THÈSE

Pour obtenir le grade de

DOCTEUR DE L'UNIVERSITÉ DE GRENOBLE

préparée dans le cadre d'une cotutelle entre l'*Université de Grenoble* et *Universidade Federal de Santa Catarina*

Spécialité : **Sciences des Polymères**

Arrêté ministériel : le 6 janvier 2005 -7 août 2006

Présentée par

« Letícia / MAZZARINO »

Thèse dirigée par **« Redouane/BORSALI »** et **« Elenara/LEMOS SENNA»**

préparée au sein du **Centre de Recherches sur les Macromolécules Végétales** et **Laboratório de Farmacotécnica**

dans **l'École Doctorale Chimie et Sciences du Vivant** et **Programa de Pós-Graduação em Farmácia**

Systèmes Nanostructurés Décorées avec du Chitosane pour la Libération Buccale de la Curcumine

Thèse soutenue publiquement le **« 24 de avril de 2013 »**,
devant le jury composé de :

Français, Redouane, BORSALI
Directeur de Recherche au Centre de Recherches sur les Macromolécules Végétales (Directeur de Thèse)
Brésilienne, Elenara, LEMOS SENNA
Professeur à l'Universidade Federal de Santa Catarina (Directeur de Thèse)
Français, Jean-Jacques, ROBIN
Directeur de Recherche à l'Université Montpellier 2 (Rapporteur)
Brésilien, Marcos Antônio, SEGATTO SILVA
Professeur à l'Universidade Federal de Santa Catarina (Rapporteur)
Français, Sami, HALILA
Maitre de Conférence au Centre de Recherches sur les Macromolécules Végétales (Examinateur)
Brésilienne, Vanessa, MOSQUEIRA
Professeur à l'Universidade Federal de Ouro Preto (Examinateur)
Français, Christophe, TRAVELET
Ingénieur d'Études au Centre de Recherches sur les Macromolécules Végétales (Examinateur)
Brésilienne, Hellen Karine, STULZER
Professeur à l'Universidade Federal de Santa Catarina (Examinateur)

Université Joseph Fourier / Université Pierre Mendès France / Université Stendhal / Université de Savoie / Grenoble INP

Letícia Mazzarino

SISTEMAS NANOESTRUTURADOS DECORADOS COM QUITOSANA PARA LIBERAÇÃO BUCAL DA CURCUMINA

Tese de doutorado em regime de co-tutela apresentada à Universidade Federal de Santa Catarina e à Université de Grenoble como requisito parcial para a obtenção dos títulos de doutora em Farmácia e em *Sciences des Polymères*, respectivamente.
Orientadores: Profa. Dra. Elenara Lemos Senna (Brasil) e Dr. Redouane Borsali (França)

Florianópolis
2013

Ficha de identificação da obra elaborada pelo autor,
através do Programa de Geração Automática da Biblioteca Universitária da UFSC.

Mazzarino, Letícia
Sistemas nanoestruturados decorados com quitosana para liberação bucal da curcumina / Letícia Mazzarino ; orientador, Elenara Lemos Senna - Florianópolis, SC, 2013.
277 p.

Tese (doutorado) - Universidade Federal de Santa Catarina, Centro de Ciências da Saúde. Programa de Pós-Graduação em Farmácia.

Inclui referências

1. Farmácia. 2. Sistemas de liberação de fármacos. 3. Nanopartículas. 4. Mucoadesão. 5. Curcumina. I. Lemos Senna, Elenara. II. Universidade Federal de Santa Catarina. Programa de Pós-Graduação em Farmácia. III. Título.

“SISTEMAS NANOESTRUTURADOS DECORADOS COM QUITOSANA PARA LIBERAÇÃO BUCAL DA CURCUMINA”

POR

Letícia Mazzarino

Tese realizada em regime de co-tutela, julgada e aprovada em sua forma final pelos Orientadores e membros da Banca Examinadora, composta pelos Doutores:

Banca Examinadora:

Dr. Sami Halila UJF/França – Membro Titular	Dr. Christophe Travelet UJF/França – Membro Externo
Prof. Dr. Marcos A. Segatto Silva UFSC – Membro Titular	Profa. Dra. Hellen Karine Stulzer UFSC – Membro Titular
Profa. Dra. Vanessa C. F. Mosqueira UFOP – Membro Titular	Prof. Dr. Jean-Jacques Robin ICG/França – Relator externo
Profa. Dra. Elenara Lemos Senna UFSC – Orientadora	Dr. Redouane Borsali UJF/França – Orientador

Profa. Dra. Tânia Beatriz Creczynski Pasa
Coordenadora do Programa de Pós-Graduação em Farmácia da UFSC

Florianópolis, 24 de abril de 2013.

Ao meu marido Lucas, pelo apoio e companheirismo em todos os momentos, ao meu pai Chico, pelos ensinamentos e pelas eternas recordações, e às minhas queridas mãe Lizete e irmã Raquel, pelo carinho.

AGRADECIMENTOS

À minha orientadora profa. Elenara Lemos Senna, pela oportunidade e orientação durante a realização desta tese e, principalmente, pela confiança no meu trabalho.

Ao meu orientador Dr. Redouane Borsali, por ter me recebido no Cermav e ter permitido que eu vivenciasse esta experiência inesquecível. Obrigada pelos ensinamentos e pela atenção durante todo o período que estive em Grenoble e, principalmente, por ter me dado liberdade e independência para conduzir esta tese, contribuindo imensamente para o meu crescimento profissional.

Ao prof. Valdir Soldi, coordenador do projeto Capes-Cofecub, pelo apoio à realização do doutorado co-tutela.

A todos funcionários e pesquisadores do CERMAV, por terem me acolhido, em especial, à equipe Physicochimie des Glycopolymères.

Aos pesquisadores e técnicos Liliane Guerente, Aymeric Audfray, Anne Imberty, Isabelle Pignot Paintrand, Amandine Durand-Terrasson, Sonia Ortega Murillo e Christophe Travelet, pela grande contribuição na realização dos experimentos.

Aos pesquisadores Issei Otsuka e Sami Halila, pela síntese do copolímero.

À profa. Maria Cláudia Santos Silva, Dra. Lorena dos Santos Bubniak e aluna Suelen Mazzucco, pela colaboração e disponibilidade para a realização dos experimentos em células e discussões.

Ao prof. Marcos A. Segatto-Silva e Dra. Andrea Mayumi Koroishi, pela colaboração que permitiu a execução dos experimentos microbiológicos.

À Gecioni Loch Neckel, pela contribuição na avaliação histológica da mucosa.

À CAPES, CNPq e CNRS, pela concessão de bolsas e apoio financeiro.

A todos amigos e professores do Laboratório de Farmacotécnica, Talitha, Cristian, Bárbara, Bruna, Luis, Georgia, Mariana(s), André, Ângela, Rosane, Diva, Sandra e Nílson, que estiveram ao meu lado e partilharam das minhas alegrias e dificuldades durante a realização deste trabalho. Em especial, à Thaísa, Clarissa, Francine e Janaína, pela amizade e pelo apoio nos momentos mais difíceis.

Aos amigos de Grenoble, por terem tornado minha estadia na França tão agradável, em especial, aos amigos Samuel, Soraia, Clayton, Carina e Reinaldo, pela parceria em todos os momentos, pelas viagens inesquecíveis e pelos vinhos compartilhados.

Às minhas seis eternas amigas Mariane, Lauren, Schanna, Tiane, Paula e Iandra.

À minha família, minha mãe Lizete e minha irmã Raquel pelo carinho e apoio. Em especial, ao meu pai Chico, meu maior exemplo de vida e maior incentivador.

Ao meu marido Lucas, por ter me acompanhado durante minha estadia em Grenoble, tornado os meus dias muito mais felizes, pela compreensão e, principalmente, pelo seu amor. Obrigada por fazer parte da minha vida e por ter estado sempre presente.

RESUMO

Este trabalho descreve o desenvolvimento de sistemas nanoestruturados mucoadesivos, incluindo nanopartículas decoradas com quitosana e filmes contendo nanopartículas, visando a liberação bucal da curcumina. Dois diferentes sistemas de nanopartículas foram desenvolvidos: as nanopartículas de policaprolactona (PCL) e as nanopartículas de xiloglucana-*bloco*-policaprolactona (XGO-*b*-PCL). As nanopartículas de PCL foram preparadas pela técnica da nanoprecipitação, enquanto as nanopartículas de XGO-*b*-PCL foram preparadas pelo método do co-solvente. Ambos sistemas coloidais apresentaram forma esférica e distribuição monodispersa de partículas. A decoração das nanopartículas com quitosana foi confirmada através das medidas de tamanho de partícula e potencial zeta. Estudos de espalhamento de luz dinâmico (DLS) mostraram raios hidrodinâmicos em torno de 100 nm para as nanopartículas de PCL, e de 50 nm para as nanopartículas de XGO-*b*-PCL. As suspensões de nanopartículas contendo curcumina apresentaram valores de eficiência de encapsulação próximos a 100 %, e teor de curcumina médio em torno de 450 μg/mL e 180 μg/mL para as nanopartículas de PCL e XGO-*b*-PCL, respectivamente. As nanopartículas também foram caracterizadas por análise do monitoramento de nanopartículas (NTA) e microscopia eletrônica de transmissão (TEM). As propriedades mucoadesivas das nanopartículas foram avaliadas pelo monitoramento das interações destes sistemas com a glicoproteína mucina (mucina submaxilar bovina, BSM) através das técnicas de espalhamento de luz dinâmico (DLS), microbalança de cristal de quartzo com monitoramento de dissipação (QCM-D) e ressonância plasmômica de superfície (SPR). Todas nanopartículas decoradas com quitosana demonstraram excelente habilidade em interagir com a mucina através de forças eletrostáticas formadas entre os grupamentos amina do polissacarídeo e os grupos negativamente carregados da glicoproteína, indicando seu potencial como carreadores mucoadesivos de fármacos. As nanopartículas de PCL também foram caracterizadas quanto a permeação e retenção de curcumina através da mucosa esofágica suína. As concentrações de curcumina retida na mucosa evidenciaram a possibilidade de aplicação destes sistemas para obtenção de efeitos locais na superfície mucosa. Estudos *in vitro* demonstraram que a nanopartículas PCL e XGO-*b*-PCL contendo curcumina apresentaram citoxicidade reduzida quando comparadas ao fármaco livre. As nanopartículas de PCL contendo curcumina também demonstraram atividade antimicrobiana contra cepas de *Candida*

albicans, sugerindo seu potencial uso no tratamento de infecções fúngicas. Os filmes mucoadesivos contendo nanopartículas foram preparados pela técnica de *casting*, após incorporação das nanopartículas de PCL em soluções de quitosana plastificadas. Os filmes obtidos usando quitosana de média e elevada massa molar mostraram-se homogêneos e flexíveis. As nanopartículas de PCL contendo curcumina apresentaram-se uniformemente distribuídas na superfície dos filmes, como evidenciado pelas imagens de microscopia de força atômica (AFM) e microscopia eletrônica de varredura de alta resolução (FEG-SEM). Análises das seções transversais dos filmes por FEG-SEM mostrou a presença das nanopartículas no interior dos filmes. Os filmes apresentaram boa hidratação em meio saliva, e liberação controlada-prolongada da curcumina *in vitro*. Assim, os resultados obtidos indicam que os sistemas mucoadesivos desenvolvidos, nanopartículas decoradas com quitosana e filmes contendo nanopartículas, oferecem uma nova estratégia para a liberação bucal da curcumina, e apresentam potenciais aplicações no tratamento local de doenças da cavidade oral.

Palavras-chave: Mucoadesão; Filmes mucoadesivos; Nanopartículas mucoadesivas; Nanopartículas decoradas com polissacarídeos; Nanopartículas decoradas com quitosana; Sistemas de liberação de fármacos; Administração bucal; Curcumina; Espalhamento de luz dinâmico (DLS); Microbalança de cristal de quartzo com monitoramento de dissipação (QCM-D); Ressonânica plasmônica de superfície (SPR); Análise de monitoramento de partículas (NTA); Microscopia eletrônica de transmissão (TEM); Microscopia de força atômica (AFM); Microscopia de varredura de alta resolução (FEG-SEM); Permeação e retenção na mucosa; Citotoxicidade *in vitro*; Atividade antifúngica.

ABSTRACT

"Nanostructured systems coated with chitosan for buccal curcumin delivery". This study describes the development of mucoadhesive nanostructured systems, including chitosan-coated nanoparticles and films containing nanoparticles, aiming the buccal delivery of curcumin. Two different systems of nanoparticles were developed: polycaprolactone (PCL) nanoparticles and xyloglucan-*block*-polycaprolactone (XGO-*b*-PCL) nanoparticles. PCL nanoparticles were prepared by the nanoprecipitation technique, while XGO-*b*-PCL nanoparticles were prepared by the co-solvent method. Both colloidal systems displayed spherical shape and monodisperse distribution of particles. The decoration of nanoparticles with chitosan was confirmed by particle size and zeta potential measurements. Dynamic light scattering (DLS) studies shown hydrodynamic radius around of 100 nm for PCL nanoparticles, and 50 nm for XGO-*b*-PCL nanoparticles. Curcumin-loaded nanoparticle suspensions exhibited encapsulation efficiency values close to 100 %, and a mean drug content about of 450 μg/mL and 180 μg/mL for PCL and XGO-*b*-PCL nanoparticles, respectively. Nanoparticle systems were also characterized by nanoparticle tracking analysis (NTA) and transmission electron microscopy (TEM). The mucoadhesive properties of nanoparticles were evaluated by monitoring the interactions of these systems with glycoprotein mucin (bovine submaxillary mucin, BSM) by dynamic light scattering (DLS), quartz crystal microbalance with dissipation monitoring (QCM-D) and surface plasmon resonance (SPR). All chitosan-coated nanoparticles demonstrate excellent ability to interact with mucin though electrostatic forces formed between amino groups of polysaccharide and negatively charged groups of glycoprotein, indicating their potential as mucoadhesive drug carriers. PCL nanoparticles were also characterized in terms of curcumin permeability and retention across the porcine esophageal mucosa. Amount of curcumin retained in the mucosa highlights the possibility of application for obtaining local effects on the mucosal surface. *In vitro* studies demonstrated that curcumin into copolymer nanoparticles showed reduced cytotoxicity when compared to free drug. Curcumin-loaded PCL nanoparticles also exhibited antimicrobial activity against *Candida albicans* strains, suggesting their potential use in the treatment of fungal infections. Mucoadhesive films containing nanoparticles were prepared using the casting technique, after the incorporation of PCL nanoparticles in plasticized chitosan solutions. Films obtained using medium and high

molar mass chitosan showed to be homogeneous and flexible. Curcumin-loaded PCL nanoparticles were uniformly distributed on the films surface, as evidenced by atomic force microscopy (AFM) and high-resolution scanning electron microscopy (FEG-SEM) images. Analyses of films cross sections by FEG-SEM demonstrate the presence of nanoparticles inside the films. In addition, films showed good rate of hydration in saliva medium, and *in vitro* prolonged-controlled delivery of curcumin. Therefore, the results obtained indicate that the developed mucoadhesive systems, chitosan-coated nanoparticles and films containing nanoparticles, offer a novel strategy to buccal curcumin delivery and have potential applications in the local treatment of oral cavity disease.

Keywords: Mucoadhesion; Mucoadhesive films; Mucoadhesive nanoparticles; Polysaccharide-coated nanoparticles; Chitosan-coated nanoparticles; Drug delivery systems; Buccal administration; Curcumin; Dynamic light scattering (DLS); Quartz crystal microbalance with dissipation monitoring (QCM-D); Surface plasmon resonance (SPR); Nanoparticle tracking analysis (NTA); Transmission electron microscopy (TEM); Atomic force microscopy (AFM); High-resolution scanning electron microscopy (FEG-SEM); Permeability and retention in the mucosa; *In vitro* cytotoxicity; Antifungal activity.

RÉSUMÉ

"Systèmes nanostructurés décorés avec du chitosane pour la libération buccale de la curcumine". Cette étude décrit le développement de systèmes nanostructurés muco-adhésives, qui comprennent les nanoparticules décorées avec du chitosane et les films contenant des nanoparticules, visant la libération buccale de la curcumine. Deux différents systèmes de nanoparticules ont été développés: les nanoparticules de polycaprolactone (PCL) et les nanoparticules xyloglucane-*bloc*-polycaprolactone (XGO-*b*-PCL). Les nanoparticules de PCL ont été préparées par la technique de nanoprécipitation, alors que les nanoparticules XGO-*b*-PCL ont été préparées par la méthode du co-solvant. Les deux systèmes colloïdaux ont montré une forme sphérique et distribution monodisperse de particules. La décoration des nanoparticules avec du chitosane a été confirmée en mesurant la taille des particules et le potentiel zêta. Les études de la diffusion dynamique de la lumière (DLS) montrent un rayon hydrodynamique autour de 100 nm pour les nanoparticules de PCL et 50 nm pour les nanoparticules de XGO-*b*-PCL. Les suspensions de nanoparticules chargées en curcumine présentent des valeurs d'efficacité d'encapsulation proche de 100 %, et un taux moyen de principe actif autour de 450 μg/mL et 180 μg/mL pour les nanoparticules de PCL et XGO-*b*-PCL, respectivement. Les systèmes de nanoparticules ont aussi été caractérisées par la technique d'analyse du suivi des nanoparticules (NTA) et microscopie électronique à transmission (MET). Les propriétés mucoadhésives des nanoparticules ont été évaluées en mesurant les interactions de ces systèmes avec la glycoprotéine mucine (mucine sous-maxillaire bovine, BSM) par diffusion dynamique de la lumière (DLS), microbalance à cristal de quartz avec la mesure de dissipation d'énergie (QCM-D) et résonance plasmonique de surface (SPR). Toutes les nanoparticules décorées avec du chitosane ont démontré une excellente capacité d'interaction avec la mucine via des forces électrostatiques formées entre les groupes amines du polysaccharide et les groupes chargés négativement de la glycoprotéine, indiquant leur potentiel comme vecteurs mucoadhésives de médicaments. Les nanoparticules PCL ont aussi été caractérisées en termes de perméabilité et de rétention de curcumine à travers la muqueuse oesophagienne de porc. La rétention de concentrations de curcumine dans la muqueuse indique la possibilité d'obtention des effets locaux sur la surface muqueuse. Les études *in vitro* ont montré que les nanoparticules de PCL et XGO-*b*-PCL contenant la curcumine ont présenté une activité cytotoxique plus petite par rapport à la curcumine

libre. Les nanoparticules de PCL contenant de la curcumine ont aussi démontré une activité antimicrobienne contre *Candida albicans*, ce qui suggère leur potentiel utilisation dans le traitement des infections fungiques. Les films mucoadhésifs contenant des nanoparticules ont été préparés par la technique de « *casting* », après l'incorporation des nanoparticules de PCL dans les solutions de chitosane plastifié. Les films obtenus en utilisant du chitosane de moyenne et haute masse molaire sont homogènes et flexibles. Les nanoparticules de PCL chargées de curcumine étaient uniformément distribuées sur les surfaces des films, comme le montrent les images de microscopie à force atomique (AFM) et de microscopie électronique à balayage de haute résolution (MEB-FEG). L'analyse par MEB-FEG des sections transversales des films a démontré la présence de nanoparticules à l'intérieur des films. En plus, les films ont montré un taux important d'hydratation en milieu salivaire et une libération contrôlée-prolongée de la curcumine. Par conséquent, les résultats obtenus indiquent que les systèmes mucoadhésives développés, nanoparticules décorées avec du chitosane et films contenant des nanoparticules, offrent une nouvelle stratégie pour la libération buccale de la curcumine, et sont potentiellement intéressant dans des applications de traitement locaux des maladies de la cavité orale.

Mots-clés: Mucoadhésion; Films mucoadhésifs; Nanoparticules mucoadhésives; Nanoparticules décorées par des polysaccharides; Nanoparticules décorées par du chitosane; Systèmes de délivrance de médicaments; Administration buccale; Curcumine; Diffusion dynamique de la lumière (DLS); Microbalance à cristal de quartz avec la mesure de dissipation d'énergie (QCM-D); Résonance plasmonique de surface (SPR); Analyse de suivi des nanoparticules (NTA); Microscopie électronique à transmission (MET); Microscopie à force atomique (AFM); Microscopie électronique à balayage de haute résolution (MEB-FEG); Perméabilité et rétention dans la muqueuse; Cytotoxicité *in vitro*; Activité antifongique.

LISTA DE FIGURAS E ESQUEMAS

Publicação: "Elaboration of chitosan-coated nanoparticles loaded with curcumin for mucoadhesive applications"

Publicação: "On the mucoadhesive properties of chitosan-coated polycaprolactone nanoparticles loaded with curcumin using QCM-D"

Publicação: *"Curcumin-loaded chitosan-decorated nanoparticles for local therapy of buccal diseases"*

Publicação: "Xyloglucan-block-poly(ε-caprolactone) copolymer nanoparticles coated with chitosan as biocompatible mucoadhesive drug delivery system"

Publicação: "Mucoadhesive films containing chitosan-coated nanoparticles: a new strategy for buccal curcumin release"

LISTA DE TABELAS

Publicação: "Elaboration of chitosan-coated nanoparticles loaded with curcumin for mucoadhesive applications"

Publicação: *"On the mucoadhesive properties of chitosan-coated polycaprolactone nanoparticles loaded with curcumin using QCM-D"*

Publicação: *"Curcumin-loaded chitosan-decorated nanoparticles for local therapy of buccal diseases"*

Publicação: "*Xyloglucan-block-poly(ε-caprolactone) copolymer nanoparticles coated with chitosan as biocompatible mucoadhesive drug delivery system*"

Publicação: "*Mucoadhesive films containing chitosan-coated nanoparticles: a new strategy for buccal curcumin release*"

LISTA DE ABREVIATURAS E SIGLAS

^{1}H NMR – Proton Nuclear Magnetic Resonance Spectroscopy; Ressonância Magnética Nuclear de Hidrogênio
AFM – Atomic Force Microscopy; Microscopia de Força Atômica
ANOVA – Analysis of Variance; Análise de Variância
BSM – Bovine Submaxillary Mucin; Mucina Submaxilar Bovina
C_0 – Initial Concentration of Drug; Concentração Inicial de Fármaco
CCD – Charge- Coupled Device; Dispositivo de Carga Acoplada
COO^- – Carboxylate; Carboxilato
Cp – Copolymer Concentration; Concentração do Copolímero
CS – Chitosan; Quitosana
CSH – High Molar Mass Chitosan; Quitosana de Elevada Massa Molar
CSHG10 – Film of High Molar Mass Chitosan and 10 % Glycerol; Filme de Quitosana de Alta Massa Molar e Glicerol 10 %
CSHG10-NP – Film of High Molar Mass Chitosan and 10 % Glycerol containing Nanoparticles; Filme de Quitosana de Alta Massa Molar e Glicerol 10 % contendo Nanopartículas
CSHG5 – Film of High Molar Mass Chitosan and 5 % Glycerol; Filme de Quitosana de Alta Massa Molar e Glicerol 5 %
CSHG5-NP – Film of High Molar Mass Chitosan and 5 % Glycerol containing Nanoparticles; Filme de Quitosana de Alta Massa Molar e Glicerol 5 % contendo Nanopartículas
CSL – Low Molar Mass Chitosan; Quitosana de Baixa Massa Molar
CSLG10 – Film of Low Molar Mass Chitosan and 10 % Glycerol; Filme de Quitosana de Baixa Massa Molar e Glicerol 10 %
CSLG10-NP – Film of Low Molar Mass Chitosan film and 10 % Glycerol containing Nanoparticles; Filme de Quitosana de Baixa Massa Molar e Glicerol 10 % contendo Nanopartículas
CSLG5 – Film of Low Molar Mass Chitosan and 5 % Glycerol; Filme de Quitosana de Baixa Massa Molar e Glicerol 5 %
CSLG5-NP – Film of Low Molar Mass Chitosan film and 5 % Glycerol containing Nanoparticles; Filme de Quitosana de Baixa Massa Molar e Glicerol 5 % contendo Nanopartículas
CSM – Medium Molar Mass Chitosan; Quitosana de Média Massa Molar
CSMG10 – Film of Medium Molar Mass Chitosan and 10 % Glycerol; Filme de Quitosana de Média Massa Molar e Glicerol 10 %
CSMG10-NP – Film of Medium Molar Mass Chitosan and 10 % Glycerol containing Nanoparticles; Filme de Quitosana de Média Massa Molar e Glicerol 10 % contendo Nanopartículas

CSMG5 – Film of Medium Molar Mass Chitosan and 5 % Glycerol; Filme de Quitosana de Média Massa Molar e Glicerol 5 %
CSMG5-Free Cur – Film of Medium Molar Mass Chitosan and 5 % Glycerol containing Free Curcumin; Filme de Quitosana de Média Massa Molar e Glicerol 5 % contendo Curcumina Livre
CSMG5-NP – Film of Medium Molar Mass Chitosan and 5 % Glycerol containing Nanoparticles; Filme de Quitosana de Média Massa Molar e Glicerol 5 % contendo Nanopartículas
CuBr – Brometo de Cobre
Cur-NP – Curcumin-Loaded Nanoparticles; Nanopartículas contendo Curcumina
Cur-NP CSH – Curcumin-Loaded Nanoparticles coated with High Molar Mass Chitosan; Nanopartículas decoradas com Quitosana de Elevada Massa Molar contendo Curcumina
Cur-NP CSL – Curcumin-Loaded Nanoparticles coated with Low Molar Mass Chitosan; Nanopartículas decoradas com Quitosana de Baixa Massa Molar contendo Curcumina
Cur-NP CSM – Curcumin-Loaded Nanoparticles coated with Medium Molar Mass Chitosan; Nanopartículas decoradas com Quitosana de Média Massa Molar contendo Curcumina
Cur-NP XGO-*b*-PCL – Curcumin-loaded Xyloglucan-*block*-Polycaprolactone Nanoparticles; Nanopartículas de Xiloglucana-*bloco*-Policaprolactona contendo Curcumina
Cur-NP XGO-*b*-PCL CS – Curcumin-loaded Xyloglucan-*block*-Polycaprolactone Nanoparticles coated with Chitosan; Nanopartículas de Xiloglucana-*bloco*-Policaprolactona decoradas com Quitosana contendo Curcumina
D – Dissipation; Dissipação
DLS – Dynamic Light Scattering, Espalhamento de Luz Dinâmico
DMEM – Dulbecco's Modified Eagle's Medium; Meio Eagle Modificado por Dulbecco
DMF – Dimethylformamide, Dimetilformamida
DP – Standard Deviation; Desvio Padrão
DPR – Relative Standard Deviation; Desvio Padrão Relativo
EDC – N-(3-Dimethylaminopropyl)-N′-Ethylcarbodiimide Hydrochloride; Cloridrato de N-(3-Dimetilaminopropil)-N'-Etilcarbodiimida
EDTA – Ethylenediamine Tetraacetic Acid; Ácido Etilenodiamino Tetra- Acético
EPR – Enhanced Permeability and Retention Effect; Efeito de Permeabilidade e Retenção Aumentadas

ETA-HCl – Ethanolamine Hydrochloride; Cloridrato de Etanolamina
F – Frequency; Frequência
FEG-SEM – Field Emission Gun Scanning Electron Microscopy ; Microscopia Eletrônica de Varredura por Emissão de Campo
HEPES – 4-(2-Hydroxyethyl)-1-Piperazineethanesulfonic Acid; Ácido 4-(2-Hidroxietil)-1-Piperazinil-Etanosulfônico
HPLC – High-Performance Liquid Chromatography; Cromatografia Líquida de Alta Eficiência
IC_{50} – 50 % Inhibitory Concentration; Concentração Inibitória 50 %
IR – Infrared; Infravermelho
J_{ss} – Steady-state Flux; Fluxo do Estado de Equilíbrio
K_D – Dissociation Constant; Constante de Dissociação
Kp – Permeability Coefficient; Coeficiente de Permeabilidade
LD – Dectection Limit; Limite de Detecção
LQ – Quantitation Limit, Limite de Quantificação
MFC - Minimum Fungicidal Concentration; Concentração Fungicida Mínima
MIC – Minimum Inhibitory Concentration; Concentração Inibitória Mínima
MPS – Mononuclear Phagocyte System; Sistema Fagocitário Mononuclear
MTT – 3-(4,5-Dimethiazol-Zyl)-2-5-Diphenyltetrazolium Bromide; Brometo de 3-(4,5-Dimetiltiazol-2-il)-2,5-Difeniltetrazólio
NH_3^+ – Amino; Amino
NHS – N-Hydroxysuccinimide; Hidroxisuccinimida
NP XGO-*b*-PCL – Unloaded Xyloglucan-*block*-Polycaprolactone Nanoparticles; Nanopartículas de Xiloglucana-*bloco*-Policaprolactona sem Fármaco
NP XGO-*b*-PCL CS – Unloaded Xyloglucan-*block*-Polycaprolactone Nanoparticles coated with Chitosan; Nanopartículas de Xiloglucana-*bloco*-Policaprolactona decoradas com Quitosana sem Fármaco
NTA – Nanoparticle Tracking Analysis; Análise do Monitoramento de Nanopartículas
PCL – Polycaprolactone; Policaprolactona
PdI – Polidispersity Index; Índice de Polidispersão
PEG – Polyethylene Glycol; Polietilenoglicol
PEO – Poly(Ethylene Oxide), Poli (Óxido de Etileno)
PLA – Poly(Lactic Acid); Poli (Ácido Lático)
PLGA – Poly(Lactic-co-Glycolic Acid); Poli (Ácido Lático-Co-Glicólico)

PMDETA – N,N,N′,N′,N″-Pentamethyldiethylenetriamine; N,N,N',N'',N''-Pentametil Dietilenotriamina
PPO – Poly(Propylene Oxide); Poli(Óxido de Propileno)
QCM-D – Quartz Crystal Microbalance with Dissipation Monitoring; Microbalança de Cristal de Quartzo com monitoramento de Dissipação
R_h – Hydrodynamic Radius; Raio Hidrodinâmico
RU – Resonance Units; Unidades de Ressonância
SDA – Sabouraud Dextrose Agar; Ágar Dextrose Sabouraud
SDS – Sodium Dodecyl Sulfate; Dodecil Sulfato de Sódio
SEC – Size Exclusion Chromatography ; Cromatografia de Exclusão por Tamanho
SEM – Scanning Electron Microscopy; Microscopia Eletrônica de Varredura
SLS – Static Light Scattering; Espalhamento de Luz Estático
SO_3^- – Sulphonate; Sulfonado
SPR – Surface Plasmon Ressonance; Ressonância Plasmônica de Superfície
TEM – Transmission Electron Microscopy; Microscopia Eletrônica de Transmissão
THF – Tetrahydrofuran; Tetrahidrofurano
T_{lag} – Lag Time; Tempo de Latência
UV/VIS – Ultraviolet-Visible Spectrophotometry ; Espectrofotometria no Ultravioleta-Visível
W_0 – Initial Weight of Film; Peso Inicial do Filme
W_t – Weight of Film at Time *t;* Peso do Filme no Tempo *t*
XGO – Xyloglucooligosaccharide; Xyloglucan Oligosaccharide; Xiloglucana Oligossacarídeo
XGO-*b*-PCL – Xyloglucan-*block*-Polycaprolactone; Xiloglucana-*bloco*-Policaprolactona

LISTA DE SÍMBOLOS

D – Diffusion Coefficient; Coeficiente de Difusão
I – Scattering Intensity; Intesidade de Espalhamento
N – Refractive Index; Índice de Refração
Q – Scattering Vector; Vetor de Espalhamento
S – Slope of the Calibration Curve; Inclinação da Curva de Calibração
T – Temperature; Temperatura
t – Time; Tempo
ζ – Zeta Potential; Potencial Zeta
η – Viscosity; Viscosidade
θ – Scattering Angle; Ângulo de Espalhamento
κ_B – Boltzmann Constant; Constante de Boltzmann
λ – Light Wavelength; Comprimendo de Onda
σ – Standard Deviation of y-Intercepts of Regression Lines; Desvio Padrão dos Interceptos das Curvas de Calibração com o Eixo Y
τ – Decay Time

SUMÁRIO

INTRODUÇÃO

Frequentemente, a absorção de fármacos através das mucosas é limitada pelo seu tempo de residência no sítio de absorção e/ou de ação. Os sistemas de liberação mucoadesivos têm sido alvo de grande interesse por serem considerados uma forma promissora para prolongar o tempo de residência das formas farmacêuticas na camada mucosa, permitindo a otimização da liberação de fármacos onde deve ocorrer o efeito terapêutico, e/ou o íntimo contato da formulação com o local de absorção (SMART, 2005a; HOMBACH; BERNKOP-SCHNURCH, 2010).

Os sistemas mucoadesivos podem ser destinados a diferentes regiões do corpo, incluindo as vias bucal, oral, vaginal, retal, nasal e ocular. Entre estas, a cavidade oral pode ser vantajosamente usada como um sítio de liberação de fármacos, visando tanto o tratamento tópico como sistêmico. A mucosa bucal é relativamente permeável, robusta e mais tolerante a substâncias potencialmente alergênicas, em comparação com outros tipos de mucosa, apresentando pouca tendência à irritação ou dano irreversível. Outras vantagens associadas à administração bucal de fármacos incluem a prevenção do metabolismo de primeira passagem hepática e da inativação por enzimas presentes no trato gastrointestinal, uma vez que o fármaco é absorvido pela mucosa e entra diretamente na circulação sanguínea. A terapia local é empregada para o tratamento da gengivite, doença periodontal, infecções fúngicas e bacterianas, úlceras aftosas e carcinomas orais. A razão para o grande interesse no tratamento local de doenças da cavidade oral provém do fato destas apresentarem uma das maiores prevalências (SMART, 2005b; SUDHAKAR; KUOTSU; BANDYOPADHYAY, 2006; SCHOLZ et al., 2008).

Entretanto, existem alguns inconvenientes associados à liberação bucal. A renovação constante da saliva, por exemplo, pode levar a rápida eliminação do fármaco no local de aplicação, necessitando a administração frequente de doses. A distribuição não uniforme da saliva pode resultar na liberação não uniforme de fármacos a partir de formas farmacêuticas sólidas ou semi-sólidas, fazendo com que algumas áreas da cavidade bucal não recebam níveis terapêuticos do fármaco. Adicionalmente, a composição da saliva pode contribuir para a modificação química de certos fármacos e para a aceitabilidade do paciente, que frente ao gosto da medicação pode não aderir ao tratamento (SMART, 2005b; SUDHAKAR; KUOTSU; BANDYOPADHYAY, 2006; SCHOLZ et al., 2008).

Formulações mucoadesivas constituem uma estratégia promissora para a administração bucal de fármacos para o tratamento de inúmeras

doenças. Além disso, o adequado desenho da forma farmacêutica permite o controle e manipulação da permeabilidade da mucosa bucal. Dentre os diferentes sistemas mucoadesivos destinados à administração bucal encontram-se os hidrogéis, filmes, comprimidos e pomadas (LEE; PARK; ROBINSON, 2000; PATHAN et al., 2008).

Apesar de poucos trabalhos descritos na literatura, as nanopartículas decoradas com polissacarídeos têm mostrado um interesse crescente como carreadores mucoadesivos de fármacos. O interesse no desenvolvimento destes sistemas provém da possibilidade de combinar as vantagens relacionadas à utilização das nanopartículas, tais como a proteção de moléculas ativas, liberação controlada e aumento da solubilidade de fármacos hidrofóbicos, com as propriedades mucoadesivas provenientes da decoração com os polissacarídeos (LEMARCHAND; GREF; COUVREUR, 2004; LEMARCHAND et al., 2006; MOHANRAJ; CHEN, 2006). Os polissacarídeos são altamente estáveis, atóxicos, hidrofílicos e biodegradáveis, além de possuírem inúmeras fontes na natureza e baixo custo. Assim, as nanopartículas decoradas com polissacarídeos mucoadesivos constituem uma alternativa promissora para prolongar o tempo de residência e, então, aumentar a absorção do fármaco encapsulado (LEMARCHAND; GREF; COUVREUR, 2004; LIU et al., 2008).

Por outro lado, o desenvolvimento de filmes mucoadesivos tem mostrado grande interesse quando a via bucal é visada, desde que permitem a fácil aplicação na mucosa. Tais sistemas de liberação são obtidos a partir de polímeros bioadesivos, e projetados de forma a proporcionar a liberação uni- ou bidirecional do fármaco, dependendo do desenho da forma farmacêutica. Outras vantagens relacionadas ao uso de filmes mucoadesivos incluem a proteção da superfície lesionada, o maior tempo de residência no local de aplicação e a maior aceitabilidade pelos pacientes, devido ao menor desconforto desta forma farmacêutica em relação aos comprimidos bucais. Relatos indicam que tais sistemas podem permanecer até 15 horas no local de aplicação, garantindo a liberação constante do fármaco (LEE; PARK; ROBINSON, 2000; SUDHAKAR; KUOTSU; BANDYOPADHYAY, 2006).

A curcumina é a substância ativa extraída do rizoma da planta *Curcuma longa* Linn, popularmente conhecida como açafrão, característica de regiões tropicais e subtropicais amplamente cultivada na Índia e China. A curcumina exibe diversas atividades farmacológicas incluindo antiinflamatória, antitumoral, antioxidante, antimicrobiana, além de estar relacionada a efeitos benéficos à saúde (GOEL;

KUNNUMAKKARA; AGGARWAL, 2008). Considerando suas atividades biológicas, a liberação bucal da curcumina pode ser útil no tratamento de várias doenças da cavidade oral. Estudos *in vivo* têm demonstrado que a administração da curcumina a ratos inibe significativamente a resposta imune inflamatória associada a doença periodontal, sugerindo o seu potencial efeito terapêutico nesta condição inflamatória crônica (GUIMARAES et al., 2011; GUIMARAES et al., 2012). A curcumina também têm demonstrado reduzir significativamente a viabilidade celular e induzir a apoptose de células de câncer oral, mostrando ser mais potente que outros polifenóis, tais como, a quercetina e a genisteína (ELATTAR; VIRJI, 2000; LIAO et al., 2011). Contudo, apesar do grande interesse farmacêutico relacionado à curcumina, seu uso terapêutico tem sido limitado devido a sua baixa solubilidade aquosa, a qual resulta em uma baixa biodisponibilidade por diferentes vias de administração. Além disso, a curcumina exibe alta taxa de decomposição em pH neutro ou básico e susceptibilidade à degradação fotoquímica (TONNESEN, 2002; TONNESEN; MASSON; LOFTSSON, 2002; ANAND et al., 2007; TOMREN et al., 2007).

Uma forma promissora para contornar os problemas de degradação, baixa solubilidade em água e reduzida biodisponibilidade é a associação da curcumina a carreadores como nanopartículas, lipossomas, ciclodextrinas, micelas e complexos fosfolipídicos (WANG et al., 2011). Assim, considerando o exposto acima, este trabalho tem como objetivo desenvolver sistemas de liberação nanoestruturados contendo curcumina para administração bucal, visando potencializar o seus efeitos farmacológicos para o tratamento local de doenças da cavidade oral. Estes sistemas são constituídos de nanopartículas poliméricas decoradas com o polissacarídeo quitosana e filmes nanoestruturados obtidos a partir destas nanopartículas. A obtenção destes sistemas é pouco descrita na literatura, evidenciando o caráter inovador deste trabalho.

OBJETIVOS

Objetivo Geral

Desenvolver e caracterizar sistemas nanoestruturados decorados com quitosana contendo curcumina com vistas à aplicação bucal.

Objetivos Específicos

- Preparar suspensões de nanopartículas decoradas com quitosana contendo curcumina a partir do polímero policaprolactona (PCL) pela técnica de nanoprecipitação;
- Preparar nanopartículas decoradas com quitosana contendo curcumina a partir do copolímero em bloco xiloglucana-policaprolactona (XGO-*b*-PCL) pela técnica do co-solvente;
- Caracterizar as suspensões de nanopartículas quanto ao tamanho de partícula, morfologia, potencial zeta, teor de curcumina e eficiência de encapsulação;
- Preparar filmes mucoadesivos contendo nanopartículas contendo curcumina;
- Caracterizar os filmes mucoadesivos quanto à massa, espessura e morfologia;
- Avaliar as propriedades mucoadesivas das nanopartículas decoradas com quitosana;
- Determinar o percentual de intumescimento dos filmes nanoestruturados em meio saliva artificial;
- Desenvolver e validar metodologia analítica por espectroscopia de fluorescência para a determinação da curcumina nos estudos de liberação, e permeação e retenção na mucosa;
- Avaliar e comparar a permeação e retenção da curcumina a partir das suspensões de nanopartículas em modelo bicompartimental de célula de difusão tipo Franz, usando mucosa esofágica suína como membrana;
- Avaliar e comparar o perfil de liberação da curcumina a partir dos diferentes filmes contendo nanopartículas desenvolvidos;
- Avaliar e comparar a citotoxicidade *in vitro* das suspensões de nanopartículas contendo curcumina em cultura de fibroblastos murino L929;
- Avaliar a atividade microbiológica *in vitro* das nanopartículas decoradas com quitosana.

CAPÍTULO 1: REVISÃO DE LITERATURA

1 ADMINISTRAÇÃO BUCAL DE FÁRMACOS

A região bucal constitui uma atrativa via para administração de fármacos. A administração bucal envolve a aplicação do princípio ativo na membrana mucosa que reveste a cavidade oral. A administração bucal de fármacos oferece algumas vantagens em relação aos outras vias, tais como, ótima acessibilidade, administração e remoção facilitada e indolor, alta aceitabilidade pelos pacientes quando comparada a outras vias não orais, baixa atividade enzimática, evita a hidrólise ácida do fármaco do trato gastrointestinal e o metabolismo de primeira passagem, levando a maior biodisponibilidade do princípio ativo. Além disso, a mucosa bucal é altamente vascularizada, robusta, apresenta rápida renovação celular e mais tolerante a alérgenos com reduzida tendência de irritação ou dano irreversível (SHOJAEI, 1998; SALAMAT-MILLER; CHITTCHANG; JOHNSTON, 2005; SUDHAKAR; KUOTSU; BANDYOPADHYAY, 2006; SCHOLZ et al., 2008).

Contudo, a baixa permeabilidade da membrana bucal, principalmente, quando comparada à membrana sublingual, a pequena superfície de absorção, o curto tempo de residência devido a remoção do fármaco pela contínua secreção de saliva e a inconveniência do uso de sistemas mucoadesivos bucais durante as ações de comer e beber são as principais limitações associadas à administração bucal de medicamentos (HAO; HENG, 2003; SALAMAT-MILLER; CHITTCHANG; JOHNSTON, 2005).

A liberação de fármacos na cavidade oral pode ocorrer em quatro regiões distintas, nomeadas bucal, sublingual, palatal e gengival, das quais as regiões bucal e sublingual são as mais adequadas para esta função (SCHOLZ et al., 2008). A liberação bucal, por sua vez, se refere especificamente à liberação de fármacos na mucosa bucal ou através da mucosa bucal para obtenção de efeitos farmacológicos locais ou sistêmicos, respectivamente. Assim, os sistemas de liberação bucal podem ser utilizados para o tratamento de doenças da cavidade oral ou para uso sistêmico (HAO; HENG, 2003). A liberação localizada é visada para o tratamento de dor de dente, doenças periodontais, cáries dentais, infecções fúngicas e bacterianas, aftas ulcerativas, líquen plano, estomatites inflamatórias e dentais. Além disso, o câncer oral está entre os cânceres malignos mais frequentes. A liberação sistêmica através dos sistemas bucais têm sido proposta, principalmente, para o tratamento de neuralgia do nervo trigêmeo, vícios, doença de Ménière e diabete (SHOJAEI, 1998; SCHOLZ et al., 2008).

1.1 Anatomia e fisiologia da mucosa bucal

A mucosa oral apresenta três camadas distintas: epitélio, membrana basal e tecido conectivo. O epitélio da mucosa oral é suportado pelo tecido conectivo, também nomeado lâmina própria, mas separado desta pela membrana basal (HAO; HENG, 2003). A composição do epitélio varia dependendo da região da cavidade oral. As áreas expostas ao estresse mecânico, como gengivas e palato duro, são queratinizadas similarmente à epiderme. Enquanto, as mucosas do palato mole, e regiões sublingual e bucal, não são queratinizadas. O epitélio queratinizado contém lipídios neutros como ceramidas e acilceramidas, os quais estão associados a função barreira, sendo relativamente impermeável à água. Já o epitélio não-queratinizado não contém acilceramidas e possui pequenas quantidades de ceramidas e lipídios polares, tais como o sulfato de colesterol e glucosilceramidas, e é considerado mais permeável à água (SHOJAEI, 1998; VASIR; TAMBWEKAR; GARG, 2003).

A mucosa bucal reveste a parte interna das bochechas e é similar ao epitélio escamoso estratificado presente no resto do corpo (Figura 1). O epitélio da mucosa bucal apresenta uma área superficial de 50,2 cm^2 e contém aproximadamente 40 à 50 camadas de células, resultando numa espessura em torno de 500 à 800 μm. O tempo de renovação do epitélio bucal varia de 5-6 dias (SHOJAEI, 1998; SUDHAKAR; KUOTSU; BANDYOPADHYAY, 2006). A função primária do epitélio bucal é a proteção do tecido subjacente. Nas regiões não-queratinizadas, a barreira de permeabilidade lipídica protege os tecidos subjacentes contra perda de líquidos e entrada de agentes potencialmente prejudiciais tais como antígenos, carcinógenos, toxinas microbianas e enzimas, presentes em alimentos e bebidas (SUDHAKAR; KUOTSU; BANDYOPADHYAY, 2006).

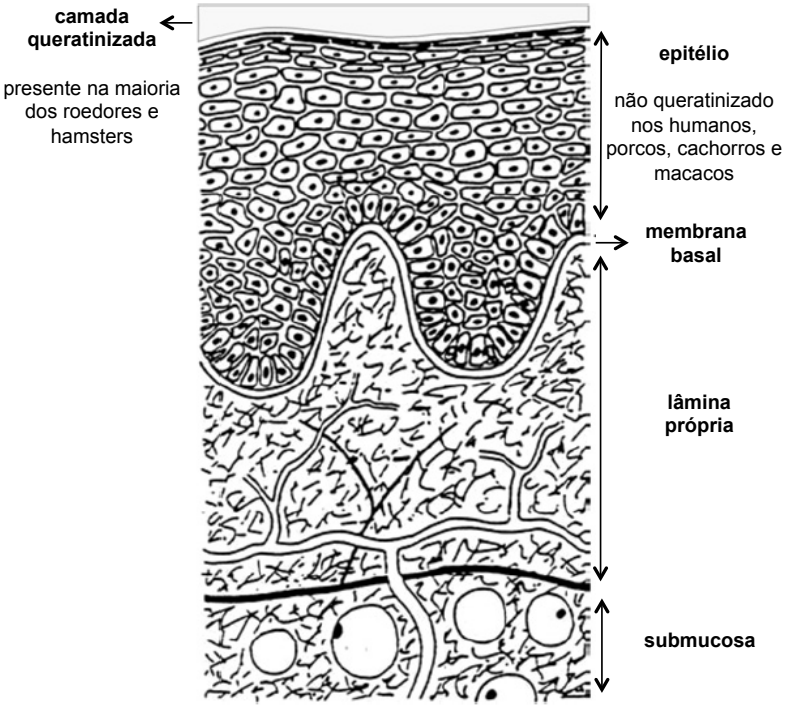

Figura 1. Representação esquemática da seção transversal da mucosa bucal. Fonte: adaptado de Morales; McConville (2011).

O fluxo sanguíneo na cavidade oral é, geralmente, mais rico e mais rápido que aquele presente na pele (HAO; HENG, 2003). As artérias que irrigam a cavidade oral encontram-se presentes na camada da lâmina própria e derivam da artéria carótida externa. O suprimento sanguíneo do revestimento das bochechas possui como principais fontes a artéria bucal, algumas ramificações terminais da artéria facial, a artéria alveolar posterior e a artéria infraorbital (SALAMAT-MILLER; CHITTCHANG; JOHNSTON, 2005). O fluxo sanguíneo da mucosa bucal é maior e mais rápido (2.4 ml/min/cm^2) que aquele apresentado pelas regiões sublingual, gengival e palatal, o que facilita a difusão passiva de fármacos através da mucosa (SUDHAKAR; KUOTSU; BANDYOPADHYAY, 2006).

A camada mucosa que reveste a cavidade oral protege a superfície contra a abrasão de materiais rugosos e agentes químicos nocivos, além de lubrificar o epitélio. O muco é um produto biológico viscoso e heterogêneo que reveste diversas superfícies epiteliais. As

células secretoras de muco, denominadas células de Globet ou caliciformes, podem ser encontradas em diferentes regiões do corpo, incluindo as mucosas nasal, ocular, e bucal, e os tratos gastrointestinal, reprodutivo e respiratório (SERRA; DOMENECH; PEPPAS, 2009). A espessura da camada de muco varia significativamente de acordo com as superfícies mucosas, sendo menor que 1 μm na cavidade oral (HOMBACH; BERNKOP-SCHNURCH, 2010).

Os principais constituintes do muco são a água (mais que 95 % do peso total), sais inorgânicos (aproximadamente 1 %), carboidratos e lipídios (menos que 1 %) e glicoproteínas (não mais que 5 %). As glicoproteínas do muco, denominadas mucinas, são constituídas por um núcleo proteico ligado a cadeias de oligossacarídeos sobre 63 % de seu comprimento (Figura 2). Os principais aminoácidos da porção proteica são a serina e a treonina, os quais estão ligados às cadeias de oligossacarídeos por ligações glicosídicas. Os resíduos de açúcar que compõe a porção oligossacarídica são a galactose, fucose, N-acetilglucosamina, N-acetilgalactosamina e ácido siálico As mucinas fornecem propriedades viscoelásticas ao muco devido a sua elevada massa molar (1 - 40 MDa), ligações peptídicas, pontes dissulfídricas intramoleculares e interações hidrofóbicas, sendo as propriedades coesivas e adesivas dependentes da concentração destas glicoproteínas. (VARUM et al., 2008; SERRA; DOMENECH; PEPPAS, 2009).

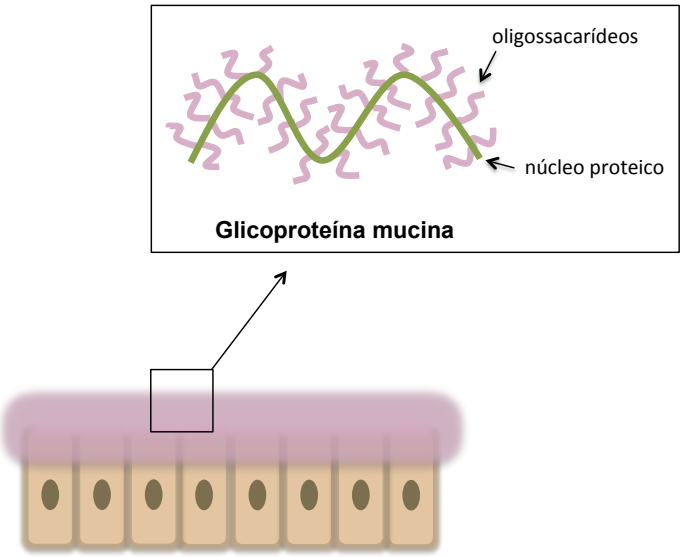

Figura 2. Representação esquemática da organização estrutural da mucina, principal responsável pelas propriedades adesivas da camada mucosa.

O muco é carregado negativamente no pH fisiológico da saliva, entre 5,8 e 7,4, devido à presença de ácidos siálico e sulfatos nas cadeias laterais de oligossacarídeos (HAO; HENG, 2003). A temperatura da cavidade oral é de 37 °C, geralmente, podendo variar por curtos períodos de tempo de 5 à 55 °C pela ingestão de comidas ou bebidas frias ou quentes (SCHOLZ et al., 2008). O volume de saliva diário varia entre 0,5 à 2 litros, sendo esta a quantidade disponível de fluido para hidratação das formas farmacêuticas administradas na mucosa oral (SHOJAEI, 1998).

1.2 Permeabilidade da mucosa bucal

Estima-se que a permeabilidade da mucosa que reveste a cavidade oral seja de 4 a 4.000 vezes maior que a da pele. Esta ampla faixa está associada às consideráveis diferenças de permeabilidade entre as diferentes regiões da cavidade oral, devido às variações de estruturas e funções das mucosas. Em geral, a permeabilidade da mucosa oral diminui na seguinte ordem: sublingual > bucal > palatal. Esta ordem baseia-se nas espessuras relativas e no grau de queratinização destes tecidos, onde a mucosa sublingual é relativamente mais fina e não-

queratinizada, a mucosa bucal é mais espessa e não-queratinizada e a região palatal possui espessura intermediária, porém é queratinizada (SHOJAEI, 1998; TANGRI; MADHAV, 2011)

As camadas superficiais do epitélio oral representam a barreira primária para a entrada de substâncias externas e microrganismos. O epitélio atua como uma barreira de permeabilidade da mucosa oral, servindo como uma camada protetora dos tecidos mais profundos. A propriedade barreira é, principalmente, atribuída à presença de material intercelular derivado dos chamados grânulos revestidos por membrana. Estes grânulos são organelas esféricas ou ovais com diâmetro entre 100 a 300 nm, encontrados em ambos epitélios queratinizados e não-queratinizados. Quando as células iniciam seu processo de diferenciação, os grânulos são formados e se fusionam com a membrana plasmática das células apicais, liberando seu conteúdo no espaço intercelular em mais de um terço da superfície epitelial (SHOJAEI, 1998; SALAMAT-MILLER; CHITTCHANG; JOHNSTON, 2005).

Apesar do epitélio ser considerado o passo limitante à penetração na mucosa, a membrana basal também pode apresentar certa resistência à passagem de substâncias entre o epitélio e o tecido conectivo. A carga dos constituintes da membrana basal pode limitar a penetração de compostos lipofílicos, que atravessam a superfície epitelial de forma relativamente fácil. Além disso, a presença de muco e saliva também pode contribuir com as propriedades de barreira da mucosa oral (SUDHAKAR; KUOTSU; BANDYOPADHYAY, 2006).

Com o intuito de aumentar a permeação de fármacos através da mucosa oral, promotores de penetração podem ser incorporados à formulação. Os promotores de penetração também são utilizados quando se deseja que o fármaco alcance a circulação sistêmica para exercer sua ação. Estas substâncias não devem ser irritantes e devem ter efeito reversível, ou seja, as propriedades de barreira do epitélio devem ser restauradas após o fármaco ter sido absorvido. Atualmente, as principais classes de promotores de penetração bucal incluem: (i) os ácidos graxos, que atuam quebrando os lipídios intercelulares; (ii) os surfactantes e, entre estes os sais biliares, que promovem a extração de lipídios e proteínas de membrana, a fluidização da membrana celular e a micelização reversa da membrana, criando canais aquosos; (iii) a azona, que atua fluidificando os lipídios intercelulares; e (iv) os álcoois, que ocasionam a reorganização dos domínios lipídicos e alteram a conformação proteica. A quitosana, também, tem demonstrado exercer considerável efeito promotor sobre a penetração de fármacos através das mucosas vaginal, bucal, intestinal e nasal. As propriedades de

penetração aumentadas da quitosana são, principalmente, atribuídas ao aumento transitório da junções entre as células (ROSSI; SANDRI; CARAMELLA, 2005).

A presença de doenças que danificam a mucosa oral, tais como líquen plano, pênfigo, infecções virais e reações alérgicas, propiciam alterações em sua permeabilidade (SMART, 2005b). Doenças hiperplásicas podem aumentar a espessura do epitélio, enquanto doenças atróficas podem torná-lo mais fino que o normal, levando até mesmo a perda desta camada como, por exemplo, no caso de lesões ulcerativas. O afinamento do epitélio altera as propriedades de barreira da mucosa, o que tende a facilitar a liberação local de fármacos para o tratamento de doenças da mucosa oral. Contudo, as alterações da superfície mucosa podem ocasionar descamação e influenciar a secreção de muco, dificultando a administração da forma farmacêutica mucoadesiva (HAO; HENG, 2003).

1.3 Vias de absorção bucal de fármacos

Os principais mecanismos responsáveis pela penetração de substâncias são difusão passiva (paracelular e transcelular), difusão mediada por carreador, transporte ativo, pinocitose e endocitose. Estudos recentes mostram que a difusão passiva é o principal mecanismo envolvido no transporte de fármacos através da mucosa bucal, embora o transporte mediado por carreadores também tenha sido relatado (SALAMAT-MILLER; CHITTCHANG; JOHNSTON, 2005).

Existem duas vias de permeação para o transporte passivo de fármacos através da mucosa bucal: a via paracelular (intercelular), que envolve o transporte de moléculas através dos espaços entre as células, e a via transcelular (intracelular), que envolve a passagem de moléculas através das membranas celulares. As moléculas de fármaco podem usar as duas rotas simultaneamente, mas, geralmente, uma é preferida em relação a outra de acordo com as propriedades físico-químicas do mesmo, tais como, lipofilicidade, carga, geometria e massa molar. Uma vez que os espaços intercelulares e o citoplasma são hidrofílicos, compostos lipofílicos apresentam baixa solubilidade neste meio. A membrana celular, por sua vez, apresenta natureza lipofílica, e substâncias hidrofílicas podem ter dificuldade de permear através dela devido ao baixo coeficiente de partição. Assim, os espaços intercelulares constituem a principal barreira para a permeação de compostos lipofílicos e a membrana celular para compostos hidrofílicos (SHOJAEI, 1998; TANGRI; MADHAV, 2011).

2 MUCOADESÃO

A bioadesão pode ser descrita como a ligação de macromoléculas naturais ou sintéticas a superfícies biológicas. Enquanto, o termo mucoadesão é utilizado quando este fenômeno de ligação ocorre especificamente com o muco ou com a membrana mucosa que reveste o epitélio. Células secretoras de muco são amplamente disseminadas em diferentes locais do corpo incluindo a mucosa nasal, ocular, bucal, gastrintestinal e o trato respiratório. As funções primárias do muco são a proteção e lubrificação do epitélio, contudo, outras funções especializadas também têm se demonstrado importantes (SMART, 2005a; SERRA; DOMENECH; PEPPAS, 2009).

Geralmente, o tempo de contato das formas farmacêuticas convencionais varia de pouco minutos (para a parte anterior do olho) até, aproximadamente, 3 horas (para o intestino delgado), com tempos intermediários para outras vias de administração, o que constitui uma barreira significativa para a liberação de fármacos. Assim, desde o início da década de 1980, a utilização de polímeros bioadesivos tem sido alvo de intensa investigação como estratégia para prolongar o tempo de contato de sistemas de liberação com as diversas membranas. A habilidade de manter o sistema de liberação de fármacos em um determinado local por um período prolongado tem se demonstrado útil no tratamento de doenças, tanto pela obtenção de efeitos locais quanto sistêmicos. (LEE; PARK; ROBINSON, 2000).

2.1 Mecanismos envolvidos na mucoadesão

Para desenvolver sistemas de liberação mucoadesivos é necessário compreender as forças e mecanismos que levam à efetiva ligação entre o polímero e a camada mucosa. Embora os mecanismos não estejam completamente elucidados, tem-se aceito que o fenômeno de mucoadesão ocorre em duas fases (Figura 3):

1. **Fase de contato:** caracteriza-se pelo estabelecimento do contato íntimo entre o polímero mucoadesivo e a membrana mucosa. Como consequência, ocorre a transferência de água da camada de muco para o polímero, resultando no intumescimento do mesmo. A hidratação do polímero é fundamental para que as cadeias de polímero adquiram maior mobilidade e possam interpenetrar com as cadeias das glicoproteínas do muco;

2. **Fase de consolidação:** mucoadesão é consolidada por meio de diferentes interações físico-químicas, levando a adesão prolongada do sistema. As interações físicas incluem o entrelaçamento das glicoproteínas mucinas com as cadeias poliméricas e a interpenetração das macromoléculas na matriz polimérica. As interações químicas são resultantes da formação de ligações químicas fracas entre o polímero e a camada mucosa, incluindo ligações iônicas, forças de Van der Waals, e ligações de hidrogênio, embora a formação de ligações covalentes seja possível em alguns casos (SMART, 2005a; VARUM et al., 2008; SERRA; DOMENECH; PEPPAS, 2009).

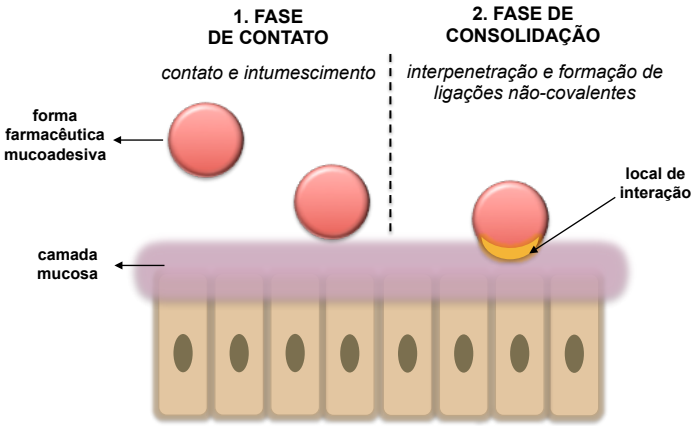

Figura 3. Fases do mecanismo de mucoadesão.

2.2 Teorias da mucoadesão

Diversas teorias têm sido propostas para fundamentar a mucoadesão. Atualmente, nenhuma destas teorias sozinhas tem sido aceita para explicar o fenômeno da mucoadesão, contudo o entendimento deste processo pode ser útil no desenvolvimento de novos produtos mucoadesivos. Entre as teorias referidas até o momento, pode-se citar:

- ***Teoria eletrônica:*** propõe que o contato entre o polímero adesivo e o muco, devido as suas diferentes características eletrônicas, ocasiona a transferência de elétrons e a formação de uma dupla camada carregada eletricamente na interface das duas superfícies. Consequentemente, a adesão ocorre devido as

forças atrativas da transferência de elétrons através desta dupla camada.

- ***Teoria da adsorção:*** relata que a atração entre o muco e o polímero mucoadesivo é alcançada através de interações específicas, tais como ligações de hidrogênio e forças de Van der Waals. Efeitos hidrofóbicos também podem exercer um importante papel quando os polímeros têm natureza anfifílica. Esta teoria também considera a adesão através da quimiossorção, onde fortes ligações covalentes são formadas entre os substratos.
- ***Teoria do umedecimento:*** considera como pré-requisito para o desenvolvimento do processo adesivo, a habilidade do sistema polimérico em espalhar-se sobre a camada mucosa. Esta teoria é, principalmente, aplicada a sistemas líquidos e semi-sólidos. Normalmente, a ótima habilidade dos polímeros em espalhar-se sobre as superfícies mucosas pode ser associada com uma excelente performance mucoadesiva. A afinidade dos sistemas pela mucosa pode ser determinada através de medidas de ângulo de contato, assim, quanto menor o ângulo de contato, maior a afinidade.
- ***Teoria da difusão:*** descreve que a ligação adesiva semi-permanente pode ser originada pela difusão e interpenetração das cadeias do polímero mucoadesivo através das cadeias glicoproteicas da camada mucosa. Esta adesão depende dos gradientes de concentração, coeficiente de difusão, massa molar, temperatura, tempo e pressão de contato e, tamanho hidrodinâmico e mobilidade das cadeias poliméricas. Polímeros com grandes cadeias podem difundir e interpenetrar numa maior extensão com a superfície mucosa; considera-se que um comprimento de cadeia mínimo de 100.000 Da seja necessário para o processo de interpenetração e entrelaçamento molecular.
- ***Teoria mecânica:*** propõe que a rugosidade da superfície favorece a adesão devido ao aumento da área de contato. Esta teoria sugere que materiais com superfície porosa e rugosa contribuem para o estabelecimento do processo mucoadesivo.
- ***Teoria da fratura:*** relaciona a ligação adesiva entre o muco e o sistema mucoadesivo à força requerida para a separação de ambos após a adesão estar estabelecida. Esta teoria é apropriada para calcular a força de fratura das ligações adesivas envolvendo sistemas mucoadesivos sólidos e rígidos, uma vez

que não considera a interpenetração e difusão das cadeias poliméricas (LEE; PARK; ROBINSON, 2000; SMART, 2005a; VARUM et al., 2008; ANDREWS; LAVERTY; JONES, 2009; SERRA; DOMENECH; PEPPAS, 2009; CARVALHO et al., 2010; KHUTORYANSKIY, 2011; MANIYAR et al., 2011).

2.3 Fatores que influenciam o processo mucoadesivo

O estabelecimento da ligação mucoadesiva pode ser influenciado por inúmeros fatores, entre os quais encontram-se os fatores relacionados com o próprio polímero mucoadesivo e os fatores relacionados ao ambiente.

2.3.1 Fatores relacionados ao polímero

Massa molar. A massa molar ideal para mucoadesão máxima depende do tipo de polímero adesivo. Estudos têm demonstrado que uma boa mucoadesão requer uma massa molar de pelo menos 100.000 Da. Um exemplo clássico é o polietilenoglicol (PEG) que com massa molar de 20.000 Da tem poucas propriedades adesivas, já com massa molar de 200.000 Da apresenta maior caráter adesivo e com 400.000 Da possui, ainda, maior adesão. Tratando-se de polímeros lineares, a baixa massa molar implica em uma crítica interpenetração das cadeias poliméricas, impossibilitando uma boa mucoadesão (LEE; PARK; ROBINSON, 2000). Contudo, ainda é difícil determinar exatamente a massa molar ótima de polímeros hidrofílicos muito grandes. Polímeros com maior massa molar podem não hidratar facilmente e não interagirem com o substrato, enquanto polímeros de menor massa molar formam géis fracos e dissolvem rapidamente (SMART, 2005a).

Concentração. A ótima mucoadesão é produzida por uma determinada concentração de polímero. A concentração do polímero adesivo pode influenciar o comprimento da cadeia disponível para penetração na camada mucosa e, assim o desenvolvimento do fenômeno mucoadesivo. Em baixas concentrações de polímero, o número de cadeias poliméricas por unidade de volume de muco é pequeno, e a interação pode ser instável. Em geral, polímeros mais concentrados podem resultar em cadeias poliméricas disponíveis mais longas e melhor capacidade de adesão. Porém, cada polímero possui uma concentração ideal e, assim, em alguns casos maiores concentrações de polímero podem até diminuir as propriedades mucoadesivas do sistema (SALAMAT-MILLER; CHITTCHANG; JOHNSTON, 2005).

Flexibilidade das cadeias. As cadeias poliméricas devem ser flexíveis a fim de permitir a interpenetração e o entrelaçamento do sistema com o muco, dando início a mucoadesão. A maior mobilidade das cadeias ocasiona maior difusão e interpenetração do polímero na camada mucosa. Polímeros muito solúveis em água podem formar ligações cruzadas (*cross-linking*) e, consequentemente, terem a mobilidade e o comprimento das suas cadeias diminuídos, o que reduz a força mucoadesiva. Geralmente, a mobilidade e flexibilidade das cadeias está relacionada a sua viscosidade e coeficiente de difusão (LEE; PARK; ROBINSON, 2000; SALAMAT-MILLER; CHITTCHANG; JOHNSTON, 2005; ANDREWS; LAVERTY; JONES, 2009).

Conformação espacial. A conformação helicoidal do polímero pode levar a diminuição da força mucoadesiva dos grupos funcionais responsáveis pelo mecanismo de adesão (FIGUEIRAS; CARVALHO; VEIGA, 2007). Por exemplo, apesar da grande diferença de massa molar dos dextranos de 200.000 Da e 19.500.000 Da, estes polímeros apresentam similar força mucoadesiva, provavelmente devido à diminuição de sítios adesivos resultante da conformação helicoidal (ANDREWS; LAVERTY; JONES, 2009). Assim, torna-se interessante a utilização de polímeros que apresentem conformação linear.

Carga. Algumas generalizações têm sido feitas em relação a carga dos polímeros mucoadesivos. Polímeros não iônicos parecem ter um menor grau de adesão comparados a polímeros aniônicos. Por outro lado, polímeros catiônicos têm demonstrado propriedades mucoadesivas superiores, principalmente, em meio neutro ou levemente alcalino. Ainda, alguns polímeros catiônicos de elevada massa molar, tais como a quitosana, têm demonstrado boas propriedades adesivas (SALAMAT-MILLER; CHITTCHANG; JOHNSTON, 2005).

2.3.2 Fatores relacionados ao ambiente

pH. O pH do meio possui um efeito significativo sobre o processo da mucoadesão pois pode alterar a carga da superfície do muco e de certos polímeros bioadesivos ionizáveis. A densidade de carga do muco pode ser alterada com o pH devido a dissociação dos grupos funcionais das moléculas de carboidratos e aminoácidos das cadeias do polipeptídio. O pH, ainda, pode afetar o grau de hidratação de alguns polímeros como, por exemplo, o ácido acrílico (LEE; PARK; ROBINSON, 2000; FIGUEIRAS; CARVALHO; VEIGA, 2007).

Tempo de contato inicial. O tempo de contato entre o sistema adesivo e a camada mucosa pode determinar a extensão dos processos de intumescimento e interpenetração das cadeias poliméricas. Além disso, tempos de contato iniciais prolongados aumentam a força mucoadesiva (LEE; PARK; ROBINSON, 2000).

Intumescimento. As características de intumescência estão relacionadas tanto ao próprio polímero adesivo como ao ambiente. O grau de intumescimento depende da concentração do polímero, força iônica e presença de água. A mucoadesão máxima ocorre em uma concentração ótima de água, uma vez que a hidratação excessiva pode diminuir a adesão (LEE; PARK; ROBINSON, 2000; FIGUEIRAS; CARVALHO; VEIGA, 2007).

Variáveis fisiológicas (tempo de renovação da mucina e condições patológicas). O tempo de renovação da mucina é considerado um fator limitante para o tempo de residência da forma farmacêutica no local de aplicação. Estima-se que este tempo de renovação varia amplamente dependendo do local, sendo relatados valores entre algumas horas até um dia (LEE; PARK; ROBINSON, 2000). Determinadas condições patológicas também podem influenciar a retenção do sistema mucoadesivo, uma vez que podem provocar alterações estruturais e físico-químicas no muco (FIGUEIRAS; CARVALHO; VEIGA, 2007). A viscosidade da camada mucosa pode ser significativamente alterada em certas doenças. A baixa viscosidade do muco resulta em fraca ligação com o sistema adesivo, enquanto viscosidade extremamente elevada dificulta a interpenetração das cadeias poliméricas e a difusão do fármaco (ANDREWS; LAVERTY; JONES, 2009). O movimento dos tecidos bucais durante as ações de comer, beber e falar, é outro fator importante que deve ser considerado no desenvolvimento de sistemas adesivos destinados à cavidade oral (SALAMAT-MILLER; CHITTCHANG; JOHNSTON, 2005).

2.4 Polímeros mucoadesivos

Um polímero mucoadesivo ideal deve apresentar as seguintes características:

- o polímero e seus produtos de degradação não devem ser tóxicos e não devem ser absorvidos pelo trato gastrointestinal;
- não deve ser irritante à membrana mucosa;
- não deve interferir nas atividades normais tais como falar e beber;

- deve formar preferencialmente ligações não-covalentes com a mucina;
- deve aderir rapidamente aos tecidos e apresentar sítio-especificidade;
- deve permitir a incorporação de fármacos hidrofílicos e hidrofóbicos e não oferecer resistência à sua liberação;
- deve facilitar e prolongar a absorção do fármaco;
- não deve se decompor durante o armazenamento da forma farmacêutica;
- não apresentar custo elevado a fim de permitir o desenvolvimento de formas farmacêuticas competitivas (PATIL et al., 2006; SUDHAKAR; KUOTSU; BANDYOPADHYAY, 2006).

Inúmeras investigações realizadas na área de polímeros têm permitido aos autores determinar as características moleculares necessárias para o estabelecimento do processo de mucoadesão. Entre as propriedades estruturais apresentadas por um bom polímero mucoadesivo estão a presença de grupos formadores de ligações de hidrogênio fortes (tais como grupos carboxila, hidroxila, amino e sulfato), fortes cargas aniônicas ou catiônicas, elevada massa molar, flexibilidade das cadeias poliméricas para penetrar na membrana mucosa, propriedades de energia de superfície adequadas ao umedecimento e espalhamento do polímero sobre a camada mucosa (PATIL et al., 2006; KHUTORYANSKIY, 2011).

De forma geral, os polímeros mucoadesivos podem ser classificados quanto à sua origem, solubilidade e carga iônica:

- ***Quanto à origem, em polímeros naturais ou sintéticos.*** A maioria dos polímeros mucoadesivos sintéticos são derivados do ácido poliacrílico e da celulose. Exemplos de polímeros baseados em ácido poliacrílico são o carbopol, policarbofil, poliacrilato, ácido poli metilvinileter-co-metacrílico, polihidroxietilmetacrilato, polimetacrilato, polialquil cianoacrilato, poli-isohexil cinoacrilato e poli-isobutil cianoacrilato. Os derivados da celulose incluem carboximetilcelulose, hidroxietilcelulose, hidroxipropilcelulose, carboximetilcelulose sódica, metilcelulose e metilhidroxietilcelulose. Polihidroxipropil metacrilamida, polioxietileno, polivinilpirrolidona, álcool polivinílico e polímeros tiolados também são incluídos nesta classificação. Enquanto os polímeros naturais ou semi-naturais incluem a

quitosana, agarose, ácido hialurônico, gelatina e várias gomas tais como guar, hakea, xantana, gelana, carragenana, pectina e alginato de sódio (LEE; PARK; ROBINSON, 2000; SALAMAT-MILLER; CHITTCHANG; JOHNSTON, 2005).

- ***Quanto à solubilidade, em polímeros solúveis ou insolúveis em água.*** Os polímeros solúveis em água ou hidrofílicos apresentam estrutura linear ou randômica, intumescem indefinidamente em contato com a água e eventualmente se dissolvem completamente. Neste caso, a duração do tempo de residência na superfície mucosa depende da velocidade de dissolução do polímero. Alguns exemplos de polímeros hidrofílicos são metilcelulose, hidroxietilcelulose, hidroxipropilmetilcelulose, carbopol, alginato de sódio, ácido poliacrílico e carboximetilcelulose sódica. Polímeros insolúveis em água, normalmente, apresentam uma rede polimérica instumescível formada por ligações covalentes ou iônicas através de um agente reticulante. Devido a insolubilidade destes polímeros em água, seu tempo de residência baseia-se no tempo de renovação do muco. Os polímeros insolúveis em água incluem policarbofil, etilcelulose, propilcelulose e quitosana (solúvel em soluções aquosas ácidas) (LEE; PARK; ROBINSON, 2000; CHOWDARY; RAO, 2004; SALAMAT-MILLER; CHITTCHANG; JOHNSTON, 2005).
- ***Quanto à carga iônica, em polímeros catiônicos, aniônicos ou não-iônicos.*** As propriedades adesivas dos polímeros aniônicos é atribuída, principalmente, aos grupos de ácidos carbônicos e, em menor extensão, aos grupamentos sulfatos e sulfonatos. Os grupamentos carboxílicos são capazes de formar ligações de hidrogênio com os grupos hidroxilas presentes nas cadeias de oligossacarídeos das mucinas. Além disso, alguns polímeros aniônicos como o carbopol exibem ótimas propriedades de gelificação através de alterações de pH. Esta característica constitui uma excelente estratégia para preparação de formulações de gelificação *in situ* usada na liberação ocular de fármacos, pois permite a aplicação ocular facilitada da forma farmacêutica sob a forma líquida cuja retenção será aumentada pela formação do gel sobre a superfície mucosa (HOMBACH; BERNKOP-SCHNURCH, 2010; KHUTORYANSKIY, 2011). Além do carbopol, polímeros aniônicos incluem carboximetilcelulose, pectina, ácido poliacrílico, propilcelulose,

alginato de sódio, carboximetilcelulose sódica e goma xantana (SALAMAT-MILLER; CHITTCHANG; JOHNSTON, 2005). Os polímeros catiônicos, por sua vez, interagem com a superfície mucosa carregada negativamente. A mucoadesão ocorre devido às interações eletrostáticas entre os grupos amino destes polímeros e os grupos siálicos da mucina presente na camada mucosa. A quitosana é o principal polímero representante desta classe e suas propriedades físico-químicas estão descritas na seção 2.4.1 (CARVALHO et al., 2010; HOMBACH; BERNKOP-SCHNURCH, 2010). Outros exemplos de polímeros catiônicos são aminodextrano, dimetilaminoetildextrano e quitosana trimetilada (SALAMAT-MILLER; CHITTCHANG; JOHNSTON, 2005). Polímeros não-iônicos, contudo, exibem menor capacidade mucoadesiva quando comparados aos polieletrólitos, formando interações fracas com a mucina. A mucoadesão de formulações preparadas com polímeros não-iônicos ocorre, principalmente, pela difusão e interpenetração das cadeias poliméricas com o muco (KHUTORYANSKIY, 2011). Entre os exemplos de polímeros não-iônicos estão hidroxipropilcelulose, polioxietileno, álcool polivinil, polivinilpirrolidona e hidroxietilamido (SALAMAT-MILLER; CHITTCHANG; JOHNSTON, 2005).

A principal desvantagem da utilização dos polímeros mucoadesivos tradicionais (primeira geração) é a falta de especificidade, ou seja, a adesão pode ocorrer em qualquer superfície mucosa. A adesão não-específica dos polímeros pode limitar o direcionamento da forma farmacêutica, principalmente, no caso de sistemas que visam a mucoadesão no trato gastrointestinal. Assim, o desenvolvimento de polímeros de nova geração (segunda geração) ligados à moléculas específicas pode aumentar os benefícios terapêuticos dos sistemas mucoadesivos e permitir a liberação sítio-específica do fármaco, além de serem menos susceptíveis à renovação do muco (CHOWDARY; RAO, 2004; ANDREWS; LAVERTY; JONES, 2009). Entre os principais representantes de segunda geração estão as lectinas e os polímeros tiolados.

Lectinas: são proteínas ou glicoproteínas capazes de reconhecer e se ligar reversivelmente a moléculas específicas de carboidratos. A afinidade específica a estas moléculas é responsável pela capacidade citoadesiva da lectina, a qual vêm sendo amplamente pesquisada na área de desenvolvimento de sistemas de liberação vetorizada. A utilização das lectinas em sistemas de liberação de fármacos pode não só permitir

a ligação à uma célula ou tecido específicos, como também aumentar a absorção do fármaco através do processo de endocitose. Apesar das inúmeras vantagens, muitas lecitinas podem ser tóxicas ou imunogênicas (ANDREWS; LAVERTY; JONES, 2009; ROY et al., 2009).

Polímeros tiolados: também designados como tiômeros, são capazes de interagir com os subdomínios ricos em cisteína da glicoproteína mucina através de ligações dissulfídicas devido a presença de grupos tióis em sua molécula. Assim, a imobilização de grupos tióis em polímeros mucoadesivos pode aumentar significativamente suas propriedades adesivas e coesivas quando comparadas ao polímero não modificado, aumentando, consequentemente, o tempo de residência da forma farmacêutica e a biodisponibilidade do fármaco. Alguns exemplos de polímers tiolados são quitosana-iminotiolano, ácido poliacrílico-cisteína, ácido poliacrílico-homocisteína, quitosana-ácido tioglicólico, quitosana-tioetilamidina, alginato-cisteína, ácido polimetacrílico-cisteína e carboximetilcelulose sódica-cisteína (BERNKOP-SCHNURCH, 2005; ANDREWS; LAVERTY; JONES, 2009).

2.4.1 Quitosana

Os polissacarídeos são polímeros naturais de monossacarídeos que possuem grande potencial para aplicações biomédicas. Os polissacarídeos são altamente estáveis, atóxicos, hidrofílicos, biocompatíveis e biodegradáveis, além de poderem ser obtidos a partir de diversas fontes naturais a um baixo custo. Muitos destes polissacarídeos, ainda, apresentam variadas propriedades farmacológicas tais como antiviral, antibacteriana e antitumoral, tornando seu uso como biomaterial bastante interessante. Estes polímeros apresentam um grande número de grupos reativos, ampla faixa de massa molar e variada composição química. Ainda, a maioria dos polissacarídeos possui grupos hidrofílicos tais como hidroxilas, carboxilas e amino, que podem formar ligações não-covalentes com os tecidos biológicos, principalmente, epitélio e membranas mucosas, promovendo a bioadesão (LIU et al., 2008).

Nos últimos 20 anos, um grande número de trabalhos têm sido realizados envolvendo a quitosana e sua potencial utilização no desenvolvimento de sistemas de liberação de fármacos. A quitosana é um polissacarídeo de caráter catiônico devido à presença de aminas primárias em sua molécula. É constituída de monômeros de glucosamina (β-(1-4)-2-amino-2-deoxi-D-glicose) e N-

acetilglucosamina (2-acetoamido-2-deoxi-D-glucose) unidos através de ligações glicosídicas β-(1-4) (Figura 4). A quitosana é obtida pela desacetilação da quitina, segundo polissacarídeo mais abundante na natureza após a celulose, encontrada no exoesqueleto de crustáceos, insetos e alguns fungos. Os polímeros de quitosana estão disponíveis em diferentes faixas de massa molar (50 kDa – 2000 kDa) e grau de desacetilação (40 % – 98 %), os quais variam de acordo com os tipos e condições de polimerização e desacetilação (ILIUM, 1998; RAY, 2011).

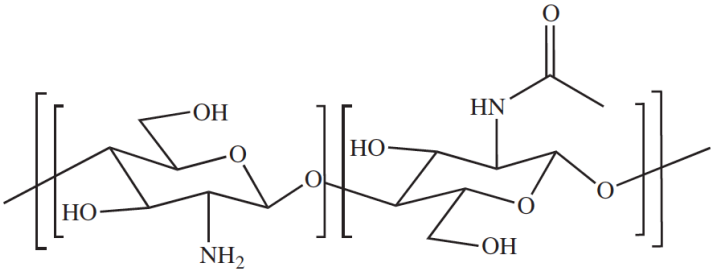

Figura 4. Estrutura da unidade monomérica da quitosana. Fonte: Croisier; Jérôme (2013).

A quitosana é solúvel em soluções de ácidos fracos diluídos, sendo o ácido acético o solvente mais empregado para sua solubilização. Porém, sua solubilidade é altamente depende do seu grau de desacetilação e pH, sendo também influenciada pela adição de sal. Por ser considerada uma base fraca com pKa em torno de 6,2 à 7,0, a quitosana é insolúvel em valores de pH neutro e alcalino. Em meio ácido, os grupos amino de sua molécula são protonados resultando na solubilização do polímero (HEJAZI; AMIJI, 2003).

A quitosana é utilizada para uma grande variedade de aplicações na área da agricultura, indústria e medicina, devido suas inúmeras propriedades. Entre as características físico-químicas e biológicas deste polissacarídeo estão a habilidade formadora de filmes, amplamente empregada no desenvolvimento de cosméticos, propriedades antimicrobianas e de cicatrização de feridas, a habilidade de se ligar a lipídios e ácidos graxos e a habilidade de aumentar a penetração de moléculas através das membranas mucosas . A natureza catiônica é a principal responsável pelas propriedades associadas à quitosana, tais como controle da liberação de fármacos, mucoadesão, gelificação *in situ*, transfecção, aumento da permeabilidade das membranas e

propriedades inibidoras da bomba de efluxo. Além disso, a quitosana apresenta boa biocompatibilidade, biodegradabilidade e propriedades toxicológicas (ANDREWS; LAVERTY; JONES, 2009; KHUTORYANSKIY, 2011; BERNKOP-SCHNURCH; DUNNHAUPT, 2012).

Entre os polímeros mucoadesivos, a quitosana têm sido amplamente investigada devido sua capacidade de interagir com as superfície mucosas e aumentar a absorção do fármaco através da abertura das junções celulares (ANDREWS; LAVERTY; JONES, 2009). A excelente mucoadesão ocorre através de interações eletrostáticas entre os grupos amina protonados da quitosana e os grupos carregados negativamente, tais como carboxilatos e sulfonatos, presentes nas cadeias laterais da mucina. Interações hidrofóbicas também podem contribuir com este processo (DEACON et al., 2000; SVENSSON; THURESSON; ARNEBRANT, 2008). Além disso, a linearidade das moléculas de quitosana fornece adequada flexibilidade às cadeias poliméricas para interpenetração na camada mucosa (ANDREWS; LAVERTY; JONES, 2009). O efeito promotor de permeação da quitosana também está relacionado às cargas positivas do polímero, as quais parecem interagir com a membrana celular resultando na reorganização estrutural das proteínas associadas às junções celulares (BERNKOP-SCHNURCH; DUNNHAUPT, 2012). As propriedades mucoadesivas da quitosana têm sido utilizadas no desenvolvimento de formas farmacêuticas destinadas, principalmente, à aplicação bucal, oral, ocular e nasal (KHUTORYANSKIY, 2011).

3 SISTEMAS MUCOADESIVOS PARA LIBERAÇÃO DE FÁRMACOS

Nas últimas décadas, os sistemas mucoadesivos têm sido alvo de grande interesse na área de liberação de fármacos pois além de possibilitar a administração de medicamentos por vias alternativas, também permitem otimizar tanto sua liberação local quanto sistêmica. A liberação localizada ou sítio-específica do fármaco pode ser alcançada devido a retenção da forma farmacêutica mucoadesiva na camada mucosa, o que permite a liberação do fármaco próxima ao local de ação e, consequentemente, o aumento da sua biodisponibilidade. A liberação sistêmica, por sua vez, é facilitada devido ao contato intenso e prolongado da formulação com a superfície absorvente, o que possibilita maior absorção do fármaco (SMART, 2005a; ANDREWS; LAVERTY; JONES, 2009).

Entre as vantagens relacionadas ao uso dos sistemas mucoadesivos para a liberação de fármacos em relação aos sistemas convencionais, pode-se citar:

- íntimo contato da formulação com as superfícies biológicas absorventes;
- tempo de residência prolongado da forma farmacêutica no sítio de aplicação, o que permite reduzir a frequência de administração de doses;
- direcionamento do fármaco a regiões ou tecidos específicos, através da utilização de moléculas bioadesivas específicas;
- evita o metabolismo associado ao efeito de primeira passagem e inativação do fármaco por enzimas presentes no trato gastrointestinal, quando administrado em rotas não orais;
- biodisponibilidade do fármaco aumentada;
- possibilidade de modificar a permeabilidade do tecido para melhor absorção de macromoléculas, tais como peptídeos e proteínas, pela adição de promotores de penetração;
- redução de custos e diminuição dos feitos colaterais indesejáveis devido a localização do fármaco no sítio de ação (CHOWDARY; RAO, 2004; ANDREWS; LAVERTY; JONES, 2009).

As formas farmacêuticas mucoadesivas podem ser formuladas sob a forma de comprimidos, cápsulas, filmes, patches, pastilhas, micro- e nanopartículas, sprays, géis, pomadas, sistemas gelificantes *in situ*, sistemas de inserções sólidas, pós e soluções, dependendo da via de administração (LEE; PARK; ROBINSON, 2000; KHUTORYANSKIY, 2011).

3.1 Nanopartículas mucoadesivas

As nanopartículas são sistemas coloidais que apresentam diâmetro inferior a 1000 nm, nas quais o fármaco pode estar encapsulado, adsorvido ou disperso. As nanopartículas são geralmente preparadas a partir de polímeros biodegradáveis, entre os quais os mais empregados incluem o poli ácido-lático, poli ácido-lático-co-glicólico, policaprolactona, poli alquil cianoacrilatos, quitosana, gelatina, entre outros (KUMARI; YADAV; YADAV, 2010). Dependendo do método e dos componentes empregados para preparação das nanopartículas, nanocápsulas ou nanoesferas podem ser obtidas (Figura 5). As nanocápsulas são sistemas nas quais o fármaco encontra-se confinado

em uma cavidade oleosa circundada por um invólucro polimérico. Por outro lado, as nanoesferas são sistemas matriciais no qual o fármaco encontra-se disperso (SCHAFFAZICK et al., 2003; MOHANRAJ; CHEN, 2006).

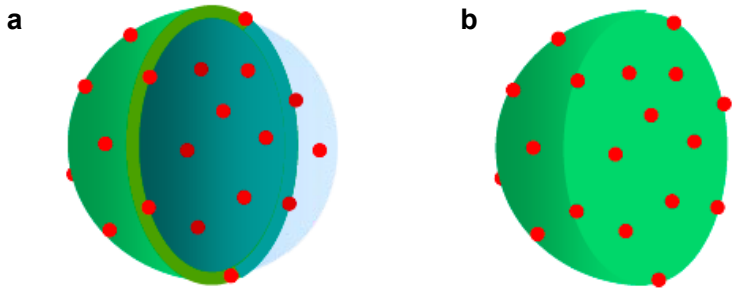

Figura 5. Representação esquemática do corte transversal de nanocápsulas (a) e nanoesferas (b). Fonte: Rossi-Bergmann (2008).

As principais vantagens da utilização de nanopartículas como sistemas de liberação de fármacos incluem o aumento da solubilidade e biodisponibilidade de fármacos pouco solúveis em água, a proteção de substâncias ativas contra a degradação em meio fisiológico, a possibilidade de vetorização do fármaco a órgãos, tecidos ou células, a possibilidade de modulação das propriedades de superfície e/ou adição de ligantes que resultam em interações específicas com certos componentes do meio fisiológico, a redução dos efeitos colaterais indesejáveis e toxicidade, além de permitir a administração por diferentes vias, incluindo as vias oral, nasal, parenteral, ocular, entre outras (MOHANRAJ; CHEN, 2006; KUMARI; YADAV; YADAV, 2010).

A possibilidade de combinar as vantagens associadas ao uso dos nanocarreadores às propriedades mucoadesivas têm sido considerada uma interessante estratégia para otimizar a administração de fármacos nas diferentes camadas mucosas. As nanopartículas mucoadesivas apresentam vantagens adicionais, pois além de encapsular e liberar o fármaco na superfície, apresentam maior contato com a mucosa, devido ao reduzido tamanho de partícula e grande área superficial do carreador, resultando numa maior absorção e biodisponibilidade do fármaco encapsulado (CHOWDARY; RAO, 2004; PATIL; SAWANT, 2008). Estes sistemas são, geralmente, administrados na forma de suspensão

aquosa, mas podem também ser aplicados através de aerossol ou incorporados a formas farmacêuticas semi-sólidas.

Recentemente, Suwannateep e colaboradores (2011) demonstraram as propriedades mucoadesivas de nanoesferas de metilcelulose e/ou etilcelulose contendo curcumina. As nanoesferas apresentaram excelente mucoadesão à mucosa gástrica após administração oral das suspensões coloidais em camundongos. As propriedades mucoadesivas foram, principalmente, atribuídas as ligações de hidrogênio formadas entre os grupamentos hidroxilas presentes na superfície das partículas e a mucina. Uma vez ligadas à mucosa gástrica, as moléculas de curcumina difundiram-se através do epitélio e foram lentamente liberadas para a circulação, onde permaneceram por até 3 horas. Além disso, a degradação da curcumina nas condições extremamente ácidas do estômago foi evitada, resultando no aumento da sua biodisponibilidade.

3.1.1 Nanopartículas decoradas com polissacarídeos

Nanopartículas decoradas com polissacarídeos podem ser preparadas por adsorção, incorporação durante a preparação, copolimerização ou utilizando copolímeros pré-formados. A adsorção simples baseia-se no revestimento de nanopartículas previamente preparadas, e pode ser governada por interações eletrostáticas, hidrofóbicas, entre outras (LEMARCHAND; GREF; COUVREUR, 2004). A decoração de nanopartículas com a quitosana é, geralmente, alcançada pela sua incorporação durante a preparação. Nanocápsulas de policaprolactona decoradas com quitosana têm sido preparadas dissolvendo o polissacarídeo na fase aquosa externa usada durante a técnica de nanoprecipitação (CALVO; VILA-JATO; ALONSO, 1997). A copolimerização pode ser realizada pelos métodos de polimerização em emulsão ou via radical. A polimerização do poli(isobutilcianoacrilato), por exemplo, pode ser iniciada pelos grupos hidroxilas presentes na molécula do dextrano, fazendo com que este polissacarídeo se ligue covalentemente ao polímero durante a formação das nanopartículas (CHAUVIERRE et al., 2004). Por fim, o revestimento de nanopartículas com polissacarídeos pode ser conseguido usando polímeros pré-formados, como, por exemplo, o copolímero dextrano-policaprolactona, composto por uma cadeia principal de polissacarídeo na qual várias cadeias secundárias de poliéster estão inseridas (GREF; RODRIGUES; COUVREUR, 2002).

As principais aplicações destes sistemas na área médica estão ilustradas na Figura 6. O revestimento da superfície das partículas com polissacarídeos promove a proteção estérica das partículas contra a adsorção de proteínas e captura por células fagocitárias. Os polissacarídeos ainda possibilitam a vetorização ativa das nanopartículas a órgãos e tecidos específicos através da adição de ligantes aos inúmeros grupos reativos disponíveis em sua molécula. As propriedades de reconhecimento molecular permite que as nanopartículas decoradas se liguem a receptores específicos presentes nas células alvo. Nanopartículas decoradas com dextrano, por exemplo, têm demonstrado prolongado tempo de residência da circulação plasmática e acúmulo em tecidos específicos, como tumores do cérebro e linfonodos, através do efeito de permeabilidade e retenção aumentadas (*EPR effect*) apresentado pelos tecidos tumorais (LEMARCHAND; GREF; COUVREUR, 2004; LEMARCHAND et al., 2006). Nanopartículas decoradas com quitosana, por sua vez, têm se mostrado eficientes carreadores para a liberação de fármacos, desde que demonstraram ser estáveis em condições fisiológicas e capazes de aumentar significativamente a penetração do fármaco encapsulado (CALVO; VILA-JATO; ALONSO, 1997; CUI; QIAN; YIN, 2006). Estes sistemas também apresentaram adequados perfis de liberação de fármaco e maior seletividade para as células de câncer de bexiga, em relação às células normais (BILENSOY et al., 2009).

Figura 6. Representação esquemática de nanopartículas decorada com polissacarídeos de diferentes conformações e suas principais aplicações na medicina. Fonte: adaptado de Lemarchand; Gref; Couvreur (2004).

Nanopartículas decoradas com polissacarídeos também apresentam interessantes propriedades bioadesivas, o que faz destes sistemas uma alternativa promissora para prolongar o tempo de residência e, assim, aumentar a absorção do fármaco encapsulado (LIU et al., 2008). O revestimento de nanopartículas com o polissacarídeo quitosana parece ser bastante interessante, uma vez que este polissacarídeo têm demonstrado excelentes propriedades mucoadesivas, mostrando-se capaz de aumentar o contato do fármaco com a mucosa. Superfícies mucosas como nasal, pulmonar e peroral são consideradas bons alvos para o reconhecimento pelos polissacarídeos (LEMARCHAND; GREF; COUVREUR, 2004).

3.2 Filmes mucoadesivos

Os filmes mucoadesivos constituem uma das formas farmacêuticas mais recentes para a administração bucal de fármacos. Os filmes oferecem algumas vantagens quando comparados a outras formas farmacêuticas mucoadesivas destinadas a aplicação bucal, como:

- menor desconforto, devido a menor espessura e maior flexibilidade em relação aos comprimidos bucais, e por isso possuem maior aceitação e adesão pelos pacientes;
- maior tempo de residência, quando comparados aos géis orais, que são facilmente lavados e removidos pela saliva;
- administração de uma dose conhecida de fármaco, o que não é possível com a aplicação de cremes, géis e pomadas;
- no caso de liberação local para doenças bucais, os filmes também ajudam a proteger a superfície lesionada, reduzindo a dor e tornando o tratamento mais efetivo (ROSSI; SANDRI; CARAMELLA, 2005; SALAMAT-MILLER; CHITTCHANG; JOHNSTON, 2005; SMART, 2005b; SUDHAKAR; KUOTSU; BANDYOPADHYAY, 2006).

Um filme ideal deve ser flexível, elástico, macio, e suficientemente forte para evitar rupturas decorrentes dos movimentos bucais. O filme também deve apresentar boa força mucoadesiva, permitindo sua retenção na mucosa bucal pelo período de tempo desejado, e não deve sofrer intumescimento excessivo, afim de prevenir o desconforto do paciente ou a perda das propriedades mucoadesivas (SALAMAT-MILLER; CHITTCHANG; JOHNSTON, 2005). Estes sistemas podem ser projetados de forma a proporcionar a liberação uni- ou bidirecional do fármaco, dependendo do desenho da forma farmacêutica. Relatos indicaram que filmes bucais podem permanecer até 15 horas no local de aplicação, garantindo a liberação constante do fármaco (LEE; PARK; ROBINSON, 2000).

Os filmes são geralmente preparados pela técnica de evaporação do solvente (*casting*). A ampla utilização desta técnica está relacionada a facilidade do processo e ao baixo custo atribuído à escala laboratorial. A preparação dos filmes pela técnica de evaporação do solvente envolve basicamente os seguintes passos: (i) preparação da solução, normalmente constituída de polímero, fármaco e excipientes (por exemplo, plastificantes) dissolvidos em um solvente ou em uma mistura de solventes; (ii) desareação da solução para remoção das bolhas de ar formadas durante o processo; (iii) transferência da solução para o

molde; (iv) secagem da solução até completa evaporação do solvente e formação do filme; e (v) corte do filme para obtenção de filmes de tamanhos adequados contendo a quantidade desejada de fármaco (MORALES; MCCONVILLE, 2011). Os filmes podem apresentar tamanhos variados, contudo tamanhos entre 1 a 3 cm^2 são preferíveis para aplicação confortável na mucosa bucal (SMART, 2005b).

Diversos trabalhos sobre a utilização de filmes mucoadesivos para administração bucal têm sido descritos na literatura. Perugini et al. (2003) prepararam filmes micromatricias constituídos de PLGA e quitosana visando a liberação da ipriflavona, um fármaco hidrofóbico utilizado visando o tratamento local da periodontite. Experimentos *in vitro* demonstraram que a liberação do fármaco a partir dos filmes micromatriciais compostos ocorreu por até 20 dias. Filmes bucais preparados a partir de polissacarídeos naturais e semissintéticos foram estudados por Juliano et al. (2008), visando a liberação da clorexidina para o tratamento da candidíase oral. Recentemente, discos mucoadesivos constituídos de nanopartículas preparadas a partir do copolímero do metilvinileter e anidrido maleico foram propostos como sistemas de liberação bucal para o cloridrato de fluoxetina. A formulação otimizada foi capaz de manter a liberação do fármaco numa velocidade constante, produzindo melhor resposta antidepressiva que a forma líquida oral, evitando efeito de primeira passagem e aumentando a biodisponibilidade do fármaco (SAPRE; PARIKH; GOHEL, 2009).

4 CURCUMINA

A curcumina é o princípio ativo extraído do rizoma da *Curcuma longa* Linn (Figura 7), uma planta amplamente distribuída em regiões tropicais e subtropicais do mundo e, principalmente, cultivada na Índia e na China. Popularmente conhecida como açafrão, esta planta é normalmente utilizada na alimentação como tempero, corante e flavorizante. O uso medicinal desta planta têm sido documentado na medicina Ayurveda (medicina Indiana) há mais de 6000 anos (ARAUJO; LEON, 2001; AGGARWAL; KUMAR; BHARTI, 2003). A curcumina apresenta diversas atividades farmacológicas incluindo antiinflamatória, antitumoral, antioxidante e antimicrobiana, além de seu uso estar relacionado a outros efeitos benéficos à saúde. Alguns dos efeitos farmacológicos descritos para a curcumina encontram-se listados na Tabela 1.

Figura 7. *Curcuma longa* Linn.

Tabela 1. Atividades farmacológicas da curcumina.

Atividade	Referências
Antiartrítica	(FUNK et al., 2006)
Antiaterogênica	(MIQUEL et al., 2002; OLSZANECKI et al., 2005)
Antimetastática	(MENON; KUTTAN; KUTTAN, 1999; OHASHI et al., 2003; HERMAN; STADELMAN; ROSELLI, 2009)
Antimicrobiana	(NEGI et al., 1999; DE et al., 2009)
Antiinflamatória	(HUANG et al., 1991; JIANG et al., 2006; JURENKA, 2009)
Antioxidante	(UNNIKRISHNAN; RAO, 1992; REDDY; LOKESH, 1994; JAYAPRAKASHA; JAGANMOHAN RAO; SAKARIAH, 2006)
Antiprotozoária	(ARAÚJO et al., 1999; CUI; MIAO, 2007)
Antitumoral	(HUANG et al., 1997; OZAKI et al., 2000; 2003; SINGH; KHAR, 2006)
Antiviral	(MAZUMDER et al., 1995; BOURNE et al., 1999)
Cardioprotetora	(NIRMALA; PUVANAKRISHNAN, 1996; MANIKANDAN et al., 2004; ANSARI; BHANDARI; PILLAI, 2007; LI et al., 2008)
Desordens respiratórias	(VENKATESAN, 2000; PUNITHAVATHI; VENKATESAN; BABU, 2003; VENKATESAN; PUNITHAVATHI; BABU, 2007)
Hepatoprotetora	(REYES-GORDILLO et al., 2007; PRIYA; SUDHAKARAN, 2008; GIRISH et al., 2009; EL-AGAMY, 2010)
Hipoglicêmica	(ARUN; NALINI, 2002; WEISBERG; LEIBEL; TORTORIELLO, 2008; KANG; KIM, 2010)
Neuroprotetora	(COLE; TETER; FRAUTSCHY, 2007; QIN; CHENG; YU, 2010)

Pesquisas clínicas e laboratoriais têm demonstrado o potencial terapêutico da curcumina na prevenção e tratamento do câncer e outras doenças crônicas. A curcumina apresenta efeitos antiproliferativos e pró-apoptóticos contra diversos tipo de tumor, incluindo tumores de cólon, duodeno, esôfago, estômago, fígado, mama, leucemia, cavidade oral e próstata (GOEL; KUNNUMAKKARA; AGGARWAL, 2008). A curcumina contribui com a inibição da formação, promoção e

progressão do tumor, sendo descrita como um bom agente antiangiogênico (DUVOIX et al., 2005).

Apesar da potencial utilização da curcumina na terapia do câncer e outras doenças, sua aplicação clínica tem sido limitada devido sua baixa solubilidade aquosa, a qual resulta numa baixa absorção pelo trato gastrointestinal após administração oral e impede a preparação de soluções aquosas para administração intravenosa. Além disso, a curcumina é instável em pH neutro e básico e bastante suscetível à degradação fotoquímica (TONNESEN, 2002; TONNESEN; MASSON; LOFTSSON, 2002; TOMREN et al., 2007). O rápido metabolismo e eliminação sistêmica da curcumina são outros fatores que contribuem aos baixos níveis séricos e teciduais deste composto e, consequentemente, a sua baixa biodisponibilidade (ANAND et al., 2007).

4.1 Características químicas e físico-químicas

As propriedades terapêuticas da *Curcuma longa* têm sido atribuídas aos constituintes ativos obtidos do rizoma da planta, denominados curcuminóides. Os principais curcuminóides presentes no açafrão são a curcumina, a demetoxicurcumina e a bisdemetoxicurcumina (Figura 8) (JURENKA, 2009), além da ciclocurcumina posteriormente identificada (KIUCHI et al., 1993). A curcumina, 1,7-bis(4-hidroxi-3-metoxifenil)-1,6-heptadieno-3,5-diona, é o principal constituinte da planta, perfazendo de 4 a 8 % de seu extrato seco (BANERJI et al., 2004). A curcumina (diferuloilmetano) é um polifenol de baixa massa molar, 368,37 g/mol, e ponto de fusão de 183 °C. É praticamente insolúvel em água, mas solúvel em etanol, acetona, dimetilsulfóxido e outros solventes orgânicos (SHARMA; GESCHER; STEWARD, 2005).

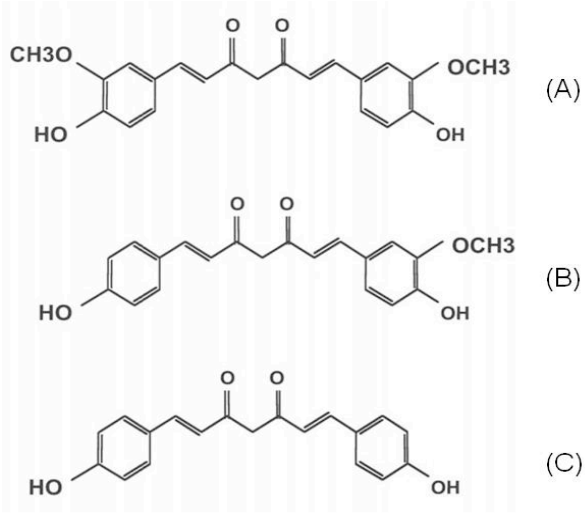

Figura 8. Estrutura química dos curcuminóides: curcumina (A), demetoxicurcumina (B) e bisdemetoxicurcumina (C).

A curcumina é estável em pH ácido, mas é instável e sofre rápida degradação hidrolítica em condições neutras ou alcalinas. A estabilidade da curcumina tem sido investigada por vários autores (WANG et al., 1997; TONNESEN, 2002; TONNESEN; MASSON; LOFTSSON, 2002; PFEIFFER et al., 2003; ANSARI et al., 2005; TOMREN et al., 2007; ZEBIB; MOULOUNGUI; NOIROT, 2010). Estudos *in vitro* têm demonstrado que mais de 90 % da curcumina é rapidamente degradada em condições fisiológicas (tampão fosfato, pH 7,2 a 37 °C). A curcumina mostrou-se mais estável em meio de cultura celular contendo 10 % de soro fetal de bezerro e em sangue humano. O trans-6-(4'-hidroxi-3'-metoxifenil)-2,4-dioxo-5-hexenal foi o principal produto de degradação, mas vanilina, ácido ferúlico e feruoilmetano também foram identificados (WANG et al., 1997). A maior estabilidade da curcumina em pH ácido está relacionada a manutenção da estrutura dieno conjugada da molécula. Quando o pH é ajustado para valores neutros ou básicos, o próton do grupo fenólico é removido levando a destruição de sua estrutura. A suscetibilidade à degradação fotoquímica é outra limitação importante demonstrada pela curcumina (TONNESEN, 2002; ZEBIB; MOULOUNGUI; NOIROT, 2010).

4.2 Associação a carreadores coloidais

Diversas estratégias têm sido propostas para aumentar a biodisponibilidade e eficácia terapêutica da curcumina. Uma forma promissora para contornar os problemas de degradação, a baixa solubilidade em água e reduzida biodisponibilidade é a associação da curcumina a carreadores coloidais, tais como, nanopartículas, lipossomas, ciclodextrinas, micelas e complexos fosfolipídicos. Estes sistemas parecem prolongar o tempo de circulação, aumentar a estabilidade nos fluidos biológicos e durante o armazenamento, e proteger a molécula dos processos metabólicos, além de permitir a preparação de sistemas aquosos facilmente dispersíveis nos fluídos biológicos, prevenindo a agregação de fármacos pouco solúveis em água após administração intravenosa (FONSECA; SIMOES; GASPAR, 2002; TORCHILIN, 2007). Um resumo dos diferentes sistemas de liberação estudados e dos benefícios produzidos encontra-se apresentado na Tabela 2.

Tabela 2. Resumo dos efeitos benéficos alcançados pelo uso de sistemas de liberação de curcumina.

Sistema de liberação	**Efeitos benéficos relatados**	**Referências**
Micelas	Aumento da solubilidade aquosa, manutenção da atividade citotóxica, possibilidade de administração intravenosa, boa estabilidade em condições fisiológicas, proteção do ativo contra degradação hidrolítica, boa estabilidade durante longo período de armazenamento, liberação controlada da curcumina em até alguns dias, prolongamento do tempo de meia-vida, tempo de residência aumentado e depuração plasmática diminuída.	(IWUNZE, 2004; MA et al., 2007; LETCHFORD; LIGGINS; BURT, 2008; MA et al., 2008; SAHU et al., 2008; SAHU; KASOJU; BORA, 2008; LAPENNA et al., 2009; SOU et al., 2009; MOHANTY et al., 2010; SAHU et al., 2010; SONG et al., 2010)
Complexos fosfolipídicos	Maiores concentrações séricas, manutenção da concentração	(LIU et al., 2006; MAITI et al., 2007; MARCZYLO et al.,

	efetiva por um maior período de tempo, propriedades antioxidantes superiores, aumento da biodisponibilidade da curcumina *in vivo*, maiores valores de picos plasmáticos e área sob a curva após administração oral, eficácia clínica na manutenção e tratamento da osteoartrite, estabilidade aumentada e melhor absorção da curcumina.	2007; BELCARO et al., 2010)
Ciclodextrinas	Aumento da solubilidade aquosa, melhor estabilidade frente à hidrólise alcalina, potencial atividade angioinibitória, liberação otimizada e maior eficácia terapêutica em células de câncer de próstata quando comparada à curcumina livre.	(TONNESEN; MASSON; LOFTSSON, 2002; HAN et al., 2004; TOMREN et al., 2007; HEGGE et al., 2008; YADAV et al., 2009; YALLAPU; JAGGI; CHAUHAN, 2010)
Lipossomas	Preparação de sistemas aquosos que possibilitam a administração intravenosa, igual ou melhor atividades antiproliferativa e antiangiogênica em células tumorais *in vitro* e *in vivo* comparadas à curcumina livre, aumento da biodisponibilidade e eficácia, maior estabilidade em tampão fosfato que a curcumina livre, redução da dose, efeito inibitório sinérgico com oxaliplatina em linhagens de células tumorais, transporte efetivo para o interior da célula, aumento da absorção	(LI; BRAITEH; KURZROCK, 2005; KUNWAR et al., 2006; LI et al., 2007; HONG et al., 2008; THANGAPAZHAM et al., 2008; WANG et al., 2008a; CHEN et al., 2009; MACH et al., 2009; TAKAHASHI et al., 2009; GOSANGARI; WATKIN, 2010; GUPTA; DIXIT, 2010)

	gastrointestinal, maior atividade antioxidante após administração oral, maior efeitos anti-idade, antioxidante e anti-rugas *in vivo* após aplicação tópica.	
Nanopartículas	Fácil dispersão no meio aquoso, possibilidade de administração intravenosa, estabilidade aumentada, liberação local sustentada por longo período, aumento da hidratação, firmeza e elasticidade da pele de voluntários após aplicação tópica, ampla distribuição nos tecidos com alta concentração de macrófagos, melhor efeito *in vivo* na terapia de fibrose cística, maior atividade anti-malária *in vivo*, biodisponibilidade aumentada, eficácia terapêutica similar ou superior contra células tumorais, maior acúmulo nos tumores, possibilidade de liberação vetorizada da curcumina, habilidade de atravessar o endotélio vascular, maior estabilidade fotoquímica da curcumina, aumento da citotoxicidade em alvos da doença de Alzheimer, aumento da biodisponibilidade após administração oral, melhoria da quimio-/radio-sensibilização em células tumorais, possibilidade de redução da dose, aumento das atividades	(BISHT et al., 2007; NAM et al., 2007; TIYABOONCHAI; TUNGPRADIT; PLIANBANGCHANG, 2007; SOU et al., 2008; GUPTA et al., 2009; MUKERJEE; VISHWANATHA, 2009; SHAIKH et al., 2009; ANAND et al., 2010; CARTIERA et al., 2010; DANDEKAR et al., 2010; DUAN et al., 2010; GAO et al., 2010; KIM et al., 2010; MAZZARINO et al., 2010b; MOHANTY; SAHOO, 2010; MULIK et al., 2010b; a; ONOUE et al., 2010; YALLAPU et al., 2010a; YALLAPU et al., 2010b; YEN et al., 2010; ZHU et al., 2010)

	antioxidante e antihepatoma, maior tempo de meia-vida *in vivo* que a curcumina livre, captura celular aumentada, maior biodisponibilidade *in vivo* que a curcumina livre.	
Nano e microemulsões	Atividade antiinflamatória aumentada, liberação controlada, aumento da solubilidade aquosa, maior absorção oral quando comparada a curcumina em suspensão, otimização da liberação transdérmica, aumento da dissolução *in vitro* e biodisponibilidade *in vivo*, maior citotoxicidade em células resistentes e melhora da biodisponibilidade oral e da eficácia terapêutica através da co-administração com o paclitaxel.	(LEE et al., 2008; WANG et al., 2008b; CUI et al., 2009; GANTA; AMIJI, 2009; GANTA; DEVALAPALLY; AMIJI, 2010; LIU; CHANG; HUNG, 2011; WU et al., 2011)

CAPÍTULO 2: DESENVOLVIMENTO DE NANOPARTÍCULAS DE POLICAPROLACTONA DECORADAS COM QUITOSANA PARA A LIBERAÇÃO BUCAL DA CURCUMINA

Nas últimas décadas, sistemas de liberação de fármacos têm sido desenvolvidos com o intuito de controlar a liberação e vetorizar fármacos a locais específicos do corpo. O uso de carreadores, tais como nanopartículas, micropartículas e lipossomas, permite modular a liberação e as características de absorção do fármaco, constituindo uma importante ferramenta no desenvolvimento de medicamentos. Contudo, o curto tempo de residência no local de absorção é um fator limitante para o sucesso destes carreadores (CHOWDARY; RAO, 2004). Assim, o desenvolvimento de carreadores mucoadesivos parece ser bastante vantajoso, visto que estes sistemas podem ficar retidos na mucosa por longos períodos de tempo e ter um íntimo contato com as membranas absorventes.

As nanopartículas decoradas com polissacarídeos constituem uma estratégia potencial na área de liberação de fármacos devido às suas propriedades de reconhecimento molecular e boas propriedades mucoadesivas. Além disso, os polissacarídeos são materiais biocompatíveis, biodegradáveis e disponíveis a partir de diversas fontes naturais. Entre os polissacarídeos mucoadesivos, a quitosana representa uma opção bastante interessante para o revestimento das nanopartículas pela sua capacidade de interagir com as superfícies mucosas e aumentar a absorção de fármacos.

Neste contexto, o desenvolvimento de nanopartículas poliméricas decoradas com quitosana visando a liberação bucal da curcumina é relatada neste trabalho. O polímero selecionado para preparação das nanopartículas foi a policaprolactona (PCL), um polímero semi-cristalino hidrofóbico cuja estrutura encontra-se representada na Figura 9. O PCL é sintetizado, principalmente, pelo processo de polimerização por abertura do anel dos monômeros da ε-caprolactona (WEI et al., 2009). Estudos de biocompatibilidade e eficácia *in vitro* e *in vivo*, têm demonstrado a adequabilidade de uma série de biomateriais e dispositivos de liberação de fármacos de PCL. O PCL é degradado pela hidrólise de suas ligações ésteres em condições fisiológicas. Além disso, este polímero é bioreabsorvível e possui degradação bem mais lenta que os outros poliésteres, o que pode ser uma característica interessante para a preparação de implantes de longa duração e sistemas de liberação prolongada (KUMARI; YADAV; YADAV, 2010; RASEKH et al., 2011).

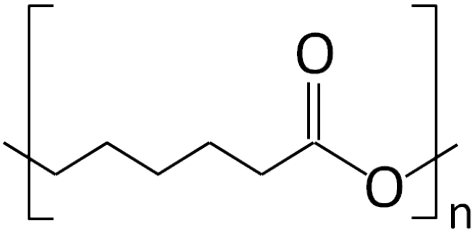

Figura 9. Estrutura da unidade monomérica da policaprolactona.

Na maioria das vezes a etapa crucial no desenvolvimento de novos sistemas mucoadesivos é a avaliação de sua habilidade em aderir ao muco. Com este intuito, diferentes métodos de caracterização têm sido descritos na literatura. Geralmente, as técnicas medem a força requerida para desligar o sistema mucoadesivo da superfície mucosa (métodos diretos) ou avaliam as interações entre os sistemas e a glicoproteína mucina (métodos indiretos) (DAVIDOVICH-PINHAS; BIANCO-PELED, 2010). Tratando-se de suspensões de nanopartículas, o estudo das interações entre a mucina e os sistemas coloidais parece ser a forma mais adequada para a caracterização de suas propriedades mucoadesivas. Neste sentido, as técnicas de microbalança de cristal de quartzo com monitoramento de dissipação (QCM-D) e ressonância plasmônica de superfície (SPR) são técnicas bastante interessantes, visto que permitem o monitoramento em tempo real das interações nanopartículas/mucina, sem a necessidade da utilização de marcadores. Além destas técnicas, estudos de espalhamento de luz dinâmico (DLS) também foram realizados para avaliar a formação dos agregados nanopartícula-mucina.

A liberação de fármacos na mucosa bucal tem sido alvo de várias pesquisas nas últimas décadas. Porém, para que o fármaco seja absorvido e destruído no organismo é essencial a sua permeação através das membranas biológicas. Modelos *in vitros* têm sido amplamente utilizados para predizer a permeação de fármacos durante o desenvolvimento de medicamentos. A metodologia *in vitro* mais empregada para avaliar a peremeabilidade de fármacos através da mucosa oral inclui o uso de células de difusão. As células de difusão possibilitam determinar a concentração total de fármaco que dinfunde através de uma membrana mucosa usada como barreira, bem como a taxa de difusão do fármaco. Normalmente, as células de difusão podem ser de dois tipos, verticais (células de Franz) ou horizontais (câmaras de Ussing) (PATEL; LIU; BROWN, 2012). As membranas usada como

barreira de difusão, pos sua vez, podem ser de origem humana, animal ou sintética. Uma membrana mucosa animal apropriada deve apresentar características de transporte e propriedades barreira que mimetizem a mucosa bucal humana. Normalmente, as mucosas suínas representam uma boa opção do ponto de vista histológico, devido a similaridade estrutural em relação à humana (HOOGSTRAATE; BODDÉ, 1993). Neste trabalho, estudos de permeação foram realizados usando células de difusão de Franz e mucosa esofágica suína como membrana.

Este capítulo descreve o desenvolvimento das nanopartículas de PCL contendo curcumina decoradas com quitosana. As nanopartículas de PCL estabilizadas pelo surfactante poloxamer foram preparadas pela técnica de nanoprecipitação. Os resultados obtidos com estes sistemas encontram-se divididos em três partes. A primeira parte descreve os resultados iniciais alcançados pela otimização das condições de preparação das nanopartículas de PCL, os quais foram publicados no *Journal of Colloid and Interface Science, v. 370, p. 58-66*, *2012*. As suspensões de nanopartículas foram preparadas e caracterizadas utilizando diferentes concentrações de surfactante, massas molares e concentrações de quitosana. Estudos de interação entre as nanopartículas decoradas com quitosana e a mucina também foram realizados pela técnica de DLS. A segunda parte do capítulo aborda a avaliação das propriedades mucoadesivas das nanopartículas de PCL decoradas com quitosana através da técnica de QCM-D, cujos resultados foram submetidos para publicação no *Journal of Biomedical Nanotechnology*. Nesta publicação, as interações entre as nanopartículas contendo curcumina, não-decoradas ou decoradas com quitosana de diferentes massas molares, e a camada de mucina formada sobre os cristais de quartzo foram monitoradas e comparadas. A terceira parte do capítulo inclui resultados obtidos na avaliação das propriedades mucoadesivas das nanopartículas através da técnica de SPR, estudos de permeação e retenção da curcumina através da mucosa, e estudos *in vitro* para avaliação da citotoxicidade e da atividade biológica destes sistemas, os quais serão submetidos para publicação no *European Journal of Pharmaceutics and Biopharmaceutics*. A validação do método analítico utilizado para a determinação da curcumina nos estudos de permeação e retenção na mucosa esofágica encontra-se descrita no Apêndice A.

Publicação: "*Elaboration of chitosan-coated nanoparticles loaded with curcumin for mucoadhesive applications"*
Journal of Colloid and Interface Science 370 (2012) 58-66

Elaboration of chitosan-coated nanoparticles loaded with curcumin for mucoadhesive applications

Letícia Mazzarino[a,b], Christophe Travelet[a], Sonia Ortega-Murillo[a], Issei Otsuka[a], Isabelle Pignot-Paintrand[a], Elenara Lemos-Senna[b] and Redouane Borsali[a,*]

[a] *Centre de Recherches sur les Macromolécules Végétales (CERMAV-CNRS), BP 53, F-38041 Grenoble Cedex 9, France - affiliated with Université Joseph Fourier and member of the Institut de Chimie Moléculaire de Grenoble; leticia.mazzarino@cermav.cnrs.fr; christophe.travelet@cermav.cnrs.fr; sonia.ortega@cermav.cnrs.fr; issei.otsuka@cermav.cnrs.fr; isabelle.paitrand@cermav.cnrs.fr; redouane.borsali@cermav.cnrs.fr*

[b] *Laboratório de Farmacotécnica, Departamento de Ciências Farmacêuticas, Centro de Ciências da Saúde, Universidade Federal de Santa Catarina, Campus Universitário Trindade, 88040-900, Florianópolis, SC, Brazil; lemos@ccs.ufsc.br*

* Corresponding author. Address: CERMAV-CNRS, BP 53, F-38041, Grenoble Cedex 9, France. Tel: +33 476037640; fax: +33 476547629. *E-mail address:* redouane.borsali@cermav.cnrs.fr

ABSTRACT

Polycaprolactone (PCL) nanoparticles decorated with a mucoadhesive polysaccharide chitosan (CS) containing curcumin were developed aiming the buccal delivery of this drug. These nanoparticles were prepared by the nanoprecipitation method using different molar masses and concentrations of chitosan and concentrations of triblock surfactant poloxamer (PEO-PPO-PEO), in order to optimize the preparation conditions. Chitosan-coated nanoparticles showed positive surface charge and a mean particle radius ranging between 114 and 125 nm, confirming the decoration of the nanoparticles with the mucoadhesive polymer, through hydrogen bonds between ether and amino groups from PEO and CS, respectively. Dynamic Light Scattering (DLS) studies at different scattering angles and concentrations have shown that the nanoparticles are monodisperse (polydispersity indices were lower than 0.3). The nanoparticle systems were also examined with Nanoparticle Tracking Analysis (NTA), and the results were in good agreement with those obtained by DLS. Colloidal systems showed mean drug content about 460 µg/mL and encapsulation efficiency higher than 99 %. Finally, when coated with chitosan, these nanoparticles show a great

ability to interact with mucin indicating also their suitability for mucoadhesive applications.

Keywords: Polysaccharide coating; Chitosan-coated nanoparticles; Mucoadhesive nanoparticles; Curcumin; Dynamic light scattering (DLS); Nanoparticle tracking analysis (NTA)

1. Introduction

Over the past decade, there has been a growing interest in the use of mucoadhesive polymers to prolong the contact time of drugs with biological membranes. The ability to maintain a delivery system at a specific site for an extended period of time can be useful for the treatment of numerous diseases either for obtaining local or systemic effects (LEE; PARK; ROBINSON, 2000). When compared to conventional dosage forms, these systems present distinct advantages, such as prolonged residence time of the dosage form at the site of application, intimate contact of the formulation with biological surface and localization in the specific site that can increase the absorption and bioavailability of the drugs (HUANG et al., 2000; CHOWDARY; RAO, 2004). Mucoadhesive formulations are considered as a potential strategy for administration of drugs due to controlled drug delivery for extended period of time and the design of pharmaceutical form that permits to control and manipulate the permeability of the mucosal surfaces (PATHAN et al., 2008).

In the last years, the use of nanoparticles coated with mucoadhesive polysaccharides has emerged as a promising strategy to prolong the residence time and to increase the absorption of drugs through the mucosa (LEMARCHAND; GREF; COUVREUR, 2004; LIU et al., 2008). Polysaccharides are important natural polymers with great potential for biomedical applications, safe, non-toxic, hydrophilic and biodegradable, besides they can be obtained from several sources in nature and low cost. In particular, chitosan is a cationic polysaccharide, derived from the deacetylation of chitin, the most abundant polysaccharide in the world, after cellulose. Among mucoadhesive polymers, chitosan has been extensively exploited due to its capacity to interact with the negatively charged mucosal surface and to enhance drug absorption by opening of the tight junctions between mucosal cells (ANDREWS; LAVERTY; JONES, 2009). Some studies have demonstrated the promising use of nanoparticles coated with this polysaccharide for drug delivery. In this way, chitosan coated-

nanoparticles have proven to be suitable to incorporate drugs and to be stable, under physiological conditions, to increase significantly the ocular penetration of the encapsulated drug. They also present favorable drug loading and release profiles as well as good selectivity to bladder cancer cells (CALVO; VILA-JATO; ALONSO, 1997; CUI; QIAN; YIN, 2006; BILENSOY et al., 2009).

Curcumin is an active principle of *Curcuma longa* Linn, commonly known as turmeric, that displays numerous pharmacological activities such as anti-oxidant, anti-inflammatory, anti-tumoral and anti-microbial (GOEL; KUNNUMAKKARA; AGGARWAL, 2008). However, its clinical application has been limited due to poor aqueous solubility, rapid hydrolysis at neutral and basic pH, and fast metabolism and systemic elimination, which together are responsible for the low bioavailability exhibited by this drug (TONNESEN, 2002; TONNESEN; MASSON; LOFTSSON, 2002; ANAND et al., 2007; TOMREN et al., 2007). Various strategies have been undertaken to overcome the limitations of the use of curcumin and to allow its therapeutic application, including the incorporation in delivery systems.

The main objective of this study is to develop and characterize mucoadhesive polysaccharide-decorated nanoparticles for the encapsulation of curcumin by the nanoprecipitation method. In order to optimize the preparation conditions, that can influence the physical characteristics of the particles, different concentrations and molar masses of chitosan and concentrations of the surfactant (poloxamer) were used.

2. Materials and methods

2.1. Materials

Curcumin and polycaprolactone (PCL, MW 60,000) were purchased from Sigma-Aldrich (St. Louis, MO, USA). Poloxamer 188 (Lutrol F68®) (PEO_{80}-PPO_{27}-PEO_{80}), a triblock copolymer with the structure of poly(ethylene oxide)-poly(propylene oxide)-poly(ethylene oxide), was kindly donated by BASF Chemical Company (Ludwigshafen, Germany). Three different molar mass chitosan: low (CSL 50,000 - 190,000), medium (CSM 190,000 - 310,000) and high molar mass (CSH 310,000 to > 375,000), were purchased from Sigma-Aldrich. The degree of deacetylation is between 75 - 85 % for CSL and CSM, and higher than 75 % for CSH, as specified. Mucin from bovine submaxillary gland (BSM, Type I-S) was purchased from Sigma-

Aldrich and used as received. BSM has a molar mass of about 1.6 MDa and a specified content of sialic acid in the range of 9 to 17 % (SVENSSON, 2008). Except for the acetonitrile of HPLC grade used in the analysis (Carlo Erba, Milan, Italy), all other used chemicals were analytical reagent grade.

2.2. Preparation of chitosan-coated polycaprolactone nanoparticles

Curcumin-loaded PCL nanoparticle suspensions (Cur-NP) were prepared using the nanoprecipitation - solvent displacement method, similar to that employed by Fessi et al. (1989). Briefly, 60 mg of PCL and 5 mg of curcumin were dissolved in 12 mL of acetone. This organic phase was poured into 24 mL of an aqueous phase containing 1 % acetic acid and 0.1, 0.25 or 0.5 % (w/v) poloxamer 188 under magnetic stirring; the pH value was adjusted to 5. The acetone was then eliminated by evaporation under reduced pressure and the colloidal suspension concentrated to the desired final volume (10 mL). The polymeric nanoparticle suspensions were filtered through 8 µm pore-sized filter paper.

The preparation of chitosan-coated PCL nanoparticles was carried out from previous dispersion with low, medium or high molar mass chitosan (CSL, CSM or CSH, respectively) in the aqueous phase. The chitosan concentration varied from 0.1 to 0.75 % (w/v) depending the final volume of colloidal suspensions. Unloaded nanoparticle suspensions were prepared and treated in the same manner as the curcumin-loaded nanoparticles.

2.3. Particle size and morphology analysis

The size distribution, mean particle size, polydispersity index and morphology of the nanoparticle suspensions were determined by Static and Dynamic Light Scattering (SLS/DLS) using an ALV 5000 (ALV-Langen, Germany) equipped with a red helium-neon laser at a wavelength of 632.8 nm operating at a power of 35 mW. After appropriate dilution in ultrapure Milli-Q®, samples were placed in cylindrical measurements cells and immersed in a toluene bath with temperature regulated at 25 °C. The scattered photons were detected by a very sensitive avalanche diode. In this study, the modulus of the scattering vector is denoted q and is equal to $(4\pi n/\lambda)\sin(\theta/2)$ where n represents the refractive index of pure water, θ is the scattering angle

and λ designates the light wavelength. Each experiment was performed during 300 s and the scattered light was measured at different angles ranging from 20 to 150° with a 2.5° stepwise increase. The scattering intensity was corrected taking into account the contributions of the solvent (water) and the toluene (standard) as well as the change of the scattering volume with the detection angle. The hydrodynamic radius (R_h) was determined using Stokes-Einstein equation, $R_h = \kappa_B T/6\pi\eta D$ where κ_B is Boltzmann constant (in J/K), T is the temperature (in K), D is the diffusion coefficient and η is the viscosity of the medium – pure water in this case (η = 0.89 cP at 25 °C). Unloaded and curcumin-loaded nanoparticles suspensions show no absorption at the wavelength used in light scattering experiments, *i.e.* 632.8 nm.

The morphology of the nanoparticle suspensions was also examined using a CM200 Philips transmission electron microscope (FEI Company, Hillsboro, USA). Drops of the dispersions diluted in ultrapure Milli-Q® water were deposited on carbon-coated copper grids and negatively stained with 2 % (w/v) uranyl acetate.

2.4. Zeta potential measurement

Zeta potential was determined by laser-doppler anemometry using a Zetasizer Nano Series (Malvern Instruments, Worcestershire, UK). Nanoparticle samples were diluted in ultrapure Milli-Q® water and placed in the electrophoretic cell where a potential of ± 150 mV was established. The ζ potential values were calculated as mean electrophoretic mobility values using Smoluchowski's equation.

2.5. Nanoparticle tracking analysis

Nanoparticle Tracking Analysis (NTA) experiments were performed using a digital microscope LM10 System (NanoSight, Salisbury, UK). Samples were diluted in Milli-Q® water and introduced into the chamber by a syringe. Video images of particles movement under Brownian motion were analyzed by the NTA analytical software version 2.1. The measurements were made at room temperature and each video clip was captured over 30 s.

2.6. Stability of the chitosan-coated nanoparticles with added salt

Chitosan-coated and uncoated nanoparticle suspensions were diluted with different concentrations of a NaCl solution previously prepared. The effects of salt addition on the particle size and zeta potential were monitoring using DLS and laser-doppler anemometry, respectively, as described in the sections 2.3 and 2.4.

2.7. Entrapment efficiency and curcumin content

Entrapment efficiency and drug content were estimated after determination of the curcumin concentration in the nanoparticle suspensions by fluorescence spectrophotometry, according to the method described by Mazzarino et al. (2010a). The entrapment efficiency (%) was estimated as being the difference between the total concentration of curcumin found in the nanoparticle suspensions after their complete dissolution in acetonitrile and the concentration of drug in the supernatant obtained by the suspension ultrafiltration/centrifugation procedure using Amicon Centrifugal Filter Devices with Ultracel-100 membrane (100 kDa, Millipore Corp., USA). Drug recovery (%) was estimated by comparing the total amount of drug found in the colloidal suspensions with the initial amount added to the formulations.

2.8. Interactions between chitosan-coated nanoparticles and mucin

Mucin from bovine submaxillary glands (BSM) was prepared in acetate buffer pH 6 at different concentrations: 100, 250 and 500 μg/mL. The effect of curcumin-loaded PCL nanoparticles decorated with chitosan on the BSM dispersions was then studied using DLS, as described in section 2.3. Nanoparticles were added to the mucin dispersion at different concentrations (0.5 to 10 %, v/v) and mixed under magnetic stirring for 15 minutes at room temperature. All measurements were performed using freshly prepared solutions.

3. Results and discussion

Nanoparticles suspensions were obtained by the nanoprecipitation method. In order to optimize the nanoparticles preparation, three main parameters were evaluated: concentration of chitosan, molar mass of chitosan and concentration of poloxamer. Polysaccharide-decorated

nanoparticles were prepared by incorporating the chitosan during of the nanoparticles preparation.

3.1. Effect of chitosan on the nanoparticle size and zeta potential

Studies performed by Quemeneur et al. (2008) have demonstrated that the molar masses of chitosan between 50,000 and 500,000 have no influence on the polymer adsorption and, consequently, on zeta potential variation. Therefore, one may conclude that the mechanism of chitosan's adsorption is the same for all molar masses and probably consists in a flat adsorption on the surface of the vesicles. Accordingly, we only used low molar mass chitosan for the preparation of decorated nanoparticles in order to choose the ideal concentration of chitosan and optimize the sample preparations. Unloaded and curcumin-loaded nanoparticles were prepared at different concentrations of chitosan: 0.1, 0.25, 0.5 and 0.75 % (w/v), with a constant poloxamer concentration of 0.25 % (w/v).

The results show that the size and surface charge of the nanoparticle suspensions were found to be dependent of chitosan concentration (see Fig. 1a and 1b). Nanoparticles prepared without chitosan showed a surface charge close to zero and becomes positive with the addition of chitosan. When chitosan concentration increased from 0 to 0.75 % (w/v), the zeta potential of unloaded and curcumin-loaded nanoparticles increased from +0.002 and -0.099 mV to +81.7 and +79.8 mV, respectively. The zeta potential of uncoated-nanoparticles tended toward zero probably due to the layer of nonionic surfactant poloxamer. The increase in the surface charge of nanoparticles is attributed to the increase of amino groups positively charged of chitosan molecules, proving that the nanoparticles were successfully coated. This adsorption is due to strong hydrogen bonds between ether and amino groups from PEO (hydrophilic block of the poloxamer) and chitosan, as it was already shown in other investigations (CALVO et al., 1997; SASHINA; VNUCHKIN; NOVOSELOV, 2006a). When chitosan concentration increases to 0.1 and 0.25 % (w/v), one observes a large increase of the zeta potential values indicating their adsorption on the nanoparticle surface. For higher added concentrations of chitosan, the zeta potential values tend to a plateau. No significant differences were observed for the zeta potential values for unloaded and curcumin-loaded nanoparticles.

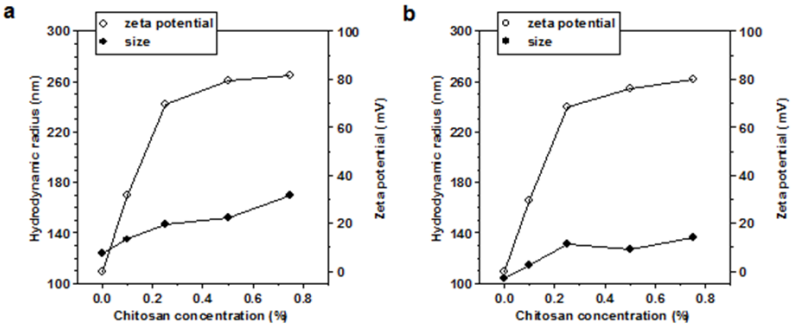

Fig. 1. Hydrodynamic radius obtained using the Contin analysis (PROVENCHER, 1976) and zeta potential of unloaded (a) and curcumin-loaded (b) nanoparticles as a function of chitosan concentration (CSL, w/v).

The mean size of the nanoparticles increased with the increase of chitosan concentration. When chitosan concentration increased from 0 to 0.75 % (w/v), the hydrodynamic radius of nanoparticles increased from 123 and 104 nm to 169 nm and 136 nm for unloaded and curcumin loaded-nanoparticles, respectively. On the hand, the size of the curcumin-loaded nanoparticles is found smaller than the unloaded curcumin. These last results suggest a strong interaction between curcumin and PCL resulting in a compaction of the core. Consequently, mucoadhesive polymer concentration of 0.1 % (w/v) was selected for the preparation of chitosan-coated nanoparticles.

3.2. Effect of poloxamer on the nanoparticles size and polydispersity

The effect of surfactant poloxamer on the characteristics of particles was also evaluated. Unloaded and curcumin-loaded nanoparticles were prepared at different concentrations of poloxamer: 0.1, 0.25 and 0.5 % (w/v), with a constant chitosan concentration of 0.1 %. In the presence of 0.1 % surfactant, aggregation and precipitate formation were observed during the nanoprecipitation process suggesting the instability of the system. In the presence of higher surfactant concentrations, nanoparticles were successfully formed. The surfactant poloxamer promotes the steric stabilization of nanoparticle dispersions at their interfaces. The triblock copolymer chains bound to the nanoparticle surface through hydrophobic interactions with PPO block whereas the external hydrophilic PEO blocks solvate and protrude

into the aqueous medium creating a steric barrier (LI; CALDWELL; RAPOPORT, 1994; SANTANDER-ORTEGA et al., 2007). Such stabilizers have been used to achieve greater stability of the colloidal particles. In the case of chitosan-coated nanoparticles, the positively charged surface also contribute to the stability of the dispersion through electrostatic forces (LOURENCO et al., 1996). The mean particle sizes and polydispersity indices of curcumin-loaded nanoparticles containing 0.25 and 0.5 % of poloxamer are listed in Table 1.

Table 1. Hydrodynamic radius and polydispersity index of curcumin-loaded nanoparticles containing 0.25 and 0.5 % (w/v) poloxamer at 90° scattering angle.

Sample	Hydrodynamic radius[a] (Polydispersity index)[b]	
	0.25 % poloxamer	**0.5 % poloxamer**
Cur-NP	104 nm (0.11)	43 and 104 nm[c]
Cur-NP CSL	114 nm (0.07)	111 nm (0.12)
Cur-NP CSM	120 nm (0.16)	41 and 119 nm[c]
Cur-NP CSH	125 nm (0.14)	37 and 125 nm[c]

[a] obtained using the Contin analysis (PROVENCHER, 1976)
[b] obtained using the cumulant analysis (WATSON, 1972; FRISKEN, 2001)
[c] samples displaying more than one peak

Hydrodynamic radius increased with the chitosan addition to the formulations, suggesting the adsorption of mucoadhesive polymer on the particle surface. Nanoparticle size was found to be dependent of the chitosan molar mass. When the molar mass increased from low to high value, the mean particle radius of nanoparticles obtained using 0.25 and 0.5 % of poloxamer increased from 114 and 111 nm to 125 nm, respectively. These results suggest that the chitosan coating layer thickness varies from approximately 10 to 20 nm for nanoparticles coated with chitosan of low and high molar masses, respectively. At the high surfactant concentration, one observed a bimodal distribution of particles (poloxamer micelles and their aggregates, and nanoparticles). The correlation function and decay time distribution obtained at 90° scattering angle are given for Cur-NP containing 0.5 % poloxamer in Fig. 2a. After treatment of the correlation function (g_2-1) using Contin analysis (PROVENCHER, 1976), two main decay times (τ_1 = 0.5 ms and τ_1 = 1.2 ms) are obtained (A). Considering equation $\tau = 1/(Dq^2)$ (BERNE; PECORA, 1976), the diffusion coefficients (D) of particles were calculated and found to be D_1 = 5.7 x 10^{-8} cm^2s^{-1} and D_2 = 2.4 x

10^{-8} cm^2s^{-1}. Each diffusion coefficient permitted to obtain hydrodynamic radius of the effective corresponding hard sphere through Stokes-Einstein equation, which were R_{h1} = 42.9 nm and R_{h2} = 103.0 nm, respectively. The micelle formation of poloxamer could also be visualized using TEM experiments as illustrated in Fig. 2b and 2c.

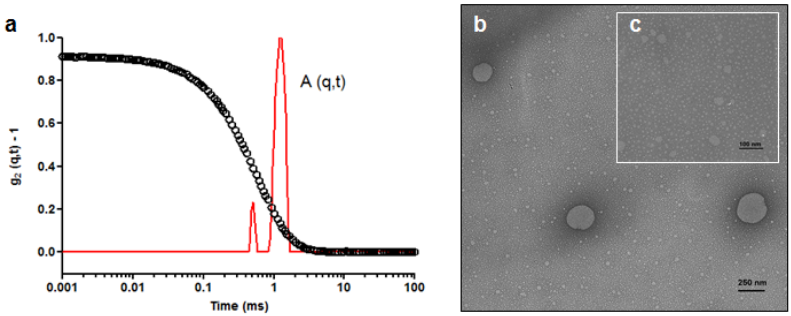

Fig. 2. Correlation function and decay time distribution obtained at 90° scattering angle for Cur-NP containing 0.5 % poloxamer (a). Transmission electron micrographs at magnification of 11500 (b) and 38000 (c).

At intermediary poloxamer concentrations, colloidal suspensions displaying monodisperse distributions of particles were obtained, as seen by the low values of polydispersity index listed in Table 1. The particle size and size distribution of these samples were also evaluated using DLS analysis at different scattering angles as shown in Table 2. The monodispersity of the samples was confirmed since all polydispersity indices were lower than 0.3 for the different measured angles. Fig. 3 shows the correlation functions and decay time distribution obtained at the scattering angles 60, 90 and 120° for sample Cur-NP CSL.

Table 2. Hydrodynamic radius and polydispersity index of curcumin-loaded nanoparticles containing 0.25 % poloxamer determined by DLS at different scattering angles (60, 90 and 120°).

Sample	Hydrodynamic radius[a] (Polydispersity index)[b]		
	60°	90°	120°
Cur-NP	115 nm (0.10)	104 nm (0.11)	103 nm (0.13)
Cur-NP CSL	132 nm (0.09)	114 nm (0.07)	108 nm (0.15)
Cur-NP CSM	138 nm (0.15)	120 nm (0.16)	124 nm (0.22)
Cur-NP CSH	152 nm (0.18)	125 nm (0.14)	130 nm (0.22)

[a] obtained using the Contin analysis (PROVENCHER, 1976)
[b] obtained using the cumulant analysis (WATSON, 1972; FRISKEN, 2001)

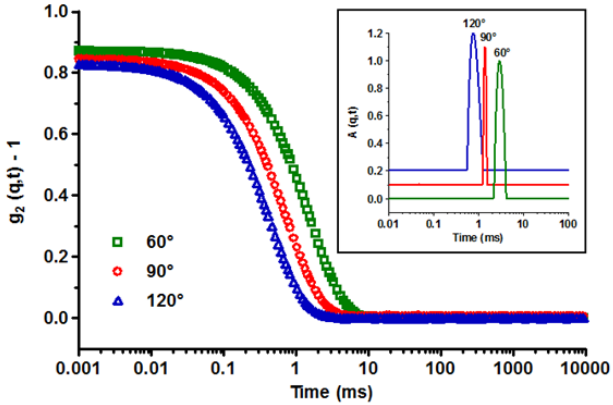

Fig. 3. Correlation function and decay time distribution obtained at different scattering angles for sample Cur-NP CSL containing 0.25 % poloxamer.

Static light scattering (SLS) measurements were also carried out for unloaded and curcumin loaded nanoparticles decorated with different chitosan molar masses. All samples presented similar behaviors indicating the same particle morphology. The scattering intensity obtained for sample Cur-NP CSH is shown in Fig. 4a, which exhibited a q^{-4}-dependence for the highest q-values and a plateau for the lowest q-values. This Porod behavior (BALE; SCHMIDT, 1984; TEIXEIRA, 1988; WILLIAMSON et al., 2003) indicates that the colloidal suspension is highly heterogeneous as far as the local density is concerned, and contains dense particles with sharp boundaries, *i.e.* small interphases, on the one hand and the less dense solvent on the other hand. Less sharp interphases would induce smoother q dependences

(AUVRAY, 1986). In Fig. 4a, we define q_0 as the particular modulus of the scattering value for which the q^{-4} dependency crosses the q^0 dependency of the scattering intensity, in the present case q_0=*0.0142* nm^{-1}. For q-values smaller than q_0, nanoparticle suspension is homogeneous and the typical particle diameter can be estimated as π/q_0 ≈ 221 nm, which is consistent with the DLS results. Fig. 4b shows the inverse decay time obtained from DLS measurements, which is proportional to q^2. The slope of this curve is equal to the diffusion coefficient and the linear dependency of the inverse decay time with q^2 proves that the diffusive Brownian motion of particles is observed.

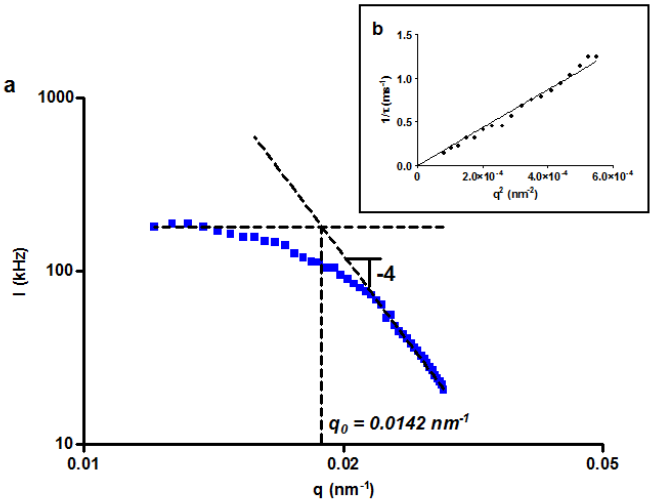

Fig. 4. Scattering intensity I *vs*. modulus of the scattering vector q (a) and inverse decay time *vs*. q^2 (b) obtained for sample Cur-NP CSH containing 0.25 % poloxamer.

TEM micrographs of chitosan-coated nanoparticles produced using 0.25 % poloxamer displayed a spherical shape as shown in Fig. 5. The uranyl acetate of the negative staining was more deposited around the nanoparticles indicating its higher affinity for the chitosan hydrophilic shell. The formulations showed a mean particle size similar to the one obtained by DLS studies. In view of the nanoparticle size and polydispersity results, the formulations containing 0.25 % (w/v) of surfactant were selected for further studies.

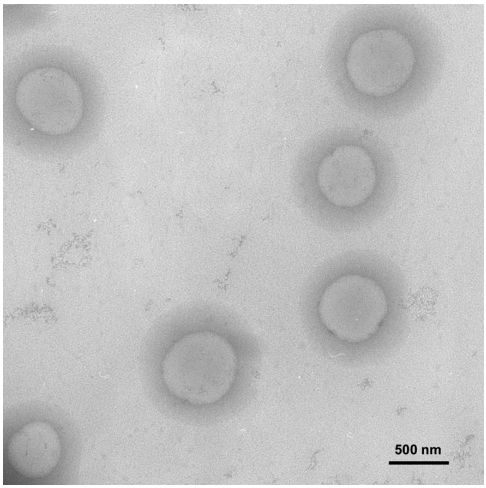

Fig. 5. Transmission electron micrograph of curcumin-loaded nanoparticles containing 0.25 % poloxamer (Cur-NP CSL).

3.3. NTA measurements

In order to confirm the results obtained using DLS that suggest the production of chitosan-coated nanoparticles with monodisperse distribution, samples were analyzed by NTA technique. This method is based on a laser illuminated microscopical technique that permits the real-time analysis of nanoparticles Brownian motion using a charge-coupled device (CCD) camera. Nanoparticles in liquid environment are visualized and tracked individually by an image analysis software that deduces the diffusion coefficient of each particle and allows the determination of its hydrodynamic radius (NANOSIGHT). This analysis method is considered very complementary to dynamic light scattering as it gives number average diameter. The nanoparticle size distribution with the corresponding video frames and three-dimensional graphs (size *vs.* intensity *vs.* concentration) are shown in Fig. 6. It is possible to observe a relatively narrow distribution for all formulations showing a good agreement with the DLS results. However, the mean diameter sizes obtained by NTA were around 170 and 180 nm for uncoated and chitosan-coated nanoparticles, respectively, which is slightly smaller than those obtained by DLS. According to Filipe et al. (2010), this shift can be explained because the size distributions obtained by DLS consist of weight distributions whereas those obtained by NTA are number distributions. In addition, the size distributions obtained by DLS towards

larger sizes due to the high contribution of a few large particles to the global scattering.

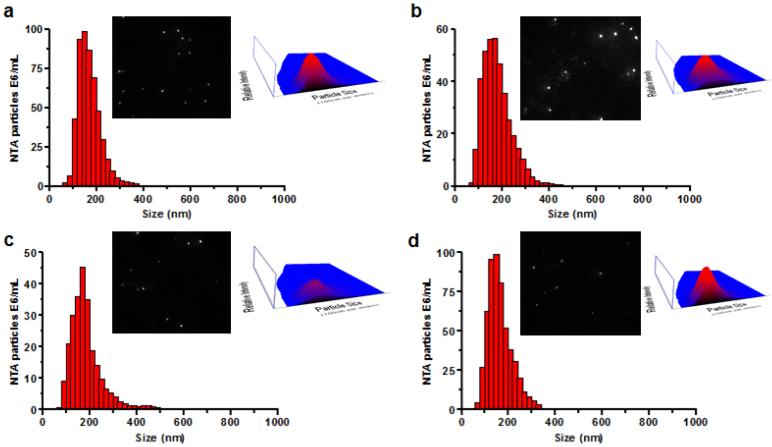

Fig. 6. Size distribution from NTA measurements with the corresponding NTA video and 3D graph size *vs*. intensity *vs*. concentration obtained for curcumin loaded-nanoparticles: Cur-NP (a), Cur-NP CSL (b), Cur-NP CSM (c) and Cur-NP CSH (d). NTA video obtained for Cur-NP CSH is available as supplementary data.

3.4. Effect of salt on the stability of chitosan-coated nanoparticles

The influence of ionic strength of the medium was studied in order to evaluate the stability of nanoparticles decorated with the cationic polyelectrolyte. The stability of nanoparticles coated with low molar mass chitosan was determined by particle size and zeta potential measurements. As shown in Fig. 7a, chitosan-coated nanoparticles were stable to salt addition (4 mol/L NaCl), presenting a similar profile with the uncoated nanoparticles. These results suggest that the mucoadhesive polymer is strongly associated with the particle, and, consequently, is not affected by salt ions. We expect similar effect on the other molar masses (CSM and CSH) as was described by Wu et al. (2005) on their results of nanoparticles made from chitosan. Indeed, their studies showed that for high molar masses of chitosan, the size of the nanoparticles is not sensitive to the effect of added salt. On the other hand, the increase of NaCl concentration reduced the zeta potential of chitosan-coated nanoparticles (Fig. 7b). This can be attributed to the

screening of electrostatic interactions by the added salt, resulting thereby in lower values of electrophoretic mobility (LOPEZ-LEON et al., 2005).

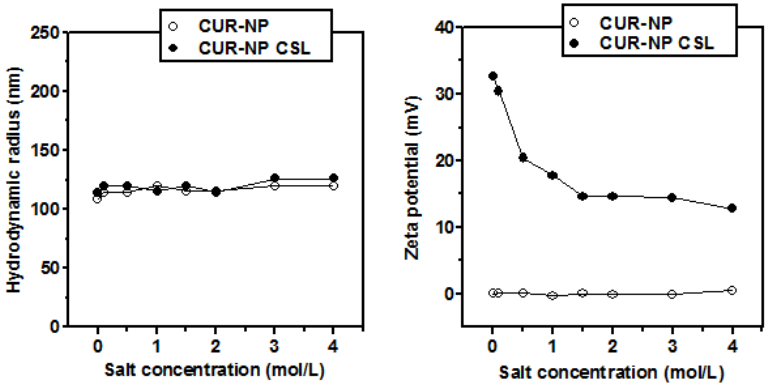

Fig. 7. Effect of salt addition on hydrodynamic radius (a) and zeta potential (b) of uncoated and chitosan-coated nanoparticles.

3.5. Determination of curcumin content

As seen in Table 3, the mean curcumin content ranged from 422 to 464 µg/mL, corresponding to a drug recovery of 84.4 to 92.7 %, in relation to the amount of drug initially added to the formulations. The encapsulation efficiency values were higher than 99 % for all formulations, probably due to the poor water solubility of curcumin in external phase of the nano-suspensions. One notes that such high percentage of loading was reached for all molar masses of chitosan.

Table 3. Entrapment efficiency and curcumin content obtained after curcumin quantification of the nanoparticle suspensions.

Sample	Curcumin content, µg/mL ± SD	Recovery, % ± SD
Cur-NP	422 ± 16.3	84.4 ± 3.3
Cur-NP CSL	460 ± 24.5	92.1 ± 4.9
Cur-NP CSM	464 ± 5.9	92.7 ± 1.2
Cur-NP CSH	456 ± 0.2	91.3 ± 0.0

Based in the above presented results, a schematic representation of chitosan-coated nanoparticles is proposed in Fig. 8, in which chitosan

molecules anchor to the polymeric nanoparticle surface stabilized by the nonionic surfactant poloxamer.

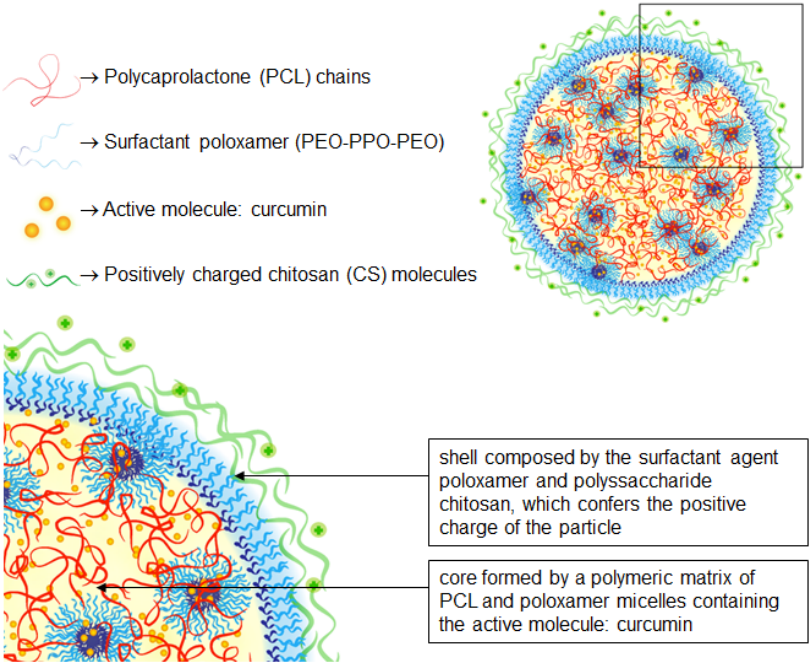

Fig. 8. Schematic representation of particles formed by a polymeric matrix of PCL and poloxamer micelles containing curcumin stabilized by surfactant shell and decorated with chitosan.

3.6. Interactions between chitosan-coated nanoparticles and mucin

According to the DLS results, the BSM dispersions displayed a high polydispersity with a main hydrodynamic radius around of 250 nm. When chitosan-coated nanoparticles were added to BSM dispersion, an increase of the hydrodynamic radius was observed, as shown in Fig. 9. The particle size increased with the nanoparticles addition to reach a maximum radius of approximately 500 nm. At higher concentrations of nanoparticles, above 2.5 % (v/v), the system undergoes a progressive precipitation mainly due to the formation of aggregates whose sizes are approaching micrometer scale.

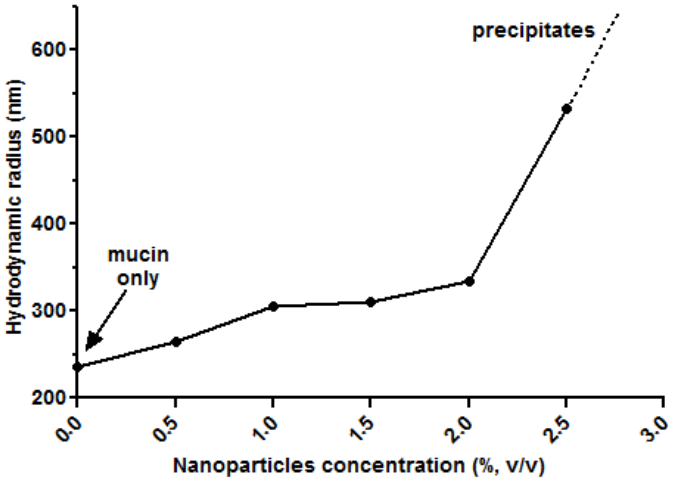

Fig. 9. Variation of the hydrodynamic radius (main peak) of the mucin colloidal system (BSM 250 μg/mL) as a function of the added concentration of the chitosan-coated nanoparticle (Cur-NP CSM), measured at 90° scattering angle. At nanoparticles concentrations higher than 2.5 % (v/v), the system precipitates.

The addition of 1 % (v/v) Cur-NP CSM (R_h = 120 nm) to mucin dispersion (R_h = 235 nm) caused an increase of about 80 nm in the radius of BSM and a narrower distribution, suggesting a strong interaction between particles and proteins, as illustrated in Fig. 10. The small peak observed at short relaxation times for BSM dispersions is attributed to internal fluctuations of the macromolecular aggregate (BASTARDO; CLAESSON; BROWN, 2002). As illustrated in Table 4, the interactions of nanoparticles with mucin are found to be dependent on the molar mass of chitosan. The hydrodynamic radius of mucin aggregates (R_{h2}) increased from 235 nm to 305, 319 and 421 nm by addition of Cur-NP CSL, Cur-NP CSM, and Cur-NP CSH, respectively.

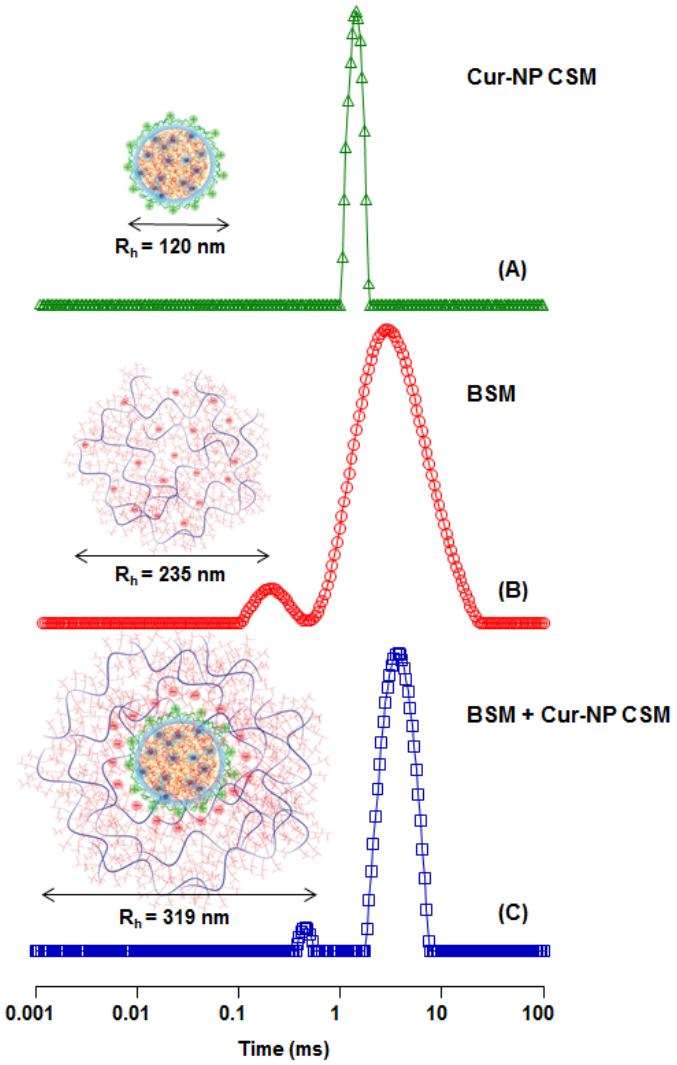

Fig. 10. Decay time distributions obtained at 90° scattering angle using CONTIN analysis for (A) Cur-NP CSM, (B) BSM 250 μg/mL, similar results were found in the range of concentration 100 - 500 μg/mL, and (C) Cur-NP CSM (1 %, v/v) added to BSM dispersion.

Table 4. Hydrodynamic radius of mucin-nanoparticles aggregates at 90° scattering angle using 1 % (v/v) of curcumin-loaded nanoparticles coated with different molar masses of chitosan.

Sample	R_{h1}[a]	R_{h2}[b]
BSM + Cur-NP CSL	12.4 nm	305 nm
BSM + Cur-NP CSM	37.7 nm	319 nm
BSM + Cur-NP CSH	75.6 nm	421 nm

[a] small peak attributed to internal fluctuations of the mucin macromolecular aggregate

[b] main peak related to mucin-nanoparticles aggregates

The interaction between chitosan-coated nanoparticles and mucin is mainly due to electrostatic forces between protonated amino groups (NH_3^+) of mucoadhesive polymer and negatively charged groups, such as carboxylate (COO^-) or sulphonate (SO_3^-) groups, of protein carbohydrate chains (DEACON et al., 2000; SVENSSON; THURESSON; ARNEBRANT, 2008). Consequently, the capacity of nanoparticles to interact with the negatively charged mucosal surface can be useful to prolong the contact time of drug delivery system in the mucosa, which would improve the therapeutic performance of curcumin or/and other drugs.

4. Conclusions

Nanoparticles coated with mucoadhesive polysaccharide were successfully prepared by the nanoprecipitation method, accompanied by the adsorption of different molar masses of chitosan (CSL, CSM or CSH) during the nanoparticles preparation. These conditions were optimized to obtain a monodisperse size distribution of surface-coated nanoparticles. The decoration of these nanoparticles with chitosan, favored by the strong H-bonds between poloxamer and chitosan, was confirmed by the changes in particle size and zeta potential values. In addition, all resulting nanoparticles showed high loading efficient of curcumin (99 %). Finally, chitosan-coated nanoparticles showed strong ability to interact with mucin through electrostatic forces that highlight their potential as mucoadhesive carriers for curcumin delivery.

Acknowledgements

The authors acknowledge the financial support from CNRS and CAPES (CAPES-COFECUB Grant N° 620/08) and the Federal University of Santa Catarina (UFSC).

References

ANAND, P.; KUNNUMAKKARA, A. B.; NEWMAN, R. A.; AGGARWAL, B. B. Bioavailability of curcumin: problems and promises. **Mol Pharm,** v. 4, n. 6, p. 807-818, 2007.

ANDREWS, G. P.; LAVERTY, T. P.; JONES, D. S. Mucoadhesive polymeric platforms for controlled drug delivery. **Eur J Pharm Biopharm,** v. 71, n. 3, p. 505-518, 2009.

AUVRAY, L. Comptes rendus de l'académie des sciences. 1986. p.859-862.

BALE, H. D.; SCHMIDT, P. W. Small-angle x-ray-scattering investigation of submicroscopic porosity with fractal properties. **Phys Rev Lett,** v. 53, n. 6, p. 596-599, 1984.

BASTARDO, L.; CLAESSON, P.; BROWN, W. Interactions between mucin and alkyl sodium sulfates in solution. A light scattering study. **Langmuir,** v. 18, n. 10, p. 3848-3853, 2002.

BERNE, B.; PECORA, R. **Dynamic light scattering with applications to chemistry, biology and physics**. Wiley, New York (USA): 1976.

BILENSOY, E.; SARISOZEN, C.; ESENDAGLI, G.; DOGAN, A. L.; AKTAS, Y.; SEN, M.; MUNGAN, N. A. Intravesical cationic nanoparticles of chitosan and polycaprolactone for the delivery of Mitomycin C to bladder tumors. **Int J Pharm,** v. 371, n. 1-2, p. 170-176, 2009.

CALVO, P.; REMUÑAN-LÓPEZ, C.; VILA-JATO, J. L.; ALONSO, M. J. Chitosan and chitosan/ethylene oxide-propylene oxide block copolymer nanoparticles as novel carriers for proteins and vaccines. **Pharm Res,** v. 14, n. 10, p. 1431-1436, 1997.

CALVO, P.; VILA-JATO, J. L.; ALONSO, M. J. Evaluation of cationic polymer-coated nanocapsules as ocular drug carriers. **Int J Pharm,** v. 153, n. 1, p. 41-50, 1997.

CHOWDARY, K. P.; RAO, Y. S. Mucoadhesive microspheres for controlled drug delivery. **Biol Pharm Bull,** v. 27, n. 11, p. 1717-1724, 2004.

CUI, F.; QIAN, F.; YIN, C. Preparation and characterization of mucoadhesive polymer-coated nanoparticles. **Int J Pharm,** v. 316, n. 1-2, p. 154-61, 2006.

DEACON, M. P.; MCGURK, S.; ROBERTS, C. J.; WILLIAMS, P. M.; TENDLER, S. J.; DAVIES, M. C.; DAVIS, S. S.; HARDING, S. E. Atomic force microscopy of gastric mucin and chitosan mucoadhesive systems. **Biochem J,** v. 348 Pt 3, p. 557-563, 2000.

FESSI, H.; PUISIEUX, F.; DEVISSAGUET, J. P.; AMMOURY, N.; BENITA, S. Nanocapsule formation by interfacial polymer deposition following solvent displacement. **Int J Pharm,** v. 55, n. 1, p. R1-R4, 1989.

FILIPE, V.; HAWE, A.; JISKOOT, W. Critical evaluation of nanoparticle tracking analysis (NTA) by NanoSight for the measurement of nanoparticles and protein aggregates. **Pharm Res,** v. 27, n. 5, p. 796-810, 2010.

FRISKEN, B. J. Revisting the method of cumulants for the analysis of dynamic light-sctattering data. **Appl Opt,** v. 40, n. 24, p. 4087-4091, 2001.

GOEL, A.; KUNNUMAKKARA, A. B.; AGGARWAL, B. B. Curcumin as ‘‘curecumin’’: from kitchen to clinic. **Biochem Pharmacol,** v. 75, n. 4, p. 787-809, 2008.

HUANG, Y.; LEOBANDUNG, W.; FOSS, A.; PEPPAS, N. A. Molecular aspects of muco- and bioadhesion: tethered structures and site-specific surfaces. **J Control Release,** v. 65, n. 1-2, p. 63-71, 2000.

LEE, J. W.; PARK, J. H.; ROBINSON, J. R. Bioadhesive-based dosage forms: the next generation. **J Pharm Sci,** v. 89, n. 7, p. 850-866, 2000.

LEMARCHAND, C.; GREF, R.; COUVREUR, P. Polysaccharide-decorated nanoparticles. **Eur J Pharm Biopharm,** v. 58, n. 2, p. 327-341, 2004.

LI, J.-T.; CALDWELL, K. D.; RAPOPORT, N. Surface properties of pluronic-coated polymeric colloids. **Langmuir,** v. 10, n. 12, p. 4475-4482, 1994.

LIU, Z.; JIAO, Y.; WANG, Y.; ZHOU, C.; ZHANG, Z. Polysaccharides-based nanoparticles as drug delivery systems. **Adv Drug Deliv Rev,** v. 60, n. 15, p. 1650-1662, 2008.

LOPEZ-LEON, T.; CARVALHO, E. L.; SEIJO, B.; ORTEGA-VINUESA, J. L.; BASTOS-GONZALEZ, D. Physicochemical characterization of chitosan nanoparticles: electrokinetic and stability behavior. **J Colloid Interface Sci,** v. 283, n. 2, p. 344-351, 2005.

LOURENCO, C.; TEIXEIRA, M.; SIMÕES, S.; GASPAR, R. Steric stabilization of nanoparticles: size and surface properties. **Int J Pharm,** v. 138, n. 1, p. 1-12, 1996.

MAZZARINO, L.; BELLETTINI, I. C.; MINATTI, E.; LEMOS-SENNA, E. Development and validation of a fluorimetric method to determine curcumin in lipid and polymeric nanocapsule suspensions. **BJPS,** v. 46, n. 2, p. 219-226, 2010.

NANOSIGHT. **Applications of nanoparticle tracking analysis (NTA) in nanoparticle research**. London: NanoSight Ltd 2011.

PATHAN, S. A.; IQBAL, Z.; SAHANI, J. K.; TALEGAONKAR, S.; KHAR, R. K.; AHMAD, F. J. Buccoadhesive drug delivery systems - extensive review on recent patents. **Recent Pat Drug Deliv Formul,** v. 2, n. 2, p. 177-188, 2008.

PROVENCHER, S. W. An eigenfunction expansion method for the analysis of exponential decay curves. **J Chem Phys,** v. 64, p. 2772-2777, 1976.

QUEMENEUR, F.; RINAUDO, M.; PEPIN-DONAT, B. Influence of molecular weight and pH on adsorption of chitosan at the surface of

large and giant vesicles. **Biomacromolecules,** v. 9, n. 1, p. 396-402, 2008.

SANTANDER-ORTEGA, M. J.; CSABA, N.; ALONSO, M. J.; ORTEGA-VINUESA, J. L.; BASTOS-GONZÁLEZ, D. Stability and physicochemical characteristics of PLGA, PLGA:poloxamer and PLGA:poloxamine blend nanoparticles: a comparative study. **Colloids Surf A Physicochem Eng Asp,** v. 296, n. 1,Äì3, p. 132-140, 2007.

SASHINA, E.; VNUCHKIN, A.; NOVOSELOV, N. A study of the thermodynamics of chitosan interaction with polyvinyl alcohol and polyethylene oxide by differential scanning calorimetry. **Russ J Appl Chem,** v. 79, n. 10, p. 1643-1646, 2006.

SVENSSON, O. **Interactions of mucins with biopolymers and drug delivery particles**. 2008. 81 (Thesis). The Faculty of Health and Society, Malmö University, Malmö.

SVENSSON, O.; THURESSON, K.; ARNEBRANT, T. Interactions between chitosan-modified particles and mucin-coated surfaces. **J Colloid Interface Sci,** v. 325, n. 2, p. 346-350, 2008.

TEIXEIRA, J. Small-angle scattering by fractal systems. **J Appl Crystallogr,** v. 21, n. 6, p. 781-785, 1988.

TOMREN, M. A.; MASSON, M.; LOFTSSON, T.; TONNESEN, H. H. Studies on curcumin and curcuminoids XXXI. Symmetric and asymmetric curcuminoids: stability, activity and complexation with cyclodextrin. **Int J Pharm,** v. 338, n. 1-2, p. 27-34, 2007.

TONNESEN, H. H. Solubility, chemical and photochemical stability of curcumin in surfactant solutions. Studies of curcumin and curcuminoids, XXVIII. **Pharmazie,** v. 57, n. 12, p. 820-824, 2002.

TONNESEN, H. H.; MASSON, M.; LOFTSSON, T. Studies of curcumin and curcuminoids. XXVII. Cyclodextrin complexation: solubility, chemical and photochemical stability. **Int J Pharm,** v. 244, n. 1-2, p. 127-135, 2002.

WATSON, T. J. Analysis of macromolecular polydispersity in intensity correlation spectroscopy: the method of cumulants. **J Chem Phys,** v. 57, n. 11, p. 4814-4820, 1972.

WILLIAMSON, D. L.; MARR, D. W. M.; YANG, J.; YAN, B.; GUHA, S. Nonuniform H distribution in thin-film hydrogenated amorphous Si by small-angle neutron scattering. **Phys Rev B,** v. 67, n. 7, p. 075314, 2003.

WU, Y.; YANG, W.; WANG, C.; HU, J.; FU, S. Chitosan nanoparticles as a novel delivery system for ammonium glycyrrhizinate. **Int J Pharm,** v. 295, n. 1-2, p. 235-245, 2005.

Publicação: "*On the mucoadhesive properties of chitosan-coated polycaprolactone nanoparticles loaded with curcumin using QCM-D"*
Submetida ao Journal of Biomedical Nanotechnology

On the mucoadhesive properties of chitosan-coated polycaprolactone nanoparticles loaded with curcumin using QCM-D

Letícia Mazzarino,[†,§] Liliane Coche-Guérente,[◦] Pierre Labbé,[◦] Elenara Lemos-Senna,[§] and Redouane Borsali[†,*]

[†]*Centre de Recherches sur les Macromolécules Végétales, CERMAV, CNRS-UPR 5301, Université Joseph Fourier, BP 53, 38041, Grenoble, Cedex 9, France*

[◦]*Département de Chimie Moléculaire, UMR CNRS-UJF 5250, ICMG FR-2607, Université Joseph Fourier, BP 53, 38041, Grenoble, Cedex 9, France*

[§]*Departamento de Ciências Farmacêuticas, Centro de Ciências da Saúde, Laboratório de Farmacotécnica, Universidade Federal de Santa Catarina, Campus Trindade, Florianópolis, 88040-900, Brazil*

ABSTRACT

Quartz Crystal Microbalance with Dissipation Monitoring (QCM-D) was used to investigate the mucoadhesive properties of nanoparticles decorated with low, medium and high molar mass chitosan (CS). Uncoated and chitosan-coated polycaprolactone (PCL) nanoparticles loaded with curcumin were prepared by nanoprecipitation method and characterized in terms of size, surface charge and drug content. The interactions between nanoparticles and mucin layer were monitored after the treatment of SAM-functionalized gold-coated quartz crystals with bovine submaxillary gland mucin (BSM). The results show that all investigated chitosan-coated nanoparticles adsorb onto the BSM layer, and the mass uptake was found to be independent of the chitosan molar mass. Uncoated nanoparticles showed, however, no affinity with BSM layer, confirming that the adsorption of colloidal systems occurs due to their decoration with chitosan. The adhesion is mainly attributed to electrostatic interactions between protonated amino groups of mucoadhesive chitosan and negatively charged groups of mucin. The results suggest that chitosan-coated nanoparticles are promising carriers for hydrophobic drugs delivery in the buccal mucosa.

Keywords: Mucoadhesive Nanoparticles; Chitosan-Coated Nanoparticles; Curcumin; Mucin; Quartz Crystal Microbalance with Dissipation Monitoring (QCM-D); Dynamic Light Scattering (DLS)

1. Introduction

Mucoadhesion has emerged as a potential strategy to improve the drug delivery by prolonging the residence time of dosage forms at mucosal membranes. The term mucoadhesion is used to define the interaction of a natural or synthetic polymer with the mucus layer covering the epithelial surface. Mucus is found in several regions of the body, including buccal, nasal and ocular mucosa and gastrointestinal, reproductive and respiratory tracts, and possesses as main functions the lubrication of epithelium and protection against pathogens and noxious substances (ANDREWS; LAVERTY; JONES, 2009; SERRA; DOMENECH; PEPPAS, 2009). Its main component besides water (approximately 95 %) is the glycoprotein mucin, in which its structure consists of branched oligosaccharide chains attached to a protein core. The carbohydrate chains are primarily composed by *N*-acetylgalactosamine, *N*-acetylglucosamine, fucose, galactose, and sialic acid, while the protein region is rich in serine and threonine amino acid residues. Mucins are responsible for the viscoelastic properties of the mucus and have a relevant role in the mucoadhesion process (BANSIL; TURNER, 2006; SVENSSON; ARNEBRANT, 2010).

Mucoadhesive drug delivery systems have been developed in order to provide intimate contact of the formulation with the biological surface and to increase its residence time at the site of application, prolonging the action of drug (PATIL et al., 2006). The advantages associated to these systems include improved drug bioavailability, reduced administration frequency, besides to permit the modification of mucosa permeability (CHOWDARY; RAO, 2004; KHUTORYANSKIY, 2011). Among the new mucoadhesive systems, nanoparticles coated with polysaccharides have demonstrated a growing interest as drug carriers due to the possibility of molecular recognition and very good mucoadhesive properties. The advantages associated to the mucoadhesive colloidal systems include the drug protection against degradation in physiologic medium, controlled release of drug at the site of action, possibility of hydrophobic drug administration as an aqueous dispersion, besides active targeting related to the polysaccharide coating (LEMARCHAND; GREF; COUVREUR, 2004; LEMARCHAND et al., 2006; LIU et al., 2008).

Chitosan is a polysaccharide obtained by the deacetylation of chitin, the second most abundant natural biopolymer found in the exoskeleton of crustaceans. It is an interesting biomaterial for the design of drug carriers and other biomedical applications since it is biodegradable, biocompatible and non-toxic, present antimicrobial and mucoadhesive properties. Moreover, the cationic polymer can interact with the negatively charged surfaces, such as mucosal membranes, and to enhance drug absorption by opening of the tight junctions between mucosal cells (DENKBAS; OTTENBRITE, 2006; SOGIAS; WILLIAMS; KHUTORYANSKIY, 2008). To gain further understanding on the mucoadhesive properties, we recently prepared chitosan-coated polymeric nanoparticles as potential carrier candidate for curcumin delivery to the buccal mucosa (MAZZARINO et al., 2012). Curcumin is a yellow polyphenol present in the turmeric that exhibits several pharmacological activities such as antioxidant, anti-inflammatory, anticancer and antimicrobial, but has limited application due to its poor aqueous solubility, instability and low oral bioavailability (GOEL; KUNNUMAKKARA; AGGARWAL, 2008). The buccal delivery of curcumin can be useful for both local disease treatments, such as gingivitis, oral lesions, periodontal diseases, and oral carcinomas, as well as for systemic effects.

The study of interactions between mucin and colloidal systems is extremely important for the characterization of their mucoadhesive properties. Therefore the Quartz Crystal Microbalance with Dissipation Monitoring (QCM-D) constitutes a useful technique that permits real-time monitoring of the nanocarriers/mucin interactions. Recent studies have demonstrated the suitability of quartz crystal microbalance in evaluating the adsorption of hydrophobically modified polysaccharides and pegylated quantum-dots to mucin-modified sensors (CHAYED; WINNIK, 2007; WIECINSKI et al., 2009). In this paper, the interactions between uncoated and chitosan-coated nanoparticles containing curcumin and bovine submaxillary gland mucin (BSM) were monitored by QCM-D. The QCM-D response is sensitive to the mass (including hydrodynamically coupled water) and the mechanical properties of the surface-bound layer. In addition, the influence of different molar masses of chitosan on the interactions with mucin layer was evaluated and compared.

2. Experimental section

2.1. Materials

Mucin from bovine submaxillary gland (BSM, Type I-S) was purchased from Sigma (St. Louis, MO, USA) and used as received. BSM has a molecular weight of around 1.6 MDa and a specified content of sialic acid in the range of 9 to 17 %.(SVENSSON, 2008) It was reported that this commercial mucin contains some residues of other proteins, e.g. bovine serum albumin (FEILER et al., 2007). Poloxamer 188 (Lutrol F68®) was kindly donated by BASF Chemical Company (Ludwigshafen, Germany). Sodium dodecyl sulfate (SDS), N-(3-dimethylaminopropyl)-N′-ethylcarbodiimide hydrochloride (EDC), N-hydroxysuccinimide (NHS), ethanolamine hydrochloride (ETA-HCl), 11-mercaptoundecanoic acid, curcumin, polycaprolactone (PCL, MW 60,000), chitosan, and all other chemicals were purchased from Sigma (St. Louis, MO, USA). Low (CSL 50,000 - 190,000), medium (CSM 190,000 - 310,000) and high (CSH 310,000 to > 375,000) molar mass chitosan were used in the experiments. The degree of deacetylation is between 75 - 85 % for CSL and CSM, and higher than 75 % for CSH.

2.2. Nanoparticles preparation

Curcumin-loaded PCL nanoparticles (Cur-NP) were prepared using the nanoprecipitation method, as previously described by Mazzarino et al. (2012). An organic solution containing 60 mg of PCL and 5 mg of curcumin in 12 mL of acetone was poured into 24 mL of an aqueous phase (pH 5) containing 1 % acetic acid and 0.25 % (w/v) poloxamer 188, under moderate magnetic stirring. The organic solvent was then eliminated by evaporation under reduced pressure and the colloidal suspension concentrated to 10 mL. The polymeric nanoparticle suspensions were filtered through 1.2 μm pore-sized filter paper. The preparation of chitosan-coated PCL nanoparticles was carried out from previous dispersion of 0.1 % (w/v) low, medium or high molar mass chitosan (CSL, CSM or CSH, respectively) in the aqueous phase.

2.3. Entrapment efficiency and drug contente

Entrapment efficiency and drug content were determined spectrophotometrically using a Perkin-Elmer Lambda 10 UV/VIS spectrophotometer at a wavelength of 420 nm. The calibration graph for

curcumin in acetonitrile was linear over the range of 1 to 6 μg mL^{-1} with a correlation coefficient of 0.997. The entrapment efficiency was calculated by the difference between the total amount of curcumin found in the nanoparticle suspensions after their complete dissolution in acetonitrile and the concentration of drug in the supernatant obtained by ultrafiltration/centrifugation at 10,000 rpm for 15 min using Amicon Centrifugal Filter Devices with Ultracel-100 membrane (100 kDa, Millipore Corp., USA). Drug recovery was calculated by comparing the total amount of drug found in the colloidal suspensions with the initial amount added to the formulations.

2.4. Zeta potential

Zeta potential was determined by laser-doppler anemometry using a Zetasizer Nano Series (Malvern Instruments, Worcestershire, UK). The measurements were performed at 25 °C after dilution of nanoparticles in Milli-Q® water. Samples were placed in electrophoretic cells where a potential of ± 150 mV was applied. The zeta potential values were calculated as mean electrophoretic mobility values using Smoluchowski's equation.

2.5. Dynamic light ccattering (DLS)

The mean particle size and polydispersity index of the nanoparticle suspensions were determined by Dynamic Light Scattering (DLS) using an ALV 5000 (ALV-Langen, Germany) equipped with a red helium-neon laser at a wavelength of 632.8 nm operating at a power of 35 mW. After appropriate dilution in ultrapure Milli-Q® water, samples were placed in cylindrical measurements cells and immersed in a toluene bath with temperature regulated at 25 °C. The scattered photons were detected by a very sensitive avalanche diode. In this study, the modulus of the scattering vector is denoted q and is equal to $(4\pi n/\lambda)\sin(\theta/2)$ where n represents the refractive index of pure water, θ is the scattering angle and λ designates the light wavelength. Each analysis was performed during 120 s and the scattered light was measured at different scattering angles ranging from 20 to 150°. The scattering intensity was corrected taking into account the contributions of the solvent (water) and the toluene as well as the change of the scattering volume with the detection angle. The hydrodynamic radius (R_h) was calculated using Stokes-Einstein equation, $R_h = \kappa_B T/6\pi\eta D$

where κ_B is Boltzmann constant (in J/K), T is the temperature (in K), D is the diffusion coefficient and η is the viscosity of the medium – pure water in this case (η = 0.89 cP at 25 °C).

2.6. Quartz crystal microbalance with dissipation monitoring (QCM-D)

QCM-D measurements were performed using QCM-D E1 and E4 systems equipped with axial flow chambers (Q-Sense, Sweden) and quartz crystals covered 100 nm gold (Q-Sense, Sweden). Both frequency (F) and dissipation (D) changes of the quartz crystal regarding mass and structural properties of adsorbed molecular layers, respectively, were measured at the fundamental resonance frequency (5 MHz) as well as at the third, fifth, seventh, ninth, eleventh, and thirteenth overtones (n = 3, 5, 7, 9, 11 and 13). The measurements were performed at 24 °C in order to avoid the bubble formation, since preliminary experiments carried out at 37 °C indicated there was no significant temperature effect on the mucin-nanoparticle interactions. All solutions were previously thermostated using a thermomixer (Eppendorf, France). Experiments were conducted in a continuous flow of buffer with a flow rate of 50 μL min^{-1} by using a peristaltic pump (ISM935C, Ismatec, Zurich, Switzerland).

In the case of homogenous, quasi-rigid films (for which $DD_n/(-DF_n/n) << 4 \times 10^{-7}$ Hz^{-1} for a 5 MHz crystal and an overlapping of the overtones), the frequency shifts are proportional to the Dm mass uptake per unit area that can be deduced from the Sauerbrey relationship:

$$Dm = -C\ DF_n/n$$

where the mass sensitivity, C, is equal to 17.7 ng cm^{-2} Hz^{-1} at f_1 = 5 MHz.

In the case of soft homogeneous films (exhibiting high values DD), the areal mass density and the viscoelastic properties of the adlayer are estimate by fitting the QCM-D data to a viscoelastic model (VOINOVA et al., 1999). Lateral homogeneity is a prerequisite for the applicability of the viscoelastic model, an additional energy dissipation mechanism can occur in laterally heterogeneous films (REVIAKINE; JOHANNSMANN; RICHTER, 2011). This is the case of films composed of discrete particles. Thus, for Cur-NP adsorbed on BSM layer, the viscoelastic model has not been applied. A decrease in the resonance frequency is usually associated in first approximation to an increase of the mass coupled to the quartz and our discussion will remain essentially on a qualitative level.

2.6.1. Substrate Preparation

The preliminary cleaning procedure of sensors included UV-ozone treatment for 10 min followed by the immersion in ethanol for 20 min under magnetic stirring. To obtain carboxylic-acid-functionalized surfaces, self-assembled monolayer of alkanethiolate containing carboxylic acid end groups was adsorbed onto gold-coated quartz crystals; this functionalized surface will be denoted SAM-COOH. It was performed by the immersion of the sensor in a 1 mM ethanolic solution of 11-mercaptoundecanoic acid for at least 12 h at room temperature. The resulting functionalized gold-coated quartz crystal was then rinsed with ethanol, dried and mounted in the QCM-D chamber.

Since quartz crystals are reusable, subsequent measurements were carried out after the regeneration of gold surfaces. The regeneration procedure of quartz was performed by keeping them overnight in a 2 % SDS solution, followed by ultrasonication in ethanol for 5 min, placing them in 2 % Hellmanex for 5 min, UV-ozone treatment for 10 min, and finally immersion in ethanol for 20 min under magnetic stirring.

2.6.2. Mucin Immobilization

Mucin was immobilized on the carboxylic acid functionalized gold-coated quartz crystals by amine-coupling method (Scheme 1). The experiments were carried out at a flow rate of 50 μL min^{-1}. Initially, the baseline was stabilized with Milli-Q water. For covalent mucin immobilization on SAM-COOH, the surface was first activated by exposing it to a 200 mM EDC and 50 mM NHS aqueous solution for 10 min, followed by rinsing it with Milli-Q water and 10 mM acetate buffer solution pH 4. Afterwards, 0.5 mg mL^{-1} BSM in acetate buffer solution pH 4 was then applied for 30 min. At saturation, the cell measurement chamber was rinsed with acetate buffer solution and the unreacted NHS-esters were deactivated by injecting 1 M ETA-HCl solution pH 8.5. After 15 min, acetate buffer solution pH 6 was injected followed by nanoparticle colloidal suspensions (0.5 mg mL^{-1}), previously diluted in the same buffer solution. Finally, the quartz was rinsed with buffer and experimental data were treated using Q-tools modeling software.

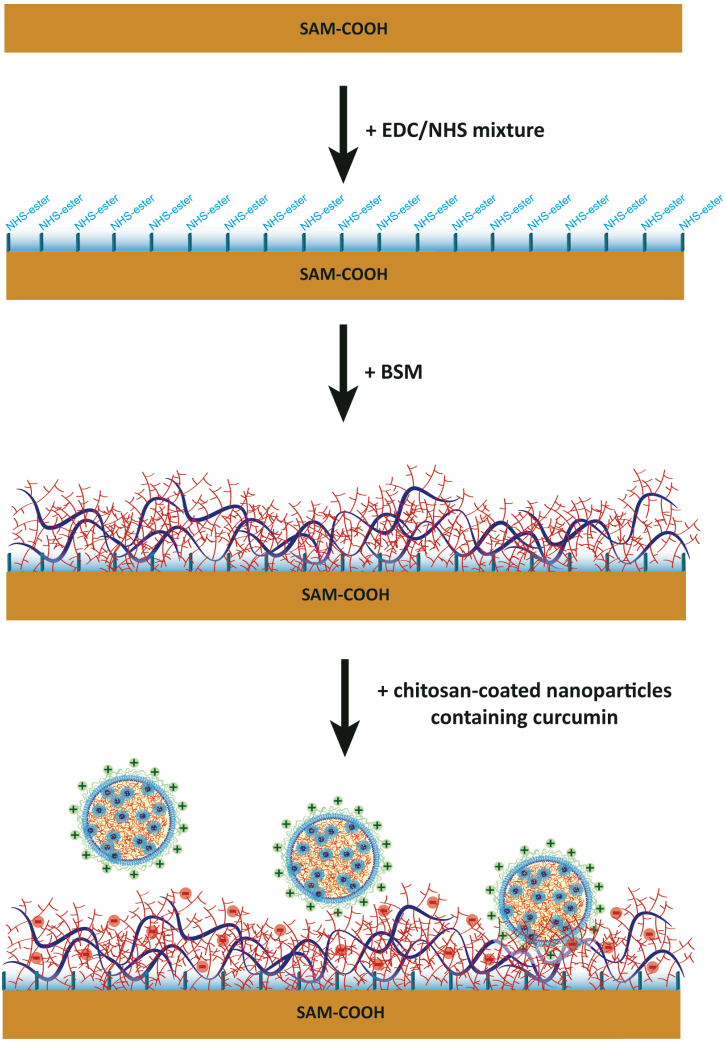

Scheme 1. Schematic representation of mucin immobilization on the gold surface followed by adsorption of chitosan-coated nanoparticles.

3. Results and discussion

In order to investigate the interactions of nanoparticles with mucin, firstly we evaluated the covalent grafting of mucin layers on SAM-COOH functionalized-gold-coated quartz crystals. Feldoto et al. (2008) demonstrated that mucin adsorbs spontaneously onto SAM-

COOH surface in spite of the negative net charges of surface and mucin and, this adsorption has been attributed to the positive amino acid residues. In order to characterize the interaction of nanoparticles with mucin layer, it seemed preferable in the present work to graft covalently the protein to the surface. The BSM covalent grafting was monitored by QCM-D, as illustrated in Figure 1. The injection of BSM in acetate buffer solution pH 4 was followed by a fast adsorption on the sensors, as evidenced by the decrease in resonance frequency, which is related to the mass uptake, and increase in dissipation, related to the slight increase in viscoelasticity of the adlayer (Figure 1). After rinsing with acetate buffer solution of same pH, no significant changes in frequency and dissipation were observed. Therefore, the mucin layer adsorbed demonstrates to exhibit high stability during its formation and after the rinsing step. The frequency shifts were analyzed according to the simple Sauerbrey equation due to the low ratio $DD/-DF_n/n$ associated with overtone overlap (REVIAKINE; JOHANNSMANN; RICHTER, 2011). An average surface density of 500 ± 30 ng/cm^2 can be evaluated from the shift in frequency by using the Sauerbrey equation.

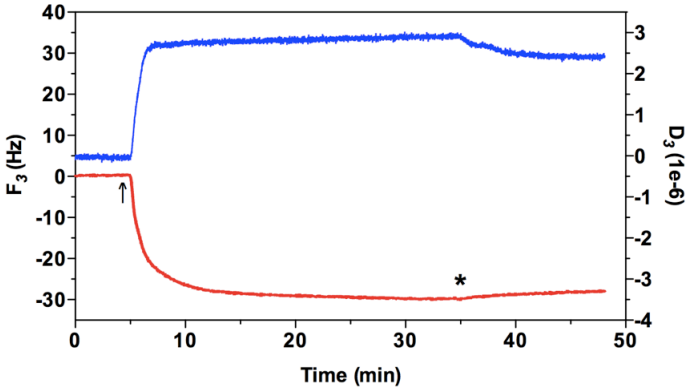

Figure 1. QCM-D profile obtained for the BSM adsorption on the functionalized gold surfaces: frequency (red lower line) and dissipation (blue upper line) shifts. Arrow indicates the BSM injection and star indicates the rinsing with buffer.

The effective immobilization of mucin on the quartz crystal resonator occurs due to covalent grafting of the protein with the functionalized surface. At low pH values, the reactive NHS-esters

formed on the gold surface after the EDC/NHS injection, interact with amino groups from the biomolecule inducing the formation of high stable covalent bonds. Mucin non-covalently bound and the remaining active groups on the surface were deactivated by the ethanolamine solution, before the injection of nanoparticle suspensions.

Curcumin-loaded nanoparticles decorated with mucoadhesive polymer chitosan were prepared by the nanoprecipitation method, after dissolution of polysaccharide in the aqueous phase. The concentrations of chitosan and poloxamer used in the nanoparticles preparation were optimized to obtain a monodisperse size distribution of surface-coated nanoparticles, as previously described by Mazzarino et al. (2012). Three different molar masses of chitosan were used for the nanoparticles preparation in order to investigate its influence on the mucoadhesive properties of the nanoparticles. Colloidal suspensions displayed a monomodal distribution of particles with hydrodynamic radius ranging from 115 to 126 nm for curcumin-loaded nanoparticles decorated with chitosan, respectively (Figure 2). Uncoated-nanoparticles were also prepared in the same conditions and investigated by QCM-D. The physicochemical characteristics of the nanoparticles are listed in Table 1. The positive surface charge displayed by the chitosan-coated nanoparticles confirmed the adsorption of mucoadhesive polymer on the nanoparticle surface, probably through hydrogen bonds between ether and amino groups of poloxamer and chitosan, respectively. Finally, all formulation showed encapsulation efficiency higher than 99 %, indicating their suitability in the encapsulation of hydrophobic drugs.

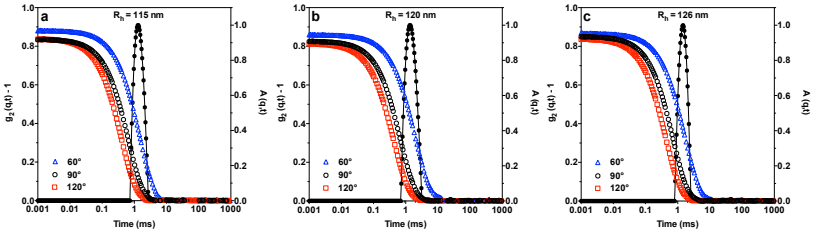

Figure 2. Autocorrelation functions $g_2(q,t)$ measured at different scattering angles (60°, 90°, and 120°) and decay time distributions $A(q,t)$ at 90°, as revealed by Contin analysis plot, for curcumin-loaded nanoparticles decorated with low (a), medium (b), and high (c) molar mass chitosan.

Table 1. Physicochemical characteristics of curcumin-loaded PCL nanoparticles.

Sample	R_h (nm)[a], PdI[b]	Zeta Potential (mV)	Drug content (μg mL^{-1})	Entrapment efficiency (%)
Cur-NP	105 (0.14)	- 0.036	467.4	99.6
Cur-NP CSL	115 (0.06)	17.8	456.3	99.6
Cur-NP CSM	120 (0.14)	24.4	512.5	99.4
Cur-NP CSH	126 (0.10)	23.4	479.0	99.8

[a] Hydrodynamic radius obtained using the Contin analysis (θ=90°).

[b] Polydispersity index obtained using the cumulant analysis (θ=90°).

Figure 3 shows the changes in frequency and dissipation recorded during the adsorption of BSM on the gold sensors followed by the addition of each nanoparticle suspension. When mucin surface was exposed to chitosan-coated nanoparticles, a rapid decrease in frequency and an increase in dissipation values were observed as a consequence of immediate adsorption of particles onto the mucin and increase of film viscoelasticity (Figures 3b, 3c and 3d). The rinsing with buffer resulted in a slight increase in frequency probably due to desorption of nonspecifically bound particles, indicating the strong interaction between BSM and chitosan-coated nanoparticles. No significant interaction between uncoated nanoparticles and BSM was detected by QCM-D (Figure 3a), confirming that the response is only related to their decoration with chitosan.

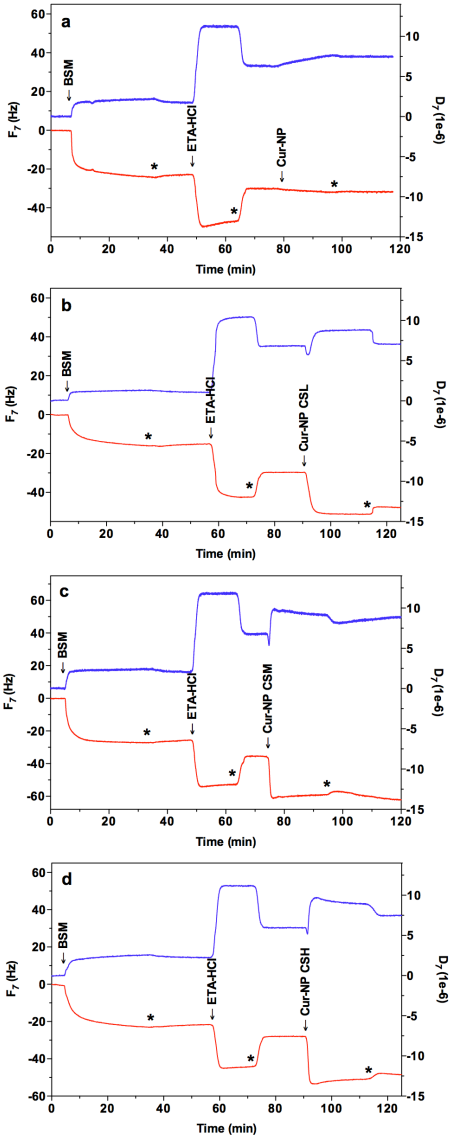

Figure 3. Frequency (red lower lines) and dissipation (blue upper lines) shifts as a function of time obtained for the adsorption of mucin on the gold sensors followed by the addition of nanoparticles: Cur-NP (a), Cur-NP CSL (b), Cur-NP CSM (c) and Cur-NP CSH (d). Presented data were obtained at the seventh

overtone. Arrows indicate the injection time of respective solutions and stars indicate the rinsing steps.

Due to a possible lateral heterogeneity of the nanoparticles layer, the viscoelastic model could not be used to determine their adsorbed mass. Consequently, our discussion remains essentially on a qualitative level. Figure 4 depicts the superposition of resonant frequency signals during the adsorption of nanoparticles on the BSM layer. The QCM-D profiles depicted in figure 4 shows that the changes in frequency are closed each other. As no significant behavior was observed between the three different molar masses decorating the Cur-NP, it allows concluding no influence of the molar mass chitosan on the adsorption of chitosan-coated nanoparticles on the BSM layer.

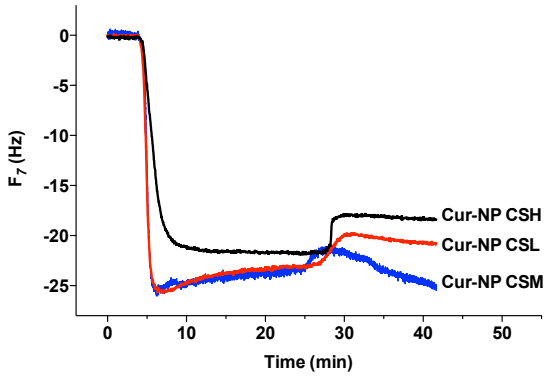

Figure 4. Superposition of resonant frequency signals (corresponding to the seventh overtone) during the adsorption of nanoparticles decorated with low (red line), medium (blue line) and high (black line) molar mass chitosan on the BSM layer.

Mucin has a pK_a of 2.6 due to the presence of sialic acid groups, and an isoelectric point of around 3 (SVENSSON, 2008). At pH=2, mucin molecules presented neutral or slightly negatively charged, however at pH=3 or higher the molecules are dissociated and then negatively charged, which favors its interaction with polycations. Previous studies reported that the interaction of chitosan (pK_a around 6.5) with BSM increases with the increase of pH, reaching a maximum value at pH 6, when the conditions for electrostatic interactions were reported to be more favorable (CHAYED; WINNIK, 2007).

The adsorption of chitosan-coated nanoparticles onto mucin layer is mainly related to electrostatic interactions between protonated amino groups (NH_3^+) of mucoadhesive polymer and negatively charged groups, like carboxylate (COO^-) or sulphonate (SO_3^-) groups, of protein carbohydrate chains. Some hydrophobic contributions can be also involved in the interactions of chitosan with mucin (DEACON et al., 2000; SVENSSON; THURESSON; ARNEBRANT, 2008).

The capacity of chitosan-coated nanoparticles to interact with the negatively charged mucosal surface is useful to prolong the contact time of drug delivery system in the mucosa, which may improve the therapeutic performance of drugs like curcumin. The intimate contact of modified curcumin-loaded nanoparticles with the mucin layer can enhance the drug absorption, by the capacity of chitosan in opening the tight junctions between mucosal cells, and, consequently, improves its bioavailability. Moreover, these mucoadhesive systems can offer the possibility of localized or systemic controlled drug delivery (CHOWDARY; RAO, 2004).

4. Conclusion

BSM was covalently grafted to the SAM-functionalized gold-coated quartz crystals forming a very stable layer. The adsorption of chitosan-coated nanoparticles containing curcumin on the mucin layer was proved by changes in frequency and dissipation, and was found to be independent to the molar mass of the mucoadhesive polysaccharide. Mucin-nanoparticle interactions were favored by electrostatic interactions between protonated amino groups of chitosan and negatively charged groups of protein. Uncoated nanoparticles showed no deposition on mucin layer, confirming that the mucoadhesive characteristics of these systems are only attributed to their decoration with chitosan. QCM-D proved to be a useful tool to evaluate the mucoadhesive properties of nanoparticles, allowing the real-time monitoring of nanocarriers/mucin interactions.

Author Information

Corresponding Author
*Author to whom correspondence should be addressed. Tel: +33 (0) 476 037 640. Fax: +33 (0) 476 547 629. E-mail: borsali@cermav.cnrs.fr.

Acknowledgments

The authors acknowledge the financial support from the CNRS and CAPES (CAPES-COFECUB Project No. 620/08).

References

ANDREWS, G. P.; LAVERTY, T. P.; JONES, D. S. Mucoadhesive polymeric platforms for controlled drug delivery. **Eur J Pharm Biopharm,** v. 71, n. 3, p. 505-518, 2009.

BANSIL, R.; TURNER, B. S. Mucin structure, aggregation, physiological functions and biomedical applications. **Curr Opin Colloid Interface Sci,** v. 11, n. 2-3, p. 164-170, 2006.

CHAYED, S.; WINNIK, F. M. In vitro evaluation of the mucoadhesive properties of polysaccharide-based nanoparticulate oral drug delivery systems. **Eur J Pharm Biopharm,** v. 65, n. 3, p. 363-370, 2007.

CHOWDARY, K. P.; RAO, Y. S. Mucoadhesive microspheres for controlled drug delivery. **Biol Pharm Bull,** v. 27, n. 11, p. 1717-1724, 2004.

DEACON, M. P.; MCGURK, S.; ROBERTS, C. J.; WILLIAMS, P. M.; TENDLER, S. J.; DAVIES, M. C.; DAVIS, S. S.; HARDING, S. E. Atomic force microscopy of gastric mucin and chitosan mucoadhesive systems. **Biochem J,** v. 348 Pt 3, p. 557-563, 2000.

DENKBAS, E. B.; OTTENBRITE, R. M. Perspectives on: chitosan drug delivery systems based on their geometries. **J Bioact Compat Polym,** v. 21, n. 4, p. 351-368, 2006.

FEILER, A. A.; SAHLHOLM, A.; SANDBERG, T.; CALDWELL, K. D. Adsorption and viscoelastic properties of fractionated mucin (BSM) and bovine serum albumin (BSA) studied with quartz crystal microbalance (QCM-D). **J Colloid Interface Sci,** v. 315, n. 2, p. 475-481, 2007.

FELDOTO, Z.; PETTERSSON, T.; DEDINAITE, A. Mucin-electrolyte interactions at the solid-liquid interface probed by QCM-D. **Langmuir,** v. 24, n. 7, p. 3348-3357, 2008.

GOEL, A.; KUNNUMAKKARA, A. B.; AGGARWAL, B. B. Curcumin as ‘‘curecumin’’: from kitchen to clinic. **Biochem Pharmacol,** v. 75, n. 4, p. 787-809, 2008.

KHUTORYANSKIY, V. V. Advances in mucoadhesion and mucoadhesive polymers. **Macromol Biosci,** v. 11, n. 6, p. 748-764, 2011.

LEMARCHAND, C.; GREF, R.; COUVREUR, P. Polysaccharide-decorated nanoparticles. **Eur J Pharm Biopharm,** v. 58, n. 2, p. 327-341, 2004.

LEMARCHAND, C.; GREF, R.; PASSIRANI, C.; GARCION, E.; PETRI, B.; MULLER, R.; COSTANTINI, D.; COUVREUR, P. Influence of polysaccharide coating on the interactions of nanoparticles with biological systems. **Biomaterials,** v. 27, n. 1, p. 108-118, 2006.

LIU, Z.; JIAO, Y.; WANG, Y.; ZHOU, C.; ZHANG, Z. Polysaccharides-based nanoparticles as drug delivery systems. **Adv Drug Deliv Rev,** v. 60, n. 15, p. 1650-1662, 2008.

MAZZARINO, L.; TRAVELET, C.; ORTEGA-MURILLO, S.; OTSUKA, I.; PIGNOT-PAINTRAND, I.; LEMOS-SENNA, E.; BORSALI, R. Elaboration of chitosan-coated nanoparticles loaded with curcumin for mucoadhesive applications. **J Colloid Interface Sci,** v. 370, n. 1, p. 58-66, 2012.

PATIL, S. B.; MURTHY, R. S. R.; MAHAJAN, H. S.; WAGH, R. D.; GATTANI, S. G. Mucoadhesive polymers: means of improving drug delivery. **Pharma Times,** v. 38, n. 4, p. 25-28, 2006.

REVIAKINE, I.; JOHANNSMANN, D.; RICHTER, R. P. Hearing what you cannot see and visualizing what you hear: interpreting quartz crystal microbalance data from solvated interfaces. **Anal Chem,** v. 83, n. 23, p. 8838-8848, 2011.

SERRA, L.; DOMENECH, J.; PEPPAS, N. A. Engineering design and molecular dynamics of mucoadhesive drug delivery systems as targeting agents. **Eur J Pharm Biopharm,** v. 71, n. 3, p. 519-528, 2009.

SOGIAS, I. A.; WILLIAMS, A. C.; KHUTORYANSKIY, V. V. Why is chitosan mucoadhesive? **Biomacromolecules,** v. 9, n. 7, p. 1837-1842, 2008.

SVENSSON, O. **Interactions of mucins with biopolymers and drug delivery particles**. 2008. 81 (Thesis). The Faculty of Health and Society, Malmö University, Malmö.

SVENSSON, O.; ARNEBRANT, T. Mucin layers and multilayers — Physicochemical properties and applications. **Curr Opin Colloid Interface Sci,** v. 15, n. 6, p. 395-405, 2010.

SVENSSON, O.; THURESSON, K.; ARNEBRANT, T. Interactions between chitosan-modified particles and mucin-coated surfaces. **J Colloid Interface Sci,** v. 325, n. 2, p. 346-350, 2008.

VOINOVA, M. V.; RODAHL, M.; JONSON, M.; KASEMO, B. Viscoelastic acoustic response of layered polymer films at fluid-solid interfaces: continuum mechanics approach. **Phys Scr,** v. 59, n. 5, p. 391-396, 1999.

WIECINSKI, P. N.; METZ, K. M.; MANGHAM, A. N.; JACOBSON, K. H.; HAMERS, R. J.; PEDERSEN, J. A. Gastrointestinal biodurability of engineered nanoparticles: development of an in vitro assay. **Nanotoxicology,** v. 3, n. 3, p. 202-214, 2009.

Publicação: ***"Curcumin-loaded chitosan-decorated nanoparticles for local therapy of buccal diseases"***
A ser submetida

Curcumin-loaded chitosan-decorated nanoparticles for local therapy of buccal diseases

Letícia Mazzarino[a,c], Gecioni Loch-Neckel[a], Andrea Mayumi Koroishi[a], Lorena dos Santos Bubniak[b], Suelen Mazzucco[b], Marcos A. Segatto-Silva[a], Maria C. Santos-Silva[b], Redouane Borsali[c] and Elenara Lemos-Senna[a,*]

[a] Departamento de Ciências Farmacêuticas, , [b]Departamento de Análises Clínicas, Centro de Ciências da Saúde, Universidade Federal de Santa Catarina, Campus Universitário Trindade, 88040-900, Florianópolis, SC, Brazil
[c] Centre de Recherches sur les Macromolécules Végétales (CERMAV-CNRS), BP 53, F-38041 Grenoble Cedex 9, France - affiliated with Université Joseph Fourier and member of the Institut de Chimie Moléculaire de Grenoble

* Corresponding author. E-mail address: lemos@ccs.ufsc.br

ABSTRACT

Mucoadhesive nanoparticles loaded with curcumin were developed in order to improve the therapeutic performance of this drug in the treatment of buccal diseases. PCL nanoparticles coated with different molar masses of mucoadhesive polysaccharide chitosan were prepared using the nanoprecipitation technique. The mucoadhesive properties of nanoparticle suspensions were demonstrated by their strong ability to interact with glycoprotein mucin through electrostatic forces. Similar permeation profiles of curcumin loaded in uncoated and chitosan-coated nanoparticles across porcine esophageal mucosa were found. Curcumin concentrations retained in the mucosa suggest the possibility of drug localizing effect. *In vitro* studies demonstrated that free curcumin and loaded into nanoparticles coated with chitosan caused significant reduction of L929 mouse fibroblast cell viability, in a concentration and time-dependent manner. However, no significant cell death was observed after 24 h of treatment with unloaded nanoparticles coated with chitosan. In addition, curcumin-loaded nanoparticles presented reduced cytotoxicity, when compared with free curcumin. Nanoparticle suspensions exhibited *in vitro* activity against *Candida albicans* strains, suggesting their potential use in the treatment of fungal infections. Then, mucoadhesive PCL nanoparticles represent a promisor strategy for the buccal delivery of curcumin aiming the local therapy of several oral diseases.

Keywords: Mucoadhesive nanoparticles; Chitosan-coated nanoparticles; Buccal delivery; Curcumin; Permeability; Cytotoxicity; Antifungal activity.

1. Introduction

The buccal region of oral cavity constitutes an attractive site for the delivery of drugs. The buccal mucosa is very convenient and easily accessible for administration of drugs, besides to be highly vascularized, more tolerant to potential allergens when compared to other mucous membranes, and has reduced tendency to irritation (SUDHAKAR; KUOTSU; BANDYOPADHYAY, 2006). The local treatment of oral cavity diseases has attracted a great interest, since it permits the drug delivery at the site of action, reducing the systemic drug distribution, and, consequently, the undesirable side effects. The localized therapy is used for the treatment of toothaches, gingivitis, periodontal diseases, dental caries, bacterial and fungal infections, aphthous ulcers, lichen planus, inflammation and dental stomatitis (SCHOLZ et al., 2008).

On the other hand, conventional drug dosage forms intended to buccal delivery often display a short residence time at the site of application due to the washing effect of saliva. The salivary secretion promotes the loss of dissolved/suspended drug, and consequently the involuntary removal of the dosage form, limiting, therefore, the drug absorption (SALAMAT-MILLER; CHITTCHANG; JOHNSTON, 2005). For this reason, the development of mucoadhesive delivery systems that are able to interact with the mucosal surface and to prolong the retention of drug at the site of action has been considered a promising approach for the treatment of oral diseases. Among the new mucoadhesive systems, polymeric nanoparticles offers additional advantages such as the much more intimate contact with the absorbing membranes, and efficient absorption due to the reduced particle size, besides to protect the drug against biological degradation, improving the bioavailability of the loaded therapeutic agent (LEMARCHAND; GREF; COUVREUR, 2004).

Nanoparticles coated with the polysaccharide chitosan have attracted a special interest as drug delivery systems due to its mucoadhesive properties. The cationic polyelectrolyte nature of chitosan provides a strong electrostatic interaction with the negatively charged mucosal surface, besides to promote a structural reorganization of tight junction-associated proteins of epithelial cells, increasing mucosal drug

transport (SCHIPPER et al., 1997). Moreover, chitosan is biocompatible, biodegradable, and exhibits good antimicrobial properties, being widely used for various pharmaceutical applications (SOGIAS; WILLIAMS; KHUTORYANSKIY, 2008; BERNKOP-SCHNURCH; DUNNHAUPT, 2012). Chitosan-coated nanoparticles have proven to be efficient drug carriers for ocular applications, since they increased significantly the corneal penetration of drugs as indomethacin and 5-fluorouracil, besides to display a good ocular tolerance (CALVO; VILA-JATO; ALONSO, 1997; NAGARWAL et al., 2010). When orally administered, chitosan-coated PLGA nanoparticles exhibited a stronger bioadhesive potency and higher pharmacological activity of insulin than uncoated PLGA nanoparticles (ZHANG et al., 2012). Mucoadhesive nanoemulsions prepared by addition of chitosan into colloidal suspensions also provided the fastest and largest extent of transport of risperidone through the nasal olfactory epithelium, when compared to a risperidone solution and risperidone-loaded nanoemulsions prepared without chitosan (KUMAR et al., 2008).

Curcumin is a yellow polyphenol extracted from the rhizome of turmeric (*Curcuma longa*) that displays numerous biological activities, including antioxidant, anti-inflammatory, anticarcinogenic, and antimicrobial effects (GOEL; KUNNUMAKKARA; AGGARWAL, 2008). Some studies have indicated the potential therapeutic application of curcumin in the treatment of yeast infections. Curcumin exhibits antifungal activity against albicans and non-albicans species of Candida, which are responsible for the oral yeast infections, via generation of oxidative stress, and inhibits hyphae development by targeting the global suppressor thyamidine uptake 1 (TUP1) (MARTINS et al., 2009; SHARMA et al., 2010).

Considering the above mentioned, in this study we evaluate the potential application of chitosan-coated PCL nanoparticles for the buccal delivery of curcumin aiming the local treatment of oral cavity diseases. The permeation profiles of curcumin through porcine esophageal mucosa as well as the mucoadhesive properties of chitosan-coated nanoparticles are evaluated. In addition, the cytotoxicity of the nanoparticles on L929 mouse fibroblast cells and the *in vitro* antifungal activity of curcumin against *Candida albicans* strains are also investigated. Recently, some studies have reported the incorporation of curcumin in mucoadhesive nanoparticles (SUWANNATEEP et al., 2011; AKHTAR; RIZVI; KAR, 2012), however the absence of studies about the development of curcumin-loaded in chitosan-coated

nanoparticles intended for the local therapy of buccal diseases evidences the novelty of this work.

2. Materials and methods

2.1. Materials

Curcumin (≥ 94% curcuminoid content, ≥ 80% curcumin), polycaprolactone (PCL, MW 60,000), chitosan, N-(3-dimethylaminopropyl)-N′-ethylcarbodiimide hydrochloride (EDC), N-hydroxysuccinimide (NHS), ethanolamine hydrochloride, and all other chemicals were purchased from Sigma (St. Louis, MO, USA). Low (CSL 50,000 - 190,000), medium (CSM 190,000 - 310,000) and high (CSH 310,000 to > 375,000) molar mass chitosan were used in the experiments. According to the manufacturer, the degree of deacetylation is between 75 - 85 % for CSL and CSM, and higher than 75 % for CSH. Poloxamer 188 (Lutrol F68®) was kindly donated by BASF Chemical Company (Ludwigshafen, Germany). Mucin from bovine submaxillary gland (BSM, Type I-S) was purchased from Sigma (St. Louis, MO, USA) and used as received.

2.2. Nanoparticles preparation

Curcumin-loaded PCL nanoparticles (Cur-NP) were prepared using the nanoprecipitation method, as previously described by Mazzarino et al. (2012) An organic solution containing 60 mg of PCL and 5 mg of curcumin in 12 mL of acetone was added into 24 mL of an aqueous phase (pH 5) containing 1 % acetic acid and 0.25 % (w/v) poloxamer 188, under moderate magnetic stirring. Acetone was then removed and the final volume adjusted to 10 mL by evaporation under reduced pressure. The polymeric nanoparticle suspensions were filtered through 1.2-µm pore-sized filter papers (Sartorius Stedim Biotech, Göttingen, Germany). For the preparation of chitosan-coated PCL nanoparticles, low, medium or high molar mass chitosan (CSL, CSM or CSH, respectively) were previously dispersed in the aqueous phase of the formulations at concentrations of 0.1 % (w/v).

2.3. Nanoparticles characterization

2.3.1. Particle size

The size distribution, mean particle size and the polydispersity index (PdI) of nanoparticle suspensions were determined by Dynamic Light Scattering (DLS) using an ALV 5000 (ALV-Langen, Germany) equipped with a red helium-neon laser at a wavelength of 632.8 nm operating at a power of 35 mW. After appropriate dilution in ultrapure Milli-Q® water, samples were placed in cylindrical measurements cells and immersed in a toluene bath with temperature regulated at 25 °C. Each analysis was performed during 120 s and the scattered light was measured at different scattering angles ranging from 20 to 150 °. The hydrodynamic radius (R_h) was calculated using Stokes-Einstein equation, $R_h = \kappa_B T/6\pi\eta D$ where κ_B is Boltzmann constant (in J/K), T is the temperature (in K), D is the diffusion coefficient and η is the viscosity of the medium – pure water in this case (η = 0.89 cP at 25 °C).

2.3.2. Zeta potential

Zeta potential was determined by laser-doppler anemometry using a Zetasizer Nano Series (Malvern Instruments, Worcestershire, UK). Samples were diluted in Milli-Q® water and placed in electrophoretic cells, where a potential of ± 150 mV was applied. The measurements were performed at 25 °C. The zeta potential values were calculated as mean electrophoretic mobility values using Smoluchowski's equation.

2.3.3. Drug content and encapsulation efficiency

Curcumin was determined by a fluorescence spectrophotometry method previously validated (MAZZARINO et al., 2010a). The total concentration of curcumin in the nanoparticle suspensions was measured after complete dissolution of the particles in acetonitrile. The encapsulation efficiency was calculated by the difference between the total concentration of curcumin found in the nanoparticle suspensions and the concentration of free drug in the ultrafiltrate obtained after the separation of nanoparticles by ultrafiltration/centrifugation at 10,000 rpm for 15 min using Amicon Centrifugal Filter Devices with Ultracel-100 membrane (100 kDa, Millipore Corp., USA). The drug content was expressed in μg of curcumin/mL of colloidal suspension.

2.4. Evaluation of mucoadhesive properties

Mucoadhesive properties of nanoparticles were evaluated by surface plasmon resonance (SPR) using a Biacore X100 instrument (GE Healthcare) at 25 °C in acetate buffer (10 mM, pH 6, 150 mM NaCl). BSM (0.5 $mg.mL^{-1}$ in acetate buffer pH 4 and centrifuged at 7,000 rpm for 5 min) was immobilized on the dextran matrix of a CM4 sensor chip (GE Healthcare Bio-Sciences AB, Uppsala, Sweden) by amino coupling method. The dextran layer was activated twice for 7 min by injection of EDC and NHS solutions at a flow rate of 10 $\mu L.min^{-1}$. Approximately 250 resonance units (RU) of mucin were immobilized to the sensor chip. Remaining active sites were then blocked with 1 M ethanolamine-HCl pH 8.5. Finally, interactions studies were performed by the injection (association 500 s, dissociation 500 s) of nanoparticle suspensions (25 $\mu g.mL^{-1}$ in acetate buffer pH 6) on the mucin layer. After each measurement, the sensor chip surface was regenerated with 6 injections of NaCl 5 M and EDTA 0.35 M solutions at a flow rate of 10 $\mu L.min^{-1}$ for 4 min.

2.5. Permeation studies

2.5.1. Tissue preparation

Porcine esophagi were obtained from a local slaughterhouse (Antônio Carlos, Brazil) and transported in simulated saliva solution pH 6.75. Esophagus was cut longitudinally and rinsed with water. Esophageal mucosae were then carefully separated from the underlying tissues using surgical scissors and placed in simulated saliva solution pH 6.75 until mounting them in the diffusion cells. Mucosae were used until 4 h after the animals were sacrificed. Permeation studies were performed using tissues from at least two animals.

2.5.2. Permeation experiments

In vitro permeation studies were carried out using vertical Franz diffusion cells with a diffusional area of 2.27 cm^2. Esophageal mucosa was clamped between the donor and receptor compartments of the diffusion cells with the epithelial side facing the donor compartment. The receptor compartment was filled with 11.5 mL of simulated saliva solution pH 6.75 containing 0.5 % (w/v) of sodium dodecyl sulfate to maintain the *sink* conditions. The mounted cells were allowed to equilibrate for 15 min in a water bath at 37^o C. Following, approximately 200 µL of each curcumin-loaded nanoparticles

suspension (100 μg of curcumin) was placed in the donor compartment. Cells were kept protected from light to avoid degradation, and the receptor medium was continuously stirred at 500 rpm. At predetermined time intervals, samples (2 mL) were withdrawn from the receptor compartment and the volume removed was immediately replaced with fresh medium. Curcumin concentration in the fresh medium was determined by a spectrofluorimetric method as described below.

At the end of the permeation experiments, the curcumin retained in the mucosa was determined. The excess of formulation was wiped with absorbent paper and the tissue was removed from the diffusion cells, cut in small pieces, and placed in glass tubes with 5 mL of methanol. The samples were vortexed, kept overnight at 4 °C protected from light, and sonicated for 50 min. The samples were, then, filtered through 0.45 μm pore-size membranes (Millipore Corp., USA), and the curcumin content was assayed by the spectrofluorimetric method as described below. All experiments were carried out in six replicates.

2.5.3. Curcumin determination

Curcumin concentration in the samples was determined by fluorescence spectrophotometry using a LS 55 Perkin Elmer Spectrophotometer. Samples were placed in a standard 1 cm quartz cell. Both slits of excitation and emission monochromators were adjusted to 5.0 nm. Samples were excited at 424 nm and the emission spectra were recorded from 435 to 700 nm. The relative fluorescence intensities for curcumin permeation and retention studies were measured at λ_{emi} of 495 nm and at λ_{emi} of 535 nm, respectively. The spectrofluorimetric method was validated using the following parameters: specificity, linearity, accuracy, precision, and limits of detection (LOD) and quantification (LOQ). A calibration curve of curcumin was constructed using simulated saliva solution pH 6.75 containing 0.5 % of sodium dodecyl sulfate and was linear over the range of 0.01 to 0.5 μg/mL ($R^2 = 0.998$). The regression equation of the media calibration graph (n = 3) was y = 513.9 x – 1.382, and LOD and LOQ values were 0.004 and 0.014 μg/mL, respectively, indicating that the method was sufficiently sensitive to determine curcumin concentration in the receiver medium. For retention studies, the calibration curve of curcumin in methanol was linear over the range of 0.05 to 1.0 μg/mL ($R^2 = 0,996$). The regression equation of the media calibration graph (n = 3) was y = 721.2 x + 24.51, and LOD and LOQ values were 0.011 and 0.034 μg/mL, respectively, and also indicating the method was sensitive to determine curcumin in

the tissue samples. The recovery values for both assays ranged from 95.5 to 107.8 %, satisfying the acceptance criteria for accuracy in these studies. The intra-day and inter-day relative standard deviation values were lower than 5 %, indicating an acceptable variability of the curcumin content determination ($P < 0.05$).

2.5.4. Data analysis

The cumulative amount of curcumin permeated per unit of area was plotted as a function of time. The steady-state flux (J_{ss}) was obtained from the slope of the linear portion of the curve using linear-regression analysis, and the lag time (T_{lag}) by the intersection of the linear portion with the abscissa axis. The permeability coefficient (Kp) was calculated using the following equation:

$$Kp = \frac{J_{ss}}{C_0}$$

where J_{ss} is the steady-state flux and C_0 is the initial concentration of drug in the donor compartment. The steady-state flux (J_{ss}) and the amount of curcumin retained in the mucosa at the end of the experiments were statistically evaluated by one-way analysis of variance followed by Bonferroni's post-hoc, using the Graph-Pad Prism software (San Diego, CA, USA).

2.6. Histological examination of mucosa

Eight hours following the treatment of esophageal mucosae with nanoparticle suspensions on Franz diffusion cells, the tissues were evaluated in order to verify possible histological changes. For that, the excess of formulation was wiped with absorbent paper and the permeated areas of mucosae were removed from the diffusion cells. Mucosae were fixed in 4 % paraformaldehyde solution, dehydrated progressively in ethanol, and embedded in paraffin. Sections of 5 μm thickness were cut vertical to the surface using a microtome, mounted on glass slides, and then deparaffinized. The sections were stained using hematoxylin/eosin (H/E) following histological standard procedures. Images of mucosae sections were acquired using a Sight DS-5 M-L1 digital camera connected to an Eclipse 50i light microscope (both from Nikon, Melville, USA).

2.7. Evaluation of in vitro cytotoxicity

L929 mouse fibroblast cells (Rio de Janeiro, Brazil) were cultured in Dulbecco's Modified Eagle's medium (DMEM, Sigma) supplemented with 10 % fetal bovine serum, 100 U/mL penicillin, 100 μg/mL streptomycin and 10 mM HEPES, pH 7.4 at 37 °C in a 5 % CO_2 humidified atmosphere. Free curcumin or curcumin-loaded PCL nanoparticles were added to cells (5 x10^5 cells/well, 2.5 x 10^5 cells/well, 1.25 x 10^4 cells/well) and incubated at 37 °C for 24, 48 or 72 hours, respectively. *In vitro* cell viability was assessed using MTT (3-(4,5-dimethiazol-zyl)-2-5-diphenyltetrazolium bromide, Sigma Chemical Co., St. Louis, MO, USA) assay (VAN DE LOOSDRECHT et al., 1991). The initial screening of curcumin and curcumin-loaded nanoparticles at 100 μM concentration was performed to identify the cytotoxic effectiveness against L929 cells. Subsequently, cells were incubated in the presence of different concentrations of curcumin (1 - 100 μM) for 24, 48 and 72 hours. Control group was only plated with cell culture medium and MTT reagent. All assays were performed in triplicate. The statistical analysis was performed using two-way analysis of variance followed by Bonferroni's post-hoc, using the Graph-Pad Prism software (San Diego, CA, USA).

2.8. Morphological assessment of apoptosis

Apoptotic death was verified as described by Geng et al. (2003). L929 cells (5 x 10^5 cells/well) were incubated with free curcumin, unloaded and curcumin-loaded PCL nanoparticles coated with chitosan at their respective 50 % inhibitory concentration (IC_{50}) values for 24 hours. Then, the coverslips covering the bottom of the plate were removed, washed with PBS and treated with 40 μL of acridine orange (10 μg/mL) and ethidium bromide (5 μg/mL) solution. Cells were examined under a fluorescence microscope (Olympus BX-FLA) and representative fields were photographed using a digital camera (Olympus BX40, Japan). Viable cells exhibited green fluorescence (acridine orange staining) whereas apoptotic cells exhibited an orange-red nuclear fluorescence (ethidium bromide staining).

2.9. Evaluation of the curcumin antifungal activity

The antifungal activity of free curcumin and incorporated in PCL nanoparticles decorated with chitosan against *Candida albicans* (ATCC No. 10231) was performed by the broth microdilution assay following the CLSI (2002). Candida growth in Sabouraud dextrose (SDA, Difco Laboratories, Detrit, MI, USA) agar were suspended in sterile saline solution to obtain a cell concentration of 1 x 10^6 colony forming units-per milliliter (0.5 McFarland). Free curcumin, unloaded and curcumin-loaded nanoparticles were diluted with Sabouraud broth to obtain a final concentrations ranging from 0.19 to 100 μg/mL. Nystatin was also evaluated as a positive control. The plates were incubated at 37 °C for 24 h and the fungal growth was visually observed. Susceptibility was expressed as minimum inhibitory concentration (MIC) and minimum fungicidal concentration (MFC). The minimum inhibitory concentration (MIC) was defined as the lowest concentration required to completely inhibit the growth of the fungi at the end of 24 h of incubation. Minimum fungicidal concentration (MFC) was determined by sub-culturing a 10 mL aliquot of the medium drawn from the culture tubes showing no macroscopic growth at the end of 24 h of culture on Sabouraud dextrose agar plates and incubated further for the appearance of yeast-like growth. The plates were scored for growth of the yeast colonies. The lowest concentration of the antifungal agent from which negative growth or fewer than 3 colonies were recorded was considered as minimum fungicidal concentration (MFC). Experiments were performed in triplicate.

3. Results and discussion

3.1. Preparation of chitosan-coated nanoparticles loaded with curcumin

Chitosan-coated PCL nanoparticles loaded with curcumin were prepared by the nanoprecipitation method using the conditions previously optimized by Mazzarino et al. (2012). In this previous study, the authors evaluated the effect of chitosan and poloxamer concentration, as well as, the effect of chitosan molar mass, on the physicochemical properties of the nanoparticle suspensions. Monodisperse colloidal dispersions (polydispersity index < 0.2) displaying hydrodynamic radius ranging from 104 to 125 were obtained when chitosan and poloxamer were employed in the aqueous phase of the formulations at concentration of 0.1 % (w/v) and 0.25 % (w/v),

respectively. The decoration of nanoparticles with chitosan was evidenced by the changes in particle size and zeta potential values of the nanoparticles. The size of the nanoparticles increased with the chitosan addition to the formulations, indicating the adsorption of mucoadhesive polysaccharide on the nanoparticle surface; the higher the chitosan molar mass, the higher the particle size. In addition, chitosan-coated nanoparticles displayed positive surface charge of about 30 mV, while zeta potential of uncoated PCL nanoparticles was close to zero. The increase in the zeta potential values was attributed to the presence of the amino groups positively charged of chitosan on the surface of the particles. Previous studies have shown that the adsorption of chitosan molecules on the nanoparticle surface occurs due to the formation of hydrogen bonds between ether and amino groups of poloxamer and chitosan, respectively (CALVO et al., 1997; SASHINA; VNUCHKIN; NOVOSELOV, 2006b) Finally, nanoparticles showed a curcumin content around of 450 μg/mL and encapsulation efficient values higher than 99 %, demonstrating their suitability in the encapsulation of curcumin. The physicochemical properties of curcumin-loaded PCL nanoparticles used in this study are summarized in Table 1.

Table 1. Physicochemical properties of uncoated and chitosan-coated nanoparticles containing curcumin.

Sample	R_h (nm)[a]	Zeta potential (mV)	Drug content (μg/mL)	Encapsulation efficiency (%)
Cur-NP	104	0.052	502	> 99
Cur-NP CSL	114	23.5	503	> 99
Cur-NP CSM	120	40.1	494	> 99
Cur-NP CSH	125	32.7	473	> 99

[a] Obtained using the Contin analysis at 90° scattering angle.

3.2. Evaluation of the mucoadhesive properties

The mucoadhesive properties of curcumin-loaded PCL nanoparticles were evaluated by means of the assessment of the interactions between mucin (BSM) and nanoparticles by surface plasmon resonance. For that, BSM was immobilized onto the surface of a CM4 sensor chip through the spontaneous formation of covalent bonds between reactive NHS-esters from dextran surface with the amino groups from glycoprotein. Mucin non-covalently bound and the

remaining active groups on the surface were deactivated by adding an ethanolamine solution, before the nanoparticle injection. The existence of interactions between the mucin (ligant) and nanoparticles (analyte) is verified by the changes in the refractive index near (within ~ 300 nm) occurred at the surface of the sensor after injection of the colloidal dispersion through the cell, under continuous flow. This refractive index change is measured in real time (sampling in a kinetic analysis experiment is taken every 0.1 s), and the result is plotted in a resonance units (RU) response *versus* time graph (termed a sensorgram).

Figure 1 shows the sensorgram obtained after the injection of uncoated and chitosan-coated nanoparticles over the mucin immobilized sensor chip. The exposure of mucin surface to the chitosan-coated nanoparticles caused a rapid increase in the RU response, as consequence of their immediate binding onto the BSM layer. At the end of their injection, no significant decrease in response was observed, indicating the strong interaction between chitosan-coated nanoparticles and mucin. However, no response was detected after the injection of uncoated nanoparticles, indicating that chitosan coating is crucial to obtain mucoadhesive PCL-based nanoparticles. It is well established that the interactions between chitosan-coated nanoparticles and mucin are mainly related to electrostatic forces between protonated amino groups of mucoadhesive polysaccharide and negatively charged groups of glycoprotein (DEACON et al., 2000; SVENSSON; THURESSON; ARNEBRANT, 2008). However, in spite of the differences observed in the RU responses obtained for Cur-NP CSL, Cur-NP CSM, and Cur-NP CSH, it is not possible to predict differences between their mucoadhesive forces; since for quantitative determination, it is necessary to calculate the dissociation constant (K_D) of each sample through kinetic analysis.

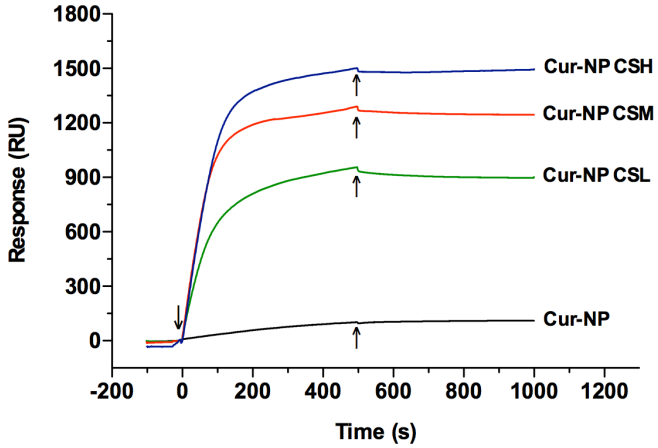

Figure 1. Sensorgram for the mucin immobilized chip after injection of uncoated (Cur-NP) and chitosan-coated (Cur-NP CSL, Cur-NP CSM and Cur-NP CSH) nanoparticles. Arrows indicate the injection (↓) and stop (↑) time of respective solutions.

3.3. Permeation studies

In vitro permeation studies were carried out using Franz diffusion cells and porcine esophageal mucosa as membrane. Porcine esophageal mucosa has been considered a suitable model for buccal permeability studies. The use of buccal mucosa in permeation studies presents some limitations, such as the limited surface area, damage caused by mastication, and hard and time-consuming excision procedure. In this way, esophageal mucosa has been proposed as a good substitute for the buccal tissue, since it offers a larger and generally intact surface area, and easier preparation. Esophageal mucosa consists of a stratified squamous non-keratinized epithelium, with a high proportion of glycosylceramides and low amount of ceramides, similarly to the buccal mucosa. Furthermore, permeability studies of drugs using both buccal and esophageal mucosae as barriers have demonstrated similar results (DIAZ DEL CONSUELO et al., 2005; DIAZ-DEL CONSUELO et al., 2005; CAON; SIMOES, 2011). Mucosa of pigs is frequently used as model for *in vitro* permeability studies due to its higher similarity to human tissue, in terms of structure and composition, that any other animal (SHOJAEI, 1998).

The permeation of curcumin-loaded nanoparticles across esophageal mucosa is shown in Figure 2. The permeability parameters

and the amount of curcumin retained in the esophageal mucosa after 8 hours of permeation experiment are listed in Table 2. As can be observed in this table, curcumin fluxes ranged from 0.096 ± 0.018 to 0.149 ± 0.025 $\mu g.cm^{-2}.h^{-1}$, depending on the composition of the formulation. However, statistically significant difference for this parameter was verified only when nanoparticles coated with low molar mass chitosan (Cur-NP CSL) was compared with that prepared with medium molar mass chitosan (Cur-NP CSM) ($P < 0.05$). The lag time is a permeation parameter that is dependent mainly on the diffusivity of the drug through the membrane and ranged from 1.08 to 2.75 h. The lowest value of curcumin retained in the esophageal mucosa was also verified when Cur-NP CSM as tested ($P < 0.05$). However, in spite of the statistical significances observed, it was not possible to assert that there was an effect of the chitosan molar mass, and even of the nanoparticle decoration with chitosan, on the permeation profile of curcumin.

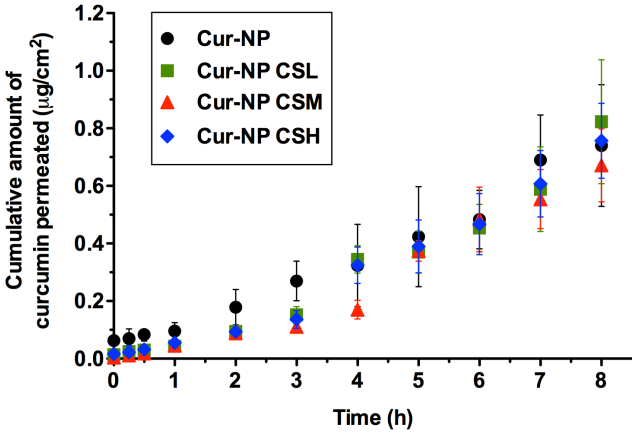

Figure 2. Permeation profiles of curcumin loaded in uncoated (Cur-NP) and chitosan-coated nanoparticles (Cur-NP CSL, Cur-NP CSM and Cur-NP CSH) through porcine esophageal mucosa. Data are presented as mean ± SD (n = 6).

Table 2. Steady-state flux (J_{ss}), lag time (T_{lag}), permeability coefficient (K_p) and amount of curcumin retained in mucosa.

Samples	J_{ss} ($\mu g.cm^{-2}.h^{-1}$)	T_{lag}[a] (h)	K_p ($cm.h^{-1}.10^{-4}$)	Drug retained ($\mu g.cm^{-2}$)
Cur-NP	0.114 ± 0.031	1.38	1.694 ± 0.463	1.367 ± 0.314
Cur-NP CSL	0.149 ± 0.025[b]	2.75	2.436 ± 0.419	1.742 ± 0.548[b]
Cur-NP CSM	0.096 ± 0.018	1.08	1.687 ± 0.309	0.854 ± 0.165
Cur-NP CSH	0.124 ± 0.020	2.02	1.921 ± 0.306	1.509 ± 0.287[b]

Data are presented as mean ± SD (n= 6). [a] Calculated from the mean permeation curves. [b] $P < 0.05$ compared to Cur-NP CSM.

There are two permeation pathways for passive transport across the mucosa: paracellular and transcellular routes. Intercellular spaces and cytoplasm are hydrophilic in character and, then, lipophilic drugs would have low solubilities in this environment. On the contrary, cell membrane is rather lipophilic in nature and permeability of hydrophilic drugs through the cell membrane is low (SANGEETHA et al., 2010). Previous studies have demonstrated that chitosan has a significant enhancing effect on the permeation of drugs across the buccal mucosa. This effect have been related to the mucoadhesive properties of chitosan, that increase the retention of the drug at the application site, and to the change in the morphology and histology of the mucosa due to the repacking of the epithelium cells up to the basal membrane and the partial disarrangement of desmosomes (SENEL et al., 2000; SENEL; HINCAL, 2001; SANDRI et al., 2006). The enhancement potential of chitosan in gel form for oral mucosa was studied by Senel and Hincal (2001) with two potential therapeutic compounds, hydrocortisone, a commonly used hydrophobic anti-inflammatory agent, and transforming growth factor beta (TGF-β), which is a bioactive peptide. *In vitro* flux of both compounds across buccal mucosa was significantly increased with chitosan gel with a greater lag time for TGF-β, which is a large peptide. However, the hydrophilicity of the compound also had an effect; hydrocortisone exhibited a relatively less penetration into the deeper tissue layers whereas more of the hydrophilic TGF-β reached the deeper layer. Then, the inability of chitosan decoration in to increase the permeation of curcumin through the esophageal mucosa demonstrated in this study may be explained by the physicochemical properties of this drug. Since curcumin is a hydrophobic drug, it will permeate preferentially through the cell membrane, i.e., by transcellular transport, which, in turn, has demonstrated to be less affected by the interactions

of chitosan with the mucosa. On the other hand, these results do not necessary represent the effect that would be observed in *in vivo* studies. Chitosan-coated PCL nanoparticles have proven to display good mucoadhesive properties that associated to their high degree of dispersibility and superficial contact area would increase the residence time at the site of application, and improve drug availability for drug absorption and therapeutic activity.

3.4. Histological examination of mucosa

The microphotographs of the mucosa sections stained with hematoxylin and eosin after treatment with the nanoparticle suspensions (Cur-NP, Cur-NP CSL, and Cur-NP CSM) are shown in Figure 3. The epithelial cells display dark stained nuclei and the cell plasma membranes appear as well-defined dark-stained borders. Untreated mucosa showed epithelia with cells tightly bonded together without any spaces between cell plasma membranes After the treatment of the tissue with curcumin-loaded nanoparticles, the epithelium appeared swollen and had thickness increased, but mainly in the mucosa treated with chitosan-coated nanoparticles, the epithelial cells of the basal and intermediate layers appears to display larger spaces between cells, indicating that some disarranging and opening of the junctions between cells may be occurred. Similar results were found in a previous study that aimed to evaluate the effect of chitosan and trimethyl chitosan on the buccal permeability of drugs (SANDRI et al., 2006).

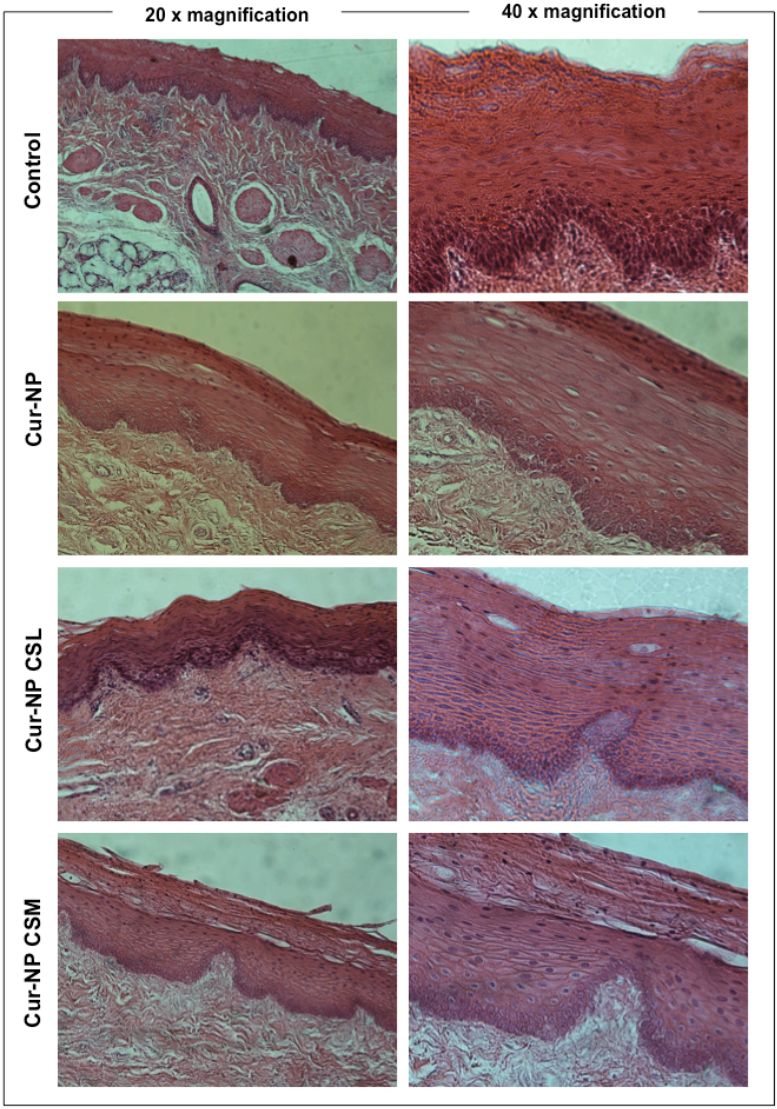

Figure 3. Light micrographs of excised porcine esophageal mucosae. Representative histological sections of mucosae control and treated with Cur-NP, Cur-NP CSL, and Cur-NP CSM for 8 hours were examined microscopically after H/E staining with magnification x20 and x40.

3.5. Cytotoxic effect on L929 cells

Cytotoxic effect of free curcumin and curcumin-loaded PCL nanoparticles coated with chitosan (Cur-NP CSL) was evaluated using L929 mouse fibroblast cells by MTT assay for 24, 48, and 72 hours (Figure 4). The incubation of L929 cells with unloaded PCL nanoparticles coated with chitosan (NP CSL) provoked an increase in the number of viable cells after 24 h of incubation; antiproliferative effects could be visualized only after 48 h of incubation. The incubation of cells with free curcumin and chitosan-coated nanoparticles loaded with curcumin at concentration of 100 mm caused a significant reduction of cell viability, in a time-dependent manner ($P < 0.05$). However, the highest cytotoxicity effect was displayed by free curcumin; the reduction in the number of viable cells after 72 h of incubation was about 90 %, while curcumin-loaded nanoparticles provoked about 40 % of reduction at the same time. This effect may be explained by the encapsulation of the drug inside the nanoparticles, which renders the drug less available to act on the cells.

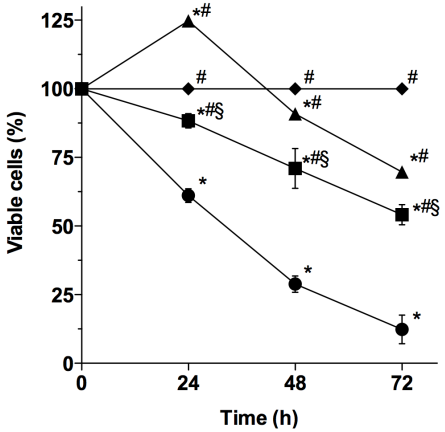

Figure 4. Cytotoxic effect of samples on L929 mouse fibroblast cells after 24, 48, and 72 hours of incubation: control (◆), NP CSL (▲), Cur-NP CSL (■), and free curcumin (●). Samples were added to cells at 100 μM concentration. Optical density of control was taking as 100 % of cell viability. The results are the mean ± SEM of at least three independent experiments. $^{*}P < 0.05$ compared with control group; $^{\#}P < 0.05$ compared with free curcumin; $^{\S}P < 0.05$ compared between NP CSL and Cur-NP CSL groups at the same concentration.

The cytotoxic effect of free curcumin and Cur-NP CSL was also dependent on drug concentration (Figure 5). The IC_{50} values of free curcumin or incorporated in chitosan-coated PCL nanoparticles were estimated, and the results are listed in Table 3. The IC_{50} values of curcumin-loaded nanoparticles were significantly higher than those presented by free curcumin at all exposure times ($P < 0.05$), supporting the above mentioned concerning the effect of the encapsulation on curcumin cytotoxicity.

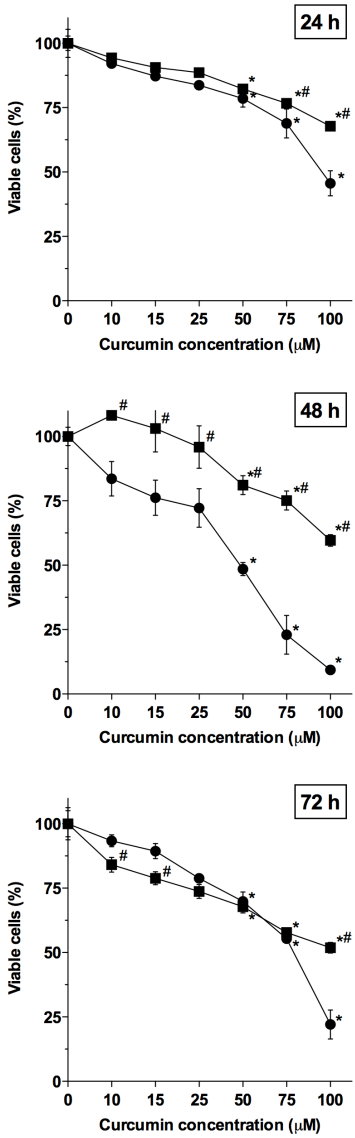

Figure 5. Cytotoxic effect of Cur-NP CSL (■) and free curcumin (●) at different concentrations on L929 mouse fibroblast cells after 24, 48, and 72 hours of incubation. Optical density of control was taking as 100 % of cell viability. The results are the mean ± SEM of at least three independent

experiments. $^{*}P < 0.05$ compared with control group; $^{\#}P < 0.05$ compared with free curcumin at the same concentration.

Table 3. IC_{50} values of free curcumin and curcumin-loaded PCL nanoparticles coated with chitosan for cell viability on L929 cells.

	IC_{50} (μM)		
	24 h	**48 h**	**72 h**
L929			
Free Curcumin	87.90 ± 2.12	46.47 ± 1.22	19.62 ± 0.98
Cur-NP CSL	219.4 ± 1.67*	215.4 ± 8.16*	92.48 ± 1.53*

The cell viability was monitored through the MTT assay. Optical density of control was taken as 100 % of cell viability. Data are presented as mean ± SEM of at least three independent experiments. $^{*}P < 0.05$ represents significant difference compared to treatment with free curcumin.

The ability of free curcumin and curcumin-loaded PCL nanoparticles to induce apoptosis on L929 mouse fibroblast cells was investigated using acridine orange/ethidium bromide staining (Figure 6). Control group (not treated cells) showed bright green nuclei with uniform intensity, evidencing the cell viability. Curcumin-treated L929 cells were intensely labeled with ethidium bromide (red fluorescence), indicating the lost of their membrane integrity and the nuclear condensation. The treatment of cells with both free curcumin and curcumin-loaded nanoparticles for 24 h increased the number of apoptotic cells, when compared with control group. The cytotoxicity exhibited by the nanoparticles may be attributed to the presence of curcumin, since unloaded nanoparticles were not able to induce significant cell death after 24 h of incubation.

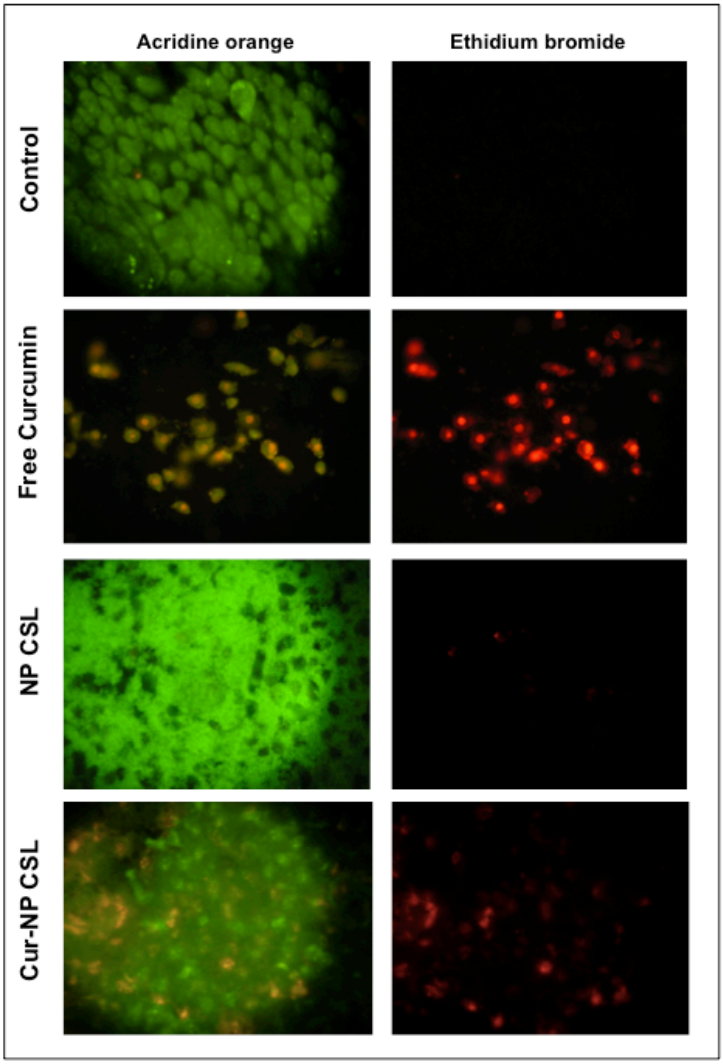

Figure 6. Detection of apoptosis on L929 fibroblast cells by acridine orange/ethidium bromide method. Cells were incubated with free curcumin, unloaded (NP CSL) and curcumin-loaded nanoparticles decorated with chitosan (Cur-NP CSL) at their respective IC_{50} values for 24 hours. Viable cells exhibited green fluorescence (acridine orange staining) whereas apoptotic cells exhibited orange-red nuclear fluorescence (ethidium bromide staining). The group without treatment was taken as control group.

3.6. Antifungal activity

The antifungal activity of curcumin-loaded nanoparticles was evaluated by their ability to inhibit growth of *C. albicans*. The oral cavity candidiasis is an opportunistic infection that affects mainly elderly and immunocompromised patients, including HIV positive patients. Considering the restricted number of commercially available antifungal drugs that not display considerable side effects, the development of new antifungal formulations appears to be an important strategy to reduce morbidity and mortality associated to fungal infections. The minimal inhibitory and fungicidal concentration values of free curcumin, and curcumin-loaded nanoparticles are summarized in Table 4. Free curcumin and curcumin-loaded nanoparticles showed a MIC of 50 μg/mL. The MFC obtained for free curcumin and Cur-NP CSH was 50 μg/mL, while 100 μg/mL was found to Cur-NP, Cur-NP CSL, and Cur-NP CSM. Nystatin, used as standard drug, showed a MIC of 0.8 μg/mL, and a MFC of 1.6 μg/mL. A representative picture of agar plates used in the growth inhibition test of *C. albicans* is shown in Figure 7.

Table 4. Minimal inhibitory concentration (MIC) and minimal fungicidal concentration (MFC) of curcumin, free or loaded in PCL nanoparticles, against *C. albicans*.

	MIC (μg/mL)	**MFC (μg/mL)**
Nystatin (positive control)	0.8	1.6
Free Curcumin	50	50
Cur-NP	50	100
Cur-NP CSL	50	100
Cur-NP CSM	50	100
Cur-NP CSH	50	50

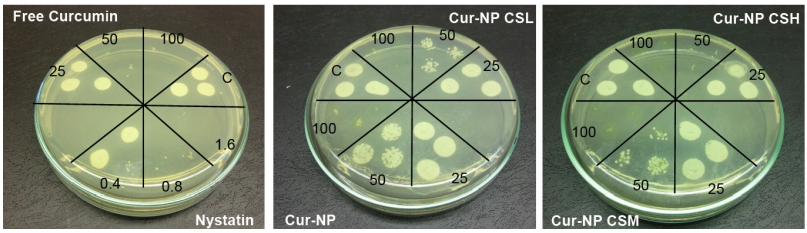

Figure 7. Growth inhibition test of *C. albicans*. Each spot was added with 10 μL sample containing different concentrations (25, 50, and 100 μg/mL) of free curcumin, curcumin-loaded nanoparticles (Cur-NP, Cur-NP CSL, Cur-NP CSM, and Cur-NP CSH), and nystatin (0.4, 0.8, and 1.6 100 μg/mL), used as reference. Control (C) received no treatment.

For comparative purposes, equal volumes of unloaded nanoparticles were also evaluated in order to verify the influence of the other formulation components. Unloaded nanoparticles showed some inhibition on the fungal growth, but no fungicidal effect was obtained at the concentrations tested (MFC > 100 μg/mL). This antifungal activity is probably related to the natural antimicrobial properties exhibited by chitosan. The presence of curcumin in the nanoparticle suspensions showed to improve the antifungal activity of nanoparticles coated with chitosan. Recent studies reported that the antifungal activity of chitosan into nanoparticles against *C. albicans* is significantly better than the solution form. The inhibitory effects on the fungal growth were influenced by the particle size and zeta potential values of chitosan nanoparticles (ING et al., 2012).

4. Conclusion

Mucoadhesive nanoparticles loaded with curcumin were successfully prepared by the decoration of PCL nanoparticles with polysaccharide chitosan. Their mucoadhesive properties were demonstrated by the strong ability of chitosan-coated nanoparticles to interact with the glycoprotein mucin through electrostatic forces. The drug retention in the mucosa after treatment with curcumin-loaded nanoparticles suggests the applicability of these systems in the therapy of numerous diseases for obtaining local effects. *In vitro* studies demonstrated that the incorporation of curcumin into chitosan-coated PCL nanoparticles was able to decrease significantly the drug toxicity on L929 fibroblast cells. In addition, all curcumin-coated nanoparticles showed effective antifungal activity, evidencing their potential use in

the treatment of oral cavity candidiasis. Therefore, mucoadhesive PCL nanoparticles constitute a good strategy to improve the residence time and the therapeutic effectiveness of curcumin on the buccal mucosa.

Acknowledgements

The authors acknowledge the financial support from CAPES (CAPES-COFECUB Project No. 620/08) and CNRS. The authors are grateful the contributions of Aymeric Audfray and Anne Imberty on the Biacore analysis, and Christophe Travelet on the light scattering experiments.

References

AKHTAR, F.; RIZVI, M. M.; KAR, S. K. Oral delivery of curcumin bound to chitosan nanoparticles cured Plasmodium yoelii infected mice. **Biotechnol Adv,** v. 30, n. 1, p. 310-320, 2012.

BERNKOP-SCHNURCH, A.; DUNNHAUPT, S. Chitosan-based drug delivery systems. **Eur J Pharm Biopharm**, 2012.

CALVO, P.; REMUÑAN-LÓPEZ, C.; VILA-JATO, J. L.; ALONSO, M. J. Chitosan and chitosan/ethylene oxide-propylene oxide block copolymer nanoparticles as novel carriers for proteins and vaccines. **Pharm Res,** v. 14, n. 10, p. 1431-1436, 1997.

CALVO, P.; VILA-JATO, J. L.; ALONSO, M. J. Evaluation of cationic polymer-coated nanocapsules as ocular drug carriers. **Int J Pharm,** v. 153, n. 1, p. 41-50, 1997.

CAON, T.; SIMOES, C. M. Effect of freezing and type of mucosa on ex vivo drug permeability parameters. **AAPS PharmSciTech,** v. 12, n. 2, p. 587-592, 2011.

CLSI. **Reference method for broth dilution antifungal susceptibility testing of yeasts**. Approved standard M27-A2. Wayne, USA: CLSI, 2002.

DEACON, M. P.; MCGURK, S.; ROBERTS, C. J.; WILLIAMS, P. M.; TENDLER, S. J.; DAVIES, M. C.; DAVIS, S. S.; HARDING, S. E.

Atomic force microscopy of gastric mucin and chitosan mucoadhesive systems. **Biochem J,** v. 348 Pt 3, p. 557-563, 2000.

DIAZ DEL CONSUELO, I.; PIZZOLATO, G.-P.; FALSON, F.; GUY, R. H.; JACQUES, Y. Evaluation of pig esophageal mucosa as a permeability barrier model for buccal tissue. **J Pharm Sci,** v. 94, n. 12, p. 2777-2788, 2005.

DIAZ-DEL CONSUELO, I.; JACQUES, Y.; PIZZOLATO, G.-P.; GUY, R. H.; FALSON, F. Comparison of the lipid composition of porcine buccal and esophageal permeability barriers. **Arch Oral Biol,** v. 50, n. 12, p. 981-987, 2005.

GENG, C. X.; ZENG, Z. C.; WANG, J. Y. Docetaxel inhibits SMMC-7721 human hepatocellular carcinoma cells growth and induces apoptosis. **World J Gastroenterol,** v. 9, n. 4, p. 696-700, 2003.

GOEL, A.; KUNNUMAKKARA, A. B.; AGGARWAL, B. B. Curcumin as ‘‘curecumin’’: from kitchen to clinic. **Biochem Pharmacol,** v. 75, n. 4, p. 787-809, 2008.

ING, L. Y.; ZIN, N. M.; SARWAR, A.; KATAS, H. Antifungal activity of chitosan nanoparticles and correlation with their physical properties. **Int J Biomater,** v. 2012, p. 632698, 2012.

KUMAR, M.; MISRA, A.; BABBAR, A. K.; MISHRA, A. K.; MISHRA, P.; PATHAK, K. Intranasal nanoemulsion based brain targeting drug delivery system of risperidone. **Int J Pharm,** v. 358, n. 1-2, p. 285-291, 2008.

LEMARCHAND, C.; GREF, R.; COUVREUR, P. Polysaccharide-decorated nanoparticles. **Eur J Pharm Biopharm,** v. 58, n. 2, p. 327-341, 2004.

MARTINS, C. V.; DA SILVA, D. L.; NERES, A. T.; MAGALHAES, T. F.; WATANABE, G. A.; MODOLO, L. V.; SABINO, A. A.; DE FATIMA, A.; DE RESENDE, M. A. Curcumin as a promising antifungal of clinical interest. **J Antimicrob Chemother,** v. 63, n. 2, p. 337-339, 2009.

MAZZARINO, L.; BELLETTINI, I. C.; MINATTI, E.; LEMOS-SENNA, E. Development and validation of a fluorimetric method to determine curcumin in lipid and polymeric nanocapsule suspensions. **BJPS,** v. 46, n. 2, p. 219-226, 2010.

MAZZARINO, L.; TRAVELET, C.; ORTEGA-MURILLO, S.; OTSUKA, I.; PIGNOT-PAINTRAND, I.; LEMOS-SENNA, E.; BORSALI, R. Elaboration of chitosan-coated nanoparticles loaded with curcumin for mucoadhesive applications. **J Colloid Interface Sci,** v. 370, n. 1, p. 58-66, 2012.

NAGARWAL, R. C.; SINGH, P. N.; KANT, S.; MAITI, P.; PANDIT, J. K. Chitosan coated PLA nanoparticles for ophthalmic delivery: characterization, in-vitro and in-vivo study in rabbit eye. **J Biomed Nanotechnol,** v. 6, n. 6, p. 648-657, 2010.

SALAMAT-MILLER, N.; CHITTCHANG, M.; JOHNSTON, T. P. The use of mucoadhesive polymers in buccal drug delivery. **Adv Drug Deliv Rev,** v. 57, n. 11, p. 1666-1691, 2005.

SANDRI, G.; POGGI, P.; BONFERONI, M. C.; ROSSI, S.; FERRARI, F.; CARAMELLA, C. Histological evaluation of buccal penetration enhancement properties of chitosan and trimethyl chitosan. **J Pharm Pharmacol,** v. 58, n. 10, p. 1327-1336, 2006.

SANGEETHA, S.; VENKATESH, D. N.; KRISHAN, P. N.; SARASWATHI, R. Mucosa as a route for systemic drug delivery. **RJPBCS,** v. 1, n. 3, p. 178-187, 2010.

SASHINA, E. S.; VNUCHKIN, A. V.; NOVOSELOV, N. P. A study of the thermodynamics of chitosan interaction with polyvinyl alcohol and polyethylene oxide by differential scanning calorimetry. **Russian Journal of Applied Chemistry,** v. 79, n. 10, p. 1643-1646, 2006.

SCHIPPER, N. G.; OLSSON, S.; HOOGSTRAATE, J. A.; DEBOER, A. G.; VARUM, K. M.; ARTURSSON, P. Chitosans as absorption enhancers for poorly absorbable drugs 2: mechanism of absorption enhancement. **Pharm Res,** v. 14, n. 7, p. 923-929, 1997.

SCHOLZ, O. A.; WOLFF, A.; SCHUMACHER, A.; GIANNOLA, L. I.; CAMPISI, G.; CIACH, T.; VELTEN, T. Drug delivery from the oral

cavity: focus on a novel mechatronic delivery device. **Drug Discov Today,** v. 13, n. 5-6, p. 247-253, 2008.

SENEL, S.; HINCAL, A. A. Drug permeation enhancement via buccal route: possibilities and limitations. **J Control Release,** v. 72, n. 1-3, p. 133-144, 2001.

SENEL, S.; KREMER, M. J.; KAS, S.; WERTZ, P. W.; HINCAL, A. A.; SQUIER, C. A. Enhancing effect of chitosan on peptide drug delivery across buccal mucosa. **Biomaterials,** v. 21, n. 20, p. 2067-2071, 2000.

SHARMA, M.; MANOHARLAL, R.; PURI, N.; PRASAD, R. Antifungal curcumin induces reactive oxygen species and triggers an early apoptosis but prevents hyphae development by targeting the global repressor TUP1 in Candida albicans. **Biosci Rep,** v. 30, n. 6, p. 391-404, 2010.

SHOJAEI, A. H. Buccal mucosa as a route for systemic drug delivery: a review. **J Pharm Pharm Sci,** v. 1, n. 1, p. 15-30, 1998.

SOGIAS, I. A.; WILLIAMS, A. C.; KHUTORYANSKIY, V. V. Why is chitosan mucoadhesive? **Biomacromolecules,** v. 9, n. 7, p. 1837-1842, 2008.

SUDHAKAR, Y.; KUOTSU, K.; BANDYOPADHYAY, A. K. Buccal bioadhesive drug delivery - a promising option for orally less efficient drugs. **J Control Release,** v. 114, n. 1, p. 15-40, 2006.

SUWANNATEEP, N.; BANLUNARA, W.; WANICHWECHARUNGRUANG, S. P.; CHIABLAEM, K.; LIRDPRAPAMONGKOL, K.; SVASTI, J. Mucoadhesive curcumin nanospheres: biological activity, adhesion to stomach mucosa and release of curcumin into the circulation. **J Control Release,** v. 151, n. 2, p. 176-182, 2011.

SVENSSON, O.; THURESSON, K.; ARNEBRANT, T. Interactions between chitosan-modified particles and mucin-coated surfaces. **J Colloid Interface Sci,** v. 325, n. 2, p. 346-350, 2008.

VAN DE LOOSDRECHT, A. A.; NENNIE, E.; OSSENKOPPELE, G. J.; BEELEN, R. H. J.; LANGENHUIJSEN, M. M. A. C. Cell mediated cytotoxicity against U 937 cells by human monocytes and macrophages in a modified colorimetric MTT assay: A methodological study. **J Immunol Methods,** v. 141, n. 1, p. 15-22, 1991.

ZHANG, X.; SUN, M.; ZHENG, A.; CAO, D.; BI, Y.; SUN, J. Preparation and characterization of insulin-loaded bioadhesive PLGA nanoparticles for oral administration. **Eur J Pharm Sci,** v. 45, n. 5, p. 632-638, 2012.

CAPÍTULO 3: DESENVOLVIMENTO DE NANOPARTÍCULAS DE XILOGLUCANA-*b*-POLICAPROLACTONA DECORADAS COM QUITOSANA PARA A LIBERAÇÃO BUCAL DA CURCUMINA

Nos últimos anos, os copolímeros em bloco constituídos por segmentos hidrofílicos e hidrofóbicos têm atraído grande atenção devido ao seu comportamento único em meio aquoso e suas potenciais aplicações nos sistemas de liberação de fármacos. A habilidade de auto-organização dos copolímeros em estruturas ordenadas ocorre devido a incompatibilidade dos diferentes blocos e depende tanto da natureza química dos blocos, quanto da estrutura molecular do copolímero. Os copolímeros em bloco anfifílicos representam uma ampla família de materiais de sequências ordenadas de dois ou mais monômeros diferentes unidos por ligações covalentes organizados em diferentes arquiteturas (QUAGLIA et al., 2008).

Na maioria dos estudos, nanopartículas são formadas a partir de copolímeros dibloco AB e triblocos do tipo ABA ou BAB, onde A é o bloco hidrofóbico formador do núcleo, e B é o bloco hidrofílico formador da casca. Assim, nanopartículas preparadas a partir de copolímeros em bloco anfifílicos são capazes de solubilizar diversas substâncias hidrofóbicas em seu núcleo. Geralmente, os blocos hidrofóbicos são polímeros hidrolisáveis em soluções aquosas e passíveis de decomposição, tais como poliamidas e poliésteres; enquanto o bloco hidrofílico, geralmente, é composto de poli (óxido de etileno) (PEO) devido as suas propriedades de circulação prolongada, apesar de nos últimos anos outros polímeros hidrofílicos estarem sendo utilizados (SACHL et al., 2007).

O desenvolvimento de nanopartículas a partir do copolímero em bloco xiloglucana-policaprolactona (XGO-*b*-PCL) é proposto neste trabalho como uma estratégia para a obtenção de sistemas coloidais sem a necessidade do uso de surfactantes. A xiloglucana é um polissacarídeo encontrado na parede celular primária da maioria das plantas terrestres, apresentando funções estruturais, regulatórias/sinalizadoras e de armazenamento (LUCYSZYN et al., 2011; FRANKOVA; FRY, 2012). Este polissacarídeo é altamente substituído, atóxico e biodegradável, sendo sua estrutura química composta por uma cadeia principal constituída de *β*-(1,4)-D-glucana parcialmente substituída por α-(1,6)-D-xilose, e alguns resíduos de xilose substituídos por β-(1,2)-D-galactoxilose (Figura 10). A xiloglucana é solúvel em água e possui vários grupos OH, os quais podem facilmente formar ligações de hidrogênio (CHEN et al., 2012).

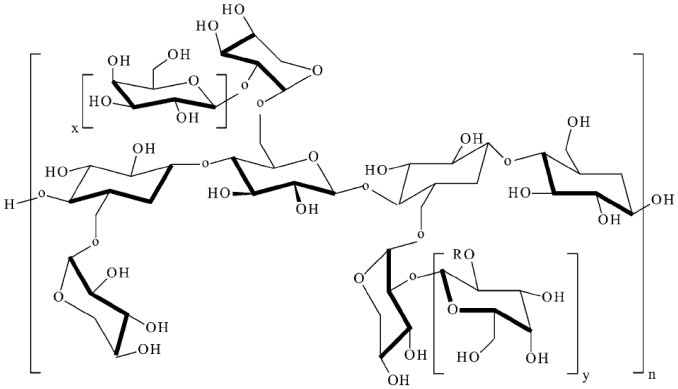

Figura 10. Estrutura da unidade monomérica da xiloglucana. Fonte: Chen et al. (2012).

A xiloglucana possui várias aplicações na indústria alimentícia, de papel, têxtil e farmacêutica. Recentemente, a utilização da xiloglucana como material biomédico vem se tornando cada vez mais popular na área médica, sendo sua aplicação na preparação de carreadores para a liberação de fármacos, peptídeos e proteínas uma das mais importantes (CHEN et al., 2012). Assim, considerando as propriedades de biocompatibilidade e biodegradabilidade da xiloglucana e da policaprolactona, a síntese do novo copolímero em bloco XGO-*b*-PCL parece ser uma alternativa interessante para a preparação de nanopartículas visando a liberação de fármacos.

Este capítulo descreve o desenvolvimento de nanopartículas de XGO-*b*-PCL decoradas com quitosana para a liberação bucal da curcumina nas mucosas. A preparação e avaliação biofarmacêutica das nanopartículas XGO-*b*-PCL contendo curcumina e decoradas com quitosana encontram-se redigidas sob a forma de artigo, o qual será submetido para publicação no periódico *Biomaterials*. Nesta publicação, as nanopartículas são preparadas utilizando diferentes concentrações de quitosana, e caracterizadas quanto ao tamanho de partícula, morfologia, potencial zeta e teor de curcumina. A avaliação das propriedades mucoadesivas pela técnica de ressonância plasmônica de superfície e da citotoxicidade *in vitro* dos sistemas também é relatada. Detalhes sobre a caracterização do copolímero estão descritos na seção *"supporting information"* desta publicação.

Publicação: ***"Xyloglucan-block-poly(ε-caprolactone) copolymer nanoparticles coated with chitosan as biocompatible mucoadhesive drug delivery system"***
A ser submetida

Xyloglucan-*block*-poly(ε-caprolactone) copolymer nanoparticles coated with chitosan as biocompatible mucoadhesive drug delivery system

Letícia Mazzarino [a,b], Issei Otsuka [a], Sami Halila [a], Lorena dos Santos Bubniak [c], Suelen Mazzucco [c], Maria C. Santos-Silva [c], Elenara Lemos-Senna [b], and Redouane Borsali [a,*]

[a] *Centre de Recherches sur les Macromolécules Végétales (CERMAV, UPR-CNRS 5301), affiliated with Université Joseph Fourier (UJF) and member of the Institut de Chimie Moléculaire de Grenoble (ICMG, FR-CNRS 2607), BP 53, F-38041 Grenoble Cedex 9, France.*
[b] *Departamento de Ciências Farmacêuticas, Centro de Ciências da Saúde, Universidade Federal de Santa Catarina (UFSC), Campus Universitário Trindade, 88040-900, Florianópolis, SC, Brazil.*
[c] *Departamento de Análises Clínicas, Centro de Ciências da Saúde, Universidade Federal de Santa Catarina (UFSC), Campus Universitário Trindade, 88040-900, Florianópolis, SC, Brazil*

* Corresponding author. E-mail: redouane.borsali@cermav.cnrs.fr; Fax: +33 4 76 03 76 29.

ABSTRACT

This paper describes the preparation of novel xyloglucan-*block*-poly(ε-caprolactone) (XGO-*b*-PCL) nanoparticles decorated with the mucoadhesive polysaccharide, chitosan, for delivering of hydrophobic drugs in mucous membranes. Monodisperse block copolymer nanoparticles were prepared by the co-solvent method. The mean hydrodynamic radius (R_h) of unloaded and curcumin-loaded XGO-*b*-PCL nanoparticles was around 50 and 55 nm, respectively. Transmission electron microscopy (TEM) images showed compact and spherical particles. Curcumin was successfully encapsulated within the PCL-based hydrophobic core, in a drug to polymer ratio of 1:5. The decoration of XGO-*b*-PCL nanoparticles with chitosan resulted in an increase of approximately 10 nm in the mean particle radius and positive surface charge. Surface plasmon resonance (SPR) measurements demonstrated the mucoadhesive properties of chitosan-coated nanoparticles by its exceptional ability to interact with mucin through electrostatic forces. Finally, *in vitro* studies demonstrated that curcumin into copolymer nanoparticles showed reduced cytotoxicity when

compared to free drug, and higher cytotoxic effects against B16F10 melanoma cells than L929 fibroblast cells.

Keywords: Block copolymer nanoparticles; Mucoadhesive nanoparticles; Polysaccharide coating; Chitosan-coated nanoparticles; Curcumin; Cytotoxicity.

1. Introduction

Amphiphilic block copolymers have attracted increasing interest in the biomedical field due to their ability to self-assemble into well-organized structures (e.g., nanoparticles, micelles, vesicles, nano-organized thin films) and their potential applications in drug delivery systems. This self-assembling tendency arises from the incompatibility of different blocks and depends on the chemical nature of the blocks as well as on the molecular structure of the copolymer (QUAGLIA et al., 2008). Generally, nanoparticles are formed of AB diblock and ABA or BAB triblock copolymers, where A is a hydrophobic core-forming block, and B is a hydrophilic shell-forming block, when dispersed in an aqueous media. These systems are especially attractive for solubilization and encapsulation of hydrophobic drugs in their cores, which may lead to the increase of drug absorption and bioavailability (SACHL et al., 2007; MERISKO-LIVERSIDGE; LIVERSIDGE, 2008).

Recent studies (OTSUKA et al., 2010; SCHATZ; LECOMMANDOUX, 2010; DE MEDEIROS MODOLON et al., 2012; OTSUKA et al., 2012a; OTSUKA et al., 2012b; ISONO et al., 2013) have shown considerable interest in the development of block copolymers containing oligo- or polysaccharides. The main motivation of using polysaccharides in block copolymer originates from their biodegradability and biocompatibility, besides they are safe, non-toxic, and have abundant natural sustainable resources. Amphiphilic block copolymers consisting of a polysaccharide segment and a synthetic one are able to self-assemble in aqueous solution into nanoparticles, which are formed by shells of the saccharidic block and cores of the synthetic block (OTSUKA et al., 2012b).

In this context, the present study aims to develop nanoparticles based on the XGO-*b*-PCL diblock copolymer. Xyloglucan is a non-toxic and biodegradable polysaccharide found in the primary cell walls of higher plants. In recent years, the use of xyloglucan as biomedical material is becoming more popular. One important application is their use as carriers and targeting systems to deliver drugs (CHEN et al.,

2012). Poly(ε-caprolactone) (PCL) is a hydrophobic biodegradable aliphatic polyester that has received considerable attention for use in drug delivery devices and others biomedical applications (WEI et al., 2009). PCL is degraded by hydrolysis of its esters linkages in physiological conditions in a much more slowly way than others polyesters, which can be interesting for the preparation of long-term implants and prolonged delivery systems (KUMARI; YADAV; YADAV, 2010; RASEKH et al., 2011).

Over the last decades, the use of carriers able to modulate the release and absorption characteristics of drugs has constituted an important approach for the development of new drug dosage forms. However, the success of these systems has been frequently limited by their short residence time at the site of absorption (CHOWDARY; RAO, 2004). In this way, the development of mucoadhesive carriers can be advantageous, since the dosage form is retained for longer period of time in intimate contact with absorbing membranes. Nanoparticles decorated with polysaccharides have shown a great potential for drug delivery via the mucous membranes of different body sites due to their molecular recognition and mucoadhesive properties (LEMARCHAND; GREF; COUVREUR, 2004; LEMARCHAND et al., 2006). The potential use of chitosan as mucoadhesive agent is highlighted by its capacity to interact with the negatively charged mucus layer and allowing an enhancement in permeation effect, based on the cationic character of these polysaccharide (BERNKOP-SCHNURCH; DUNNHAUPT, 2012)

In this study, monodisperse nanoparticles are prepared from the new XGO-*b*-PCL diblock copolymer by cosolvent method. These systems were coated with the mucoadhesive polysaccharide, chitosan, and loaded with a hydrophobic active compound. The ability of XGO-*b*-PCL nanoparticles to load hydrophobic drugs was evaluated using curcumin, a natural polyphenol extracted from *Curcuma longa* (turmeric). This drug displays various interesting pharmacological activities (e.g., antitumor, anti-inflammatory, and antimicrobial), but has limited therapeutic application due to its poor aqueous solubility and low bioavailability (ANAND et al., 2007). The mucoadhesive properties of chitosan-coated XGO-*b*-PCL nanoparticles were evaluated for their ability to interact with the glycoprotein mucin. Finally, *in vitro* studies were carried out to evaluate the cytotoxicity of these systems on L929 mouse fibroblast and B16F10 mouse melanoma cells.

2. Experimental Section

2.1. Materials

Curcumin (≥ 94% curcuminoid content, ≥ 80% curcumin), chitosan, *N*-(3-dimethylaminopropyl)-N′-ethylcarbodiimide hydrochloride (EDC), *N*-hydroxysuccinimide (NHS), ethanolamine hydrochloride, *N,N,N',N'',N''*-pentamethyldiethylenetriamine (PMDETA, purity = 99%) and copper(I) bromide (CuBr, purity > 99.999%), and all other chemicals were purchased from Sigma (St. Louis, MO, USA). Low molar mass chitosan of approximately 50,000 - 190,000 Da and a degree of deacetylation between 75 % and 85 % was used in the experiments. Mucin from bovine submaxillary gland (BSM, Type I-S) was also purchased from Sigma and used as received. Diblock copolymer containing xyloglucooligosaccharide and polycaprolactone (XGO-*b*-PCL) was synthesized by "click" reaction between a propargyl group at the reducing end of XGO (propargyl-XGO) (HALILA et al., 2008) and a PCL having a terminal azido group (PCL-N_3; M_n = 10,320 determined by ^{1}H NMR spectrum) (OTSUKA et al., 2012a), according methodology previously reported in the literature. Details of characterization of the diblock copolymer are described in supporting information.

2.2. Synthesis of XGO-b-PCL

A degassed solution of propargyl-XGO (100 mg, 0.074 mmol) and PMDETA (18 μL, 0.085 mmol) in DMF (20 mL) was added to a degassed solution of PCL-N_3 (0.57 g, 0.057 mmol) and CuBr (12 mg, 0.085 mmol) in DMF (15 mL) under argon atmosphere. The mixture was stirred at 60 °C for 5 days. After cooling to room temperature, the reaction mixture was passed through a pad of alumina and eluted with THF. The polymer was purified by reprecipitation using DMF as a good solvent and cold MeOH as a poor solvent to give XGO-*b*-PCL as a white solid (0.57 g). Yield, 88%.

2.3. Nanoparticles preparation

Diblock copolymer nanoparticles (NP XGO-*b*-PCL, Cp = 1.0 mg/mL) were prepared using the cosolvent method. Typically, 5.0 mg of XGO-*b*-PCL copolymer was added to a closed vial containing 2.0 mL of THF. After stirring for at least 3 hours, the nanoparticles formation was

obtained by the addition of the copolymer solution in 10 mL of Milli-Q water. Subsequently, the suspension was stirred for 1 hour and the organic solvent was removed by evaporation under reduced pressure and the colloidal suspension concentrated to 5 mL. The preparation of curcumin-loaded nanoparticles (Cur-NP XGO-*b*-PCL) was carried out from previous addition with curcumin in THF.

2.4. Nanoparticles decoration with chitosan

The preparation of chitosan-decorated XGO-*b*-PCL nanoparticles (NP XGO-*b*-PCL CS) was carried out by single adsorption. Adsorption of chitosan was preformed by the addition of a 1 % (w/v) chitosan solution to the copolymer nanoparticle suspension. Chitosan solution was prepared in 1 % (v/v) acetic acid under magnetic stirring at room temperature. The final chitosan concentration in the nanoparticle suspensions varied from 0.01 % to 0.25 % (w/v).

2.5. Determination of the drug content in the nanoparticles

Curcumin content in the nanoparticle suspension was determined using a Perkin-Elmer Lambda 10 UV/VIS spectrophotometer at 420 nm. The calibration graph for curcumin in acetonitrile was linear over the range of 1.0 to 6.0 μg/mL with a correlation coefficient of 0.997. For determination of the entrapment efficiency, each sample was placed in Amicon Centrifugal Filter Devices with Ultracel-100 membrane (100 kDa, Millipore Corp., USA) and centrifuged at 10,000 rpm for 15 min to separate the free drug in the supernatant from the curcumin-loaded nanoparticles. Curcumin entrapment efficiency was calculated from the difference between the total concentration of curcumin ($Conc_{total}$) found in the nanoparticle suspensions, after their complete dissolution in acetonitrile, and the concentration of drug in the supernatant ($Conc_{supernatant}$), according to the following equation:

$$\text{Entrapment Efficiency (\%)} = \frac{\text{Conc}_{\text{total}} - \text{Conc}_{\text{supernatant}}}{\text{Conc}_{\text{total}}} \times 100$$

Drug recovery was calculated from the difference between the total concentration of drug found in the colloidal suspensions with the initial concentration ($Conc_{initial}$) added to the formulations, according to the following equation:

$$\text{Drug Recovery (\%)} = \frac{\text{Conc}_{\text{initial}} - \text{Conc}_{\text{total}}}{\text{Conc}_{\text{initial}}} \times 100$$

2.6. Zeta potential measurements

Zeta potential was determined by laser-doppler anemometry using a Zetasizer Nano Series (Malvern Instruments, Worcestershire, UK). Nanoparticle samples were diluted in ultrapure Milli-Q® water and placed in the electrophoretic cell where a potential of ± 150 mV was established. The ζ potential values were calculated as mean electrophoretic mobility values using Smoluchowski's equation.

2.7. Dynamic light scattering (DLS) measurements

Scattering measurements were performed using an ALV 5000 (ALV-Langen, Germany) equipped with a red helium-neon laser at a wavelength of 632.8 nm operating at a power of 35 mW. After dilution in ultrapure Milli-Q® water, nanoparticle samples were placed in cylindrical measurements cells and immersed in a toluene bath with temperature regulated at 25 °C. The scattered photons were detected by a very sensitive avalanche diode. In this study, the modulus of the scattering vector is denoted q and is equal to $(4\pi n/\lambda)\sin(\theta/2)$ where n represents the refractive index of pure water, θ is the scattering angle and λ designates the light wavelength. Each experiment was performed during 120 s and the scattered light was measured at different angles ranging from 20 to 155 °. The scattering intensity was corrected taking into account the contributions of the solvent (water) and the toluene (standard) as well as the change of the scattering volume with the detection angle. The hydrodynamic radius (R_h) was determined using Stokes-Einstein equation, $R_h = \kappa_B T/6\pi\eta D$ where κ_B is Boltzmann constant (in J/K), T is the temperature (in K), D is the diffusion coefficient and η is the viscosity of the medium – pure water in this case (η = 0.89 cP at 25 °C). Curcumin-loaded nanoparticles show no absorption at the wavelength used in light scattering experiments, *i.e.* 632.8 nm.

2.8. Transmission electron microscopy (TEM) examinations

The morphology of the nanoparticles was examined using a CM200 Philips transmission electron microscope (FEI Company, Hillsboro, USA). Nanoparticle suspension previously diluted in ultrapure Milli-Q® water was dropped on a carbon-coated copper grid and negatively stained with 2% (w/v) uranyl acetate.

2.9. Nanoparticle tracking analysis (NTA) measurements

NTA experiments were performed using a digital microscope LM10 System (NanoSight, Salisbury, UK). Samples were diluted in Milli-Q® water and introduced into the chamber by a syringe. Video images of particles movement under Brownian motion were analyzed by the NTA analytical software version 2.1. The measurements were made at room temperature and each video clip was captured over 30 s.

2.10. Surface plasmon resonance (SPR)

SPR experiments were performed on a Biacore X100 instrument (GE Healthcare) at 25 °C in acetate buffer (10 mM, pH 6, 150 mM NaCl) at a flow rate of 10 µL/min. BSM (0.5 mg/mL in acetate buffer pH 4 and previously centrifuged at 7,000 rpm for 5 min) was immobilized on the dextran matrix of a CM4 sensor chip (GE Healthcare Bio-Sciences AB, Uppsala, Sweden) by amino coupling method. The dextran layer was activated twice for 7 min by injection of EDC and NHS solutions at a flow rate of 10 µL/min. Approximately 250 resonance units (RU) of mucin were immobilized to the sensor chip. Remaining active sites were then blocked with 1 M ethanolamine-HCl pH 8.5. Finally, interactions studies were performed by the injection (association 500 s, dissociation 500 s) of nanoparticle suspensions (25 µg/mL in acetate buffer pH 6) on the mucin layer. After each measurement, the sensor chip surface was regenerated with 6 injections of NaCl 5 M and EDTA 0.35 M solutions at a flow rate of 10 µL/min for 4 min.

2.11. Evaluation of in vitro cytotoxicity

L929 mouse fibroblast and B16F10 mouse melanoma cells (Rio de Janeiro, Brazil) were cultured in Dulbecco's Modified Eagle's medium (DMEM, Sigma) supplemented with 10 % fetal bovine serum, 100 U/mL penicillin, 100 µg/mL streptomycin and 10 mM HEPES, pH 7.4 at 37 °C in a 5 % CO_2 humidified atmosphere. Free curcumin, unloaded and curcumin-loaded chitosan-coated nanoparticles were added to L929 and B16F10 cells (5.0×10^4, 2.5×10^4, 1.25×10^4 cells/well) and incubated at 37 °C for 24, 48 or 72 hours, respectively. Cell viability was assessed using MTT (3-(4,5-dimethiazol-zyl)-2-5-diphenyltetrazolium bromide, Sigma Chemical Co., St. Louis, MO, USA) assay (VAN DE LOOSDRECHT et al., 1991). The initial

screening of free curcumin and curcumin-loaded nanoparticles at 100 μM concentration was performed to identify the cytotoxic effectiveness against L929 and B16F10 cells. Subsequently, cells were incubated in the presence of different concentrations of curcumin (1- 100 μM) for 24, 48, and 72 hours, in order to calculate the 50 % inhibitory concentration (IC_{50}) values. Experiments were performed in triplicate. The statistical analysis was performed using two-way analysis of variance (Two-way ANOVA) followed by Bonferroni's post-hoc, using the Graph-Pad Prism software (San Diego, CA, USA). *P*-values of less 0.05 were considered indicative of significance. The IC_{50} values were determined by graphical interpolation from the individual experiments.

2.12. Morphological assessment of apoptosis

Apoptotic death was verified as described by Geng et al. (2003). L929 and B16F10 cells (5 x 10^5 cells/well) were incubated with free curcumin, unloaded nanoparticles, and curcumin-loaded nanoparticles uncoated or coated with chitosan at their respective IC_{50} values for 24 hours. Then, the coverslips covering the bottom of the plate were removed, washed with PBS and treated with 40 μL of acridine orange (10 μg/mL) and ethidium bromide (5 μg/mL) solution. Cells were examined under a fluorescence microscope (Olympus BX-FLA) and representative fields were photographed using a digital camera (Olympus BX40, Japan). Viable cells exhibited green fluorescence (acridine orange staining) whereas apoptotic cells exhibited an orange-red nuclear fluorescence (ethidium bromide staining).

3. Results and discussion

3.1. Self-assembly of XGO-b-PCL into nanoparticles

The development of nanoparticles from XGO-*b*-PCL copolymer was proposed as a strategy for obtaining colloidal systems without the use of surfactants, which may induces potential irritation and damage to the mucosa. The amphiphilic block copolymer used in this study consists of a nanoparticle shell-forming XGO block and a core-forming PCL block. The method of preparation of block copolymer nanoparticles essentially depends on the hydrophilicity/hydrophobicity of copolymers. For copolymers insoluble in water, the use of organic solvents can be required (XIAO et al., 2010). Preliminary solubility

studies indicated that water-miscible THF was the best choice, since it solubilizes the block copolymer and it is easy to be removed by evaporation. Then, nanoparticles were prepared by dissolving the block copolymer in THF followed by its mixture with water, which is a selective solvent for the XGO block, and induces the desolvation of PCL block to form the nanoparticle core. XGO-*b*-PCL nanoparticles were successfully obtained by this method. It was established that the initial polymer concentration in the organic solvent, the rate of water addition, and the final water content, before dialysis or evaporation, are relevant parameters for the successful preparation of nanoparticles with narrow size distribution (GIACOMELLI et al., 2009). In this study, these parameters were previously evaluated in order to optimize the preparation conditions (data not shown).

In order to evaluate the efficiency of XGO-*b*-PCL copolymer nanoparticles in the encapsulation of hydrophobic compounds, different concentrations of curcumin (1 mg, 2.5 mg, and 5 mg) were added during the nanoparticles preparation. At higher curcumin concentrations (2.5 mg and 5 mg), the presence of precipitates was observed during the nanoparticles formation, suggesting there was an excess of the hydrophobic active molecule. On the other hand, when 1 mg of curcumin was added, no precipitate was observed. Therefore, at the drug to copolymer ratio of 1 to 5, the complete encapsulation of curcumin was verified. The mean curcumin content was 181 μg/mL, corresponding to a drug recovery of 90.5 %, regarding to the amount of drug initially added to the formulations.

DLS analysis revealed the presence of a monodisperse distribution of particles. Figure 1 shows the correlation functions and decay time distributions obtained at the scattering angles 60, 90 and 120° for unloaded XGO-*b*-PCL nanoparticles. The hydrodynamic radius and polydispersity indices of unloaded and curcumin-loaded XGO-*b*-PCL nanoparticles at different scattering angles are shown in Table 1. The mean hydrodynamic radius (R_h) of unloaded and curcumin-loaded nanoparticles was around of 50 and 55 nm, respectively. These results suggest that the incorporation of curcumin in the XGO-*b*-PCL nanoparticles causes an increase of approximately 10 nm in the mean particle diameter. Moreover, all polydispersity indices were lower than 0.3 for the different measured angles, confirming the monodispersity of the samples.

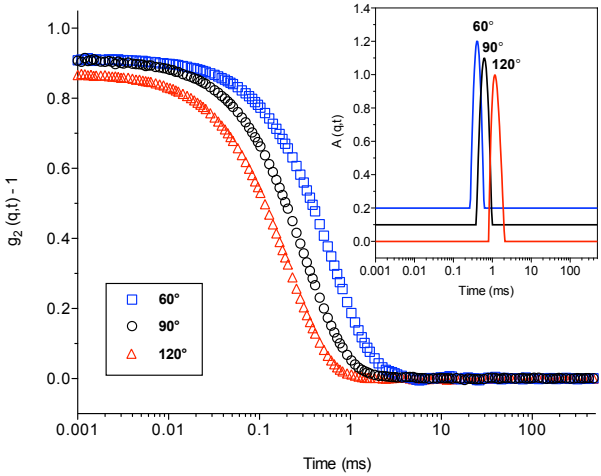

Figure 1. Correlation function and decay time distribution obtained at different scattering angles (θ = 60, 90 and 120 °) for unloaded XGO-*b*-PCL nanoparticles.

Table 1. Hydrodynamic radius (nm) and polydispersity index (PdI) of unloaded and curcumin-loaded XGO-*b*-PCL nanoparticles determined by DLS at different scattering angles (θ = 60, 90 and 120 °).

Sample	Hydrodynamic radius (nm)[a] (PdI)[b]		
	60°	90°	120°
NP XGO-*b*-PCL	52.2 (0.07)	52.0 (0.07)	51.4 (0.11)
Cur-NP XGO-*b*-PCL	57.3 (0.18)	55.8 (0.10)	51.4 (0.14)

[a] obtained using the Contin analysis
[b] obtained using the cumulant analysis

TEM observations of the XGO-*b*-PCL nanoparticles demonstrated the spherical shape of the systems as shown in Figure 2a. Curcumin-loaded nanoparticles displayed an increase in particle size and higher electron density when compared with unloaded nanoparticles, confirming the encapsulation of curcumin in their cores (Figure 2b). Moreover, copolymer nanoparticles size displayed a mean particle size similar to that obtained by DLS studies. The slight difference between the particle sizes obtained by TEM and DLS can be accounted for the preparation conditions of the samples; for DLS

measurements nanoparticles are dispersed in aqueous medium, while for TEM analysis, water is removed from the samples.

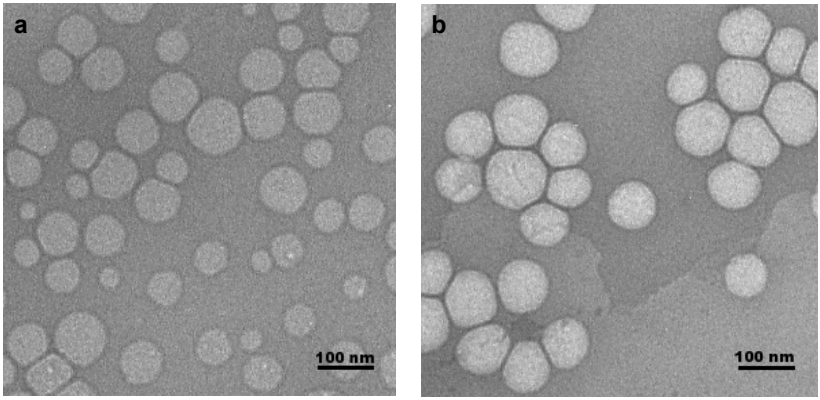

Figure 2. Transmission electron micrographs of unloaded (a) and curcumin-loaded (b) XGO-*b*-PCL nanoparticles (bar 100 nm).

3.2. Decoration of XGO-b-PCL nanoparticles with chitosan

The decoration of nanoparticles with the mucoadhesive polysaccharide was carried out by single adsorption by adding a concentrated chitosan solution (1 %, w/v) to the nanoparticle suspension. In order to evaluate the effect of chitosan concentration, decorated XGO-*b*-PCL nanoparticles were prepared with final concentrations of chitosan ranging from 0.01 to 0.25 % (w/v). The nanoparticle decoration process was investigated by DLS and zeta potential measurements, and the results are shown in Figure 3.

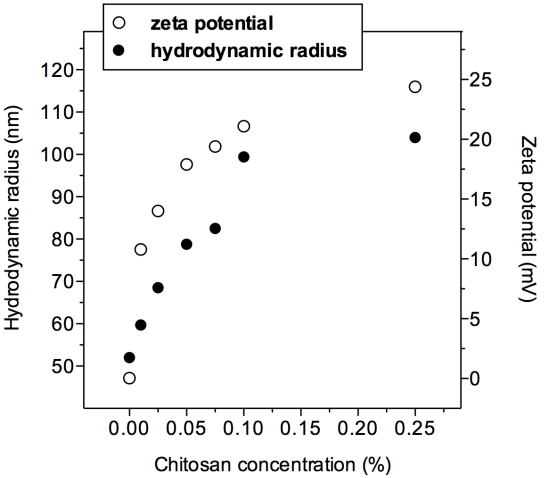

Figure 3. Variation of the hydrodynamic radius (main peak, θ = 90 °, *dark circles*), obtained using the Contin analysis, and zeta potential (*white circles*) of unloaded XGO-*b*-PCL nanoparticles as a function of chitosan concentration (w/v).

Uncoated XGO-*b*-PCL nanoparticles showed a surface charge close to zero, attributed to the external nonionic xyloglucan blocks. The stabilization of uncoated nanoparticle suspensions into the aqueous medium is probably induced by the steric repulsive forces of the XGO shell and by the hydrophobic interactions inside the PCL core. The addition of chitosan into the external phase of the colloidal suspensions provoked an increase of the zeta potential, which was dependent on chitosan concentration. When chitosan concentration was 0.25 % (w/v), the zeta potential value varied from +0.038 mV to +24.4 mV. However, the nanoparticles zeta potential values tended to a plateau for the highest chitosan concentration, indicating the maximum degree of nanoparticles decoration was achieved. The increase of the surface charge of XGO-*b*-PCL nanoparticles may be attributed to the high content of amino groups brought by chitosan and demonstrated that the nanoparticles were successfully coated. The adsorption of chitosan on the copolymer nanoparticle surface may be attributed to the strong hydrogen bonding between the OH / NH_3^+ groups of chitosan and the OH group of XGO in acidic conditions, as previously described (SIMI; ABRAHAM, 2010). No significant differences were observed for the zeta potential values for unloaded and curcumin-loaded nanoparticles.

The mean particle size increased with the increase of chitosan concentration. When chitosan concentration increased from 0 to 0.25 % (w/v), the hydrodynamic radius of copolymer nanoparticles increased from 52 nm to 104 nm. In addition, the increase of chitosan concentration in the colloidal systems led to an increase in their polydispersity indices (data not shown). Bimodal distributions were observed for concentrations of chitosan higher than 0.05 % (w/v). In this way, the mucoadhesive polymer concentration of 0.01 % (w/v) was chosen for the decoration of copolymer nanoparticles.

3.3. Nanoparticle tracking analysis (NTA) measurements

Direct and real-time visualization of Brownian motion of nanoparticles was carried out by NTA. XGO-*b*-PCL copolymer nanoparticles in aqueous medium were identified and tracked individually by an image analysis software, which deduces the diffusion coefficient of each particle and allows the determination of its hydrodynamic diameter. This method is considered a complementary analysis to DLS as it gives the number average diameter. Nanoparticle size distributions with the corresponding video frames and three-dimensional graphs (size *vs.* intensity *vs.* concentration) are shown in Figure 4. All nanoparticle suspensions exhibited a narrow distribution of size, showing a good agreement with DLS results. However, the mean diameters around of 80 and 85 nm obtained for uncoated and chitosan-coated nanoparticles, respectively, were slightly smaller than those obtained by DLS. This shift can be explained because the size distributions obtained by DLS consist of weight distributions, whereas those obtained by NTA are number distributions.

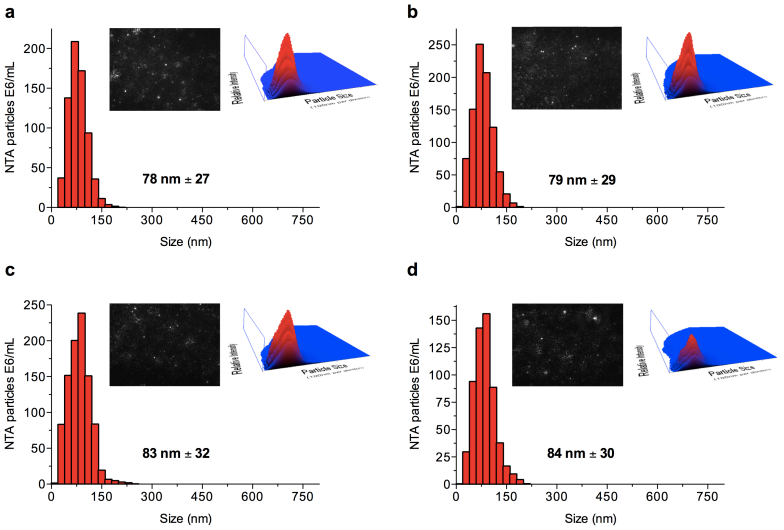

Figure 4. Size distribution from NTA measurements with the corresponding NTA video and 3D graph size vs. intensity vs. concentration of copolymer nanoparticles: NP XGO-b-PCL (a), Cur-NP XGO-b-PCL (b), NP XGO-b-PCL CS (c), Cur-NP XGO-b-PCL CS (d). NTA video obtained for NP XGO-b-PCL is available as supplementary data.

3.4. Evaluation of mucoadhesive properties

The interactions between mucin (BSM) and uncoated and chitosan-coated XGO-*b*-PCL nanoparticles were monitored using a Biacore instrument. The principle of this system is based on the optical phenomenon of Surface Plasmon Resonance (SPR). The SPR response is a measurement of the refractive index, which changes when molecules in solution interact with the sensor chip (TAKEUCHI et al., 2005). The binding or dissociation of molecules on the sensor surface is proportional to the mass of bound material and is recorded in a sensorgram. The main advantage of this technique is the ability to monitor label-free molecular interactions in real-time. For the detection of mucoadhesive properties of nanoparticles, BSM was immobilized onto the surface of a CM4 sensor chip. The adsorption of mucin onto the functionalized surface occurs due to the spontaneous formation of covalent bonds between reactive NHS-esters from dextran surface with the amino groups from the glycoprotein. Mucin non-covalently bound

and the remaining active groups on the surface were deactivated by adding an ethanolamine solution, before nanoparticle injection.

Figure 5 shows the sensorgram obtained by the passing of uncoated and chitosan-coated XGO-*b*-PCL nanoparticles over the mucin immobilized sensor chip. When mucin surface was exposed to chitosan-coated nanoparticles, a rapid increase in the RU response is observed as a consequence of their binding onto the BSM layer. No decrease in response is seen at the end of chitosan-coated nanoparticles injection, indicating the strong interaction between them and mucin. In addition, no significant RU responses were detected upon exposure of the BSM layer to uncoated copolymer nanoparticles, indicating that the interactions between nanoparticles and mucin occur only due to their decoration with chitosan. The lack of mucoadhesive properties of uncoated nanoparticles is probably related to the low molar mass of xyloglucan block (M_n = 1,360), which limit the interpenetration of polymeric chains with the mucin layer. Then, the decoration of XGO-*b*-PCL nanoparticles with chitosan was essential for obtaining mucoadhesive carriers. The interactions between chitosan-coated XGO-*b*-PCL nanoparticles and mucin are mainly related to electrostatic forces between protonated amino groups (NH_3^+) of mucoadhesive polymer and negatively charged groups, like carboxylate (COO^-) or sulphonate (SO_3^-) groups, of protein (DEACON et al., 2000; SVENSSON; THURESSON; ARNEBRANT, 2008).

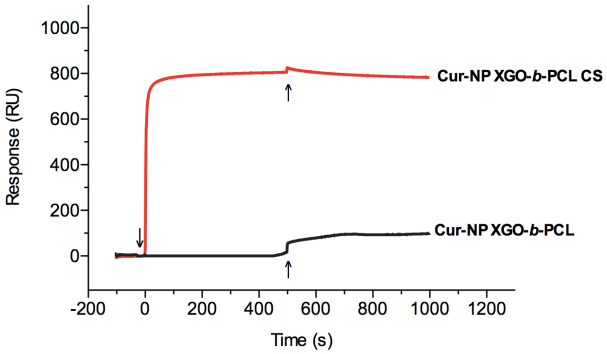

Figure 5. Sensorgram for the mucin immobilized chip after injection of uncoated (Cur-NP XGO-*b*-PCL, *black line*) and chitosan-coated (Cur-NP XGO-*b*-PCL CS, *red line*) copolymer nanoparticles. Arrows indicate the injection (↓) and stop (↑) time of respective solutions.

3.5. Cytotoxic studies

In vitro cytotoxicity studies of free curcumin, unloaded, and curcumin-loaded nanoparticles were carried out on L929 mouse fibroblast and B16F10 mouse melanoma cell lines. Fibroblast culture cells are often employed to evaluate the cytotoxicity of new materials intended to medical applications as an indicator of biocompatibility. In particular, L929 fibroblast cells, derived from an immortalized mouse fibroblast cell line, have been widely used in these studies, since they are able to maintain their characteristics for long periods of culture, resulting in better experimental reproducibility (LUNA et al., 2011). On the other hand, curcumin has shown to inhibit the proliferation of several cancer cells in culture, to prevent carcinogen-induced cancer in rodents, and to inhibit the growth of human tumors in animal models alone or in association with other antitumor drugs (BANERJI et al., 2004; KUNNUMAKKARA; ANAND; AGGARWAL, 2008; LEE et al., 2010; MAZZARINO et al., 2011). In particular, studies have described the anti-proliferative properties of curcumin on B16F10 melanoma cells by targeting the cyclic nucleotide phosphodiesterases-1 (PDE1), an enzyme that inhibits cell proliferation via UHRF1, DNMT1, cyclin A, p21 and p27 regulations (ABUSNINA et al., 2011). Then, the B16F10 mouse melanoma cell line was also chosen to evaluate the cytotoxicity effect of free curcumin and XGO-*b*-PCL nanoparticles. .

The *in vitro* cytotoxicity results obtained for free curcumin, unloaded, and curcumin loaded nanoparticles after 24, 48, and 72 hours of incubation at 100 μM concentration is shown in Figure 6. Unloaded nanoparticles prepared from the new copolymer exhibited similar cytotoxic profiles for L929 fibroblast and B16F10 melanoma cells, causing about 10 % reduction in the number of viable cells after 72 h of incubation. In spite of statistical significance when compared with the control group, cytotoxicity of unloaded NP XGO-*b*-PCL was significant lower than those obtained for free drug and curcumin-loaded nanoparticles. At 100 μM concentration, free curcumin displayed the highest cytotoxicity effect; the reduction in the number of viable cells after 72 h of incubation was around 90 % for both cell lines. After incubation with L929 cells at the same time, Cur-NP XGO-*b*-PCL and Cur-NP XGO-*b*-PCL CS caused a reduction of about 50 % in the number of viable cells, and no statistical significance was verified between these groups ($P < 0.05$). On the other hand, after incubation with B16F10 melanoma cells, the cytotoxic effect was increased in the

following order: free curcumin > Cur-NP XGO-*b*-PCL CS > Cur-NP XGO-*b*-PCL ($P < 0.05$). As expected, the lower cytotoxicity exhibited by curcumin-loaded nanoparticles, when compared with free curcumin, occurred probably due to the encapsulation of curcumin into nanoparticles, rendering the drug less available to act on the cells. However, the cytotoxic effect of curcumin-loaded nanoparticles showed a significant increase at higher exposition times (48 and 72 hours), probably due to the release of the encapsulated drug over time (Figure 6). On the other hand, it is noteworthy that Cur-NP XGO-*b*-PCL CS exhibited a higher cytotoxicity than Cur-NP XGO-*b*-PCL (without chitosan). In fact, chitosan nanoparticles have demonstrated to elicit dose-dependent inhibitory effects on the proliferation of various tumor cell lines, while have exhibited low toxicity against normal cells (QI et al., 2005a; QI et al., 2005b). Then, the higher cytotoxic effect verified for nanoparticles decorated with chitosan could be related, to some extent, to the toxicity of this polysaccharide against tumor cells.

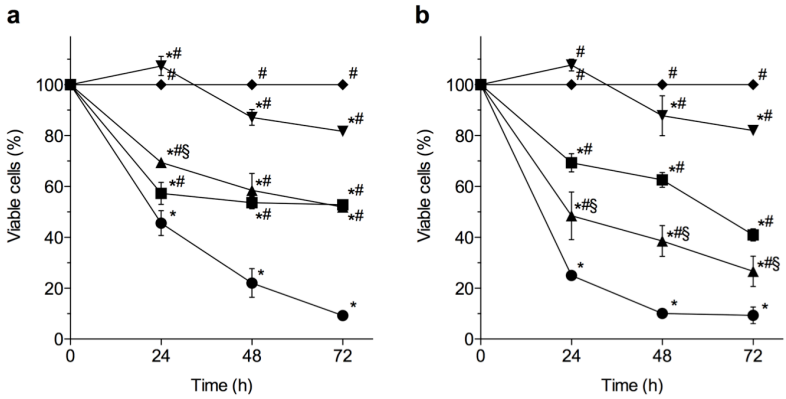

Figure 6. Cytotoxic effect of samples on L929 mouse fibroblast (a) and B16F10 mouse melanoma (b) cells after 24, 48, and 72 hours of incubation: control (◆), NP XGO-*b*-PCL (▼), Cur-NP XGO-*b*-PCL (■), Cur-NP XGO-*b*-PCL CS (▲), and free curcumin (●). Samples were added to cells at 100 μM concentration. Optical density of control was taking as 100 % of cell viability. The results are the mean ± SEM of at least three independent experiments. $^{*}P < 0.05$ compared with control group; $^{\#}P < 0.05$ compared with free curcumin; $^{\S}P < 0.05$ compared between Cur-NP XGO-*b*-PCL and Cur-NP XGO-*b*-PCL CS groups at the same concentration.

Free curcumin and curcumin-loaded nanoparticles decorated or not with chitosan displayed cytotoxic effect in a concentration-

dependent manner (Figure 7). The IC_{50} values estimated from cytotoxicity profiles as a function of curcumin concentration are listed in Table 2. The IC_{50} values of free curcumin were significantly lower than those exhibited by curcumin-loaded nanoparticles for the at all exposure times, supporting the results discussed above. Besides, after 24 h of incubation, free drug and curcumin-loaded nanoparticles displayed a higher cytotoxicity against B16F10 melanoma cells than L929 fibroblast cells.

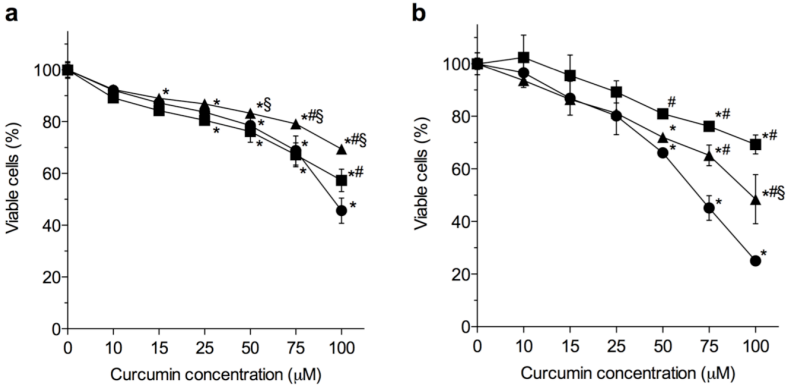

Figure 7. Cytotoxic effect of samples at different concentrations on L929 mouse fibroblast (a) and B16F10 mouse melanoma (b) cells after 24 hours of incubation: Cur-NP XGO-*b*-PCL (■), Cur-NP XGO-*b*-PCL CS (▲), and free curcumin (●). Optical density of control was taking as 100 % of cell viability. The results are the mean ± SEM of at least three independent experiments. $^{*}P < 0.05$ compared with control group; $^{\#}P < 0.05$ compared with free curcumin; $^{\S}P < 0.05$ compared between Cur-NP XGO-*b*-PCL and Cur-NP XGO-*b*-PCL CS groups at the same concentration.

Table 2. IC_{50} values of free curcumin and curcumin-loaded XGO-*b*-PCL nanoparticles for cell viability on L929 and B16F10 cells.

	IC_{50} (μM)		
	24 h	**48 h**	**72 h**
L929			
Free Curcumin	87.90 ± 2.12	46.47 ± 1.22	19.62 ± 0.98
Cur-NP XGO-*b*-PCL	135.0 ± 2.27*	113.3 ± 1.68*	95.33 ± 1.81*
Cur-NP XGO-*b*-PCL CS	231.8 ± 2.66*	139.0 ± 3.02*	103.2 ± 1.47*
B16F10			
Free Curcumin	40.16 ± 8.49	23.34 ± 0.83	18.45 ± 0.77
Cur-NP XGO-*b*-PCL	233.1 ± 6.09*	171.9 ± 1.80*	79.01 ± 1.20*
Cur-NP XGO-*b*-PCL CS	115.7 ± 2.11*	64.62 ± 1.08*	48.48 ± 1.25*

The cell viability was monitored through the MTT assay. Optical density of control was taken as 100 % of cell viability. Data are presented as mean ± SEM of at least three independent experiments. $^{*}P < 0.05$ represents significant difference compared to treatment with free curcumin.

Induction of apoptosis or programmed cell death is a common death mechanism exhibited by several antitumor agents. The ability of free curcumin and curcumin-loaded nanoparticles to induce apoptosis on L929 fibroblast and B16F10 melanoma cells was investigated using acridine orange/ethidium bromide staining (Figure 8). Control group (not treated cells) showed characteristic green color by stained with acridine orange and nuclei integrity, indicating the cell viability. The treatment of cells with free curcumin or loaded in nanoparticles coated with chitosan for 24 hours increased the number of apoptotic cells when compared with control group. Cells treated with curcumin showed morphological features of apoptosis. Early apoptotic cells still have intact membrane and were identified as green cells with chromatin condensation and nuclear fragmentation. Late apoptotic cells lost their membrane integrity and were stained by ethidium bromide with an orange/red color. The cytotoxic effect exhibited by nanoparticles may be attributed to the presence of curcumin, since unloaded nanoparticles were not able to induce significant cell death, when compared to the control group. However, the apoptosis mechanism of curcumin still requires a more detailed investigation.

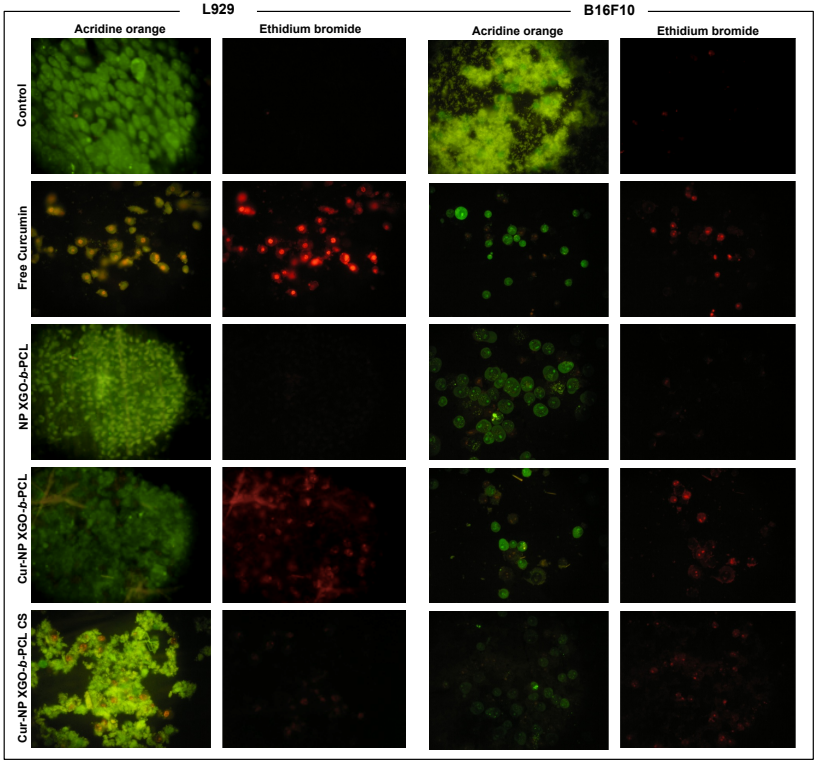

Figure 8. Detection of apoptosis on L929 fibroblast and B16F10 melanoma cells using the acridine orange/ethidium bromide staining assay. Cells were incubated with free curcumin, unloaded (NP XGO-*b*-PCL) and curcumin-loaded nanoparticles (Cur-NP XGO-*b*-PCL), and curcumin-loaded nanoparticles coated with chitosan (Cur-NP XGO-*b*-PCL CS) at their respective IC_{50} values for 24 hours. Viable cells exhibited green fluorescence (acridine orange staining) whereas apoptotic cells exhibited orange-red nuclear fluorescence (ethidium bromide staining). The group without treatment was taken as control group.

4. Conclusions

Monodisperse self-assembled nanoparticles based on the amphiphilic block copolymer XGO-*b*-PCL were prepared using the co-solvent method for the first time to the best of our knowledge. Mucoadhesive drug delivery systems were successful obtained by decoration of XGO-*b*-PCL nanoparticles with chitosan. In addition,

curcumin-loaded copolymer nanoparticles showed higher cytotoxic effects on B16F10 mouse melanoma cells than L929 mouse fibroblast cells. Therefore, the novel chitosan-coated XGO-*b*-PCL nanoparticles constitutes a good strategy to improve the therapeutic effectiveness of hydrophobic drugs for administration in mucosal surfaces.

Acknowledgments

The authors acknowledge the financial support from CNRS and CAPES (CAPES-COFECUB Project No. 620/08). The authors are grateful for the help of A. Durand-Terrasson in the technical assistance with microscopy and C. Travelet for light scattering experiments. We also thank the contributions of A. Audfray and A. Imberty on the Biacore analysis and discussions, and T. Kakuchi and T. Satoh for the synthesis of PCL-N_3.

References

ABUSNINA, A.; KERAVIS, T.; YOUGBARE, I.; BRONNER, C.; LUGNIER, C. Anti-proliferative effect of curcumin on melanoma cells is mediated by PDE1A inhibition that regulates the epigenetic integrator UHRF1. **Mol Nutr Food Res,** v. 55, n. 11, p. 1677-89, 2011.

ANAND, P.; KUNNUMAKKARA, A. B.; NEWMAN, R. A.; AGGARWAL, B. B. Bioavailability of curcumin: problems and promises. **Mol Pharm,** v. 4, n. 6, p. 807-818, 2007.

BANERJI, A.; CHAKRABARTI, J.; MITRA, A.; CHATTERJEE, A. Effect of curcumin on gelatinase A (MMP-2) activity in B16F10 melanoma cells. **Cancer Lett,** v. 211, n. 2, p. 235-242, 2004.

BERNKOP-SCHNURCH, A.; DUNNHAUPT, S. Chitosan-based drug delivery systems. **Eur J Pharm Biopharm**, 2012.

CHEN, D.; GUO, P.; CHEN, S.; CAO, Y.; JI, W.; LEI, X.; LIU, L.; ZHAO, P.; WANG, R.; QI, C.; LIU, Y.; HE, H. Properties of xyloglucan hydrogel as the biomedical sustained-release carriers. **J Mater Sci Mater Med,** v. 23, n. 4, p. 955-962, 2012.

CHOWDARY, K. P.; RAO, Y. S. Mucoadhesive microspheres for controlled drug delivery. **Biol Pharm Bull,** v. 27, n. 11, p. 1717-1724, 2004.

DE MEDEIROS MODOLON, S.; OTSUKA, I.; FORT, S.; MINATTI, E.; BORSALI, R.; HALILA, S. Sweet block copolymer nanoparticles: preparation and self-assembly of fully oligosaccharide-based amphiphile. **Biomacromolecules,** v. 13, n. 4, p. 1129-1135, 2012.

DEACON, M. P.; MCGURK, S.; ROBERTS, C. J.; WILLIAMS, P. M.; TENDLER, S. J.; DAVIES, M. C.; DAVIS, S. S.; HARDING, S. E. Atomic force microscopy of gastric mucin and chitosan mucoadhesive systems. **Biochem J,** v. 348 Pt 3, p. 557-563, 2000.

GENG, C. X.; ZENG, Z. C.; WANG, J. Y. Docetaxel inhibits SMMC-7721 human hepatocellular carcinoma cells growth and induces apoptosis. **World J Gastroenterol,** v. 9, n. 4, p. 696-700, 2003.

GIACOMELLI, C.; SCHMIDT, V.; PUTAUX, J. L.; NARUMI, A.; KAKUCHI, T.; BORSALI, R. Aqueous self-assembly of polystyrene chains end-functionalized with beta-cyclodextrin. **Biomacromolecules,** v. 10, n. 2, p. 449-453, 2009.

HALILA, S.; MANGUIAN, M.; FORT, S.; COTTAZ, S.; HAMAIDE, T.; FLEURY, E.; DRIGUEZ, H. Syntheses of well-defined glyco-polyorganosiloxanes by "click" chemistry and their surfactant properties. **Macromolecular Chemistry and Physics,** v. 209, n. 12, p. 1282-1290, 2008.

ISONO, T.; OTSUKA, I.; KONDO, Y.; HALILA, S.; FORT, S.; ROCHAS, C.; SATOH, T.; BORSALI, R.; KAKUCHI, T. Sub-10 nm nano-organization in AB2- and AB3-type miktoarm star copolymers consisting of maltoheptaose and polycaprolactone. **Macromolecules,** v. 46, n. 4, p. 1461-1469, 2013.

KUMARI, A.; YADAV, S. K.; YADAV, S. C. Biodegradable polymeric nanoparticles based drug delivery systems. **Colloids Surf B Biointerfaces,** v. 75, n. 1, p. 1-18, 2010.

KUNNUMAKKARA, A. B.; ANAND, P.; AGGARWAL, B. B. Curcumin inhibits proliferation, invasion, angiogenesis and metastasis

of different cancers through interaction with multiple cell signaling proteins. **Cancer Lett,** v. 269, n. 2, p. 199-225, 2008.

LEE, J. H.; JANG, J. Y.; PARK, C.; KIM, B. W.; CHOI, Y. H.; CHOI, B. T. Curcumin suppresses alpha-melanocyte stimulating hormone-stimulated melanogenesis in B16F10 cells. **Int J Mol Med,** v. 26, n. 1, p. 101-6, 2010.

LEMARCHAND, C.; GREF, R.; COUVREUR, P. Polysaccharide-decorated nanoparticles. **Eur J Pharm Biopharm,** v. 58, n. 2, p. 327-341, 2004.

LEMARCHAND, C.; GREF, R.; PASSIRANI, C.; GARCION, E.; PETRI, B.; MULLER, R.; COSTANTINI, D.; COUVREUR, P. Influence of polysaccharide coating on the interactions of nanoparticles with biological systems. **Biomaterials,** v. 27, n. 1, p. 108-118, 2006.

LUNA, S. M.; SILVA, S. S.; GOMES, M. E.; MANO, J. F.; REIS, R. L. Cell adhesion and proliferation onto chitosan-based membranes treated by plasma surface modification. **J Biomater Appl,** v. 26, n. 1, p. 101-16, 2011.

MAZZARINO, L.; SILVA, L. F.; CURTA, J. C.; LICINIO, M. A.; COSTA, A.; PACHECO, L. K.; SIQUEIRA, J. M.; MONTANARI, J.; ROMERO, E.; ASSREUY, J.; SANTOS-SILVA, M. C.; LEMOS-SENNA, E. Curcumin-loaded lipid and polymeric nanocapsules stabilized by nonionic surfactants: an in vitro and In vivo antitumor activity on B16-F10 melanoma and macrophage uptake comparative study. **J Biomed Nanotechnol,** v. 7, n. 3, p. 406-14, 2011.

MERISKO-LIVERSIDGE, E. M.; LIVERSIDGE, G. G. Drug nanoparticles: formulating poorly water-soluble compounds. **Toxicol Pathol,** v. 36, n. 1, p. 43-8, 2008.

OTSUKA, I.; FUCHISE, K.; HALILA, S.; FORT, S.; AISSOU, K.; PIGNOT-PAINTRAND, I.; CHEN, Y.; NARUMI, A.; KAKUCHI, T.; BORSALI, R. Thermoresponsive vesicular morphologies obtained by self-assemblies of hybrid oligosaccharide-block-poly(N-isopropylacrylamide) copolymer systems. **Langmuir,** v. 26, n. 4, p. 2325-2332, 2010.

OTSUKA, I.; ISONO, T.; ROCHAS, C.; HALILA, S.; FORT, S.; SATOH, T.; KAKUCHI, T.; BORSALI, R. 10 nm Scale Cylinder–Cubic Phase Transition Induced by Caramelization in Sugar-Based Block Copolymers. **ACS Macro Letters,** v. 1, n. 12, p. 1379-1382, 2012a.

OTSUKA, I.; TRAVELET, C.; HALILA, S.; FORT, S.; PIGNOT-PAINTRAND, I.; NARUMI, A.; BORSALI, R. Thermoresponsive self-assemblies of cyclic and branched oligosaccharide-block-poly(N-isopropylacrylamide) diblock copolymers into nanoparticles. **Biomacromolecules,** v. 13, n. 5, p. 1458-1465, 2012b.

QI, L.; XU, Z.; JIANG, X.; LI, Y.; WANG, M. Cytotoxic activities of chitosan nanoparticles and copper-loaded nanoparticles. **Bioorg Med Chem Lett,** v. 15, n. 5, p. 1397-9, 2005a.

QI, L. F.; XU, Z. R.; LI, Y.; JIANG, X.; HAN, X. Y. In vitro effects of chitosan nanoparticles on proliferation of human gastric carcinoma cell line MGC803 cells. **World J Gastroenterol,** v. 11, n. 33, p. 5136-41, 2005b.

QUAGLIA, F.; OSTACOLO, L.; NESE, G.; CANCIELLO, M.; DE ROSA, G.; UNGARO, F.; PALUMBO, R.; LA ROTONDA, M. I.; MAGLIO, G. Micelles based on amphiphilic PCL-PEO triblock and star-shaped diblock copolymers: potential in drug delivery applications. **Journal of Biomedical Materials Research Part A,** v. 87A, n. 3, p. 563-574, 2008.

RASEKH, M.; AHMAD, Z.; DAY, R.; WICKHAM, A.; EDIRISINGHE, M. Direct writing of polycaprolactone polymer for potential biomedical engineering applications. **Advanced Engineering Materials,** v. 13, n. 9, p. B296-B305, 2011.

SACHL, R.; UCHMAN, M.; MATEJICEK, P.; PROCHAZKA, K.; STEPANEK, M.; SPIRKOVA, M. Preparation and characterization of self-assembled nanoparticles formed by poly(ethylene oxide)-block-poly(epsilon-caprolactone) copolymers with long poly(epsilon-caprolactone) blocks in aqueous solutions. **Langmuir,** v. 23, n. 6, p. 3395-3400, 2007.

SCHATZ, C.; LECOMMANDOUX, S. Polysaccharide-containing block copolymers: synthesis, properties and applications of an emerging family of glycoconjugates. **Macromol Rapid Commun,** v. 31, n. 19, p. 1664-1684, 2010.

SIMI, C.; ABRAHAM, T. Biodegradable biocompatible xyloglucan films for various applications. **Colloid & Polymer Science,** v. 288, n. 3, p. 297-306, 2010.

SVENSSON, O.; THURESSON, K.; ARNEBRANT, T. Interactions between chitosan-modified particles and mucin-coated surfaces. **J Colloid Interface Sci,** v. 325, n. 2, p. 346-350, 2008.

TAKEUCHI, H.; THONGBORISUTE, J.; MATSUI, Y.; SUGIHARA, H.; YAMAMOTO, H.; KAWASHIMA, Y. Novel mucoadhesion tests for polymers and polymer-coated particles to design optimal mucoadhesive drug delivery systems. **Adv Drug Deliv Rev,** v. 57, n. 11, p. 1583-1594, 2005.

VAN DE LOOSDRECHT, A. A.; NENNIE, E.; OSSENKOPPELE, G. J.; BEELEN, R. H. J.; LANGENHUIJSEN, M. M. A. C. Cell mediated cytotoxicity against U 937 cells by human monocytes and macrophages in a modified colorimetric MTT assay: A methodological study. **Journal of Immunological Methods,** v. 141, n. 1, p. 15-22, 1991.

WEI, X.; GONG, C.; GOU, M.; FU, S.; GUO, Q.; SHI, S.; LUO, F.; GUO, G.; QIU, L.; QIAN, Z. Biodegradable poly(epsilon-caprolactone)-poly(ethylene glycol) copolymers as drug delivery system. **Int J Pharm,** v. 381, n. 1, p. 1-18, 2009.

XIAO, R. Z.; ZENG, Z. W.; ZHOU, G. L.; WANG, J. J.; LI, F. Z.; WANG, A. M. Recent advances in PEG-PLA block copolymer nanoparticles. **Int J Nanomedicine,** v. 5, p. 1057-1065, 2010.

Supporting Information

Xyloglucan-*block*-poly(ε-caprolactone) copolymer nanoparticles coated with chitosan as biocompatible mucoadhesive drug delivery system

Letícia Mazzarino [a,b], Issei Otsuka [a], Sami Halila [a], Lorena dos Santos Bubniak [c], Suelen Mazzucco [c], Maria C. Santos-Silva [c], Elenara Lemos-Senna [b], and Redouane Borsali [a,*]

Synthesis of XGO-b-PCL

The diblock copolymer (XGO-*b*-PCL) was synthesized by Cu(I)-catalyzed 1,3-dipolar azide/alkyne cycloaddition ("click" reaction) of propargyl-XGO and PCL-N_3. The "click" reactions was performed in DMF using CuBr and N,N,N',N'',N''-pentamethyldiethylenetriamine (PMDETA) as catalytic system at 60 °C for 5 days (Scheme S1). The reaction mixtures were purified by filtering through alumina short column two times to remove the catalysts and then precipitated in cold methanol to remove the excess propargyl-XGO. The reactions were monitored by checking IR spectra as shown in Figure S1. The signal corresponding to the azido group of PCL-N_3 around 2,100 cm^{-1} disappeared in the spectra of the products, indicating that the azido group of PCL-N_3 was completely reacted with alkyne groups of propargyl-XGO. The obtained products were then characterized by ^1H NMR analysis. Signals corresponding to the protons of PCL blocks (Figure S2, the signals shown in green), the methine protons of triazole rings (Figure S2, the signal shown in red), and oligosaccharidic protons (Figure S2, the signals shown in blue) were observed in the spectra of the products. In addition, the SEC traces of the products shown in Figure S3 displayed clearly shifted signals toward higher molar mass region as compared to that of PCL-N_3 and propargyl-XGO, indicating that the products had efficient conjugation of the XGO blocks to the PCL block. Thus, the obtained products were assigned to the diblock copolymers containing PCL and XGO blocks.

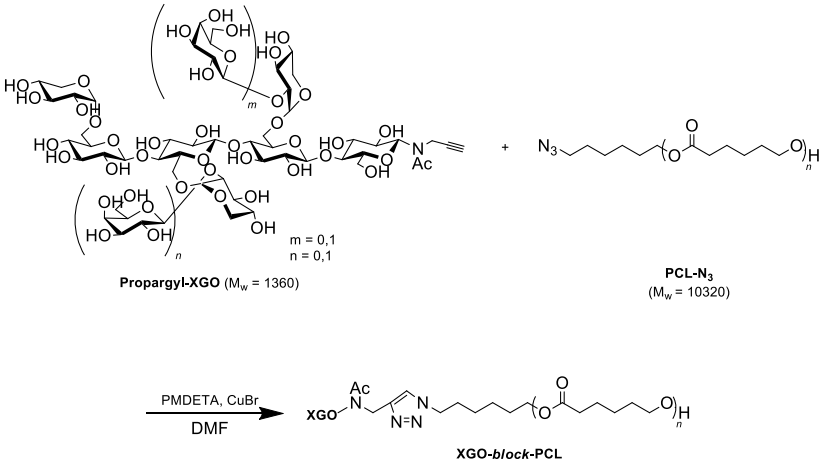

Scheme S1. Synthesis of XGO-*b*-PCL.

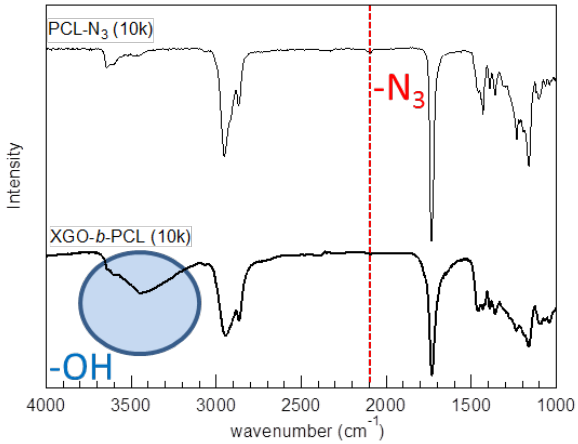

Figure S1. IR spectra of PCL-N_3 (top) and XGO-*b*-PCL (bottom).

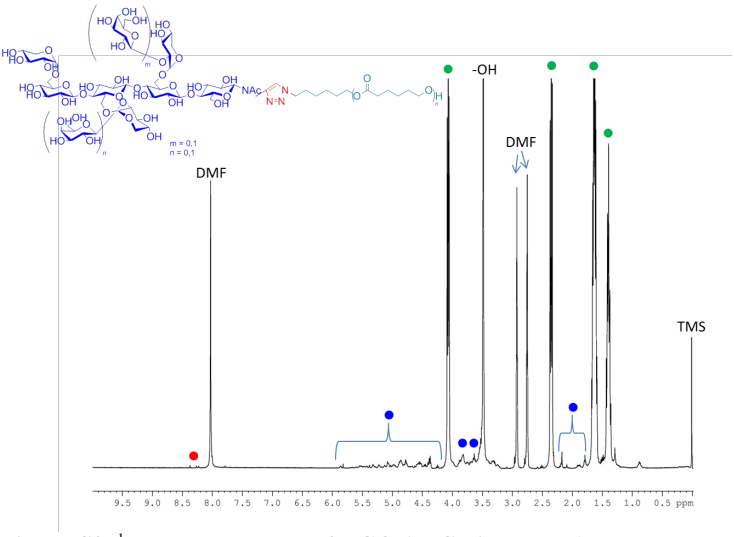

Figure S2. ^{1}H NMR spectrum of XGO-*b*-PCL in DMF-d_7.

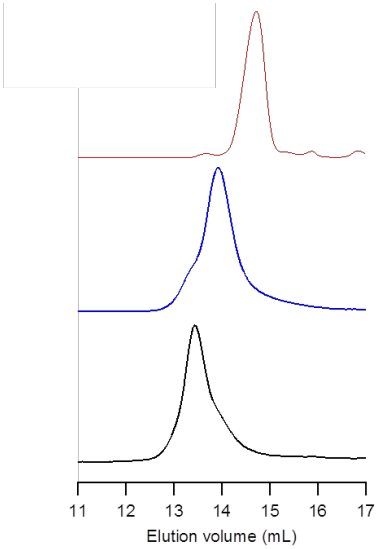

Figure S3. SEC traces of propargyl-XGO (red line), PCL-N_3 (blue line), and XGO-*b*-PCL (black line).

CAPÍTULO 4: DESENVOLVIMENTO DE FILMES NANOESTRUTURADOS PARA A LIBERAÇÃO BUCAL DA CURCUMINA

Recentemente, diferentes formas farmacêuticas mucoadesivas têm sido desenvolvidas visando a administração bucal de fármacos. Entre elas, os filmes mucoadesivos têm atraído grande atenção devido as vantagens adicionais em termos de flexibilidade e conforto, quando comparados aos comprimidos bucais, e maior tempo de residência, quando comparados aos géis e pomadas. Além disso, os filmes protegem fisicamente a superfície bucal lesionada, reduzindo a dor e tornando o tratamento mais eficaz (PEH; WONG, 1999). O uso das nanopartículas como carreadores de fármacos, por sua vez, permite o aumento da solubilidade de moléculas hidrofóbicas, a proteção contra a degradação prematura em meio fisiológico e a modulação da liberação do princípio ativo (KUMARI; YADAV; YADAV, 2010). Assim, a possibilidade de combinar as vantagens relacionadas à utilização dos filmes mucoadesivos e as propriedades de liberação controlada das nanopartículas em um único sistema parece ser uma estratégia bastante interessante para a administração bucal de fármacos.

Nos últimos anos, poucos trabalhos envolvendo sistemas similares têm sido descritos na literatura. Cui e colaboradores (2007) descreveram a preparação de filmes bilaminados, constituídos de uma camada mucoadesiva de hidrogel ácido etilenodiamino tetra-acético-quitosana e uma camada hidrofóbica de etilcelulose, contendo nanopartículas de quitosana carboxilada. Pequenas porções dos filmes foram colocadas em cápsulas com revestimento entérico com o intuito de melhorar a administração de proteínas por via oral. Sapre e colaboradores (2009), por sua vez, desenvolveram discos mucoadesivos a partir de nanopartículas do copolímero do metilvinileter e anidrido maleico pela técnica de compactação, visando a liberação do cloridrato de fluoxetina através da mucosa bucal. Os discos permitiram controlar a velocidade de liberação do fármaco, produzindo melhor resposta antidepressiva que a forma líquida oral de liberação imediata. Por fim, recentemente, filmes de quitosana contendo paclitaxel (fármaco hidrofóbico) encapsulado em nanopartículas de PLGA e carboxifluoresceína (modelo de fármaco hidrofílico) foram desenvolvidos por Tada e colaboradores (2010) visando a aplicação no revestimento de implantes médicos. Os filmes de quitosana contendo as nanopartículas de PLGA mostraram-se capazes de incorporar e liberar fármacos de diferentes polaridades constituindo uma plataforma para a liberação dupla de fármacos localizada.

Este trabalho descreve o desenvolvimento de novos filmes nanoestruturados visando a liberação bucal da curcumina. Os filmes nanoestruturados foram constituídos de uma suspensão do

polissacarídeo mucoadesivo quitosana e glicerol contendo curcumina encapsulada em nanopartículas de PCL. Os filmes mucoadesivos foram preparados pela técnica de evaporação do solvente (*casting*), devido a sua facilidade e baixo custo laboratorial. Diferentes massas molares de quitosana e concentrações do plastificante foram testadas a fim de permitir a obtenção de filmes homogêneos e flexíveis. Filmes sem nanopartículas também foram preparados para fins de comparação durante a realização dos experimentos.

Apesar dos relatos encontrados na literatura, a inexistência de trabalhos que descrevam a fácil preparação de filmes mucoadesivos contendo nanopartículas e sua detalhada caracterização evidencia o caráter inovador deste trabalho.

Publicação: ***"Mucoadhesive films containing chitosan-coated nanoparticles: a new strategy for buccal curcumin release"***
A ser submetida

Mucoadhesive films containing chitosan-coated nanoparticles: a new strategy for buccal curcumin release

Letícia Mazzarino[1,2], Elenara Lemos-Senna[2], and Redouane Borsali[1,*]

[1] Centre de Recherches sur les Macromolécules Végétales (CERMAV, UPR-CNRS 5301), affiliated with Université Joseph Fourier (UJF) and member of the Institut de Chimie Moléculaire de Grenoble (ICMG, FR-CNRS 2607), BP 53, F-38041 Grenoble Cedex 9, France.
[2] Departamento de Ciências Farmacêuticas, Centro de Ciências da Saúde, Universidade Federal de Santa Catarina (UFSC), Campus Universitário Trindade, 88040-900, Florianópolis, SC, Brazil.

* Corresponding author. E-mail: redouane.borsali@cermav.cnrs.fr; Fax: +33 4 76 03 76 29.

ABSTRACT

Mucoadhesive films containing curcumin-loaded nanoparticles were developed aiming to prolong the residence time of the dosage form in the oral cavity and to increase the drug absorption through the buccal mucosa. Chitosan-coated polycaprolactone (PCL) nanoparticles containing curcumin were prepared by the nanoprecipitation technique. Films were prepared by the casting method after incorporation of nanoparticles into plasticized chitosan solutions. Different molar masses of mucoadhesive polymer chitosan and concentrations of plasticizer glycerol were used in order to optimize the preparation conditions. Chitosan-coated nanoparticles exhibited an average diameter ranging from 230 to 252 nm with narrow polydispersity, and high encapsulation efficiency values (> 98 %). Films obtained using medium and high molar mass chitosan showed to be homogeneous and flexible. Curcumin-loaded nanoparticles were uniformly distributed in the films surface, as evidenced by Atomic Force Microscopy (AFM) and high-resolution Scanning Electron Microscopy (FEG-SEM) images. Analyses of film cross sections using FEG-SEM demonstrate the presence of nanoparticles inside the films. In addition, films proved to have a good rate of hydration in simulated saliva, displaying a maximum swelling of around 80 %, and *in vitro* prolonged-controlled delivery of curcumin. These results indicate that the mucoadhesive films containing PCL nanoparticles offer a promising approach for buccal delivery of curcumin, which may be particularly useful in the treatment of periodontal diseases that requires a sustained drug delivery.

Keywords: Buccal delivery; Mucoadhesive systems; Mucoadhesive films; Chitosan-coated nanoparticles; Chitosan; Curcumin; Prolonged-controlled delivery.

1. Introduction

The buccal cavity constitutes an attractive route for administration of drugs. Among the various mucosal membranes available, buccal mucosa is the most convenient and easily accessible for delivery of therapeutic agents either for local or systemic effects. Besides, this region is highly vascularized and permits the direct access to the systemic circulation through the internal jugular vein bypassing the first pass metabolism, improving the systemic bioavailability of drugs (SUDHAKAR; KUOTSU; BANDYOPADHYAY, 2006). Buccal route has a high patient acceptability when compared to others non-oral routes of drug administration (SALAMAT-MILLER; CHITTCHANG; JOHNSTON, 2005). However, the short residence time at the site of application displayed by conventional formulations due to the washing effect of saliva limits the absorption of drugs through buccal mucosa (SCHOLZ et al., 2008).

Mucoadhesive systems including tablets, gels, ointments, and films have shown to improve the drug delivery by prolonging the residence time at the site of application and providing an intimate contact with the absorbing membranes. Among the mucoadhesive dosage forms designed for buccal administration, films are preferable in terms of flexibility and comfort over buccal tablets, and circumvent the relatively short residence time of gels and ointments on the mucosa. Moreover, buccal films also provide physical protection to the wound surfaces, reducing the pain and increasing the treatment effectiveness (PEH; WONG, 1999; PERIOLI et al., 2004). Some studies have demonstrated the promising use of films for drug delivery into the periodontal pocket. Films have proved to be suitable to incorporate and to promote a sustained release of several therapeutic agents. Chitosan/poly(D,L-lactide-co-glycolide) (PLGA) films has shown to prolong the ipriflavone release, a synthetic flavonoid derivative, for 20 days. Additionally, these systems showed good morphological characteristics, such as thickness and flexibility, desirable for application in the oral cavity (PERUGINI et al., 2003). Recently, the development of films consisting of ethylcellulose for delivery of antibacterial agent ornidazole in the treatment of periodontitis has also been reported. The polymeric films showed a sustained release of

ornidazole over a period of time of 9 days, and *in vitro* antibacterial activity against oral bacteria *Streptococcus mutans* (SHANKRAIAH et al., 2011).

More recently, the use of mucoadhesive carriers, such as micro- and nanoparticles, has emerged as other potential strategy for drug delivery through the mucosa. The additional advantages related to the use of colloidal carriers include the possibility to modify the release and absorption characteristics of drugs, drug protection against biological degradation, improved drug bioavailability, and possibility of hydrophobic drug administration as an aqueous dispersion (CHOWDARY; RAO, 2004; LEMARCHAND; GREF; COUVREUR, 2004; PATIL; SAWANT, 2008). Nanoparticles decorated with the polysaccharide chitosan has have attracted a special interest for mucoadhesive applications, mainly, due to its ability to interact with the negatively charged mucosal surface and increase the absorption of drugs by reorganizing the tight junctions between mucosal cells (BERNKOP-SCHNURCH; DUNNHAUPT, 2012).

Based on the above considerations, the possibility to combine the advantages of mucoadhesive films to the controlled release properties related to nanoparticles in one single system seems to be an interesting strategy for buccal administration of drugs. In the last years, few studies on the films containing nanoparticles have been described in the literature (CUI et al., 2007; TADA et al., 2010). So, this work is motivated by the need to develop new mucoadhesive delivery systems that not only prolong the residence time of dosage forms as also modulate the drug delivery. Herein, we report the development of nanostructured films aiming the buccal delivery of curcumin. Curcumin, a natural polyphenol compound derived from turmeric, has been shown to exhibit several pharmacological activities (e.g., antioxidant, anti-inflammatory, antiviral, antimicrobial, and anticancer) and thus presents a potential therapeutic role in different diseases (GOEL; KUNNUMAKKARA; AGGARWAL, 2008). The buccal delivery of curcumin may be useful for the treatment of many disorders that affect the oral cavity, including gingivitis, periodontal diseases, bacterial and fungal infections, aphthous ulcers, inflammations and oral cancers. Nanostructured films were composed by mucoadhesive matrix of chitosan containing curcumin-loaded nanoparticles decorated with chitosan. Different concentrations of the mucoadhesive polysaccharide chitosan and concentrations of plasticizer agent were used in order to obtain homogenous and flexible films. The nanostructured films were

evaluated in terms of weight, thickness, morphology, swelling, and *in vitro* release properties.

2. Materials and methods

2.1. Materials

Curcumin (≥ 94 % curcuminoid content), polycaprolactone (PCL, MW 60,000) and glycerol (ReagentPlus®, ≥ 99 %) were purchased from Sigma-Aldrich (St. Louis, MO, USA). Poloxamer 188 (Lutrol F68®) was kindly donated by BASF Chemical Company (Ludwigshafen, Germany). Three different molar mass chitosan: low (CSL 50,000 - 190,000), medium (CSM 190,000 - 310,000) and high molar mass (CSH 310,000 to > 375,000), were purchased from Sigma-Aldrich. The degree of deacetylation is between 75 - 85 % for CSL and CSM, and higher than 75 % for CSH.

2.2. Preparation of chitosan-coated polycaprolactone nanoparticles

Chitosan-coated PCL nanoparticles loaded with curcumin (Cur-NP) were prepared using the nanoprecipitation method as previously described by Mazzarino et al. (2012). Briefly, 60 mg of PCL and 5 mg of curcumin were dissolved in 12 mL of acetone. This organic phase was poured into 24 mL of an aqueous phase (pH 5) containing 1 % acetic acid, 0.25 % (w/v) poloxamer 188, and 0.1 % low, medium or high molar mass chitosan (CSL, CSM or CSH, respectively), under magnetic stirring. The acetone was then eliminated by evaporation under reduced pressure and the colloidal suspension was concentrated to 10 mL. Finally, the polymeric nanoparticle suspensions were filtered through 1.2- µm pore-size filter paper.

2.3. Preparation of chitosan films containing nanoparticles

Films were prepared by casting/solvent evaporation method. Initially, 1 % (w/v) low, medium or high molar mass chitosan solutions were prepared in 1 % of acetic acid and filtered through non-woven gauzes to remove any suspended impurities. Glycerol at 5 or 10 % (w/w) was added to the chitosan solutions as plasticizer agent. Films containing chitosan-coated nanoparticles loaded with curcumin were prepared according to the same procedure by adding 1 mL of the

nanoparticle suspensions to 2 mL of the plasticized chitosan solution followed by magnetic stirring during 15 min. The obtained mixtures were cast onto polystyrene dishes (9.62 cm^2) overnight under room temperature. Finally, films were cut in 0.785-cm^2 circles. For comparative purposes, films containing free curcumin were also prepared.

2.4. Characterization of chitosan-coated polycaprolactone nanoparticles

2.4.1. Particle size

The size distribution, mean particle size and polydispersity index of the nanoparticle suspensions were determined by Dynamic Light Scattering (DLS) using an ALV 5000 (ALV-Langen, Germany) equipped with a red helium-neon laser at a wavelength of 632.8 nm and a power of 35 mW. After appropriate dilution in ultrapure Milli-Q® water, samples were placed in cylindrical measurements cells and immersed in a toluene bath with temperature regulated at 25 °C. Each analysis was performed during 300 s and the scattered light was measured at different angles ranging from 20 to 150°. The hydrodynamic radius (R_h) was determined using Stokes-Einstein equation, $R_h = \kappa_B T/6\pi\eta D$ where κ_B is Boltzmann constant (in J/K), T is the temperature (in K), D is the diffusion coefficient and η is the viscosity of the medium – pure water in this case (η = 0.89 cP at 25 °C).

2.4.2. Zeta potential measurements

Zeta potential was determined by laser-doppler anemometry using a Zetasizer Nano Series (Malvern Instruments, Worcestershire, UK). Nanoparticle samples were diluted in ultrapure Milli-Q® water and placed in the electrophoretic cell where a potential of ± 150 mV was established. The zeta potential values were calculated as mean electrophoretic mobility values using Smoluchowski's equation.

2.4.3. Nanoparticles drug content

Curcumin content in the nanoparticle suspensions was determined using a Perkin-Elmer Lambda 10 UV/VIS spectrophotometer at 420 nm. The calibration graph for curcumin in acetonitrile was linear over the range of 1.0 to 6.0 μg/mL with a correlation coefficient of 0.997. For determination of the entrapment efficiency, each sample was placed in Amicon Centrifugal Filter Devices with Ultracel-100 membrane (100 kDa, Millipore Corp., USA)

and centrifuged at 10,000 rpm for 15 min to separate the free drug in the supernatant from the curcumin incorporated in the nanoparticles. The amount of drug incorporated in nanoparticles was calculated from the difference between the total concentration of curcumin found in the nanoparticle suspensions after their complete dissolution in acetonitrile and the concentration of drug in the supernatant. Drug recovery was calculated from the difference between the total concentration of drug found in the colloidal suspensions and the initial concentration added to the formulations.

2.5. Characterization of films containing chitosan-coated polycaprolactone nanoparticles

2.5.1. Film weight and thickness

Mean weight of 0.785-cm^2 films was obtained using an analytical balance (Denver Instrument, New York, USA), while thickness was measured using a Digimatic Micrometer (Mitutoyo, Tokyo, Japan). Both were determined on six samples for each film formulation.

2.5.2. Atomic force microscopy (AFM)

The morphological characteristics of films surfaces were observed by AFM using a Pico Plus (Molecular Imaging) commercial instrument. Topography images were obtained using intermittent mode, silicon probes with a spring constant of 48 N/m, and a frequency of 190 kHz. All measurements were performed at room temperature.

2.5.3. High resolution scanning electron microscopy (FEG-SEM)

For high resolution SEM analysis, the film was formed on a grid (usually used for TEM). The grid was then mounted onto aluminum stub and observed in secondary electron imaging mode with a Zeiss ultra 55 FEG-SEM (CMTC-INPG, Grenoble) at an accelerating voltage of 3 kV, using an in-lens detector. Cross-sections of films were also visualized by FEG-SEM after preparation using an Ultramicrotome Leica UC6 equipped with a Cryochamber EM FC7.

2.5.4. Measurement of film swelling

The films swelling studies were performed by measuring the weight increase after contact with simulated saliva solution (PEH; WONG, 1999). Each film was weighted and immersed in a Petri plate containing simulated saliva solution, pH 6.75. At predetermined time intervals, films were removed, wiped off from the excess water using

filter paper and weighted. This procedure was repeated until a constant weight was observed.

The percentage of swelling was calculated using the equation below, where W_0 is the initial weight of film and W_t is the weight of film at time *t*.

$$\text{Swelling (\%)} = \frac{W_t - W_0}{W_0} \times 100$$

2.5.5. *In vitro* curcumin release studies

In vitro release of curcumin from mucoadhesive films was carried out using Franz diffusion cells and commercial dialysis cellulose membranes (MW cut-off 12,000 Da, Sigma-Aldrich, St. Louis, MO, USA) as barrier. The prehydrated membranes were mounted between the donor and receptor compartments of the diffusion cells. The receptor compartment was filled with 12 mL of simulated saliva solution pH 6.75 containing 0.5 % (w/v) of sodium dodecyl sulfate to maintain the *sink* conditions, and allowed to equilibrate at 37 °C. The receptor medium was continuously stirred at 600 rpm. Films displaying a diffusional area of 0.785-cm^2, containing approximately 40 μg of curcumin, were placed in the donor compartment. Cells were protected from light to avoid drug degradation. Release studies were conducted for 24 h. At predetermined time intervals, samples (2 mL) were withdrawn from the receptor compartment and immediately replaced with the same volume of fresh medium. The permeated amount of curcumin was determined using a LS 55 Perkin Elmer Spectrophotometer. Both slits of excitation and emission monochromators were adjusted to 5.0 nm. Samples were excited at 424 nm and the emission spectra were recorded from 435 to 700 nm. The relative fluorescence intensities for curcumin release studies were measured at λ_{emi} of 495 nm. The spectrofluorimetric method was validated using the following parameters: specificity, linearity, accuracy, precision, and limits of detection (LOD) and quantification (LOQ). A calibration curve of curcumin was constructed using simulated saliva solution pH 6.75 containing 0.5 % of sodium dodecyl sulfate and was linear over the range of 0.01 to 0.5 μg/mL (R^2 = 0.998). The regression equation of the media calibration graph (n = 3) was y = 513.9 x – 1.382, and LOD and LOQ values were 0.004 and 0.014 μg/mL, respectively, indicating that the method was sufficiently sensitive to determine curcumin concentration in the release medium. The recovery values for both assays ranged from 96.7 to 107.8 %,

satisfying the acceptance criteria for accuracy in this study. The intra-day and inter-day relative standard deviation values were lower than 5 %, indicating an acceptable variability of the curcumin content determination ($P < 0.05$). The cumulative amount of curcumin released (%) as a function of time (h) was plotted. The percentage of drug released after 24 h was statistically evaluated by analysis of variance (ANOVA) followed by Bonferroni's post-hoc, using the Graph-Pad Prism software (San Diego, CA, USA). All experiments were carried out in six replicates.

3. Results and discussion

3.1. Characterization of curcumin-loaded chitosan-coated nanoparticles

Physicochemical characteristics of curcumin-loaded nanoparticles are listed in Table 1. The decoration of nanoparticles with chitosan was confirmed by the changes in particle size and zeta potential values. Nanoparticle suspensions displayed a monodisperse distribution of particles with hydrodynamic diameter ($2R_h$) ranging between 210 to 252 nm. The mean particle size increased with the chitosan addition to the formulations, indicating the adsorption of mucoadhesive polysaccharide on the nanoparticle surface. Figure 1 shows the correlation functions obtained at the scattering angles 60, 90 and 120° and the decay time distribution obtained at 90° for curcumin-loaded nanoparticles decorated with low, medium and high molar mass chitosan. Chitosan-coated nanoparticles showed positive surface charge, which is attributed to the amino groups positively charged of chitosan molecules. The zeta potential of uncoated nanoparticles tended toward zero probably due to the layer of nonionic surfactant poloxamer. Finally, nanoparticles showed a curcumin content varying from 423 to 484 μg/mL and an encapsulation efficient higher than 98 %, demonstrating their suitability for curcumin encapsulation.

Table 1. Hydrodynamic diameter ($2R_h$), polydispersity index (PdI), zeta potential and curcumin content obtained for uncoated and chitosan-coated nanoparticles.

Sample	$2R_h$[a], PdI[b]	Zeta potential	Drug content	Drug recovery
Cur-NP	210 nm (0.14)	0.047 mV	423 µg/mL	93.1 %
Cur-NP CSL	230 nm (0.06)	22.6 mV	458 µg/mL	91.5 %
Cur-NP CSM	240 nm (0.14)	37.5 mV	468 µg/mL	93.6 %
Cur-NP CSH	252 nm (0.10)	38.5 mV	484 µg/mL	96.8 %

[a] Obtained using the Contin analysis at 90° scattering angle (PROVENCHER, 1976). [b] Obtained using the cumulant analysis at 90° scattering angle (WATSON, 1972; FRISKEN, 2001).

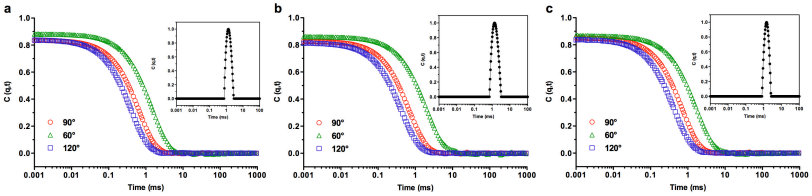

Figure 1. Correlation functions obtained at the scattering angles 60, 90 and 120° and decay time distribution obtained at 90° for Cur-NP CSL (a), Cur-NP CSM (b) and Cur-NP CSH.

3.2. Characterization of films containing curcumin-loaded chitosan-coated nanoparticles

The main goal of this work was to develop new mucoadhesive films containing nanoparticles for buccal administration of drugs. Chitosan was selected as mucoadhesive polymer due to its interesting properties such as biocompatibility, low toxicity, and enhanced absorption effect, besides great film-forming properties. On the other hand, chitosan-coated nanoparticles were added in order to permit the control of curcumin release.

The first step for the development of new mucoadhesive films containing nanoparticles was the optimization of preparation conditions. With this aim, films were prepared using a constant amount (1 %, w/w) of three different molar masses of mucoadhesive polysaccharide chitosan (CSL, CSM and CSH) and different concentrations of plasticizer glycerol (5 % or 10 %, w/w). Curcumin-loaded nanoparticles

decorated with low, medium or high molar mass chitosan were incorporated into the plasticized chitosan solutions before the film casting. Films without nanoparticles were also prepared in order to evaluate their influence on the physicochemical characteristics of the films. Films obtained using medium and high molar mass chitosan showed to be homogeneous, flexible, and transparent or yellow, depending on the presence of curcumin-loaded nanoparticles, as shown in Figure 2. However, low molar mass chitosan resulted in heterogeneous films, even with the increase of polysaccharide concentration to 2 % (w/v) (Figure 2a). Consequently, films obtained using low molar mass chitosan were not considered for further studies.

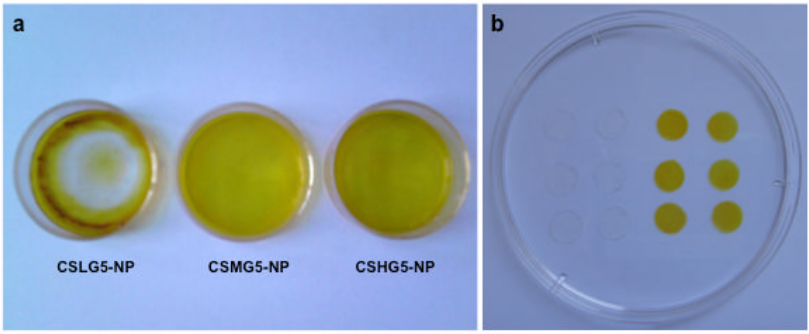

Figure 2. Physical appearance of the different formulated films. Polystyrene supports containing films after the casting (a). Films prepared with (yellow) or without (transparent) chitosan-coated nanoparticles loaded with curcumin cut in portions of 0.785-cm2 (b).

All films were characterized by weight and thickness, as illustrate in Table 2. Films prepared with 5 % glycerol showed a mean weight about of 8 mg, while films containing 10 % glycerol showed a mean weight around 16 mg. When films thickness was examined, values of about 85 μm and 150 μm were observed for films containing 5 % and 10 % of plasticizer agent, respectively. Differences in weight and thickness were mainly attributed to the concentration of glycerol in the films. No significant changes were observed in the presence of nanoparticles.

Table 2. Mean weight, thickness, and swelling of developed formulations (n = 6).

Parameters	CSMG5	CSMG5-NP	CSMG10	CSMG10-NP	CSHG5	CSHG5-NP	CSHG10	CSHG10-NP
Weight (mg)	7.83 ± 1.73	8.60 ± 1.36	13.96 ± 1.69	15.74 ± 1.53	8.74 ± 1.41	8.32 ± 1.28	16.24 ± 1.87	15.92 ± 1.73
Thickness (μm)	86.8 ± 17.2	87.4 ± 17.1	137.2 ± 22.6	154.0 ± 22.4	84.4 ± 15.8	85.6 ± 7.60	151.7 ± 26.5	153.2 ± 14.6
Swelling (%)*	71.6 ± 11.2	68.5 ± 9.02	-	70.4 ± 15.1	66.5 ± 8.06	79.1 ± 12.5	-	52.6 ± 6.0

* Swelling after 45 min of immersion in simulated saliva solution pH 6.75.

3.2.1. Morphological characterization

Morphological characteristics of nanostructured films were investigated by AFM and FEG-SEM. Through microscopy observations, it was possible to visualize the uniform distribution of nanoparticles into the films. AFM images clearly shows nanoparticles sized between 200 and 700 nm dispersed in a uniform surface of chitosan. The largest sizes displayed by nanoparticles on the film surface can be related to their covering by the chitosan film layer. The presence of nanoparticles on the films surface was also confirmed by FEG-SEM images (Figure 4a), showing a good agreement with AFM. Finally, the distribution of nanoparticles inside the chitosan films was observed through cross-sections images using FEG-SEM. Curcumin-loaded nanoparticles inside the film cross-sections showed a mean particle size very similar to the one obtained by DLS studies, as seen in Figure 4b.

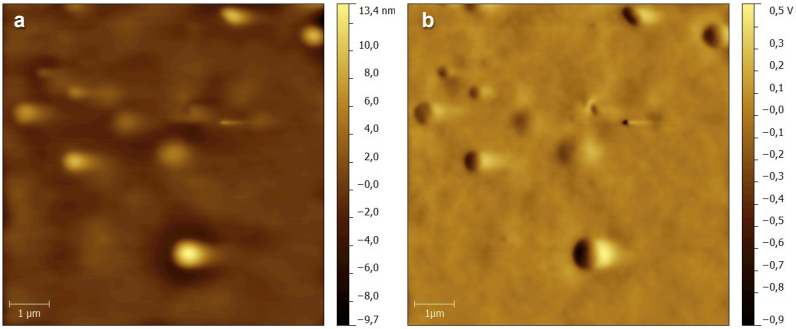

Figure 3. AFM image of film containing curcumin-loaded nanoparticles (CSMG5-NP). Topography (a) and phase (b) images.

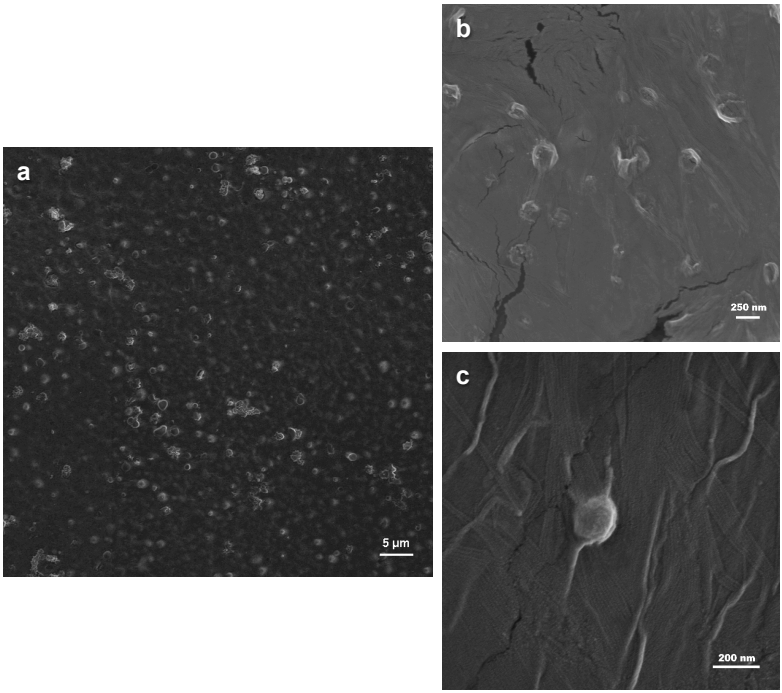

Figure 4. FEG-SEM images of films containing curcumin-loaded nanoparticles. Nanoparticles were observed on the surface of CSMG5-NP film (a), and into the CSHG5-NP film cross-sections (b and c).

3.2.2. Swelling studies

Films swelling profiles were estimated from the comparison between the initial and the final weights after their immersion in simulated saliva solution. The swelling behavior was monitored until a constant weight, which occurred after approximately 1 h. Figure 5 shows the swelling profiles of chitosan films prepared in the presence and absence of nanoparticles, and containing different concentrations of plasticizer. The highest water uptake was obtained with formulations containing 10 % glycerol without the addition of nanoparticles (CSMG10 and CSHG10), which reach 100 % hydration in few minutes (Figure 5b). Formulations containing 5 % glycerol displayed a maximum swelling of 70 - 80 % after 45 minutes of immersion in saliva medium, and no significant difference ($P > 0.05$) was verified comparing to the films prepared in the presence of nanoparticles (Figure 5a). However, chitosan films containing 10 % glycerol showed

fragmentation throughout the experiment. The highest weight losses were observed for films prepared without nanoparticles, being impossible to handle and to weight the films after 30 min of experiment. This high fragility can be associated to the large swelling showed by films containing 10 % glycerol, which probably resulted from the high concentration of plasticizer. The presence of nanoparticles seemed to reduce the swelling of films prepared with 10 % glycerol, and consequently to improve their integrity. No significant difference ($P > 0.05$) was observed in the swelling profile displayed by intact films prepared with medium or high molar mass chitosan. The swelling percentage of films after 45 min of immersion in simulated saliva solution is illustrated in Table 2.

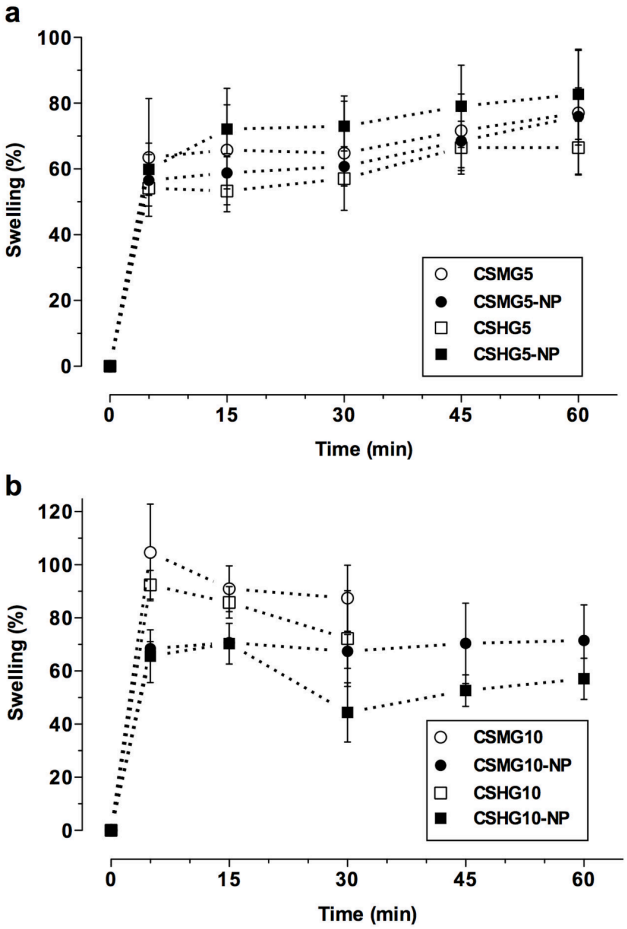

Figure 5. Swelling profiles of films containing 5 % (a) and 10 % (b) glycerol in simulated saliva solution pH 6.75. Data are presented as mean ± SD (n = 3).

Previous studies carried out to asses the bioadhesion of a wide variety of bioadhesives on oral mucosa have shown a direct relationship between the rate of hydratation in vitro and the bioadhesion properties in vivo (NEEDLEMAN; MARTIN; SMALES, 1998). So, the swelling profile of the polymer seems to be a decisive factor for its bioadhesiveness. The adhesion process occurs shortly after the beginning of swelling, but the bond formed is not very strong. The

adhesion will increase with the polymer hydration, however the excessive hydration can leads to an abrupt drop in adhesive strength due to the dilution of functional groups available for adhesive interaction between the film and the mucus surface (PEH; WONG, 1999; EOUANI et al., 2001).

In this context, the adequately hydration shown by nanostructured films containing 5 % of glycerol can predict their good adhesiveness. The mucoadhesive properties of chitosan films are mainly attributed to electrostatic interactions between protonated amino groups of polymer chitosan and negatively charged mucus layer of buccal cavity. Hydroxyl and amino groups of chitosan may also interact with mucus via hydrogen bonding. Additionally, chitosan molecules have sufficient chain flexibility to interpenetrate with mucin chains (ANDREWS; LAVERTY; JONES, 2009). Once overhydration and fragmentation of dosage is undesirable for mucoadhesive systems, films containing 10 % glycerol were thus not considered for further studies.

3.2.3. Release studies

Figure 6 shows the *in vitro* release profiles of curcumin released from chitosan films containing 5 % of glycerol in simulated saliva solution pH 6.75 containing 0.5 % (w/v) of sodium dodecyl sulfate at 37 °C. Films prepared with different molar masses of chitosan containing nanoparticles showed similar curcumin release profiles. CSHG5-NP and CSMG5-NP showed the highest drug release rates, delivering approximately 3.4 % and 2.8 % of curcumin, respectively, over 24 hours. Films containing free curcumin (CSMG5-Free Cur) showed significant slower release of curcumin ($P < 0.05$), when compared to the films containing curcumin-loaded nanoparticles. Only 1 % of drug was released from CSMG5-Free Cur after 24 hours of experiment. This release profile may be related to the low solubility of the hydrophobic drug into the chitosan films. The drug present in a solid dispersion form must be firstly dissolved after penetration of the solvent into the delivery system before to diffuse towards to the saliva medium. Then, the loading of curcumin into PCL nanoparticles showed to increase significantly the release rate of drug from the mucoadhesive films, probably due to the presence of a molecular dispersion of the drug inside or even on the surface of the particles. The films containing nanoparticles may be useful for the localized delivery of curcumin in the treatment of oral diseases, particularly periodontal disorders where prolonged-controlled delivery is desired.

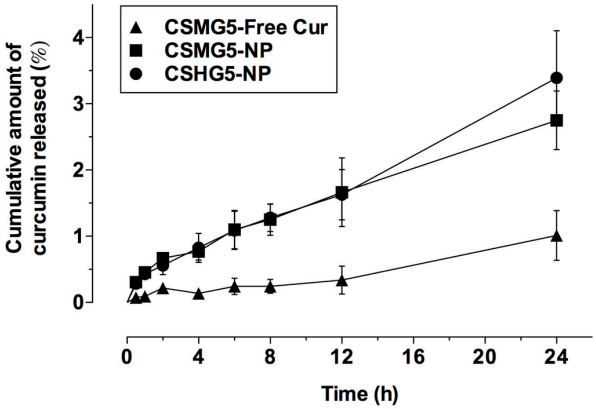

Figure 6. *In vitro* release profiles of curcumin from films containing 5 % glycerol in simulated saliva solution pH 6.75 containing 0.5 % (w/v) of sodium dodecyl sulfate at 37 °C. Data are presented as mean ± SD (n = 6).

4. Conclusions

New mucoadhesive films containing curcumin-loaded nanoparticles decorated with chitosan were successfully prepared by the casting method, after incorporation of nanoparticles into plasticized chitosan solutions. The main advantage of developed films is that it contains nanoparticles able to deliver the loaded drug in a controlled way directly on the site of application for prolonged periods of time. In addition, the use of chitosan for the films preparation and decoration of nanoparticles may improve the drug bioavailability due to its property of increase the penetration of molecules across the mucosal surface. Films obtained using medium and high molar mass chitosan exhibited good morphological characteristics for buccal application, such as homogeneity, flexibility and thickness. Moreover, mucoadhesive films containing curcumin-loaded nanoparticles showed a good hydration in simulated saliva medium and prolonged-controlled release properties, demonstrating their suitability in the treatment of several buccal diseases.

Acknowledgments

The authors acknowledge the financial support from CNRS and CAPES (CAPES-COFECUB Project No. 620/08). The authors are

grateful for the help of Amandine Durand-Terrasson and Isabelle Pignot-Paintrand in the technical assistance with scanning electron microscopy, Sonia Ortega-Murillo for atomic force microscopy, and Christophe Travelet for light scattering experiments.

References

ANDREWS, G. P.; LAVERTY, T. P.; JONES, D. S. Mucoadhesive polymeric platforms for controlled drug delivery. **Eur J Pharm Biopharm,** v. 71, n. 3, p. 505-518, 2009.

BERNKOP-SCHNURCH, A.; DUNNHAUPT, S. Chitosan-based drug delivery systems. **Eur J Pharm Biopharm**, 2012.

CHOWDARY, K. P.; RAO, Y. S. Mucoadhesive microspheres for controlled drug delivery. **Biol Pharm Bull,** v. 27, n. 11, p. 1717-1724, 2004.

CUI, F.; HE, C.; YIN, L.; QIAN, F.; HE, M.; TANG, C.; YIN, C. Nanoparticles incorporated in bilaminated films: a smart drug delivery system for oral formulations. **Biomacromolecules,** v. 8, n. 9, p. 2845-2850, 2007.

EOUANI, C.; PICCERELLE, P.; PRINDERRE, P.; BOURRET, E.; JOACHIM, J. In-vitro comparative study of buccal mucoadhesive performance of different polymeric films. **Eur J Pharm Biopharm,** v. 52, n. 1, p. 45-55, 2001.

FRISKEN, B. J. Revisting the method of cumulants for the analysis of dynamic light-sctattering data. **Appl Opt,** v. 40, n. 24, p. 4087-4091, 2001.

GOEL, A.; KUNNUMAKKARA, A. B.; AGGARWAL, B. B. Curcumin as ‘‘curecumin’’: from kitchen to clinic. **Biochem Pharmacol,** v. 75, n. 4, p. 787-809, 2008.

LEMARCHAND, C.; GREF, R.; COUVREUR, P. Polysaccharide-decorated nanoparticles. **Eur J Pharm Biopharm,** v. 58, n. 2, p. 327-341, 2004.

MAZZARINO, L.; TRAVELET, C.; ORTEGA-MURILLO, S.; OTSUKA, I.; PIGNOT-PAINTRAND, I.; LEMOS-SENNA, E.; BORSALI, R. Elaboration of chitosan-coated nanoparticles loaded with curcumin for mucoadhesive applications. **J Colloid Interface Sci,** v. 370, n. 1, p. 58-66, 2012.

NEEDLEMAN, I. G.; MARTIN, G. P.; SMALES, F. C. Characterisation of bioadhesives for periodontal and oral mucosal drug delivery. **J Clin Periodontol,** v. 25, n. 1, p. 74-82, 1998.

PATIL, S. B.; SAWANT, K. K. Mucoadhesive microspheres: a promising tool in drug delivery. **Curr Drug Deliv,** v. 5, n. 4, p. 312-318, 2008.

PEH, K. K.; WONG, C. F. Polymeric films as vehicle for buccal delivery: swelling, mechanical, and bioadhesive properties. **J Pharm Pharm Sci,** v. 2, n. 2, p. 53-61, 1999.

PERIOLI, L.; AMBROGI, V.; ANGELICI, F.; RICCI, M.; GIOVAGNOLI, S.; CAPUCCELLA, M.; ROSSI, C. Development of mucoadhesive patches for buccal administration of ibuprofen. **J Control Release,** v. 99, n. 1, p. 73-82, 2004.

PERUGINI, P.; GENTA, I.; CONTI, B.; MODENA, T.; PAVANETTO, F. Periodontal delivery of ipriflavone: new chitosan/PLGA film delivery system for a lipophilic drug. **Int J Pharm,** v. 252, n. 1-2, p. 1-9, 2003.

PROVENCHER, S. W. An eigenfunction expansion method for the analysis of exponential decay curves. **J Chem Phys,** v. 64, p. 2772-2777, 1976.

SALAMAT-MILLER, N.; CHITTCHANG, M.; JOHNSTON, T. P. The use of mucoadhesive polymers in buccal drug delivery. **Adv Drug Deliv Rev,** v. 57, n. 11, p. 1666-1691, 2005.

SCHOLZ, O. A.; WOLFF, A.; SCHUMACHER, A.; GIANNOLA, L. I.; CAMPISI, G.; CIACH, T.; VELTEN, T. Drug delivery from the oral cavity: focus on a novel mechatronic delivery device. **Drug Discov Today,** v. 13, n. 5-6, p. 247-253, 2008.

SHANKRAIAH, M.; NAGESH, C.; VENKATESH, J. S.; NARSU, M. L.; SETTY, S. R. Sustained release device containing ornidazole for periodontitis. **IRJP,** v. 2, n. 4, p. 217-221, 2011.

SUDHAKAR, Y.; KUOTSU, K.; BANDYOPADHYAY, A. K. Buccal bioadhesive drug delivery - a promising option for orally less efficient drugs. **J Control Release,** v. 114, n. 1, p. 15-40, 2006.

TADA, D. B.; SINGH, S.; NAGESHA, D.; JOST, E.; LEVY, C. O.; GULTEPE, E.; CORMACK, R.; MAKRIGIORGOS, G. M.; SRIDHAR, S. Chitosan film containing poly(D,L-lactic-co-glycolic acid) nanoparticles: a platform for localized dual-drug release. **Pharm Res,** v. 27, n. 8, p. 1738-1745, 2010.

WATSON, T. J. Analysis of macromolecular polydispersity in intensity correlation spectroscopy: the method of cumulants. **J Chem Phys,** v. 57, n. 11, p. 4814-4820, 1972.

DISCUSSÃO GERAL

A curcumina, princípio ativo extraído da *Curcuma longa* (açafrão), apresenta diversas atividades farmacológicas incluindo as atividades antiinflamatória, antitumoral, antioxidante e antimicrobiana. Contudo, apesar da sua potencial utilização, o uso terapêutico da curcumina têm sido limitado devido a sua baixa solubilidade aquosa, elevada susceptibilidade à degradação biológica e rápido metabolismo, os quais contribuem para a sua baixa biodisponibilidade (TONNESEN, 2002; TONNESEN; MASSON; LOFTSSON, 2002; TOMREN et al., 2007). Diante destes aspectos, a encapsulação da curcumina em nanopartículas mucoadesivas visando a sua administração bucal foi proposta com o intuito de contornar as limitações relacionadas ao seu uso clínico e, assim, melhorar sua performance terapêutica no tratamento de doenças da cavidade oral. A liberação bucal da curcumina pode ser útil no tratamento de várias doenças da cavidade oral, tais como, gengivite, doenças periodontais, infecções bacterianas e fúngicas, lesões e carcinomas orais.

Nos últimos anos, o uso de formulações mucoadesivas têm surgido como uma promissora estratégia para a administração bucal de fármacos, visto que podem permanecer retidas na cavidade oral por períodos prolongados e promover o íntimo contato da formulação com as membranas absorventes (LEE; PARK; ROBINSON, 2000). Entre os novos sistemas mucoadesivos, as nanopartículas decoradas com polissacarídeos capazes de interagir com diferentes superfícies mucosas têm mostrado um interesse crescente como carreadores de fármacos. Além das vantagens associadas à decoração com polissacarídeos, as nanopartículas são capazes de proteger o fármaco contra degradação biológica, alterar a liberação do princípio ativo e aumentar a solubilidade de substâncias hidrofóbicas, permitindo sua administração em meios aquosos (LEMARCHAND; GREF; COUVREUR, 2004). Os filmes mucoadesivos, por sua vez, constituem uma das formas farmacêuticas mais recentes para a administração bucal de fármacos. Entre as vantagens da utilização dos filmes em relação às outras formas farmacêuticas mucoadesivas destinadas a aplicação bucal estão o maior conforto e flexibilidade, quando comparados aos comprimidos bucais, e maior tempo de residência, quando comparados aos géis e pomadas. Outras vantagens incluem a proteção da superfície lesionada no caso de doenças bucais e a maior aceitabilidade pelos pacientes (PEH; WONG, 1999).

Neste trabalho, sistemas nanoestruturados mucoadesivos, incluindo nanopartículas decoradas com quitosana e filmes contendo nanopartículas, foram desenvolvidos visando a liberação bucal da

curcumina. Para melhor compreensão, este trabalho foi dividido em quatro capítulos: (1) revisão de literatura, (2) desenvolvimento de nanopartículas de policaprolactona decoradas com quitosana para a liberação bucal da curcumina, (3) desenvolvimento de nanopartículas de xiloglucana-*b*-policaprolactona decoradas com quitosana para a liberação bucal da curcumina, e (4) desenvolvimento de filmes nanoestruturados para a liberação bucal da curcumina.

Entre os polissacarídeos mucoadesivos existentes, a quitosana foi selecionada para a decoração das nanopartículas devido suas excelentes propriedades mucoadesivas e capacidade de aumentar a absorção de fármacos (ANDREWS; LAVERTY; JONES, 2009). Entre os polímeros utilizados para a preparação de nanopartículas, a policaprolactona (PCL) e a xiloglucana (XGO) foram propostas considerando suas características de biodegradabilidade e biocompatibilidade, além de suas potenciais aplicações no desenvolvimento de carreadores para liberação de fármacos (RASEKH et al., 2011; CHEN et al., 2012).

Dois diferentes sistemas de nanopartículas poliméricas foram preparadas neste trabalho, as nanopartículas de policaprolactona (PCL) estabilizadas por surfactante e as nanopartículas do copolímero em bloco xiloglucana-*b*-policaprolactona (XGO-*b*-PCL). As nanopartículas de PCL foram preparadas através da técnica de nanoprecipitação, que constitui o método mais amplamente utilizado para a preparação de nanopartículas a partir de polímeros pré-formados. A nanoprecipitação envolve a dissolução do polímero em um solvente orgânico miscível em água, o qual é adicionado à uma fase aquosa contendo um surfactante hidrofílico, sob agitação magnética moderada. Com a adição da fase orgânica sobre a fase aquosa, o solvente orgânico se difunde imediatamente na fase externa aquosa, levando a precipitação do polímero e formação das nanopartículas (LETCHFORD; BURT, 2007). A origem do mecanismo de formação das nanopartículas pode ser explicada em termos da turbulência interfacial ou agitação espontânea da interface entre as duas fases líquidas em desequilíbrio, envolvendo fluxo, difusão e processos de superfície (FESSI et al., 1989; QUINTANAR-GUERRERO et al., 1998). Enquanto, as nanopartículas XGO-*b*-PCL foram preparadas pela técnica do co-solvente. Esta técnica consiste na dissolução do copolímero em um solvente comum, ou seja, termodinamicamente bom para ambos os blocos, e miscível em água. A formação das nanopartículas ocorre após a mistura desta solução com um solvente seletivo (água), o qual provoca mudanças na qualidade do solvente em relação a cada bloco, tornando-o bom para um bloco e ruim para o outro (GIACOMELLI, 2007).

A decoração das nanopartículas de PCL com o polissacarídeo mucoadesivo foi alcançada através da incorporação da quitosana durante a sua preparação. Enquanto, a decoração das nanopartículas XGO-*b*-PCL foi realizada por simples adsorção, adicionando uma solução de quitosana às suspensões de nanopartículas previamente preparadas. A adsorção da quitosana à superfície das nanopartículas ocorre através da formação de fortes ligações de hidrogênio entre os grupos amina da quitosana e os blocos PEO do surfactante poloxamer e XGO do copolímero, presentes na interface das nanopartículas de PCL e XGO-*b*-PCL, respectivamente. Todas nanopartículas decoradas com quitosana apresentaram excelente habilidade em interagir com a mucina submaxilar bovina (BSM), demonstrando as fortes propriedades mucoadesivas destes sistemas. Esta interação é, principalmente, atribuída às forças elestrostáticas entre os grupos amina do polímero mucoadesivo quitosana e os grupos carregados negativamente da glicoproteína mucina (DEACON et al., 2000; SVENSSON; THURESSON; ARNEBRANT, 2008).

Ambos sistemas de nanopartículas apresentaram grande habilidade na encapsulação do princípio ativo hidrofóbico curcumina. Elevados valores de eficiência de encapsulação foram alcançados, o que pode ser explicado pela baixa solubilidade da curcumina na fase aquosa externa e alta afinidade pela partícula durante a preparação. O menor teor de curcumina apresentado pelas nanopartículas de XGO-*b*-PCL, quando comparadas às nanopartículas de PCL, pode ser relacionado à baixa concentração de copolímero utilizada (Cp = 1 mg/mL).

Um método fluorimétrico foi desenvolvimento visando a determinação da curcumina nos estudos de liberação, e permeação e retenção na mucosa esofágica suína. O método mostrou ser específico, linear, exato, preciso e sensível para a quantificação da curcumina nos meios aceptor e extrator. As nanopartículas contendo curcumina decoradas e não decoradas com quitosana apresentaram perfis de permeação similares através da mucosa esofágica suína. A concentração de curcumina retida na mucosa sugere a possibilidade de obtenção de efeitos localizados do princípio ativo, evidenciando a potencial aplicação destes sistemas no tratamento local de doenças bucais. Ainda, análise de cortes histológicos demonstraram que o tratamento da mucosa com as nanopartículas contendo curcumina promoveu a hidratação do tecido, o que facilita a penetração de fármacos nas camadas mais profundas da mucosa.

Ambas nanopartículas de PCL e XGO-*b*-PCL, preparados sem curcumina, apresentaram reduzida toxicidade *in vitro* em linhagem de

células normais de fibroblastos murino L929, o que demonstra a segurança destes sistemas. As suspensões de nanopartículas contendo curcumina apresentaram menor atividade citotóxica quando comparadas a curcumina livre, provavelmente devido a mais lenta liberação do fármaco encapsulado. A citotoxicidade *in vitro* das nanopartículas de XGO-*b*-PCL também foi avaliada em linhagem de células tumorais de melanoma murino B16F10. As nanopartículas contendo curcumina apresentaram citotoxicidade significativamente maior contra células tumorais em relação àquela observada em células normais, sugerindo a possível aplicação terapêutica destes sistemas no tratamento de doenças cancerígenas. O potencial terapêutico *in vitro* das suspensões de nanopartículas de PCL, por sua vez, foi avaliado em modelo microbiológico de *Candida albicans*. Apesar das nanopartículas preparadas sem curcumina terem apresentado certa atividade antifúngica, provavelmente devido as propriedades antimicrobianas da quitosana, a presença de curcumina nas nanopartículas aumentou a atividade antifúngica das mesmas. As nanopartículas de PCL contendo curcumina apresentaram mesmos valores de MIC e MFC que a curcumina livre, evidenciando seu potencial no tratamento de infecções fúngicas da cavidade oral.

Os filmes nanoestruturados desenvolvidos neste trabalho foram preparados pela técnica de *casting*/evaporação do solvente, que constitui o processo de fabricação de filmes mais amplamente descrito na literatura. As principais vantagens desta técnica são a facilidade do processo e o baixo custo associado à realização em escala laboratorial (MORALES; MCCONVILLE, 2011). Os filmes foram preparados após a incorporação das nanopartículas de PCL em soluções de quitosana contendo agente plastificante. A escolha do polissacarídeo quitosana para a preparação dos filmes mucoadesivos baseou-se nas suas características físico-químicas e biológicas, tais como, habilidade formadora de filme, propriedades antimicrobiana e de cicatrização de feridas, além das excelentes propriedades mucoadesivas e boas características de biocompatibilidade e biodegradabilidade exibidas pela quitosana, anteriormente descritas (KHUTORYANSKIY, 2011).

As nanopartículas apresentaram-se uniformemente distribuídas tanto na superfície quanto no interior dos filmes. Além disso, os filmes obtidos usando quitosana de média e elevada massa molar mostraram-se homogêneos e flexíveis, e apresentaram boa hidratação em solução saliva simulada. Os filmes contendo nanopartículas apresentaram liberação lenta da curcumina, o que pode estar relacionado as propriedades de liberação controlada das nanopartículas de PCL. Os

resultados obtidos sugerem que a aplicação dos filmes desenvolvidos pode ser útil no tratamento local de doenças bucais, principalmente no caso de doenças periodontais onde a liberação controlada-prolongada é desejada. Contudo, apesar das propriedades mucoadesivas da quitosana já serem bem conhecidas, ressalta-se a importância da realização de estudos futuros que avaliem as propriedades mucoadesivas dos filmes a fim de assegurar a adequabilidade dos mesmos para a administração bucal da curcumina.

CONSIDERAÇÕES FINAIS

- A preparação das nanopartículas de PCL e XGO-*b*-PCL contendo curcumina pelas técnicas de nanoprecipitação e do co-solvente, respectivamente, demonstrou-se viável e de simples execução.
- A decoração das nanopartículas com o polissacarídeo mucoadesivo quitosana foi confirmada pelas alterações dos valores de tamanho de partícula e potencial zeta, e ocorre através da formação de fortes ligações de hidrogênio entre os grupos amina do polissacarídeo e os blocos PEO do surfactante poloxamer e XGO do copolímero presentes na interface das nanopartículas de PCL e XGO-*b*-PCL, respectivamente.
- As nanopartículas apresentaram elevados valores de eficiência de encapsulação, indicando que a curcumina encontra-se preferencialmente associada às partículas e demonstrando a adequabilidade destas na encapsulação do fármaco hidrofóbico.
- Todas as nanopartículas decoradas com quitosana apresentaram excelente habilidade em interagir com a mucina através de forças eletrostáticas entre os grupos amina protonados do polissacarídeo e os grupos negativamente carregados da glicoproteína, confirmando as propriedades mucoadesivas das mesmas.
- Um método por espectroscopia de fluorescência foi desenvolvido e validado para a determinação da curcumina nos estudos de liberação e, permeação e retenção na mucosa esofágica suína. O método mostrou ser específico, linear, exato, preciso e sensível.
- A retenção da curcumina incorporada em nanopartículas de PCL na mucosa esofágica suína, sugere a potencial aplicação destes sistemas no tratamento local de doenças bucais.
- A segurança do uso das suspensões de nanopartículas de PCL e XGO-*b*-PCL foi demonstrada pela reduzida toxicidade destes sistemas em linhagem celular de fibroblastos murino L929.
- O potencial terapêutico das nanopartículas XGO-*b*-PCL contendo curcumina no tratamento do câncer foi evidenciado pelo pronunciado efeito citotóxico destes sistemas em células de melanoma murino B16F10.
- As nanopartículas de PCL contendo curcumina apresentaram atividade antimicrobiana contra *Candida albicans*, sugerindo a aplicabilidade destes sistemas no tratamento de infecções fúngicas da cavidade oral.
- Filmes homogêneos e flexíveis contendo curcumina encapsulada em nanopartículas de PCL foram facilmente preparados através da técnica de *casting*/evaporação do solvente.

- A presença das nanopartículas nos filmes mucoadesivos foi confirmada através da análise morfológica da superfície e de seções transversais dos mesmos.
- Os filmes mucoadesivos contendo nanopartículas apresentaram boa hidratação em solução saliva simulada e liberação controlada-prolongada da curcumina, indicando sua adequabilidade para o tratamento de doenças bucais, principalmente, doenças periodontais, onde a liberação prolongada-controlada do fármaco é desejável.
- Por fim, os sistemas nanoestruturados mucoadesivos desenvolvidos, nanopartículas decoradas com quitosana e filmes contendo nanopartículas, demonstraram constituir uma boa estratégia para aumentar o tempo de residência e a efetividade terapêutica da curcumina no tratamento de doenças da cavidade oral.

REFERÊNCIAS

ABUSNINA, A.; KERAVIS, T.; YOUGBARE, I.; BRONNER, C.; LUGNIER, C. Anti-proliferative effect of curcumin on melanoma cells is mediated by PDE1A inhibition that regulates the epigenetic integrator UHRF1. **Mol Nutr Food Res,** v. 55, n. 11, p. 1677-1689, 2011.

AGGARWAL, B. B.; KUMAR, A.; BHARTI, A. C. Anticancer potential of curcumin: preclinical and clinical studies. **Antic Res,** v. 23, p. 363-398, 2003.

AKHTAR, F.; RIZVI, M. M.; KAR, S. K. Oral delivery of curcumin bound to chitosan nanoparticles cured Plasmodium yoelii infected mice. **Biotechnol Adv,** v. 30, n. 1, p. 310-320, 2012.

ANAND, P.; KUNNUMAKKARA, A. B.; NEWMAN, R. A.; AGGARWAL, B. B. Bioavailability of curcumin: problems and promises. **Mol Pharm,** v. 4, n. 6, p. 807-818, 2007.

ANAND, P.; NAIR, H. B.; SUNG, B.; KUNNUMAKKARA, A. B.; YADAV, V. R.; TEKMAL, R. R.; AGGARWAL, B. B. Design of curcumin-loaded PLGA nanoparticles formulation with enhanced cellular uptake, and increased bioactivity in vitro and superior bioavailability in vivo. **Biochem Pharmacol,** v. 79, n. 3, p. 330-338, 2010.

ANDREWS, G. P.; LAVERTY, T. P.; JONES, D. S. Mucoadhesive polymeric platforms for controlled drug delivery. **Eur J Pharm Biopharm,** v. 71, n. 3, p. 505-518, 2009.

ANSARI, M. J.; AHMAD, S.; KOHLI, K.; ALI, J.; KHAR, R. K. Stability-indicating HPTLC determination of curcumin in bulk drug and pharmaceutical formulations. **J Pharm Biomed Anal,** v. 39, n. 1-2, p. 132-138, 2005.

ANSARI, M. N.; BHANDARI, U.; PILLAI, K. K. Protective role of curcumin in myocardial oxidative damage induced by isoproterenol in rats. **Hum Exp Toxicol,** v. 26, n. 12, p. 933-938, 2007.

ARAÚJO, C. A. C.; ALEGRIO, L. V.; GOMES, D. C. F.; LIMA, M. E. F.; GOMES-CARDOSO, L.; LEON, L. L. Studies on the effectiveness of diarylheptanoids derivatives against Leishmania amazonensis. **Mem Inst Oswaldo Cruz,** v. 94, n. 6, p. 791-794, 1999.

ARAUJO, C. C.; LEON, L. L. Biological activities of Curcuma longa L. **Mem Inst Oswaldo Cruz,** v. 96, n. 5, p. 723-728, 2001.

ARUN, N.; NALINI, N. Efficacy of turmeric on blood sugar and polyol pathway in diabetic albino rats. **Plant Foods Hum Nutr,** v. 57, n. 1, p. 41-52, 2002.

AUVRAY, L. Comptes rendus de l'académie des sciences. 1986. p.859-862.

BALE, H. D.; SCHMIDT, P. W. Small-angle x-ray-scattering investigation of submicroscopic porosity with fractal properties. **Phys Rev Lett,** v. 53, n. 6, p. 596-599, 1984.

BANERJI, A.; CHAKRABARTI, J.; MITRA, A.; CHATTERJEE, A. Effect of curcumin on gelatinase A (MMP-2) activity in B16F10 melanoma cells. **Cancer Lett,** v. 211, n. 2, p. 235-242, 2004.

BANSIL, R.; TURNER, B. S. Mucin structure, aggregation, physiological functions and biomedical applications. **Curr Opin Colloid Interface Sci,** v. 11, n. 2-3, p. 164-170, 2006.

BASTARDO, L.; CLAESSON, P.; BROWN, W. Interactions between mucin and alkyl sodium sulfates in solution. A light scattering study. **Langmuir,** v. 18, n. 10, p. 3848-3853, 2002.

BELCARO, G.; CESARONE, M. R.; DUGALL, M.; PELLEGRINI, L.; LEDDA, A.; GROSSI, M. G.; TOGNI, S.; APPENDINO, G. Product-evaluation registry of Meriva , a curcumin-phosphatidylcholine complex, for the complementary management of osteoarthritis. **Panminerva medica,** v. 52, n. 2 Suppl 1, p. 55-62, 2010.

BERNE, B.; PECORA, R. **Dynamic light scattering with applications to chemistry, biology and physics**. Wiley, New York (USA): 1976.

BERNKOP-SCHNURCH, A. Mucoadhesive systems in oral drug delivery. **Drug Discov Today Technol,** v. 2, n. 1, p. 83-87, 2005.

BERNKOP-SCHNURCH, A.; DUNNHAUPT, S. Chitosan-based drug delivery systems. **Eur J Pharm Biopharm**, 2012.

BILENSOY, E.; SARISOZEN, C.; ESENDAGLI, G.; DOGAN, A. L.; AKTAS, Y.; SEN, M.; MUNGAN, N. A. Intravesical cationic nanoparticles of chitosan and polycaprolactone for the delivery of Mitomycin C to bladder tumors. **Int J Pharm,** v. 371, n. 1-2, p. 170-176, 2009.

BISHT, S.; FELDMANN, G.; SONI, S.; RAVI, R.; KARIKAR, C.; MAITRA, A.; MAITRA, A. Polymeric nanoparticle-encapsulated curcumin ("nanocurcumin"): a novel strategy for human cancer therapy. **J Nanobiotechnology,** v. 5, p. 3, 2007.

BOURNE, K. Z.; BOURNE, N.; REISING, S. F.; STANBERRY, L. R. Plant products as topical microbicide candidates: assessment of in vitro and in vivo activity against herpes simplex virus type 2. **Antiviral Res,** v. 42, n. 3, p. 219-226, 1999.

CALVO, P.; REMUÑAN-LÓPEZ, C.; VILA-JATO, J. L.; ALONSO, M. J. Chitosan and chitosan/ethylene oxide-propylene oxide block copolymer nanoparticles as novel carriers for proteins and vaccines. **Pharm Res,** v. 14, n. 10, p. 1431-1436, 1997.

CALVO, P.; VILA-JATO, J. L.; ALONSO, M. J. Evaluation of cationic polymer-coated nanocapsules as ocular drug carriers. **Int J Pharm,** v. 153, n. 1, p. 41-50, 1997.

CAON, T.; SIMOES, C. M. Effect of freezing and type of mucosa on ex vivo drug permeability parameters. **AAPS PharmSciTech,** v. 12, n. 2, p. 587-592, 2011.

CARTIERA, M. S.; FERREIRA, E. C.; CAPUTO, C.; EGAN, M. E.; CAPLAN, M. J.; SALTZMAN, W. M. Partial correction of cystic fibrosis defects with PLGA nanoparticles encapsulating curcumin. **Mol Pharm,** v. 7, n. 1, p. 86-93, 2010.

CARVALHO, F. V. C.; BRUSCHI, M. L.; EVANGELISTA, R. C.; GREMI√£O, M. P. D. Mucoadhesive drug delivery systems. **BJPS,** v. 46, p. 1-17, 2010.

CHAUVIERRE, C.; VAUTHIER, C.; LABARRE, D.; HOMMEL, H. Evaluation of the surface properties of dextran-coated

poly(isobutylcyanoacrylate) nanoparticles by spin-labelling coupled with electron resonance spectroscopy. **Colloid Polym Sci,** v. 282, n. 9, p. 1016-1025, 2004.

CHAYED, S.; WINNIK, F. M. In vitro evaluation of the mucoadhesive properties of polysaccharide-based nanoparticulate oral drug delivery systems. **Eur J Pharm Biopharm,** v. 65, n. 3, p. 363-370, 2007.

CHEN, C.; JOHNSTON, T. D.; JEON, H.; GEDALY, R.; MCHUGH, P. P.; BURKE, T. G.; RANJAN, D. An in vitro study of liposomal curcumin: stability, toxicity and biological activity in human lymphocytes and Epstein-Barr virus-transformed human B-cells. **Int J Pharm,** v. 366, n. 1-2, p. 133-139, 2009.

CHEN, D.; GUO, P.; CHEN, S.; CAO, Y.; JI, W.; LEI, X.; LIU, L.; ZHAO, P.; WANG, R.; QI, C.; LIU, Y.; HE, H. Properties of xyloglucan hydrogel as the biomedical sustained-release carriers. **J Mater Sci Mater Med,** v. 23, n. 4, p. 955-962, 2012.

CHOWDARY, K. P.; RAO, Y. S. Mucoadhesive microspheres for controlled drug delivery. **Biol Pharm Bull,** v. 27, n. 11, p. 1717-1724, 2004.

CLSI. **Reference method for broth dilution antifungal susceptibility testing of yeasts**. Approved standard M27-A2. Wayne, USA: CLSI, 2002.

COLE, G. M.; TETER, B.; FRAUTSCHY, S. A. Neuroprotective effects of curcumin. **Adv Exp Med Biol,** v. 595, p. 197-212, 2007.

CROISIER, F.; JÉRÔME, C. Chitosan-based biomaterials for tissue engineering. **Eur Polym J,** v. 49, n. 4, p. 780-792, 2013.

CUI, F.; HE, C.; YIN, L.; QIAN, F.; HE, M.; TANG, C.; YIN, C. Nanoparticles incorporated in bilaminated films: a smart drug delivery system for oral formulations. **Biomacromolecules,** v. 8, n. 9, p. 2845-2850, 2007.

CUI, F.; QIAN, F.; YIN, C. Preparation and characterization of mucoadhesive polymer-coated nanoparticles. **Int J Pharm,** v. 316, n. 1-2, p. 154-61, 2006.

CUI, J.; YU, B.; ZHAO, Y.; ZHU, W.; LI, H.; LOU, H.; ZHAI, G. Enhancement of oral absorption of curcumin by self-microemulsifying drug delivery systems. **Int J Pharm,** v. 371, n. 1-2, p. 148-155, 2009.

CUI, L.; MIAO, J. Cytotoxic effect of curcumin on malaria parasite Plasmodium falciparum: inhibition of histone acetylation and generation of reactive oxygen species. **Antimicrob Agents Chemother,** v. 51, n. 2, p. 488-494, 2007.

DANDEKAR, P. P.; JAIN, R.; PATIL, S.; DHUMAL, R.; TIWARI, D.; SHARMA, S.; VANAGE, G.; PATRAVALE, V. Curcumin-loaded hydrogel nanoparticles: application in anti-malarial therapy and toxicological evaluation. **J Pharm Sci,** v. 99, n. 12, p. 4992-5010, 2010.

DAVIDOVICH-PINHAS, M.; BIANCO-PELED, H. Mucoadhesion: a review of characterization techniques. **Expert Opin Drug Deliv,** v. 7, n. 2, p. 259-271, 2010.

DE MEDEIROS MODOLON, S.; OTSUKA, I.; FORT, S.; MINATTI, E.; BORSALI, R.; HALILA, S. Sweet block copolymer nanoparticles: preparation and self-assembly of fully oligosaccharide-based amphiphile. **Biomacromolecules,** v. 13, n. 4, p. 1129-1135, 2012.

DE, R.; KUNDU, P.; SWARNAKAR, S.; RAMAMURTHY, T.; CHOWDHURY, A.; NAIR, G. B.; MUKHOPADHYAY, A. K. Antimicrobial activity of curcumin against Helicobacter pylori isolates from India and during infections in mice. **Antimicrob Agents Chemother,** v. 53, n. 4, p. 1592-1597, 2009.

DEACON, M. P.; MCGURK, S.; ROBERTS, C. J.; WILLIAMS, P. M.; TENDLER, S. J.; DAVIES, M. C.; DAVIS, S. S.; HARDING, S. E. Atomic force microscopy of gastric mucin and chitosan mucoadhesive systems. **Biochem J,** v. 348 Pt 3, p. 557-563, 2000.

DENKBAS, E. B.; OTTENBRITE, R. M. Perspectives on: chitosan drug delivery systems based on their geometries. **J Bioact Compat Polym,** v. 21, n. 4, p. 351-368, 2006.

DIAZ DEL CONSUELO, I.; PIZZOLATO, G.-P.; FALSON, F.; GUY, R. H.; JACQUES, Y. Evaluation of pig esophageal mucosa as a

permeability barrier model for buccal tissue. **J Pharm Sci,** v. 94, n. 12, p. 2777-2788, 2005.

DIAZ-DEL CONSUELO, I.; JACQUES, Y.; PIZZOLATO, G.-P.; GUY, R. H.; FALSON, F. Comparison of the lipid composition of porcine buccal and esophageal permeability barriers. **Arch Oral Biol,** v. 50, n. 12, p. 981-987, 2005.

DUAN, J.; ZHANG, Y.; HAN, S.; CHEN, Y.; LI, B.; LIAO, M.; CHEN, W.; DENG, X.; ZHAO, J.; HUANG, B. Synthesis and in vitro/in vivo anti-cancer evaluation of curcumin-loaded chitosan/poly(butyl cyanoacrylate) nanoparticles. **Int J Pharm,** v. 400, n. 1-2, p. 211-220, 2010.

DUVOIX, A.; BLASIUS, R.; DELHALLE, S.; SCHNEKENBURGER, M.; MORCEAU, F.; HENRY, E.; DICATO, M.; DIEDERICH, M. Chemopreventive and therapeutic effects of curcumin. **Cancer Lett,** v. 223, n. 2, p. 181-190, 2005.

EL-AGAMY, D. S. Comparative effects of curcumin and resveratrol on aflatoxin B(1)-induced liver injury in rats. **Arch Toxicol,** v. 84, n. 5, p. 389-396, 2010.

ELATTAR, T. M.; VIRJI, A. S. The inhibitory effect of curcumin, genistein, quercetin and cisplatin on the growth of oral cancer cells in vitro. **Anticancer Res,** v. 20, n. 3A, p. 1733-8, 2000.

EOUANI, C.; PICCERELLE, P.; PRINDERRE, P.; BOURRET, E.; JOACHIM, J. In-vitro comparative study of buccal mucoadhesive performance of different polymeric films. **Eur J Pharm Biopharm,** v. 52, n. 1, p. 45-55, 2001.

FEILER, A. A.; SAHLHOLM, A.; SANDBERG, T.; CALDWELL, K. D. Adsorption and viscoelastic properties of fractionated mucin (BSM) and bovine serum albumin (BSA) studied with quartz crystal microbalance (QCM-D). **J Colloid Interface Sci,** v. 315, n. 2, p. 475-481, 2007.

FELDOTO, Z.; PETTERSSON, T.; DEDINAITE, A. Mucin-electrolyte interactions at the solid-liquid interface probed by QCM-D. **Langmuir,** v. 24, n. 7, p. 3348-3357, 2008.

FESSI, H.; PUISIEUX, F.; DEVISSAGUET, J. P.; AMMOURY, N.; BENITA, S. Nanocapsule formation by interfacial polymer deposition following solvent displacement. **Int J Pharm,** v. 55, n. 1, p. R1-R4, 1989.

FIGUEIRAS, A.; CARVALHO, R.; VEIGA, F. Mucoadhesive drug delivery systems in the oral cavity: mucoadhesive mechanism and mucoadhesive polymers. **Revista Lusófona de Ciências e Tecnologias da Saúde,** v. 4, n. 2, p. 216-233, 2007.

FILIPE, V.; HAWE, A.; JISKOOT, W. Critical evaluation of nanoparticle tracking analysis (NTA) by NanoSight for the measurement of nanoparticles and protein aggregates. **Pharm Res,** v. 27, n. 5, p. 796-810, 2010.

FONSECA, C.; SIMOES, S.; GASPAR, R. Paclitaxel-loaded PLGA nanoparticles: preparation, physicochemical characterization and in vitro anti-tumoral activity. **J Control Release,** v. 83, n. 2, p. 273-286, 2002.

FRANKOVA, L.; FRY, S. C. Trans-alpha-xylosidase, a widespread enzyme activity in plants, introduces (1-->4)-alpha-d-xylobiose side-chains into xyloglucan structures. **Phytochemistry,** v. 78, p. 29-43, 2012.

FRISKEN, B. J. Revisting the method of cumulants for the analysis of dynamic light-sctattering data. **Appl Opt,** v. 40, n. 24, p. 4087-4091, 2001.

FUNK, J. L.; OYARZO, J. N.; FRYE, J. B.; CHEN, G.; LANTZ, R. C.; JOLAD, S. D.; SÓLYOM, A. M.; TIMMERMANN, B. N. Turmeric extracts containing curcuminoids prevent experimental rheumatoid arthritis. **J Nat Prod,** v. 69, p. 351-355, 2006.

GANTA, S.; AMIJI, M. Coadministration of Paclitaxel and Curcumin in Nanoemulsion Formulations To Overcome Multidrug Resistance in Tumor Cells. **Mol Pharm,** v. 6, n. 3, p. 928-939, 2009.

GANTA, S.; DEVALAPALLY, H.; AMIJI, M. Curcumin enhances oral bioavailability and anti-tumor therapeutic efficacy of paclitaxel upon

administration in nanoemulsion formulation. **J Pharm Sci,** v. 99, n. 11, p. 4630-4641, 2010.

GAO, Y.; LI, Z.; SUN, M.; GUO, C.; YU, A.; XI, Y.; CUI, J.; LOU, H.; ZHAI, G. Preparation and characterization of intravenously injectable curcumin nanosuspension. **Drug Deliv**, 2010.

GENG, C. X.; ZENG, Z. C.; WANG, J. Y. Docetaxel inhibits SMMC-7721 human hepatocellular carcinoma cells growth and induces apoptosis. **World J Gastroenterol,** v. 9, n. 4, p. 696-700, 2003.

GIACOMELLI, C. **Nouveaux développements dans l'encapsulation de molécules hydrophobes via l'auto-assemblage de copolymères à blocs amphiphiles**. 2007. 211p. (Thesis). École Doctorale des Sciences Chimiques, Université de Bordeaux, Bordeaux, France.

GIACOMELLI, C.; SCHMIDT, V.; PUTAUX, J. L.; NARUMI, A.; KAKUCHI, T.; BORSALI, R. Aqueous self-assembly of polystyrene chains end-functionalized with beta-cyclodextrin. **Biomacromolecules,** v. 10, n. 2, p. 449-453, 2009.

GIRISH, C.; KONER, B. C.; JAYANTHI, S.; RAMACHANDRA RAO, K.; RAJESH, B.; PRADHAN, S. C. Hepatoprotective activity of picroliv, curcumin and ellagic acid compared to silymarin on paracetamol induced liver toxicity in mice. **Fundam Clin Pharmacol,** v. 23, n. 6, p. 735-745, 2009.

GOEL, A.; KUNNUMAKKARA, A. B.; AGGARWAL, B. B. Curcumin as ‘‘curecumin’’: from kitchen to clinic. **Biochem Pharmacol,** v. 75, n. 4, p. 787-809, 2008.

GOSANGARI, S. L.; WATKIN, K. L. Effect of preparation techniques on the properties of curcumin liposomes: Characterization of size, release and cytotoxicity on a squamous oral carcinoma cell line. **Pharm Dev Technol**, 2010.

GREF, R.; RODRIGUES, J.; COUVREUR, P. Polysaccharides grafted with polyesters: Novel amphiphilic copolymers for biomedical applications. **Macromolecules,** v. 35, n. 27, p. 9861-9867, 2002.

GUIMARAES, M. R.; COIMBRA, L. S.; DE AQUINO, S. G.; SPOLIDORIO, L. C.; KIRKWOOD, K. L.; ROSSA, C., JR. Potent anti-inflammatory effects of systemically administered curcumin modulate periodontal disease in vivo. **J Periodontal Res,** v. 46, n. 2, p. 269-279, 2011.

GUIMARAES, M. R.; DE AQUINO, S. G.; COIMBRA, L. S.; SPOLIDORIO, L. C.; KIRKWOOD, K. L.; ROSSA, C., JR. Curcumin modulates the immune response associated with LPS-induced periodontal disease in rats. **Innate Immun,** v. 18, n. 1, p. 155-163, 2012.

GUPTA, N. K.; DIXIT, V. K. Development and evaluation of vesicular system for curcumin delivery. **Arch Dermatol Res**, 2010.

GUPTA, V.; ASEH, A.; RIOS, C. N.; AGGARWAL, B. B.; MATHUR, A. B. Fabrication and characterization of silk fibroin-derived curcumin nanoparticles for cancer therapy. **Int J Nanomedicine,** v. 4, p. 115-122, 2009.

HALILA, S.; MANGUIAN, M.; FORT, S.; COTTAZ, S.; HAMAIDE, T.; FLEURY, E.; DRIGUEZ, H. Syntheses of well-defined glyco-polyorganosiloxanes by "click" chemistry and their surfactant properties. **Macromol Chem Phys,** v. 209, n. 12, p. 1282-1290, 2008.

HAN, G.; XU, J.; LI, W.; NING, C. Study on preparation of the inclusion compound of curcumin with beta-cyclodextrin. **Zhong Yao Cai,** v. 27, n. 12, p. 946-948, 2004.

HAO, J.; HENG, P. W. Buccal delivery systems. **Drug Dev Ind Pharm,** v. 29, n. 8, p. 821-832, 2003.

HEGGE, A. B.; SCHULLER, R. B.; KRISTENSEN, S.; TONNESEN, H. H. In vitro release of curcumin from vehicles containing alginate and cyclodextrin. Studies of curcumin and curcuminoides. XXXIII. **Pharmazie,** v. 63, n. 8, p. 585-592, 2008.

HEJAZI, R.; AMIJI, M. Chitosan-based gastrointestinal delivery systems. **J Control Release,** v. 89, n. 2, p. 151-165, 2003.

HERMAN, J. G.; STADELMAN, H. L.; ROSELLI, C. E. Curcumin blocks CCL2-induced adhesion, motility and invasion, in part, through down-regulation of CCL2 expression and proteolytic activity. **Int J Oncol,** v. 34, n. 5, p. 1319-1327, 2009.

HOMBACH, J.; BERNKOP-SCHNURCH, A. Mucoadhesive drug delivery systems. **Handb Exp Pharmacol**, n. 197, p. 251-266, 2010.

HONG, W.; CHEN, D.-W.; ZHAO, X.-L.; QIAO, M.-X.; HU, H.-Y. Preparation and study in vitro of long-circulating nanoliposomes of curcumin. **Zhongguo Zhong Yao Za Zhi,** v. 33, n. 8, p. 889-892, 2008.

HOOGSTRAATE, A. J.; BODDÉ, H. E. Methods for assessing the buccal mucosa as a route of drug delivery. **Adv Drug Deliv Rev,** v. 12, n. 1–2, p. 99-125, 1993.

HUANG, M. T.; LYSZ, T.; FERRARO, T.; ABIDI, T. F.; LASKIN, J. D.; CONNEY, A. H. Inhibitory effects of curcumin on in vitro lipoxygenase and cyclooxygenase activities in mouse epidermis. **Cancer Res,** v. 51, n. 3, p. 813-819, 1991.

HUANG, M. T.; MA, W.; YEN, P.; XIE, J. G.; HAN, J.; FRENKEL, K.; GRUNBERGER, D.; CONNEY, A. H. Inhibitory effects of topical application of low doses of curcumin on 12-O-tetradecanoylphorbol-13-acetate-induced tumor promotion and oxidized DNA bases in mouse epidermis. **Carcinogenesis,** v. 18, n. 1, p. 83-8, 1997.

HUANG, Y.; LEOBANDUNG, W.; FOSS, A.; PEPPAS, N. A. Molecular aspects of muco- and bioadhesion: tethered structures and site-specific surfaces. **J Control Release,** v. 65, n. 1-2, p. 63-71, 2000.

ILIUM, L. Chitosan and Its Use as a Pharmaceutical Excipient. **Pharm Res,** v. 15, n. 9, p. 1326-1331, 1998.

ING, L. Y.; ZIN, N. M.; SARWAR, A.; KATAS, H. Antifungal activity of chitosan nanoparticles and correlation with their physical properties. **Int J Biomater,** v. 2012, p. 632698, 2012.

ISONO, T.; OTSUKA, I.; KONDO, Y.; HALILA, S.; FORT, S.; ROCHAS, C.; SATOH, T.; BORSALI, R.; KAKUCHI, T. Sub-10 nm nano-organization in AB2- and AB3-type miktoarm star copolymers

consisting of maltoheptaose and polycaprolactone. **Macromolecules,** v. 46, n. 4, p. 1461-1469, 2013.

IWUNZE, M. O. Binding and distribution characteristics of curcumin solubilized in CTAB micelle. **J Mol Liq,** v. 111, n. 1-3, p. 161-165, 2004.

JAYAPRAKASHA, G. K.; JAGANMOHAN RAO, L.; SAKARIAH, K. K. Antioxidant activities of curcumin, demethoxycurcumin and bisdemethoxycurcumin. **Food Chem,** v. 98, p. 720-724, 2006.

JIANG, H.; DENG, C. S.; ZHANG, M.; XIA, J. Curcumin-attenuated trinitrobenzene sulphonic acid induces chronic colitis by inhibiting expression of cyclooxygenase-2. **World J Gastroenterol,** v. 12, n. 24, p. 3848-3853, 2006.

JULIANO, C.; COSSU, M.; PIGOZZI, P.; RASSU, G.; GIUNCHEDI, P. Preparation, in vitro characterization and preliminary in vivo evaluation of buccal polymeric films containing chlorhexidine. **AAPS PharmSciTech,** v. 9, n. 4, p. 1153-1158, 2008.

JURENKA, J. S. Anti-inflammatory properties of curcumin, a major constituent of Curcuma longa: a review of preclinical and clinical research. **Altern Med Rev,** v. 14, n. 2, p. 141-153, 2009.

KANG, C.; KIM, E. Synergistic effect of curcumin and insulin on muscle cell glucose metabolism. **Food Chem Toxicol,** v. 48, n. 8-9, p. 2366-2373, 2010.

KHUTORYANSKIY, V. V. Advances in mucoadhesion and mucoadhesive polymers. **Macromol Biosci,** v. 11, n. 6, p. 748-764, 2011.

KIM, T. H.; JIANG, H. H.; YOUN, Y. S.; PARK, C. W.; TAK, K. K.; LEE, S.; KIM, H.; JON, S.; CHEN, X.; LEE, K. C. Preparation and characterization of water-soluble albumin-bound curcumin nanoparticles with improved antitumor activity. **Int J Pharm**, 2010.

KIUCHI, F.; GOTO, Y.; SUGIMOTO, N.; AKAO, N.; KONDO, K.; TSUDA, Y. Nematocidal activity of turmeric: synergistic action of curcuminoids. **Chem Pharm Bull (Tokyo),** v. 41, n. 9, p. 1640-3, 1993.

KUMAR, M.; MISRA, A.; BABBAR, A. K.; MISHRA, A. K.; MISHRA, P.; PATHAK, K. Intranasal nanoemulsion based brain targeting drug delivery system of risperidone. **Int J Pharm,** v. 358, n. 1-2, p. 285-291, 2008.

KUMARI, A.; YADAV, S. K.; YADAV, S. C. Biodegradable polymeric nanoparticles based drug delivery systems. **Colloids Surf B Biointerfaces,** v. 75, n. 1, p. 1-18, 2010.

KUNNUMAKKARA, A. B.; ANAND, P.; AGGARWAL, B. B. Curcumin inhibits proliferation, invasion, angiogenesis and metastasis of different cancers through interaction with multiple cell signaling proteins. **Cancer Lett,** v. 269, n. 2, p. 199-225, 2008.

KUNWAR, A.; BARIK, A.; PANDEY, R.; PRIYADARSINI, K. I. Transport of liposomal and albumin loaded curcumin to living cells: An absorption and fluorescence spectroscopic study. **Biochim Biophys Acta,** v. 1760, n. 10, p. 1513-1520, 2006.

LAPENNA, S.; BILIA, A. R.; MORRIS, G. A.; NILSSON, M. Novel artemisinin and curcumin micellar formulations: drug solubility studies by NMR spectroscopy. **J Pharm Sci,** v. 98, n. 10, p. 3666-3675, 2009.

LEE, J. H.; JANG, J. Y.; PARK, C.; KIM, B. W.; CHOI, Y. H.; CHOI, B. T. Curcumin suppresses alpha-melanocyte stimulating hormone-stimulated melanogenesis in B16F10 cells. **Int J Mol Med,** v. 26, n. 1, p. 101-106, 2010.

LEE, J. W.; PARK, J. H.; ROBINSON, J. R. Bioadhesive-based dosage forms: the next generation. **J Pharm Sci,** v. 89, n. 7, p. 850-866, 2000.

LEE, M.-H.; LIN, H.-Y.; CHEN, H.-C.; THOMAS, J. L. Ultrasound mediates the release of curcumin from microemulsions. **Langmuir : the ACS journal of surfaces and colloids,** v. 24, n. 5, p. 1707-13, 2008.

LEMARCHAND, C.; GREF, R.; COUVREUR, P. Polysaccharide-decorated nanoparticles. **Eur J Pharm Biopharm,** v. 58, n. 2, p. 327-341, 2004.

LEMARCHAND, C.; GREF, R.; PASSIRANI, C.; GARCION, E.; PETRI, B.; MULLER, R.; COSTANTINI, D.; COUVREUR, P. Influence of polysaccharide coating on the interactions of nanoparticles with biological systems. **Biomaterials,** v. 27, n. 1, p. 108-118, 2006.

LETCHFORD, K.; BURT, H. A review of the formation and classification of amphiphilic block copolymer nanoparticulate structures: micelles, nanospheres, nanocapsules and polymersomes. **Eur J Pharm Biopharm,** v. 65, n. 3, p. 259-269, 2007.

LETCHFORD, K.; LIGGINS, R.; BURT, H. Solubilization of hydrophobic drugs by methoxy poly(ethylene glycol)-block-polycaprolactone diblock copolymer micelles: theoretical and experimental data and correlations. **J Pharm Sc,** v. 97, n. 3, p. 1179-1190, 2008.

LI, H. L.; LIU, C.; DE COUTO, G.; OUZOUNIAN, M.; SUN, M.; WANG, A. B.; HUANG, Y.; HE, C. W.; SHI, Y.; CHEN, X.; NGHIEM, M. P.; LIU, Y.; CHEN, M.; DAWOOD, F.; FUKUOKA, M.; MAEKAWA, Y.; ZHANG, L.; LEASK, A.; GHOSH, A. K.; KIRSHENBAUM, L. A.; LIU, P. P. Curcumin prevents and reverses murine cardiac hypertrophy. **J Clin Invest,** v. 118, n. 3, p. 879-893, 2008.

LI, J.-T.; CALDWELL, K. D.; RAPOPORT, N. Surface properties of pluronic-coated polymeric colloids. **Langmuir,** v. 10, n. 12, p. 4475-4482, 1994.

LI, L.; AHMED, B.; MEHTA, K.; KURZROCK, R. Liposomal curcumin with and without oxaliplatin: effects on cell growth, apoptosis, and angiogenesis in colorectal cancer. **Mol Cancer Ther,** v. 6, n. 4, p. 1276-1282, 2007.

LI, L.; BRAITEH, F. S.; KURZROCK, R. Liposome-encapsulated curcumin: in vitro and in vivo effects on proliferation, apoptosis, signaling, and angiogenesis. **Cancer,** v. 104, n. 6, p. 1322-1331, 2005.

LIAO, S.; XIA, J.; CHEN, Z.; ZHANG, S.; AHMAD, A.; MIELE, L.; SARKAR, F. H.; WANG, Z. Inhibitory effect of curcumin on oral carcinoma CAL-27 cells via suppression of Notch-1 and NF-kappaB signaling pathways. **J Cell Biochem,** v. 112, n. 4, p. 1055-1065, 2011.

LIU, A.; LOU, H.; ZHAO, L.; FAN, P. Validated LC/MS/MS assay for curcumin and tetrahydrocurcumin in rat plasma and application to pharmacokinetic study of phospholipid complex of curcumin. **J Pharm Biomed Anal,** v. 40, n. 3, p. 720-727, 2006.

LIU, C.-H.; CHANG, F.-Y.; HUNG, D.-K. Terpene microemulsions for transdermal curcumin delivery: Effects of terpenes and cosurfactants. **Colloids Surf B Biointerfaces,** v. 82, n. 1, p. 63-70, 2011.

LIU, Z.; JIAO, Y.; WANG, Y.; ZHOU, C.; ZHANG, Z. Polysaccharides-based nanoparticles as drug delivery systems. **Adv Drug Deliv Rev,** v. 60, n. 15, p. 1650-1662, 2008.

LOPEZ-LEON, T.; CARVALHO, E. L.; SEIJO, B.; ORTEGA-VINUESA, J. L.; BASTOS-GONZALEZ, D. Physicochemical characterization of chitosan nanoparticles: electrokinetic and stability behavior. **J Colloid Interface Sci,** v. 283, n. 2, p. 344-351, 2005.

LOURENCO, C.; TEIXEIRA, M.; SIMÕES, S.; GASPAR, R. Steric stabilization of nanoparticles: size and surface properties. **Int J Pharm,** v. 138, n. 1, p. 1-12, 1996.

LUCYSZYN, N.; LUBAMBO, A. F.; ONO, L.; JO, T. A.; DE SOUZA, C. F.; SIERAKOWSKI, M. R. Chemical, physico-chemical and cytotoxicity characterisation of xyloglucan from Guibourtia hymenifolia (Moric.) J. Leonard seeds. **Food Hydrocolloids,** v. 25, n. 5, p. 1242-1250, 2011.

LUNA, S. M.; SILVA, S. S.; GOMES, M. E.; MANO, J. F.; REIS, R. L. Cell adhesion and proliferation onto chitosan-based membranes treated by plasma surface modification. **J Biomater Appl,** v. 26, n. 1, p. 101-116, 2011.

MA, Z.; HADDADI, A.; MOLAVI, O.; LAVASANIFAR, A.; LAI, R.; SAMUEL, J. Micelles of poly(ethylene oxide)-b-poly(ε-caprolactone) as vehicles for the solubilization, stabilization, and controlled delivery of curcumin. **J Biomed Mater Res A,** v. 86A, n. 2, p. 300-310, 2008.

MA, Z.; SHAYEGANPOUR, A.; BROCKS, D. R.; LAVASANIFAR, A.; SAMUEL, J. High-performance liquid chromatography analysis of

curcumin in rat plasma: application to pharmacokinetics of polymeric micellar formulation of curcumin. **Biomed Chromatogr,** v. 21, n. 5, p. 546-552, 2007.

MACH, C. M.; MATHEW, L.; MOSLEY, S. A.; KURZROCK, R.; SMITH, J. A. Determination of minimum effective dose and optimal dosing schedule for liposomal curcumin in a xenograft human pancreatic cancer model. **Anticancer Res,** v. 29, n. 6, p. 1895-1899, 2009.

MAITI, K.; MUKHERJEE, K.; GANTAIT, A.; SAHA, B. P.; MUKHERJEE, P. K. Curcumin-phospholipid complex: Preparation, therapeutic evaluation and pharmacokinetic study in rats. **Int J Pharm,** v. 330, n. 1-2, p. 155-163, 2007.

MANIKANDAN, P.; SUMITRA, M.; AISHWARYA, S.; MANOHAR, B. M.; LOKANADAM, B.; PUVANAKRISHNAN, R. Curcumin modulates free radical quenching in myocardial ischaemia in rats. **Int J Biochem Cell Biol,** v. 36, n. 10, p. 1967-1980, 2004.

MANIYAR, A.; PATIL, R. M.; KALE, M. T.; JAIN, D. K.; BAVISKAR, D. T. Mucoadhesion: a new polymeric controlled drug delivery. **Int J Pharm Sci Res,** v. 8, n. 2, p. 54-60, 2011.

MARCZYLO, T.; VERSCHOYLE, R.; COOKE, D.; MORAZZONI, P.; STEWARD, W.; GESCHER, A. Comparison of systemic availability of curcumin with that of curcumin formulated with phosphatidylcholine. **Cancer Chemother Pharmacol,** v. 60, n. 2, p. 171-177, 2007.

MARTINS, C. V.; DA SILVA, D. L.; NERES, A. T.; MAGALHAES, T. F.; WATANABE, G. A.; MODOLO, L. V.; SABINO, A. A.; DE FATIMA, A.; DE RESENDE, M. A. Curcumin as a promising antifungal of clinical interest. **J Antimicrob Chemother,** v. 63, n. 2, p. 337-339, 2009.

MAZUMDER, A.; RAGHAVAN, K.; WEINSTEIN, J.; KOHN, K. W.; POMMIER, Y. Inhibition of human immunodeficiency virus type-1 integrase by curcumin. **Biochem Pharmacol,** v. 49, n. 8, p. 1165-1170, 1995.

MAZZARINO, L.; BELLETTINI, I. C.; MINATTI, E.; LEMOS-SENNA, E. Development and validation of a fluorimetric method to determine curcumin in lipid and polymeric nanocapsule suspensions. **BJPS,** v. 46, n. 2, p. 219-226, 2010a.

MAZZARINO, L.; DORA, C. L.; BELLETTINI, I. C.; MINATTI, E.; CARDOSO, S. G.; LEMOS-SENNA, E. Curcumin-loaded polymeric and lipid nanocapsules: Preparation, characterization and chemical stability evaluation. **Lat Am J Pharm,** v. 29, n. 6, p. 933-940, 2010b.

MAZZARINO, L.; SILVA, L. F.; CURTA, J. C.; LICINIO, M. A.; COSTA, A.; PACHECO, L. K.; SIQUEIRA, J. M.; MONTANARI, J.; ROMERO, E.; ASSREUY, J.; SANTOS-SILVA, M. C.; LEMOS-SENNA, E. Curcumin-loaded lipid and polymeric nanocapsules stabilized by nonionic surfactants: an in vitro and In vivo antitumor activity on B16-F10 melanoma and macrophage uptake comparative study. **J Biomed Nanotechnol,** v. 7, n. 3, p. 406-414, 2011.

MAZZARINO, L.; TRAVELET, C.; ORTEGA-MURILLO, S.; OTSUKA, I.; PIGNOT-PAINTRAND, I.; LEMOS-SENNA, E.; BORSALI, R. Elaboration of chitosan-coated nanoparticles loaded with curcumin for mucoadhesive applications. **J Colloid Interface Sci,** v. 370, n. 1, p. 58-66, 2012.

MENON, L. G.; KUTTAN, R.; KUTTAN, G. Anti-metastatic activity of curcumin and catechin. **Cancer Lett,** v. 141, n. 1-2, p. 159-165, 1999.

MERISKO-LIVERSIDGE, E. M.; LIVERSIDGE, G. G. Drug nanoparticles: formulating poorly water-soluble compounds. **Toxicol Pathol,** v. 36, n. 1, p. 43-48, 2008.

MIQUEL, J.; BERND, A.; SEMPERE, J. M.; DÍAS-ALPERI, J.; A., R. The curcuma antioxidants: pharmacological effects and prospects for future clinical use. A review. **Arch Gerontol Geriatr,** v. 34, n. 1, p. 37-46, 2002.

MOHANRAJ, V. J.; CHEN, Y. Nanoparticles - a review. **Trop J Pharm Res,** v. 5, n. 1, p. 561-573, 2006.

MOHANTY, C.; ACHARYA, S.; MOHANTY, A. K.; DILNAWAZ, F.; SAHOO, S. K. Curcumin-encapsulated MePEG/PCL diblock copolymeric micelles: a novel controlled delivery vehicle for cancer therapy. **Nanomedicine,** v. 5, n. 3, p. 433-449, 2010.

MOHANTY, C.; SAHOO, S. K. The in vitro stability and in vivo pharmacokinetics of curcumin prepared as an aqueous nanoparticulate formulation. **Biomaterials,** v. 31, n. 25, p. 6597-6611, 2010.

MORALES, J. O.; MCCONVILLE, J. T. Manufacture and characterization of mucoadhesive buccal films. **Eur J Pharm Biopharm,** v. 77, n. 2, p. 187-199, 2011.

MUKERJEE, A.; VISHWANATHA, J. K. Formulation, characterization and evaluation of curcumin-loaded PLGA nanospheres for cancer therapy. **Anticancer Res,** v. 29, n. 10, p. 3867-3875, 2009.

MULIK, R. S.; MONKKONEN, J.; JUVONEN, R. O.; MAHADIK, K. R.; PARADKAR, A. R. ApoE3 mediated poly(butyl) cyanoacrylate nanoparticles containing curcumin: study of enhanced activity of curcumin against beta amyloid induced cytotoxicity using in vitro cell culture model. **Mol Pharm,** v. 7, n. 3, p. 815-825, 2010a.

MULIK, R. S.; MONKKONEN, J.; JUVONEN, R. O.; MAHADIK, K. R.; PARADKAR, A. R. Transferrin mediated solid lipid nanoparticles containing curcumin: Enhanced in vitro anticancer activity by induction of apoptosis. **Int J Pharm,** v. 398, n. 1-2, p. 190-203, 2010b.

NAGARWAL, R. C.; SINGH, P. N.; KANT, S.; MAITI, P.; PANDIT, J. K. Chitosan coated PLA nanoparticles for ophthalmic delivery: characterization, in-vitro and in-vivo study in rabbit eye. **J Biomed Nanotechnol,** v. 6, n. 6, p. 648-657, 2010.

NAM, S. H.; NAM, H. Y.; JOO, J. R.; BAEK, I. S.; PARK, J.-S. Curcumin-loaded PLGA nanoparticles coating onto metal stent by electrophoretic deposition techniques. **Bull Korean Chem Soc,** v. 28, n. 3, p. 397-402, 2007.

NANOSIGHT. **Applications of nanoparticle tracking analysis (NTA) in nanoparticle research**. London: NanoSight Ltd, 2011.

NEEDLEMAN, I. G.; MARTIN, G. P.; SMALES, F. C. Characterisation of bioadhesives for periodontal and oral mucosal drug delivery. **J Clin Periodontol,** v. 25, n. 1, p. 74-82, 1998.

NEGI, P. S.; JAYAPRAKASHA, G. K.; JAGAN MOHAN RAO, L.; SAKARIAH, K. K. Antibacterial activity of turmeric oil: a byproduct from curcumin manufacture. **J Agric Food Chem,** v. 47, n. 10, p. 4297-4300, 1999.

NIRMALA, C.; PUVANAKRISHNAN, R. Effect of curcumin on certain lysosomal hydrolases in isoproterenol-induced myocardial infarction in rats. **Biochem Pharmacol,** v. 51, n. 1, p. 47-51, 1996.

OHASHI, Y.; TSUCHIYA, Y.; KOIZUMI, K.; SAKURAI, H.; SAIKI, I. Prevention of intrahepatic metastasis by curcumin in an orthotopic implantation model. **Oncology,** v. 65, n. 3, p. 250-258, 2003.

OLSZANECKI, R.; JAWIEN, J.; GAJDA, M.; MATEUSZUK, L.; GEBSKA, A.; KORABIOWSKA, M.; CHLOPICKI, S.; KORBUT, R. Effect of curcumin on atherosclerosis in apoE/LDLR-double knockout mice. **J Physiol Pharmacol,** v. 56, n. 4, p. 627-635, 2005.

ONOUE, S.; TAKAHASHI, H.; KAWABATA, Y.; SETO, Y.; HATANAKA, J.; TIMMERMANN, B.; YAMADA, S. Formulation design and photochemical studies on nanocrystal solid dispersion of curcumin with improved oral bioavailability. **J Pharm Sci,** v. 99, n. 4, p. 1871-1881, 2010.

OTSUKA, I.; FUCHISE, K.; HALILA, S.; FORT, S.; AISSOU, K.; PIGNOT-PAINTRAND, I.; CHEN, Y.; NARUMI, A.; KAKUCHI, T.; BORSALI, R. Thermoresponsive vesicular morphologies obtained by self-assemblies of hybrid oligosaccharide-block-poly(N-isopropylacrylamide) copolymer systems. **Langmuir,** v. 26, n. 4, p. 2325-2332, 2010.

OTSUKA, I.; ISONO, T.; ROCHAS, C.; HALILA, S.; FORT, S.; SATOH, T.; KAKUCHI, T.; BORSALI, R. 10 nm Scale Cylinder–Cubic Phase Transition Induced by Caramelization in Sugar-Based Block Copolymers. **ACS Macro Letters,** v. 1, n. 12, p. 1379-1382, 2012a.

OTSUKA, I.; TRAVELET, C.; HALILA, S.; FORT, S.; PIGNOT-PAINTRAND, I.; NARUMI, A.; BORSALI, R. Thermoresponsive self-assemblies of cyclic and branched oligosaccharide-block-poly(N-isopropylacrylamide) diblock copolymers into nanoparticles. **Biomacromolecules,** v. 13, n. 5, p. 1458-1465, 2012b.

OZAKI, K.; KAWATA, Y.; AMANO, S.; HANAZAWA, S. Stimulatory effect of curcumin on osteoclast apoptosis. **Biochem Pharmacol,** v. 59, n. 12, p. 1577-1581, 2000.

PATEL, V. F.; LIU, F.; BROWN, M. B. Modeling the oral cavity: in vitro and in vivo evaluations of buccal drug delivery systems. **J Control Release,** v. 161, n. 3, p. 746-756, 2012.

PATHAN, S. A.; IQBAL, Z.; SAHANI, J. K.; TALEGAONKAR, S.; KHAR, R. K.; AHMAD, F. J. Buccoadhesive drug delivery systems - extensive review on recent patents. **Recent Pat Drug Deliv Formul,** v. 2, n. 2, p. 177-188, 2008.

PATIL, S. B.; MURTHY, R. S. R.; MAHAJAN, H. S.; WAGH, R. D.; GATTANI, S. G. Mucoadhesive polymers: means of improving drug delivery. **Pharma Times,** v. 38, n. 4, p. 25-28, 2006.

PATIL, S. B.; SAWANT, K. K. Mucoadhesive microspheres: a promising tool in drug delivery. **Curr Drug Deliv,** v. 5, n. 4, p. 312-318, 2008.

PEH, K. K.; WONG, C. F. Polymeric films as vehicle for buccal delivery: swelling, mechanical, and bioadhesive properties. **J Pharm Pharm Sci,** v. 2, n. 2, p. 53-61, 1999.

PERIOLI, L.; AMBROGI, V.; ANGELICI, F.; RICCI, M.; GIOVAGNOLI, S.; CAPUCCELLA, M.; ROSSI, C. Development of mucoadhesive patches for buccal administration of ibuprofen. **J Control Release,** v. 99, n. 1, p. 73-82, 2004.

PERUGINI, P.; GENTA, I.; CONTI, B.; MODENA, T.; PAVANETTO, F. Periodontal delivery of ipriflavone: new chitosan/PLGA film delivery system for a lipophilic drug. **Int J Pharm,** v. 252, n. 1-2, p. 1-9, 2003.

PFEIFFER, E.; HÖHLE, S.; SOLYOM, A. M.; METZLER, M. Studies on the stability of turmeric constituents. **J Food Eng,** v. 56, n. 2-3, p. 257-259, 2003.

PRIYA, S.; SUDHAKARAN, P. R. Curcumin-induced recovery from hepatic injury involves induction of apoptosis of activated hepatic stellate cells. **Indian J Biochem Biophys,** v. 45, n. 5, p. 317-325, 2008.

PROVENCHER, S. W. An eigenfunction expansion method for the analysis of exponential decay curves. **J Chem Phys,** v. 64, p. 2772-2777, 1976.

PUNITHAVATHI, D.; VENKATESAN, N.; BABU, M. Protective effects of curcumin against amiodarone-induced pulmonary fibrosis in rats. **Br J Pharmacol,** v. 139, n. 7, p. 1342-1350, 2003.

QI, L.; XU, Z.; JIANG, X.; LI, Y.; WANG, M. Cytotoxic activities of chitosan nanoparticles and copper-loaded nanoparticles. **Bioorg Med Chem Lett,** v. 15, n. 5, p. 1397-1399, 2005a.

QI, L. F.; XU, Z. R.; LI, Y.; JIANG, X.; HAN, X. Y. In vitro effects of chitosan nanoparticles on proliferation of human gastric carcinoma cell line MGC803 cells. **World J Gastroenterol,** v. 11, n. 33, p. 5136-5141, 2005b.

QIN, X. Y.; CHENG, Y.; YU, L. C. Potential protection of curcumin against intracellular amyloid beta-induced toxicity in cultured rat prefrontal cortical neurons. **Neurosci Lett,** v. 480, n. 1, p. 21-24, 2010.

QUAGLIA, F.; OSTACOLO, L.; NESE, G.; CANCIELLO, M.; DE ROSA, G.; UNGARO, F.; PALUMBO, R.; LA ROTONDA, M. I.; MAGLIO, G. Micelles based on amphiphilic PCL-PEO triblock and star-shaped diblock copolymers: potential in drug delivery applications. **J Biomed Mater Res A,** v. 87A, n. 3, p. 563-574, 2008.

QUEMENEUR, F.; RINAUDO, M.; PEPIN-DONAT, B. Influence of molecular weight and pH on adsorption of chitosan at the surface of large and giant vesicles. **Biomacromolecules,** v. 9, n. 1, p. 396-402, 2008.

QUINTANAR-GUERRERO, D.; ALLEMANN, E.; DOELKER, E.; FESSI, H. Preparation and characterization of nanocapsules from preformed polymers by a new process based on emulsification-diffusion technique. **Pharm Res,** v. 15, n. 7, p. 1056-1062, 1998.

RASEKH, M.; AHMAD, Z.; DAY, R.; WICKHAM, A.; EDIRISINGHE, M. Direct writing of polycaprolactone polymer for potential biomedical engineering applications. **Adv Eng Mater,** v. 13, n. 9, p. B296-B305, 2011.

RAY, S. D. Potential aspects of chitosan as pharmaceutical excipient. **Acta Pol Pharm,** v. 68, n. 5, p. 619-22, 2011.

REDDY, A. C.; LOKESH, B. R. Effect of dietary turmeric (Curcuma longa) on iron-induced lipid peroxidation in the rat liver. **Food Chem Toxicol,** v. 32, n. 3, p. 279-283, 1994.

REVIAKINE, I.; JOHANNSMANN, D.; RICHTER, R. P. Hearing what you cannot see and visualizing what you hear: interpreting quartz crystal microbalance data from solvated interfaces. **Anal Chem,** v. 83, n. 23, p. 8838-8848, 2011.

REYES-GORDILLO, K.; SEGOVIA, J.; SHIBAYAMA, M.; VERGARA, P.; MORENO, M. G.; MURIEL, P. Curcumin protects against acute liver damage in the rat by inhibiting NF-kappaB, proinflammatory cytokines production and oxidative stress. **Biochim Biophys Acta,** v. 1770, n. 6, p. 989-996, 2007.

ROSSI, S.; SANDRI, G.; CARAMELLA, C. M. Buccal drug delivery: a challenge already won? **Drug Discov Today,** v. 2, n. 1, p. 59-65, 2005.

ROSSI-BERGMANN, B. Introdução à nanobiotecnologia. Workshop Avanços em Engenharia de Proteínas e Síntese de Peptídeos, 2008, Instituto Oswaldo Cruz, Rio de Janeiro.

ROY, S.; PAL, K.; ANIS, A.; PRAMANIK, K.; PRABHAKAR, B. Polymers in mucoadhesive drug-delivery systems: a Brief note. **Des Monomers Polym,** v. 12, n. 6, p. 483-495, 2009.

SACHL, R.; UCHMAN, M.; MATEJICEK, P.; PROCHAZKA, K.; STEPANEK, M.; SPIRKOVA, M. Preparation and characterization of

self-assembled nanoparticles formed by poly(ethylene oxide)-block-poly(epsilon-caprolactone) copolymers with long poly(epsilon-caprolactone) blocks in aqueous solutions. **Langmuir,** v. 23, n. 6, p. 3395-3400, 2007.

SAHU, A.; BORA, U.; KASOJU, N.; GOSWAMI, P. Synthesis of novel biodegradable and self-assembling methoxy poly(ethylene glycol)-palmitate nanocarrier for curcumin delivery to cancer cells. **Acta Biomaterialia,** v. 4, n. 6, p. 1752-1761, 2008.

SAHU, A.; KASOJU, N.; BORA, U. Fluorescence study of the curcumin-casein micelle complexation and its application as a drug nanocarrier to cancer cells. **Biomacromolecules,** v. 9, n. 10, p. 2905-2912, 2008.

SAHU, A.; KASOJU, N.; GOSWAMI, P.; BORA, U. Encapsulation of Curcumin in Pluronic Block Copolymer Micelles for Drug Delivery Applications. **J Biomater Appl**, 2010.

SALAMAT-MILLER, N.; CHITTCHANG, M.; JOHNSTON, T. P. The use of mucoadhesive polymers in buccal drug delivery. **Adv Drug Deliv Rev,** v. 57, n. 11, p. 1666-1691, 2005.

SANDRI, G.; POGGI, P.; BONFERONI, M. C.; ROSSI, S.; FERRARI, F.; CARAMELLA, C. Histological evaluation of buccal penetration enhancement properties of chitosan and trimethyl chitosan. **J Pharm Pharmacol,** v. 58, n. 10, p. 1327-1336, 2006.

SANGEETHA, S.; VENKATESH, D. N.; KRISHAN, P. N.; SARASWATHI, R. Mucosa as a route for systemic drug delivery. **RJPBCS,** v. 1, n. 3, p. 178-187, 2010.

SANTANDER-ORTEGA, M. J.; CSABA, N.; ALONSO, M. J.; ORTEGA-VINUESA, J. L.; BASTOS-GONZÁLEZ, D. Stability and physicochemical characteristics of PLGA, PLGA:poloxamer and PLGA:poloxamine blend nanoparticles: a comparative study. **Colloids Surf A Physicochem Eng Asp,** v. 296, n. 1, p. 132-140, 2007.

SAPRE, A.; PARIKH, R.; GOHEL, M. Diskettes of mucoadhesive polymeric nanoparticles for oral (buccal) transmucosal delivery of

fluoxetine hydrochloride: formulation and characterization. Nanotech Conference and Expo, 2009, Houston, Texas.

SASHINA, E.; VNUCHKIN, A.; NOVOSELOV, N. A study of the thermodynamics of chitosan interaction with polyvinyl alcohol and polyethylene oxide by differential scanning calorimetry. **Russ J Appl Chem,** v. 79, n. 10, p. 1643-1646, 2006a.

SASHINA, E. S.; VNUCHKIN, A. V.; NOVOSELOV, N. P. A study of the thermodynamics of chitosan interaction with polyvinyl alcohol and polyethylene oxide by differential scanning calorimetry. **Russian Journal of Applied Chemistry,** v. 79, n. 10, p. 1643-1646, 2006b.

SCHAFFAZICK, S. R.; GUTERRES, S. S.; FREITAS, L. D. L.; POHLMANN, A. R. Caracterização e estabilidade físico-química de sistemas poliméricos nanoparticulados para administração de fármacos. **Química Nova,** v. 26, p. 726-737, 2003.

SCHATZ, C.; LECOMMANDOUX, S. Polysaccharide-containing block copolymers: synthesis, properties and applications of an emerging family of glycoconjugates. **Macromol Rapid Commun,** v. 31, n. 19, p. 1664-1684, 2010.

SCHIPPER, N. G.; OLSSON, S.; HOOGSTRAATE, J. A.; DEBOER, A. G.; VARUM, K. M.; ARTURSSON, P. Chitosans as absorption enhancers for poorly absorbable drugs 2: mechanism of absorption enhancement. **Pharm Res,** v. 14, n. 7, p. 923-929, 1997.

SCHOLZ, O. A.; WOLFF, A.; SCHUMACHER, A.; GIANNOLA, L. I.; CAMPISI, G.; CIACH, T.; VELTEN, T. Drug delivery from the oral cavity: focus on a novel mechatronic delivery device. **Drug Discov Today,** v. 13, n. 5-6, p. 247-253, 2008.

SENEL, S.; HINCAL, A. A. Drug permeation enhancement via buccal route: possibilities and limitations. **J Control Release,** v. 72, n. 1-3, p. 133-144, 2001.

SENEL, S.; KREMER, M. J.; KAS, S.; WERTZ, P. W.; HINCAL, A. A.; SQUIER, C. A. Enhancing effect of chitosan on peptide drug delivery across buccal mucosa. **Biomaterials,** v. 21, n. 20, p. 2067-2071, 2000.

SERRA, L.; DOMENECH, J.; PEPPAS, N. A. Engineering design and molecular dynamics of mucoadhesive drug delivery systems as targeting agents. **Eur J Pharm Biopharm,** v. 71, n. 3, p. 519-528, 2009.

SHAIKH, J.; ANKOLA, D. D.; BENIWAL, V.; SINGH, D.; KUMAR, M. N. V. R. Nanoparticle encapsulation improves oral bioavailability of curcumin by at least 9-fold when compared to curcumin administered with piperine as absorption enhancer. **Eur J Pharm Sci,** v. 37, n. 3-4, p. 223-230, 2009.

SHANKRAIAH, M.; NAGESH, C.; VENKATESH, J. S.; NARSU, M. L.; SETTY, S. R. Sustained release device containing ornidazole for periodontitis. **IRJP,** v. 2, n. 4, p. 217-221, 2011.

SHARMA, M.; MANOHARLAL, R.; PURI, N.; PRASAD, R. Antifungal curcumin induces reactive oxygen species and triggers an early apoptosis but prevents hyphae development by targeting the global repressor TUP1 in Candida albicans. **Biosci Rep,** v. 30, n. 6, p. 391-404, 2010.

SHARMA, R. A.; GESCHER, A. J.; STEWARD, W. P. Curcumin: the story so far. **Eur J Cancer,** v. 41, n. 13, p. 1955-1968, 2005.

SHOJAEI, A. H. Buccal mucosa as a route for systemic drug delivery: a review. **J Pharm Pharm Sci,** v. 1, n. 1, p. 15-30, 1998.

SIMI, C.; ABRAHAM, T. Biodegradable biocompatible xyloglucan films for various applications. **Colloid Polym Sci,** v. 288, n. 3, p. 297-306, 2010.

SINGH, S.; KHAR, A. Biological effects of curcumin and its role in cancer chemoprevention and therapy. **Anticancer Agents Med Chem,** v. 6, n. 3, p. 259-270, 2006.

SMART, J. D. The basics and underlying mechanisms of mucoadhesion. **Adv Drug Deliv Rev,** v. 57, n. 11, p. 1556-1568, 2005a.

SMART, J. D. Buccal drug delivery. **Expert Opin Drug Deliv,** v. 2, n. 3, p. 507-517, 2005b.

SOGIAS, I. A.; WILLIAMS, A. C.; KHUTORYANSKIY, V. V. Why is chitosan mucoadhesive? **Biomacromolecules,** v. 9, n. 7, p. 1837-1842, 2008.

SONG, Z.; FENG, R.; SUN, M.; GUO, C.; GAO, Y.; LI, L.; ZHAI, G. Curcumin-loaded PLGA-PEG-PLGA triblock copolymeric micelles: preparation, pharmacokinetics and distribution in vivo. **J Colloid Interface Sci**, 2010.

SOU, K.; INENAGA, S.; TAKEOKA, S.; TSUCHIDA, E. Loading of curcumin into macrophages using lipid-based nanoparticles. **International Journal of Pharmaceutics,** v. 352, n. 1-2, p. 287-93, 2008.

SOU, K.; OYAJOBI, B.; GOINS, B.; PHILLIPS, W. T.; TSUCHIDA, E. Characterization and cytotoxicity of self-organized assemblies of curcumin and amphiphatic poly(ethylene glycol). **J Biomed Nanotechnol,** v. 5, n. 2, p. 202-208, 2009.

SUDHAKAR, Y.; KUOTSU, K.; BANDYOPADHYAY, A. K. Buccal bioadhesive drug delivery - a promising option for orally less efficient drugs. **J Control Release,** v. 114, n. 1, p. 15-40, 2006.

SUWANNATEEP, N.; BANLUNARA, W.; WANICHWECHARUNGRUANG, S. P.; CHIABLAEM, K.; LIRDPRAPAMONGKOL, K.; SVASTI, J. Mucoadhesive curcumin nanospheres: biological activity, adhesion to stomach mucosa and release of curcumin into the circulation. **J Control Release,** v. 151, n. 2, p. 176-182, 2011.

SVENSSON, O. **Interactions of mucins with biopolymers and drug delivery particles**. 2008. 81 (Thesis). The Faculty of Health and Society, Malmö University, Malmö.

SVENSSON, O.; ARNEBRANT, T. Mucin layers and multilayers — Physicochemical properties and applications. **Curr Opin Colloid Interface Sci,** v. 15, n. 6, p. 395-405, 2010.

SVENSSON, O.; THURESSON, K.; ARNEBRANT, T. Interactions between chitosan-modified particles and mucin-coated surfaces. **J Colloid Interface Sci,** v. 325, n. 2, p. 346-350, 2008.

TADA, D. B.; SINGH, S.; NAGESHA, D.; JOST, E.; LEVY, C. O.; GULTEPE, E.; CORMACK, R.; MAKRIGIORGOS, G. M.; SRIDHAR, S. Chitosan film containing poly(D,L-lactic-co-glycolic acid) nanoparticles: a platform for localized dual-drug release. **Pharm Res,** v. 27, n. 8, p. 1738-1745, 2010.

TAKAHASHI, M.; UECHI, S.; TAKARA, K.; ASIKIN, Y.; WADA, K. Evaluation of an Oral Carrier System in Rats: Bioavailability and Antioxidant Properties of Liposome-Encapsulated Curcumin. **J Agric Food Chem,** v. 57, n. 19, p. 9141-9146, 2009.

TAKEUCHI, H.; THONGBORISUTE, J.; MATSUI, Y.; SUGIHARA, H.; YAMAMOTO, H.; KAWASHIMA, Y. Novel mucoadhesion tests for polymers and polymer-coated particles to design optimal mucoadhesive drug delivery systems. **Adv Drug Deliv Rev,** v. 57, n. 11, p. 1583-1594, 2005.

TANGRI, P.; MADHAV, N. V. S. Oral mucoadhesive drug delivery systems: a review. **IJB,** v. 2, n. 1, p. 36-46, 2011.

TEIXEIRA, J. Small-angle scattering by fractal systems. **J Appl Crystallogr,** v. 21, n. 6, p. 781-785, 1988.

THANGAPAZHAM, R. L.; PURI, A.; TELE, S.; BLUMENTHAL, R.; MAHESHWARI, R. K. Evaluation of a nanotechnology-based carrier for delivery of curcumin in prostate cancer cells. **Int J Oncol,** v. 32, n. 5, p. 1119-1123, 2008.

TIYABOONCHAI, W.; TUNGPRADIT, W.; PLIANBANGCHANG, P. Formulation and characterization of curcuminoids loaded solid lipid nanoparticles. **Int J Pharm,** v. 337, n. 1-2, p. 299-306, 2007.

TOMREN, M. A.; MASSON, M.; LOFTSSON, T.; TONNESEN, H. H. Studies on curcumin and curcuminoids XXXI. Symmetric and asymmetric curcuminoids: stability, activity and complexation with cyclodextrin. **Int J Pharm,** v. 338, n. 1-2, p. 27-34, 2007.

TONNESEN, H. H. Solubility, chemical and photochemical stability of curcumin in surfactant solutions. Studies of curcumin and curcuminoids, XXVIII. **Pharmazie,** v. 57, n. 12, p. 820-824, 2002.

TONNESEN, H. H.; MASSON, M.; LOFTSSON, T. Studies of curcumin and curcuminoids. XXVII. Cyclodextrin complexation: solubility, chemical and photochemical stability. **Int J Pharm,** v. 244, n. 1-2, p. 127-135, 2002.

TORCHILIN, V. P. Micellar nanocarriers: pharmaceutical perspectives. **Pharm Res,** v. 24, n. 1, p. 1-16, 2007.

UNNIKRISHNAN, M. K.; RAO, M. N. Curcumin inhibits nitrite-induced methemoglobin formation. **FEBS Lett,** v. 301, n. 2, p. 195-196, 1992.

VAN DE LOOSDRECHT, A. A.; NENNIE, E.; OSSENKOPPELE, G. J.; BEELEN, R. H. J.; LANGENHUIJSEN, M. M. A. C. Cell mediated cytotoxicity against U 937 cells by human monocytes and macrophages in a modified colorimetric MTT assay: A methodological study. **J Immunol Methods,** v. 141, n. 1, p. 15-22, 1991.

VARUM, F. O.; BASIT, A. W.; SOUSA, J.; VEIGA, F. Estudos de mucoadesão no trato gastrointestinal para o aumento da biodisponibilidade oral de fármacos. **RBCF,** v. 44, p. 535-548, 2008.

VASIR, J. K.; TAMBWEKAR, K.; GARG, S. Bioadhesive microspheres as a controlled drug delivery system. **Int J Pharm,** v. 255, n. 1-2, p. 13-32, 2003.

VENKATESAN, N. Pulmonary protective effects of curcumin against paraquat toxicity. **Life Sci,** v. 66, n. 2, p. PL21-PL28, 2000.

VENKATESAN, N.; PUNITHAVATHI, D.; BABU, M. Protection from acute and chronic lung diseases by curcumin. **Adv Exp Med Biol,** v. 595, p. 379-405, 2007.

VOINOVA, M. V.; RODAHL, M.; JONSON, M.; KASEMO, B. Viscoelastic acoustic response of layered polymer films at fluid-solid interfaces: continuum mechanics approach. **Phys Scr,** v. 59, n. 5, p. 391-396, 1999.

WANG, D.; VEENA, M. S.; STEVENSON, K.; TANG, C.; HO, B.; SUH, J. D.; DUARTE, V. M.; FAULL, K. F.; MEHTA, K.;

SRIVATSAN, E. S.; WANG, M. B. Liposome-encapsulated curcumin suppresses growth of head and neck squamous cell carcinoma in vitro and in xenografts through the inhibition of nuclear factor kappaB by an AKT-independent pathway. **Clin Cancer Res,** v. 14, n. 19, p. 6228-6236, 2008a.

WANG, S.; TAN, M.; ZHONG, Z.; CHEN, M.; WANG, Y. Nanotechnologies for curcumin: an ancient puzzler meets modern solutions. **J Nanomater,** v. 2011, 2011.

WANG, X.; JIANG, Y.; WANG, Y.-W.; HUANG, M.-T.; HO, C.-T.; HUANG, Q. Enhancing anti-inflammation activity of curcumin through O/W nanoemulsions. **Food Chem,** v. 108, n. 2, p. 419-424, 2008b.

WANG, Y. J.; PAN, M. H.; CHENG, A. L.; LIN, L. I.; HO, Y. S.; HSIEH, C. Y.; LIN, J. K. Stability of curcumin in buffer solutions and characterization of its degradation products. **J Pharm Biomed Anal,** v. 15, n. 12, p. 1867-1876, 1997.

WATSON, T. J. Analysis of macromolecular polydispersity in intensity correlation spectroscopy: the method of cumulants. **J Chem Phys,** v. 57, n. 11, p. 4814-4820, 1972.

WEI, X.; GONG, C.; GOU, M.; FU, S.; GUO, Q.; SHI, S.; LUO, F.; GUO, G.; QIU, L.; QIAN, Z. Biodegradable poly(epsilon-caprolactone)-poly(ethylene glycol) copolymers as drug delivery system. **Int J Pharm,** v. 381, n. 1, p. 1-18, 2009.

WEISBERG, S. P.; LEIBEL, R.; TORTORIELLO, D. V. Dietary curcumin significantly improves obesity-associated inflammation and diabetes in mouse models of diabesity. **Endocrinology,** v. 149, n. 7, p. 3549-3458, 2008.

WIECINSKI, P. N.; METZ, K. M.; MANGHAM, A. N.; JACOBSON, K. H.; HAMERS, R. J.; PEDERSEN, J. A. Gastrointestinal biodurability of engineered nanoparticles: development of an in vitro assay. **Nanotoxicology,** v. 3, n. 3, p. 202-214, 2009.

WILLIAMSON, D. L.; MARR, D. W. M.; YANG, J.; YAN, B.; GUHA, S. Nonuniform H distribution in thin-film hydrogenated amorphous Si

by small-angle neutron scattering. **Phys Rev B,** v. 67, n. 7, p. 075314, 2003.

WU, X.; XU, J.; HUANG, X.; WEN, C. Self-microemulsifying drug delivery system improves curcumin dissolution and bioavailability. **Drug Dev Ind Pharm,** v. 37, n. 1, p. 15-23, 2011.

WU, Y.; YANG, W.; WANG, C.; HU, J.; FU, S. Chitosan nanoparticles as a novel delivery system for ammonium glycyrrhizinate. **Int J Pharm,** v. 295, n. 1-2, p. 235-245, 2005.

XIAO, R. Z.; ZENG, Z. W.; ZHOU, G. L.; WANG, J. J.; LI, F. Z.; WANG, A. M. Recent advances in PEG-PLA block copolymer nanoparticles. **Int J Nanomedicine,** v. 5, p. 1057-1065, 2010.

YADAV, V.; SURESH, S.; DEVI, K.; YADAV, S. Effect of Cyclodextrin Complexation of Curcumin on its Solubility and Antiangiogenic and Anti-inflammatory Activity in Rat Colitis Model. **AAPS PharmSciTech,** v. 10, n. 3, p. 752-762, 2009.

YALLAPU, M. M.; GUPTA, B. K.; JAGGI, M.; CHAUHAN, S. C. Fabrication of curcumin encapsulated PLGA nanoparticles for improved therapeutic effects in metastatic cancer cells. **J Colloid Interface Sci,** v. 351, n. 1, p. 19-29, 2010a.

YALLAPU, M. M.; JAGGI, M.; CHAUHAN, S. C. [beta]-Cyclodextrin-curcumin self-assembly enhances curcumin delivery in prostate cancer cells. **Colloids Surf B Biointerfaces,** v. 79, n. 1, p. 113-125, 2010.

YALLAPU, M. M.; MAHER, D. M.; SUNDRAM, V.; BELL, M. C.; JAGGI, M.; CHAUHAN, S. C. Curcumin induces chemo/radio-sensitization in ovarian cancer cells and curcumin nanoparticles inhibit ovarian cancer cell growth. **J Ovarian Res,** v. 3, n. 11, 2010b.

YEN, F. L.; WU, T. H.; TZENG, C. W.; LIN, L. T.; LIN, C. C. Curcumin nanoparticles improve the physicochemical properties of curcumin and effectively enhance its antioxidant and antihepatoma activities. **J Agric Food Chem,** v. 58, n. 12, p. 7376-7382, 2010.

ZEBIB, B.; MOULOUNGUI, Z.; NOIROT, V. Stabilization of curcumin by complexation with divalent cations in glycerol/water system. **Bioinorg Chem Appl**, 2010.

ZHANG, X.; SUN, M.; ZHENG, A.; CAO, D.; BI, Y.; SUN, J. Preparation and characterization of insulin-loaded bioadhesive PLGA nanoparticles for oral administration. **Eur J Pharm Sci,** v. 45, n. 5, p. 632-638, 2012.

ZHU, X. Q.; SUN, M.; ZHU, F. P.; DING, T. T.; ZHAI, Y. J.; ZHAI, G. X. Preparation and characterization of curcumin polybutylcyanoacrylate nanoparticles. **Zhong Yao Cai,** v. 33, n. 5, p. 797-801, 2010.

APÊNDICE

Validação do Método Analítico para a Determinação da Curcumina nos Estudos de Liberação, Permeação e Retenção na Mucosa Esofágica

1 METODOLOGIA

1.1 Método fluorimétrico

As análises foram realizadas por espectrofotometria usando um espectrofluorímetro Perkin Elmer LS 55. As amostras foram colocadas em cubeta de quartzo de 1 cm. Ambos slits de excitação e emissão foram ajustados para 5 nm. As amostras foram excitadas a 424 nm e o espectro de emissão foi gravado de 435 a 700 nm. Para os estudos de permeação e retenção, as intensidades de fluorescência foram medidas em 495 nm e 535 nm, respectivamente.

1.2 Especificidade

A especificidade do estudo de permeação foi avaliada pela análise do meio aceptor puro (solução saliva artificial pH 6,75 contendo 0,5 % de lauril sulfato de sódio), contaminado com nanopartículas brancas, e daquele obtido após 8 horas do estudo de permeação. A especificidade do estudo de retenção foi avaliada pela análise do meio extrator (metanol) contaminado com nanopartículas brancas e daquele obtido após o procedimento de extração da mucosa. As soluções foram analisadas por espectrofotometria conforme metodologia descrita no item 1. O objetivo das análises é verificar se os componentes do meio, das suspensões de nanopartículas ou da mucosa interferem na quantificação da curcumina.

1.3 Linearidade

Para avaliar a linearidade do método, uma solução estoque foi preparada pela dissolução de, exatamente, 10 mg de curcumina em 10 mL de metanol. Esta solução foi, então, diluída com solução saliva artificial pH 6,75 contendo 0,5 % de lauril sulfato de sódio ou metanol para a obtenção de soluções com concentrações variando de 0,01 a 0,5 μg/mL, e 0,05 a 1,0 μg/mL, respectivamente. As soluções foram preparadas em triplicata e analisadas por espectrofotometria. O gráfico da curva de calibração foi obtido plotando as intensidades de fluorescência *versus* as concentrações teóricas das soluções padrão. A

linearidade foi avaliada através da análise de regressão linear pelo método dos mínimos quadrados.

1.4 Limites de Detecção e de Quantificação

O limite de detecção (LD) é definido como a menor concentração da curva de calibração que pode ser detectada, mas não necessariamente quantificada como um valor exato. O valor do LD foi calculado diretamente a partir da curva de calibração, usando a seguinte equação:

$$LD = \frac{3{,}3\,\sigma}{S}$$

Onde, σ é o desvio padrão dos interceptos das curvas com o eixo Y e S é a inclinação da curva de calibração.

O limite de quantificação (LQ), por sua vez, é definido como a menor concentração da curva de calibração que pode ser medida com precisão e exatidão adequadas. O valor do LQ foi calculado diretamente a partir da curva de calibração, usando a seguinte equação:

$$LQ = \frac{10\,\sigma}{S}$$

Onde, σ é o desvio padrão dos interceptos das curvas com o eixo Y e S é a inclinação da curva de calibração.

1.5 Precisão

A precisão do método foi determinada pela medida da repetibilidade (precisão intra-dia) e da precisão intermediária (precisão inter-dia), ambos expressos como desvio padrão relativo (DPR). A precisão foi avaliada pela análise de soluções padrão contendo diferentes concentrações de curcumina em solução saliva artificial pH 6,75 contendo 0,5 % de lauril sulfato de sódio (0,025; 0,1 e 0,5 μg/mL) e em metanol (0,1; 0,5 e 1,0 μg/mL). A repetibilidade foi avaliada pela medida de cada solução padrão em triplicata, no mesmo dia, sob as mesmas condições experimentais. A precisão intermediária foi avaliada pela análise de cada solução padrão em três dias diferentes.

1.6 Exatidão

A exatidão do método foi avaliada através da determinação da recuperação de curcumina após contaminação da mucosa e do meio

aceptor obtido do estudo de permeação *in vitro* (sem aplicação de amostra).

1.6.1 Recuperação da Curcumina no Meio Aceptor

A recuperação da curcumina no meio aceptor foi avaliada pela contaminação do meio obtido após o estudo de permeação *in vitro* com uma solução padrão de curcumina. Soluções com diferentes concentrações finais de curcumina (baixa, média e alta) foram obtidas e a curcumina foi quantificada por espectrofotometria, conforme descrito no item 1.1. Todas as análises foram realizadas em triplicata.

1.6.2 Recuperação da Curcumina na Mucosa

Para avaliação da recuperação da curcumina na mucosa, amostras deste tecido com área de 2,27 cm^2 foram cortadas e colocadas em tubos de ensaio. As mucosas foram contaminadas com soluções padrão de diferentes concentrações de curcumina em metanol. Após, procedeu-se a extração da curcumina pela adição de 5 mL de metanol, agitação em vortex durante 30 s, armazenamento *overnight* a 4 °C e sonicação em banho de ultrassom por 50 min. As soluções foram, então, filtradas em membranas de 0,45 μm (PVDF, Millipore, EUA) e a curcumina quantificada por espectrofotometria, conforme descrito no item 1.1. Todas as análises foram realizadas em triplicata.

2 RESULTADOS E DISCUSSÃO

A validação do método analítico é indispensável para assegurar a sua adequabilidade ao objetivo pretendido. Assim, a validação do método analítico para a determinação da curcumina nos estudos de permeação e retenção na mucosa esofágica torna-se essencial para a obtenção de dados confiáveis. Devido as suas propriedades de fluorescência, a quantificação da curcumina permeada e retida na mucosa foi determinada através de método fluorimétrico.

2.1 Especificidade

O espectro de emissão da curcumina no meio aceptor (solução saliva artificial pH 6,75 contendo 0,5 % de lauril sulfato de sódio) é apresentado na Figura 11. Este espectro mostra uma banda de emissão

intensa na região de comprimento de onda entre 435 - 650 nm, exibindo uma intensidade máxima de fluorescência em 495 nm. A fim de provar a especificidade do método na análise do meio aceptor obtido após o estudo de permeação, foram analisados o meio aceptor puro, contaminado com nanopartículas brancas, e aquele obtido após 8 horas do estudo de permeação (Figura 11). A análise dos espectros mostra que os componentes do meio aceptor exibem certa intensidade de fluorescência no comprimento de onda de 495 nm, a qual foi descontada durante os cálculos da quantificação de curcumina permeada. Os componentes da formulação e da camada mucosa não apresentaram interferência no comprimento de onda de 495 nm, indicando que o método foi específico para as condições fluorimétricas empregadas.

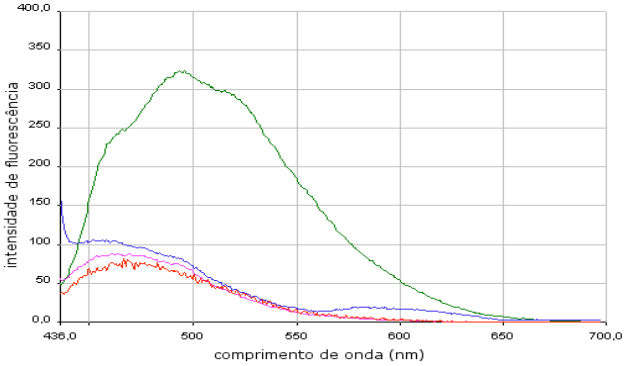

Figura 11. Espectros de fluorescência obtidos para: solução padrão de curcumina no meio aceptor, 0,5 μg/mL (verde); meio aceptor contaminado com suspensão de nanopartículas brancas (azul); meio aceptor puro (rosa); meio aceptor obtido após 8 horas do estudo de permeação (vermelho).

O espectro de emissão da curcumina no meio extrator (metanol) é apresentado na Figura 12. Este espectro mostra uma banda de emissão intensa na região de comprimento de onda entre 440 - 650 nm, exibindo uma intensidade máxima de fluorescência em 535 nm. A fim de provar a especificidade do método na análise do meio extrator obtido no estudo de retenção, foram analisados o meio extrator contaminado com nanopartículas brancas, e aquele obtido após o procedimento de extração da mucosa (Figura 12). A análise dos espectros mostra que os componentes da formulação não apresentaram interferência, enquanto os componentes da camada mucosa extraídos pelo metanol emitiram pequena intensidade de fluorescência no comprimento de onda de 535

nm, a qual foi descontada durante os cálculos da quantificação de curcumina retida.

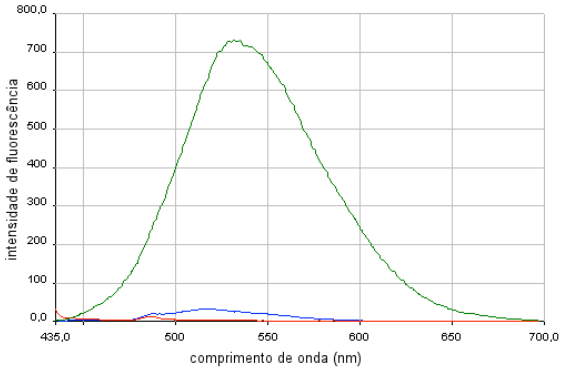

Figura 12. Espectros de fluorescência obtidos para: solução padrão de curcumina no meio extrator, 1,0 μg/mL (verde); meio extrator contaminado com suspensão de nanopartículas brancas (vermelho); meio extrator obtido após o procedimento de extração da mucosa (azul).

2.2 Linearidade

O gráfico de linearidade da curcumina em solução saliva artificial pH 6,75 contendo 0,5 % de lauril sulfato de sódio, utilizada como meio aceptor nos estudos de permeação está apresentado na Figura 13. A curva de calibração demonstrou-se linear na faixa de 0,01 a 0,5 μg/mL, com coeficiente de correlação de 0,998. A equação da reta da curva de calibração média obtida foi y = 513,9 x – 1,382. A validade do método foi verificada por análise de variância (ANOVA), a qual confirmou a linearidade da equação ($F_{calculado}$ = 3970,63 > $F_{crítico}$ = 1,07 x 10^{-9}, P = 5 %).

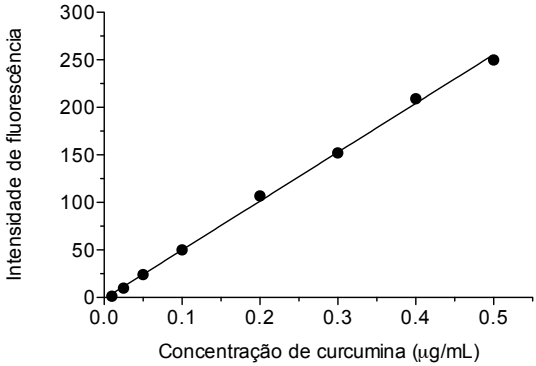

Figura 13. Curva de calibração da curcumina em solução saliva artificial pH 6,75 contendo 0,5 % de lauril sulfato de sódio.

O gráfico de linearidade da curcumina em metanol, utilizado como meio extrator nos estudos de retenção, está apresentado na Figura 14. A curva de calibração demonstrou-se linear na faixa de 0,05 a 1,0 μg/mL, com coeficiente de correlação de 0,996. A equação da reta foi y = 721,2 x + 24,51. A análise de variância (ANOVA) confirmou que a equação foi linear ($F_{calculado}$ = 1053,64 > $F_{crítico}$ = 5,37 x 10^{-6}, P = 5 %).

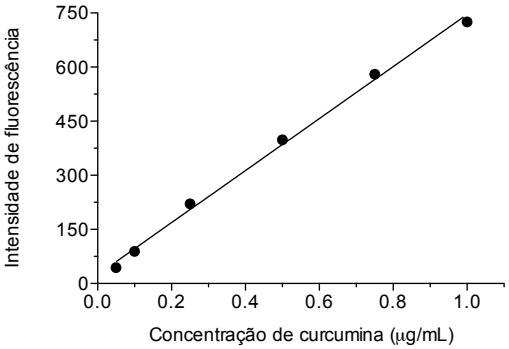

Figura 14. Curva de calibração da curcumina em metanol.

2.3 Limites de Detecção e de Quantificação

Os limites de detecção (LD) e quantificação (LQ) foram calculados usando os valores de intercepto e inclinação obtidos da média das três curvas de calibração originadas. Para a curva de curcumina em solução saliva artificial pH 6,75 contendo 0,5 % de lauril sulfato de sódio, o desvio padrão dos interceptos e a inclinação média das curvas foram de 0,696 e 513,9, respectivamente. Assim, os valores calculados de LD e LQ para a curcumina neste meio foram de 0,004 e 0,014 μg/mL, respectivamente.

Para a curva de curcumina em metanol, o desvio padrão dos interceptos e a inclinação média das curvas foram de 2,46 e 721,2, respectivamente. Os valores calculados de LD e LQ para a curcumina neste meio foram de 0,011 e 0,034 μg/mL, respectivamente.

2.4 Precisão

Os resultados dos ensaios de repetibilidade e precisão intermediária da curcumina nos meios aceptor e extrator estão mostrados nas Tabelas 3 e 4, respectivamente. As intensidades de fluorescência indicaram variabilidade intra- e inter-dia satisfatória, com valores de DPR menores que 5 %, indicando a precisão do método.

Tabela 3. Resultados obtidos na avaliação da precisão do método usando solução saliva artificial pH 6,75 contendo 0,5 % de lauril sulfato de sódio (meio aceptor).

Concentração teórica (µg/ml)	**Dia**		**Intensidade média**	**DP**	**DPR (%)**
0,025	Intra-dia	1	82,24	1,39	1,69
		2	87,45	2,37	2,71
		3	85,63	0,72	0,84
	Inter-dia	1, 2, 3	85,11	2,16	2,54
0,1	Intra-dia	1	122,53	0,47	0,38
		2	127,80	1,49	1,16
		3	134,00	2,57	1,92
	Inter-dia	1, 2, 3	128,11	4,69	3,66
0,5	Intra-dia	1	322,27	5,16	1,60
		2	331,17	8,89	2,69
		3	356,20	5,93	1,66
	Inter-dia	1, 2, 3	336,55	14,37	4,27

Tabela 4. Resultados obtidos na avaliação da precisão do método usando metanol (meio extrator).

Concentração teórica (µg/ml)	Dia		Intensidade média	DP	DPR (%)
0,1	Intra-dia	1	88,79	2,35	2,64
		2	89,05	1,32	1,49
		3	90,05	1,16	1,29
	Inter-dia	1, 2, 3	89,30	0,54	0,61
0,5	Intra-dia	1	398,63	12,50	3,14
		2	404,75	9,92	2,45
		3	407,23	9,09	2,23
	Inter-dia	1, 2, 3	403,54	3,61	0,90
1,0	Intra-dia	1	725,32	6,67	0,92
		2	726,18	10,77	1,48
		3	691,89	10,51	1,52
	Inter-dia	1, 2, 3	714,46	15,97	2,23

2.5 Exatidão

A exatidão do método foi determinada pela análise das amostras de mucosa e de meio aceptor, obtido após o estudo de permeação, contaminadas com soluções de concentrações conhecidas de curcumina. A recuperação de curcumina foi expressa como a porcentagem média de fármaco encontrada nas soluções de três níveis diferentes (baixa, média e alta concentração). Os resultados demonstram que o método apresentou exatidão adequada para ambas amostras analisadas (Tabela 5).

Tabela 5. Resultados obtidos na avaliação da exatidão do método.

Amostra	Concentração de curcumina (µg/ml)		Recuperação (%)	DP	DPR
	teórica	medida			
Meio aceptor	0,025	0,024	96,7	0,70	0,72
	0,10	0,10	103,9	1,34	1,29
	0,50	0,54	107,8	0,66	0,61
Mucosa	0,10	0,10	100,5	3,87	3,85
	0,49	0,47	96,8	0,61	0,63
	0,98	0,94	95,5	0,09	0,09

ANEXO

NOTE A L'ATTENTION
DES RAPPORTEURS SUR LES TRAVAUX DES CANDIDATS AU DIPLOME DE DOCTORAT DE L'UNIVERSITE JOSEPH FOURIER

Vu les décisions du Conseil Scientifique (séance du 11 avril 2003) et du Conseil d'Administration (séance du 15 avril 2003) de l'Université Joseph Fourier :

Il est demandé aux rapporteurs qui établissent les rapports préalables de bien vouloir compléter la grille d'évaluation suivante et de la joindre à leur rapport : (merci de respecter cette grille, sans ajouter d'autres items)

Nom du rapporteur : Marcos Antônio Segatto Silva				
Nom du doctorant : Letícia Mazzarino				
Niveau scientifique :	Satisfaisant	Bon	Très bon	Exceptionnel
	[ ]	[ ]	[ ]	[X]

SERVIÇO PÚBLICO FEDERAL
UNIVERSIDADE FEDERAL DE SANTA CATARINA
Centro de Ciências da Saúde
Departamento de Ciências Farmacêuticas
LABORATÓRIO DE CONTROLE DE QUALIDADE
CAMPUS UNIVERSITÁRIO - TRINDADE CEP: 88040-900 - FLORIANÓPOLIS - SC
TELEFONE (048) 3721-5066 - FAX (048) 3721-9542

Florianópolis, 28 de março de 2013.

The work titled "Sistemas Nanoestruturados decorados com quitosana para liberação bucal de curcumina" (Nanostructured Systems decorated with chitosan for oral curcumin release) describes the development of nanostructured mucoadhesive systems, including decorated with chitosan nanoparticles and films containing nanoparticles, aiming release oral curcumin. Nanoparticles have been developed polycaprolactone (PCL) and nanoparticles xiloglucana polycaprolactone-block-(XGO-b-PCL) prepared by the techniques of nanoprecipitation and by the method of co-solvent, respectively. Numerous methods were used for the determination of particle size and zeta potential, studies of dynamic light scattering (DLS), nanoparticle tracking analysis (NTA), transmission electron microscopy (TEM), dynamic light scattering (DLS), microbalance quartz crystal with dissipation monitoring (QCM-D), plasmonics surface resonance (SPR), permeation and retention of curcumin through porcine esophageal mucosa, in vitro cytotoxicity and antimicrobial activity.

The mucoadhesive films containing nanoparticles were prepared by the casting technique, with characterization by atomic force microscopy (AFM) and scanning electron microscopy, high-resolution (FEG-SEM).

The results indicate that the mucoadhesive systems developed, nanoparticles decorated with chitosan and films nanoparticles containing offer a new strategy for the release oral curcumin and have potential applications in the local treatment of diseases of the oral cavity. For all that has been seen, the work was adequate scientific and technological level, provided an excellent training and work experience outside your country.

Prof. Dr. Marcos Antonio Segatto Silva

NOTE A L'ATTENTION
DES RAPPORTEURS SUR LES TRAVAUX DES CANDIDATS AU DIPLOME DE DOCTORAT DE L'UNIVERSITE JOSEPH FOURIER

Vu les décisions du Conseil Scientifique (séance du 11 avril 2003) et du Conseil d'Administration (séance du 15 avril 2003) de l'Université Joseph Fourier :

Il est demandé aux rapporteurs qui établissent les rapports préalables de bien vouloir compléter la grille d'évaluation suivante et de la joindre à leur rapport : (merci de respecter cette grille, sans ajouter d'autres items)

Nom du rapporteur : ROBIN				
Nom du doctorant :Leticia Mazzarino				
Niveau scientifique :	Satisfaisant	Bon	Très bon	Exceptionnel
	[ ]	[ ]	[ ]	■

Rapport sur le mémoire de thèse présenté par Madame Leticia Mazzarino intitulé « Systèmes nanostructurés décorés avec du chitosan pour la libération buccale de la curcumine »

Le manuscrit soumis aux rapporteurs par Madame Leticia Mazzarino s'intitule « Systèmes nanostructurés décorés avec du chitosan pour la libération buccale de la curcumine ». Ce travail s'inscrit dans le cadre d'une co-tutelle avec le Brésil, aussi, le manuscrit, est présenté dans les deux langues des pays de la co-tutelle. Le document qui intègre plusieurs publications dont une est déjà acceptée, se décompose en quatre grands chapitres auxquels viennent s'ajouter une discussion générale ainsi que des documents annexes.

Ce travail s'inscrit dans une problématique générale parfaitement d'actualité qu'est l'absorption de médicaments au travers de muqueuses. Les systèmes dits mucoadhésifs, ont la particularité de prolonger le temps de séjour des médicaments dans la couche muqueuse, permettant par là même d'optimiser la libération progressive des molécules à effet thérapeutique. La cavité buccale constitue un site privilégié pour l'administration des médicaments du fait de sa forte perméabilité. Cette voie de traitement permet de traiter directement des affections comme les gengivites, les périodonties. Cependant, la production continue de salive pose des problèmes de libération non uniforme du médicament mais aussi de dilution. Aussi, le développement de systèmes mucoadhésifs constitue un mode d'administration prometteur pour pallier ces inconvénients. A partir de cette problématique posée, Madame Leticia Mazzarino a envisagé d'étudier l'élaboration de nanoparticules décorées par des polysaccharides, visant à combiner une protection des molécules actives (parfois très hydrophobes), leur libération contrôlée, et le caractère adhésif de ces systèmes. Le chapitre 1 du manuscrit est donc consacré à l'état de l'art dans le domaine des voies d'administration buccale de médicaments mais également, à la compréhension des mécanismes de diffusion buccale des principes actifs. Une revue des différents polymères utilisés et de leur mise en forme pour une telle application dans ce domaine est présentée au lecteur avec une analyse critique des performances atteintes. L'étudiante ayant choisi de s'intéresser à la curcumine, reconnue pour ses nombreuses propriétés biologiques décrites dans bon nombre de publications scientifiques, elle en fait une présentation des principales structures rencontrées et de leurs principales propriétés. Cependant, cette molécule est sensible à pH neutre ou basique, et peu soluble en milieu aqueux. Son association à des transporteurs, tels que les nanoparticules, permet de pallier ces lacunes, ce qui justifie tout le travail présenté dans ce manuscrit.

Le chapitre 2 vise l'obtention de nanoparticules de polyepsilon caprolactone (Poly CAPA) décorées par des chaines de chitosan en vue d'encapsuler de la curcumine. A partir de (Poly CAPA) commerciale et en utilisant la technique de nano-précipitation et de déplacement de solvant en présence de tensio-actifs non ioniques, des nanoparticules ont ainsi pu être obtenues selon le protocole connu décrit en 1989 par *Fessi et al*. Ces nanoparticules ont alors été décorées par des chaines de chitosan de différentes masses molaires. Ces conditions de préparation ont été optimisées en faisant varier différents paramètres. Selon ce procédé, des particules parfaitement sphériques d'une centaine de

INGENIERIE ET ARCHITECTURES MACROMOLECULAIRES
Groupe Synthèse et Organisations Macromoléculaires
Université Montpellier II - Bat. 17 – CC1702 - Place Eugène Bataillon 34095 Montpellier cedex 5
Téléphone : (33) (0)4 67 14 41 57 – Secrétariat : (33) (0)4 67 14 49 89

nanomètres, comme l'attestent les clichés de TEM, ont pu être obtenues avec une répartition monodisperse. Il est clairement montré que la concentration de la solution de chitosan a un effet sur l'étape de décoration, alors que la masse moléculaire du polysaccharide n'a pas d'incidence sur le rayon hydrodynamique des particules formées. Le mécanisme d'adhésion est essentiellement dicté par les liaisons hydrogène comme cela est prouvé par des mesures de potentiel Zéta. Le taux d'encapsulation en curcumine se situe aux alentours de 99%, cette valeur élevée étant expliquée par sa très faible solubilité dans l'eau. Les différentes techniques de caractérisation physico-chimiques ont permis de déboucher sur une représentation schématique de l'organisation du système à quatre composants mis en oeuvre. Enfin, ces nano-particules ont montré leur caractère adhésif vis-à-vis de mucines grâce à des mesures de tailles de particules après mise en contact. La faisabilité du concept est ainsi prouvée et ouvre la voie à d'autres systèmes.

Les propriétés de mucoadhésivité sont étudiées dans un deuxième temps et font l'objet d'un manuscrit soumis à Journal of Biomedical Nanotechnology. L'utilisation d'une microbalance à cristal de quartz a permis de montrer que toutes les nanoparticules préparées interagissent avec la mucine sous-maxillaire bovine, et ceci, quelle que soit la masse molaire des chaines de chitosan décorant les nanoparticules. L'absence de décoration ne conduit pas la propriété de mucoadhésivité. A partir des valeurs de charges des entités en présence, l'étudiante propose un mécanisme d'interaction basé sur des forces électrostatiques dues aux groupements carboxylates ou sulfonates des protéines et ammonium du chitosan. Cette hypothèse n'exclut pas pour autant l'intervention d'autres mécanismes intégrant des contributions hydrophobes comme cela a été montré par le passé et rapporté dans la littérature.

Par la suite, les nanoparticules ont été étudiées sur le plan de leur perméation au travers de la muqueuse œsophagienne issue du porc, selon des protocoles bien connus dans ce domaine. L'examen des profils de perméation de la curcumine ne semblent pas révéler un effet de la taille des chaines de chitosan ni même un effet de la présence de ces chaines. L'examen histologique de coupes révèle que les cellules épithéliales semblent influencées dans leur arrangement par la présence des nanoparticules recouvertes de chitosan, ce qui est en accord avec la littérature. L'étude de cytotoxicité sur des fibroblasts L929 montre clairement que la protection de la curcumine au sein des nanoparticules réduit notablement la cytotoxicité de cette molécule. Par ailleurs, la présence de curcumine au sein des nanoparticules exacerbe l'activité antifongique, même si des études récentes montrent une activité antifongique du chitosan seul. Au terme de cette partie, il semble que le système d'encapsulation de la curcumine soit une solution d'intérêt pour la délivrance de cette molécule dans le cas de traitement de maladies de la bouche.

A partir de ce concept, l'étudiante s'est alors intéressée à l'élaboration de nouveaux systèmes à base de copolymères à blocs xyloglucan-*bloc*-polyepsilon caprolactone organisés sous la forme de nanoparticules décorées par du chitosan. Les copolymères ont été préparés par chimie click à partir de leurs précurseurs fonctionnalisés par une triple liaison ou une fonction azidure. Après couplage des blocs, les copolymères ont été mis sous la forme de nanoparticules par la méthode des co-solvants en présence de curcumine. L'étude physico-chimique révèle l'obtention d'objets monodisperses d'un diamètre hydrodynamique moyen voisin de 50 nanomètres, la présence de curcumine dans le milieu conduisant à la formation de nanoparticules légèrement plus grosses. L'examen TEM des objets montre qu'il s'agit bien de particules sphériques dont la taille augmente après décoration par du chitosan. Le potentiel Zéta est très nettement changé après cette étape de décoration et atteint une valeur maximale de 24mV due aux charges amenées par les fonctions ammonium. La liaison entre le chitosan et les nanoparticules semble imputable à des liaisons hydrogène, ce qui a déjà été mis en évidence par le passé dans des travaux antérieurs. Les propriétés de mucoadhésivité ont été évaluées par résonance plasmonique de surface et montre très nettement l'effet de la décoration par le chitosan. Là, comme précédemment dans le cas de la première génération de nanoparticules, les interactions avec la mucine sont d'origine électrostatique. Les nanoparticules chargées en curcumine révèlent une activité cytotoxique importante envers des cellules tumorales de mélanome B16F10 ce qui à terme peut présenter un intérêt dans le traitement de maladies cancéreuses.

La dernière partie du travail vise la formation de films intégrant des nanoparticules décorées. Ici, la stratégie est différente et Madame Leticia Mazzarino a voulu prolonger le temps de résidence de ses nanoparticules en les incorporant au sein de films de chitosan plastifié. La mise au point des films

avec une distribution homogène des nanoparticules a constitué un défi qui a été relevé comme l'attestent les caractérisations des films obtenus par AFM et FEG-SEM. Ces films s'hydratent jusqu'à 80% dans un milieu simulant la salive. Le relargage de la curcumine s'effectue selon une cinétique d'ordre zéro, ce qui est tout à fait intéressant dans l'objectif d'une distribution lente d'un principe actif.

En résumé, Madame Leticia Mazzarino présente ici un mémoire soigné, consacré à l'utilisation de la curcumine comme principe actif. Compte-tenu de la fragilité de cette molécule, il est nécessaire de la protéger et d'envisager sa distribution. Pour atteindre cet objectif, l'étudiante a choisi la voie de la protection par des nanoparticules. Il s'agit d'un travail particulièrement d'actualité dont les retombées potentielles sont importantes.

Le travail allie des aspects de synthèse, de caractérisation physico-chimiques mais également, de biologie, et on ne peut que souligner la polyvalence de Madame Leticia Mazzarino qui a su aborder avec maîtrise ces différents domaines. L'analyse des nombreux résultats qu'elle a obtenus lui a permis de tirer des conclusions claires sur les performances des systèmes qu'elle a mis au point.

Il s'agit d'un travail de qualité qui apporte une contribution non négligeable aux connaissances liées à la vectorisation de médicaments par la voie des nanoparticules. On peut considérer ce travail comme abouti, et je tiens à souligner au terme de ce rapport, la quantité impressionnante de travail fourni par Madame Leticia Mazzarino. Compte tenu de tous ces éléments, il est tout à fait digne d'être défendu et j'émets un avis favorable à sa soutenance devant le jury retenu.

Fait à Montpellier, le 1 Avril 2013

Prof. J.J. ROBIN

RÉSUMÉ EN FRANÇAIS

Systèmes Nanostructurés Décorées avec du Chitosane pour la Libération Buccale de la Curcumine

Introduction et contexte

Généralement l'absorption de médicaments à travers des muqueuses est limitée par le temps de séjour sur le site d'absorption et/ou action. Les systèmes de libération mucoadhésifs font l'objet d'un intérêt notable, puisqu'ils sont considérés comme une voie prometteuse de prolonger la durée du séjour des formes posologiques dans la couche muqueuse, permettant l'optimisation de la libération de médicaments et produire l'effet thérapeutique et/ou un grand contact de la formulation avec le lieu d'absorption (SMART, 2005a; HOMBACH; BERNKOP-SCHNURCH, 2010).

Les systèmes mucoadhésifs peuvent être destinés à différentes régions du corps, y compris par voie buccale, orale, vaginale, rectale, nasale et oculaire. Parmi celles-ci, la cavité buccale peut être avantageusement utilisée comme site pour l'administration de médicaments, visant le traitement topique ainsi que systémique. La muqueuse buccale est relativement plus perméable, robuste et tolérante à des substances potentiellement allergisantes, si on compare à d'autres types de muqueuses; elle présente aussi une faible tendance à une irritation ou des nuisances irréversibles. D'autres avantages associés à l'administration buccale de médicaments incluent la prévention du métabolisme de premier passage hépatique et l'inactivation par les enzymes présentes dans le tractus gastro-intestinal, lorsque que le médicament est absorbé par la muqueuse et pénètre directement dans la circulation sanguine. Le traitement local sert au traitement de la gingivite, de la périodontie, des infections fongiques et bactériennes, des ulcères aphteux et des carcinomes oraux. La raison pour laquelle il existe un grand intérêt au traitement local des maladies de la cavité buccale vient du fait que ces types de maladies montrent une de plus élevées prévalences (SMART, 2005b; SUDHAKAR; KUOTSU; BANDYOPADHYAY, 2006; SCHOLZ et al., 2008).

Cependant, il existe quelques inconvénients associés à la libération orale. Le renouvellement constant de la salive, par exemple, peut conduire à une élimination rapide du médicament au niveau du lieu d'application, ce qui demande l'administration fréquente de doses. La distribution non uniforme de la salive peut entraîner la libération non-uniforme de médicaments à partir de formes pharmaceutiques solides ou semi-solides, et pour cette raison certaines régions de la cavité

buccale ne reçoivent pas les niveaux thérapeutiques du médicament. En outre, la composition de la salive peut contribuer à la modification chimique de certains médicaments et à l'acceptabilité du patient qui, à cause du goût, peut ne pas adhérer à un traitement (SMART, 2005b; SUDHAKAR; KUOTSU; BANDYOPADHYAY, 2006; SCHOLZ et al., 2008).

Les formulations mucoadhésives constituent une stratégie prometteuse pour l'administration buccale de médicaments afin de traiter diverses maladies. Outre cela, l'adéquate conception de la forme pharmaceutique permet le contrôle et la manipulation de la perméabilité de la muqueuse buccale. Parmi les différents systèmes mucoadhésifs destinés à l'administration orale, on peut en lister: les hydrogels, les films, les comprimés et les pommades (LEE; PARK; ROBINSON, 2000; PATHAN et al., 2008).

Bien que très peu de travaux existent dans la littérature, les nanoparticules décorées avec des polysaccharides suscitent un intérêt croissant comme vecteurs mucoadhésifs de médicaments. L'intérêt envers le développement de ces systèmes réside dans la possibilité de combiner les avantages liés à l'utilisation de nanoparticules; comme la protection de molécules actives, la libération contrôlée et une croissance de la solubilité de médicaments hydrophobes, avec les propriétés mucoadhésives provenant de la décoration avec les polysaccharides (LEMARCHAND; GREF; COUVREUR, 2004; LEMARCHAND et al., 2006; MOHANRAJ; CHEN, 2006). Les polysaccharides sont fortement stables, non toxiques, hydrophiliques et biodégradables, en prime d'avoir de nombreuses sources dans la nature à un faible coût. Ainsi, les nanoparticules décorées de polysaccharide mucoadhésif représentent une alternative prometteuse pour prolonger la durée de séjour des principes actifs et donc d'augmenter l'absorption du médicament encapsulé (LEMARCHAND; GREF; COUVREUR, 2004; LIU et al., 2008).

Par ailleurs, le développement de films mucoadhésifs - à condition de permettre une application facile à la muqueuse - a aussi montré un grand intérêt s'agissant de la voie buccale. Ces vecteurs sont obtenus à partir de polymères bioadhésifs, et conçus pour fournir une libération uni-ou bidirectionnelle du médicament en fonction de la conception de la forme posologique. D'autres avantages liés à l'utilisation de films mucoadhésifs comprennent la protection de la zone lésée, un temps supérieur de séjour sur la zone d'application et une meilleure acceptation par les patients grâce à un moindre effort avec cette forme posologique par rapport aux comprimés buccaux. Des

rapports indiquent que de tels systèmes peuvent rester jusqu'à 15 heures sur la zone d'application, assurant la libération constante du médicament (LEE; PARK; ROBINSON, 2000; SUDHAKAR; KUOTSU; BANDYOPADHYAY, 2006).

La curcumine est le principe actif extrait du rhizome de la *Curcuma Longa* Linn, (communément appelé safran) plante caractéristique des régions tropicales et subtropicales, largement cultivé en Inde et en Chine. La curcumine présente différentes activités pharmacologiques y compris les fonctions anti-inflammatoire, anti-tumorale, anti-oxydante, antimicrobienne, au-delà d'être liée aux effets bénéfiques pour la santé de façon générale (GOEL; KUNNUMAKKARA; AGGARWAL, 2008). Etant donné ses activités biologiques, la libération buccale de la curcumine peut être utile dans le traitement de diverses maladies de la cavité buccale. Des études *in vitro* ont montré que l'administration de la curcumine à des souris inhibe significativement la réponse immunitaire inflammatoire associée à la maladie parodontale, ce qui suggère son effet potentiel thérapeutique dans cette condition d'inflammation chronique (GUIMARAES et al., 2011; GUIMARAES et al., 2012). La curcumine démontre aussi son efficacité à réduire significativement la faisabilité cellulaire et induire l'apoptose des cellules cancéreuses oraux. De cette façon, elle serait plus puissante que d'autres polyphénols, tels comme la quércetine et la génistéine (ELATTAR; VIRJI, 2000; LIAO et al., 2011). Cependant, malgré l'intérêt scientifique concernant la curcumine, son usage thérapeutique est limité à cause de sa basse solubilité aqueuse, ce qui résulte à une faible biodisponibilité par des différentes voies d'administration. En outre, la curcumine démontre un grand taux de décomposition à pH neutre ou basique et une susceptibilité à la dégradation photochimique (TONNESEN, 2002; TONNESEN; MASSON; LOFTSSON, 2002; ANAND et al., 2007; TOMREN et al., 2007).

Un moyen prometteur de contourner les problèmes de dégradation, de faible solubilité dans l'eau et de biodisponibilité réduite, est l'association de la curcumine à des transporteurs comme des nanoparticules, des liposomes, des cyclodextrines, des micelles et des complexes phospholipidiques (WANG et al., 2011). Ainsi**,** et en tenant compte de ce qui a été exposé, cette étude a comme objectif de développer des systèmes de libération nanostructurés contenant la curcumine pour l'administration buccale, ce qui envisage à utiliser potentiellement ses effets pharmacologiques pour le traitement local des maladies de la cavité buccale. Ces systèmes sont constitués de

nanoparticules polymériques décorées avec un polysaccharide tel que le chitosane et des films nanostructurés obtenus à partir de ces nanoparticules. L'obtention de ces systèmes est peu décrite dans la littérature, ce qui montre le caractère novateur de ce travail.

Objectif Général

Développer et caractériser des systèmes nanostructurés décorés avec du chitosane contenant la curcumine ayant comme objectif leurs utilisations dans des applications buccales.

Objectif Spécifiques

- Préparer des suspensions de nanoparticules décorées avec du chitosane contenant de la curcumine à partir du polymère polycaprolactone (PCL) par la technique de nanoprécipitation;
- Préparer des nanoparticules décorées avec du chitosan contenant de la curcumine à partir du copolymère en bloc xyloglucan-polycaprolactone (XGO-*b*-PCL) par la technique du co-solvant;
- Caractériser les suspensions de nanoparticules quant à la taille des particules, la morphologie, le potentiel zêta, le taux de curcumine et l'efficacité d'encapsulation;
- Préparer des films mucoadhésifs contenant des nanoparticules encapsulant de la curcumine;
- Caractériser les films mucoadhésifs quant à la masse, l'épaisseur et la morphologie ;
- Évaluer les propriétés mucoadhésives des nanoparticules décorées avec du chitosane;
- Déterminer le pourcentage de gonflement des films nanostructurés dans un milieu salive artificielle;
- Développer et valider une méthode d'analyse par spectroscopie de fluorescence pour la détermination de la curcumine dans les études de libération, perméation et de rétention au niveau de la muqueuse;
- Évaluer et comparer la perméation et la rétention de la curcumine à partir des suspensions de nanoparticules dans le modèle bicompartimental de cellule de diffusion de type Franz, en utilisant la muqueuse oesophagienne de porc comme membrane;

- Évaluer et comparer le profil de libération de la curcumine à partir des différents films contenant des nanoparticules développées;
- Évaluer et comparer la cytotoxicité *in vitro* des suspensions de nanoparticules contenant de la curcumine dans des cultures de fibroblastes murins L929;
- Évaluer l'activité microbiologique *in vitro* des nanoparticules décorées avec du chitosane.

Discussion générale

Des systèmes mucoadhésifs nanostructurés, y compris des nanoparticules décorées avec du chitosane et des films contenant des nanoparticules, ont été développés pour la libération buccale de la curcumine. Pour une meilleure compréhension, cette étude a été divisé en quatre chapitres: (1) état des lieux bibliographique, (2) le développement de nanoparticules de polycaprolactone décorées avec du chitosane pour la libération buccale de la curcumine, (3) le développement de nanoparticules xyloglucan-*b*-polycaprolactone décorées avec du chitosane pour la libération buccale de la curcumine, et (4) le développement de films nanostructurés pour libération buccale de la curcumine.

Parmi les polysaccharides mucoadhésifs existants, le chitosane a été sélectionné pour la décoration des nanoparticules en raison de ses excellentes propriétés mucoadhésives, et aussi en raison de sa capacité d'améliorer l'absorption des médicaments (ANDREWS; LAVERTY; JONES, 2009). Parmi les polymères utilisés pour la préparation des nanoparticules, la polycaprolactone (PCL) et le xyloglucan (XGO) ont été proposées grâce à leurs caractéristiques de biodégradabilité et de biocompatibilité et leurs potentielles applications dans le développement de transporteurs pour la libération de médicaments (RASEKH et al., 2011; CHEN et al., 2012).

Deux différents systèmes de nanoparticules ont été préparés dans ce travail, les nanoparticules de polycaprolactone (PCL) stabilisées par un agent tensioactif (poloxamère) et les nanoparticules du copolymère en bloc xyloglucan-*b*-polycaprolactone (XGO-*b*-PCL). Les nanoparticules de PCL ont été préparées à partir de la technique de nanoprécipitation, qui constitue la méthode la plus largement utilisée pour la préparation de nanoparticules à partir de polymères préformés. La nanoprécipitation implique la dissolution du polymère dans un

solvant organique miscible avec l'eau, lequel est additionné à une phase aqueuse contenant un agent tensioactif, sous agitation magnétique modérée. Avec l'addition de la phase organique sur la phase aqueuse, le solvant organique se diffuse immédiatement dans la phase externe aqueuse, ce qui amène la précipitation du polymère et la formation des nanoparticules (LETCHFORD; BURT, 2007). L'origine du mécanisme de formation des nanoparticules peut être expliquée en termes de la turbulence interfaciale ou de l'agitation spontanée de l'interface entre les deux phases liquides en déséquilibre, impliquant le flux, la diffusion et les processus de surface (FESSI et al., 1989; QUINTANAR-GUERRERO et al., 1998). Les nanoparticules XGO-*b*-PCL ont été préparées par la technique du co-solvant. Cette technique consiste à la dissolution du copolymère dans un solvant commun, en d'autres termes, thermodynamiquement bon pour les deux blocs, et miscible avec l'eau. La formation des nanoparticules se produit après le mélange de cette solution avec un solvant sélectif (de l'eau), lequel provoque des changements dans la qualité du solvant par rapport à chaque bloc, en le rendant bon pour un bloc et mauvais pour l'autre (GIACOMELLI, 2007).

La décoration des nanoparticules de PCL avec le polysaccharide mucoadhésif a été réalisée en incorporant du chitosane pendant la préparation. Concernant la décoration des nanoparticules XGO-*b*-PCL, elle a été produite par une simple adsorption, en ajoutant une solution de chitosane aux suspensions de nanoparticules précédemment préparées. L'adsorption du chitosane à la surface des nanoparticules se produit via la formation de fortes liaisons d'hydrogène entre les groupes amine du chitosane et les blocs PEO de l'agent tensioactif poloxamère et XGO du copolymère, présents à l'interface des nanoparticules de PCL et XGO-*b*-PCL, respectivement. Toutes les nanoparticules décorées avec du chitosane ont présenté une grande habilité à interagir avec la mucine sous-maxillaire bovine (BSM), ce qui démontre les fortes propriétés mucoadhésives de ces systèmes. Cette interaction est, principalement, attribuée aux forces électrostatiques entre les groupes amines du polymère mucoadhésif chitosane et les groupes négativement chargés de la glycoprotéine mucine (DEACON et al., 2000; SVENSSON; THURESSON; ARNEBRANT, 2008).

Les deux systèmes de nanoparticules ont présenté une grande habilité dans l'encapsulation du principe actif hydrophobe: curcumine. Des valeurs élevées d'efficacité d'encapsulation ont été atteints, ce qui peut être expliqué par la faible solubilité de la curcumine dans la phase aqueuse externe et la forte affinité pour la particule pendant la

préparation. Le plus petit taux de curcumine présenté par les nanoparticules de XGO-*b*-PCL, quand comparées aux nanoparticules de PCL, peut être lié à la faible concentration de copolymère utilisée (Cp = 1 mg/mL).

Une méthode d'analyse par spectroscopie de fluorescence a été utilisée pour la détermination de la curcumine dans les études de libération, perméation et de rétention dans la muqueuse de oesophagienne de porc. Cette méthode a démontré son efficacité: elle est spécifique, linéaire, exacte, précise et sensible pour la quantification de la curcumine dans les milieux acepteur et extrateur. Les nanoparticules contenant de la curcumine non décorées et décorées avec du chitosane ont montré des profils de perméation similaires à travers la muqueuse oesophagienne de porc. La rétention des concentrations de curcumine suggère la possibilité d'obtention des effets localisés du principe actif, attestant du potentiel dans l'application de ces systèmes dans le traitement local des maladies buccales. L'analyse histologique de la muqueuse a démontré que le traitement de la muqueuse avec des nanoparticules contenant de la curcumine a occasionné l'hydratation du tissu, ce qui facilite la pénétration des médicaments dans les couches profondes de la muqueuse.

Les deux systèmes de nanoparticules PCL et XGO-*b*-PCL, préparés sans la curcumine, ont présenté reduite toxicité *in vitro* dans des lignages de cellules normales de fibroblastes murins L929, ce qui démontre une sécurité dans l'utilisation de ces systèmes. Les suspensions des nanoparticules contenant de la curcumine ont montré une activité cytotoxique plus petite par rapport à la curcumine libre, probablement due à la libération lente du médicament encapsulé. La cytotoxicité *in vitro* des nanoparticules de XGO-*b*-PCL a également été évaluée dans la lignée cellulaire tumorale de mélanome murin B16F10. Les nanoparticules contenant de la curcumine ont montré une cytotoxicité significativement plus élevée contre les cellules tumorales par rapport à celle observée dans les cellules normales, suggérant une potentielle application thérapeutique de ces systèmes dans le traitement des maladies cancéreuses. Le potentiel thérapeutique *in vitro* des suspensions de nanoparticules de PCL a été évaluée dans le modèle microbiologique de *Candida albicans*. Malgré que les nanoparticules préparées sans curcumine aient présenté une activité antifongique, probablement à cause des propriétés antimicrobiennes du chitosane, la présence de curcumine dans les nanoparticules a augmenté leur activité antifongique. Les nanoparticules de PCL contenant de la curcumine ont montré les mêmes valeurs de MIC et MFC par rapport à la curcumine,

démontrant aussi son potentiel dans le traitement des infections fongiques de la cavité orale.

Les films nanostructurés développés dans cette étude ont été préparés par la technique de *casting*/évaporation du solvant, qui constitue le processus de fabrication des films le plus largement décrit dans la littérature. Les principaux avantages de cette technique sont la facilité du processus et le bas coût associés à réalisation à l'échelle du laboratoire (MORALES; MCCONVILLE, 2011). Les films ont été préparés après l'incorporation de nanoparticules de PCL dans des solutions du chitosane contenant un l'agent plastifiant (glycérol). Le choix du polysaccharide chitosane pour la préparation des films mucoadhésif était basé sur ses propriétés physico-chimiques et biologiques, tel que, la capacité de formation de film, des propriétés antimicrobiennes et de cicatrisation des plaies, en plus d'excellentes propriétés mucoadhésives et une bonne biocompatibilité et biodégradabilité présenté par du chitosane, précédemment décrites (KHUTORYANSKIY, 2011).

Les nanoparticules se sont présentées uniformément distribuées dans la surface ainsi qu'à l'intérieur des films de chitosane. Par ailleurs, les films obtenus en utilisant du chitosane de masse molaire moyenne et élevée se sont montrés homogènes et flexibles, et ont présenté une bonne hydratation en solution de salive simulée. Les films contenant des nanoparticules ont montré une libération lente de la curcumine, qui peut être liée aux propriétés de libération contrôlée des nanoparticules de PCL. Les résultats suggèrent que l'application de films développés peut être utiles dans le traitement local des maladies buccales, surtout dans le cas des maladies parodontales, où la libération contrôlée-prolongée est souhaitée. Cependant, malgré les propriétés mucoadhésives du chitosane qui est déjà bien connus, la réalisation des études futures afin d'évaluer les propriétés mucoadhésives des films est nécessaire pour assurer l'adéquation de ces systèmes pour l'administration buccale de la curcumine.